Ollscoil na hÉireann, Corcaigh

National University of Ireland, Cork

University College Cork, Ireland
Coláiste na hOllscoile Corcaigh

Workforce Fatigue Prediction via Wearable Sensor Data Analytics

Thesis presented by

Patricia O'Sullivan, BEng

ORCID: 0000-0002-5024-2564

for the degree of

Doctor of Philosophy

University College Cork

Electrical and Electronic Engineering

Head of School: Dr. Alan Morrison

Supervisors: Prof. Brendan O'Flynn, Dr. Dimitrios-Sokratis Komaris, Dr. Matteo Menolotto

Advisor: Dr. Andrea Visentin

March 2026

Table of Contents

DECLARATION ..... **IV**

ABSTRACT ..... **V**

ACKNOWLEDGEMENTS ..... **VII**

ABBREVIATIONS ..... **VIII**

LIST OF FIGURES ..... **X**

LIST OF TABLES ..... **XIII**

LIST OF APPENDICES ..... **XIV**

CHAPTER 1 INTRODUCTION **1**

1.1 Background 1

1.1.1 The Smart Factory Workforce of the Future *1*

1.1.2 Ergonomic Risk, Fatigue and WMSDs *2*

1.2 Identified Gaps in the State-of-the-Art 9

1.3 Research Framework 10

1.3.1 Research Hypothesis and Objectives *10*

1.3.2 Research Gaps Addressed and Novel Contributions *13*

1.3.3 Thesis Structure and Scope *22*

CHAPTER 2 STATE-OF-THE-ART IN WORKPLACE FATIGUE, WEARABLES, AND WMSD PREVENTION **28**

2.1. Understanding and Assessing Fatigue in the Workplace 28

2.1.1 Fatigue: Definitions, Classifications, and Contributing Factors *28*

2.1.2 Measurement and Prediction Methods *32*

2.1.3 Current Fatigue and WMSD Interventions *46*

2.2 Literature Review 54

2.2.1 Wearable Technologies for Occupational Well-Being *54*

2.2.2 Ergonomic Applications of Wearables *55*

2.2.3 Fatigue Assessment and Modelling *58*

2.2.4 Machine Learning and Artifical Intelligence in Ergonomics and Fatigue Modelling *59*

2.2.5 Innovative Approaches for Upper Limb WMSD Prevention *60*

2.2.6 Identified Gaps in the State-of-the-Art *60*

2.3 Thesis Rational and Research Direction 64

CHAPTER 3 ENDURANCE MODELLING **66**

3.1 Estimation of Maximum Shoulder and Elbow Joint Torque Based on Demographics and Anthropometrics 67

3.1.1 Introduction *68*
3.1.2 Methodology *69*
3.1.3 Results *71*
3.1.4 Discussion *74*
3.1.5 Conclusion *77*
3.2 Validation of Endurance Model for Manual Tasks 77
3.2.1 Introduction *77*
3.2.2 Methodology *79*
3.2.3 Results *82*
3.2.4 Discussion *84*
3.2.5 Conclusion *85*
3.3 Improving Dynamic Endurance Time Predictions for Shoulder Fatigue: A Comparative Evaluation 86
3.3.1 Introduction *86*
3.3.2 Material and Methods *88*
3.3.3 Results *93*
3.3.4 Discussion *97*
3.3.5 Conclusion *101*
CHAPTER 4 LOAD AND TASK ESTIMATION 102
4.1 Evaluating Wearable Sensor Technologies for Predicting Shoulder Endurance 103
4.1.1 Introduction *103*
4.1.2 Methods *104*
4.1.3 Results *106*
4.1.4 Discussion *109*
4.1.5 Conclusion *110*
4.2 AI-based Task Classification Using Pressure Insoles for Occupational Safety 111
4.2.1 Introduction *111*
4.2.2 Methodology *115*
4.2.3 Results *119*
4.2.4 Discussion *125*
4.2.5 Conclusion *129*
CHAPTER 5 SYSTEM FOR ACTIVITY-AWARE FATIGUE EVALUATION (SAFE) FRAMEWORK: PREDICTIVE FATIGUE MODELLING FOR OCCUPATIONAL TASKS 130
5.1 Introduction 131
5.2 SAFE Framework 132
5.2.1 Framework Overview *132*
5.2.2 Modelling Approach *134*
5.3 SAFE System 138

5.3.1 Hardware ... *139*
5.3.2 Software ... *140*
5.4 VALIDATION ... 142
5.4.1 Subjects ... *142*
5.4.2 Validation Equipment ... *143*
5.4.3 Protocol ... *143*
5.4.4 Data Analysis ... *147*
5.4.5 Results ... *151*
5.5 DISCUSSION ... 155
5.5.1 SAFE Framework ... *155*
5.5.2 Framework Validation ... *158*
5.5.3 Limitations and Future work ... *159*
5.6 CONCLUSION ... 162

CHAPTER 6 DISCUSSION, CONCLUSIONS AND FUTURE DIRECTIONS ... 163

6.1 SUMMARY OF KEY FINDINGS AND CONTRIBUTIONS ... 163
6.1.1 Contribution 1: Torque-based Endurance Modelling and Calibration Method ... *163*
6.1.2 Contribution 2: Explainable Task Classification and Open Datasets ... *164*
6.1.3 Contribution 3: SAFE Framework Integration and Prototype Deployment ... *165*
6.2 LIMITATIONS ... 167
6.3 FUTURE DIRECTIONS ... 170
6.3.1 System and Framework Development ... *172*
6.3.2 Individual and Physiological Factors ... *175*
6.3.3 Generalisability ... *176*
6.4 IMPLICATIONS OF FINDINGS ... 178
6.4.1 Commercial Opportunities and Reduced WMSDs ... *178*
6.4.2 Implications on the Employee, Employer and Organisation ... *182*
6.4.3 Standards and Policy ... *184*
6.5 CONCLUSION ... 186

APPENDICES ... 188

REFERENCES ... 232

Declaration

This is to certify that the work I am submitting is my own and has not been submitted for another degree, either at University College Cork or elsewhere. All external references and sources are clearly acknowledged and identified within the contents. I have read and understood the regulations of University College Cork concerning plagiarism and intellectual property.

Signature: Patricia O'Sullivan

Abstract

Work-related musculoskeletal disorders (WMSDs) remain a critical challenge in labour-intensive professions, often leading to disability, reduced productivity, and significant healthcare costs. Common ergonomic risk factors, such as repetitive tasks, heavy lifting, and awkward postures, contribute to localised muscle fatigue, which over time can cause chronic injury according to fatigue failure theory. Although observational risk assessments are widely used and influential in setting standards for WMSD prevention, they primarily offer static, reactive evaluations of ergonomic risk and fatigue. This thesis introduces a **S**ystem for **A**ctivity-aware **F**atigue **E**valuation (SAFE) framework using torque-based biomechanical endurance modelling to predict the time to physical fatigue during static and dynamic tasks in an individualised and task generalisable manner. The framework addresses limitations of ergonomic assessments, force-based endurance models, and other wearable ergonomic systems. The feasibility of the framework was demonstrated using a custom MATLAB application supporting wearable data streaming, manual entry of anthropometric and task-related data, and output of endurance metrics. This solution shows potential for proactive fatigue forecasting in real-time and fills important gaps in the field.

Preliminary testing with a torque-based endurance model showed large errors for one-handed static (28.62%) and two-handed dynamic (49.21%) fatiguing shoulder flexion tasks which led to exploring alternative models and inputs. Subsequently, six different models and four different methods of obtaining maximum torque ($Torque_{max}$), an input which indicates the maximum strength of the individual, were compared. This included regression models that predicted $Torque_{max}$ based on individual factors developed in the present work ($R^2 \approx .6$, $P<.05$). However, a novel method to determine $Torque_{max}$ with the new improved consumed endurance (NICE) model produced the lowest errors across all model-$Torque_{max}$ combinations for all tasks. The new method achieved RMSE=19.11 s compared to the errors of other models and methods which ranged from 41.08 s to 65.54 s. The novel method developed used data from a static task at a given load relative to the maximum voluntary contraction (MVC) force to solve for $Torque_{max}$. The torque-based endurance modelling approach is an important contribution that replaces traditional force inputs with torque, improving

prediction accuracy and allowing the model to account for multi-joint dynamics, and therefore different tasks, and inter-individual variability.

The system developed to validate the SAFE framework comprises of inertial measurement units, pressure insoles, and a custom MATLAB application to continuously refine predictions based on upper extremity configuration, task type, and load, requiring minimal manual input. Prior to deployment of the framework, the influence of these sensor types on endurance predictions was assessed offline where predictions were calculated using non-wearable data (laboratory-based equipment and manual input) and wearables data. Pressure insoles were not found to be a reliable method for estimating the load (mean absolute errors of 29.8%), and it was decided to automate the input of task-related parameters, such as external load, component shape and geometry, using task prediction methodologies. Machine learning techniques were employed to identify task types using pressure insole data with high accuracy (83% for 5 s window), demonstrating the feasibility of automated load input to the endurance model while achieving explainability and enabling low data throughput.

The SAFE framework was preliminarily tested during simulated industrial tasks with human subjects. Results confirmed the reliability of joint angle estimation compared to gold-standard technology (RMSD≤13.9°, MAE≤10.6°, .51≤CMC≤.95). Very strong correlations between the endurance metric describing cumulative fatigue, consumed endurance (CE), with subjective fatigue ratings (rmm≥.883, P < .001), and time (rmm≥.909, P < .001) demonstrated the strong potential of the framework as a task generalisable (adjusting predictions using task-specific coefficients) yet individualised (using the novel approach to calculate $Torque_{max}$, consideration of anthropometrics and individuals' perception of fatigue) tool for WMSD prevention. Endurance measures generated by the framework successfully differentiated between ergonomically high- and low-risk tasks (P<.050) while overcoming the shortcomings of self-report measures and ergonomic risk assessment tools. This is the first known implementation of an endurance model with task classification into a wearable ergonomic system, offering a biomechanical perspective grounded in real-world data rather than purely theoretical models, with applicability to various dynamic tasks involving the upper extremities. This work marks a step toward proactive real-time physical fatigue management and potentially WMSD prevention.

Acknowledgements

I would like to express my sincere gratitude to my supervisors, Dr. Brendan O'Flynn, Dr. Dimitrios-Sokratis Komaris, Dr. Matteo Menolotto, and advisor, Dr. Andrea Visentin, for their guidance, encouragement, and invaluable feedback throughout my PhD journey. Their expertise and support have been instrumental in shaping both this research and my development as a researcher.

I am deeply grateful to my examiners, Dr. Andy Kerr and Prof. Liam Marnane, for their time, careful review of the thesis, and constructive and insightful feedback.

I would like the thank all the participants who generously volunteered their time and effort to take part in my studies. Without their contribution, this work would not have been possible.

I would like to acknowledge the support of Taighde Éireann – Research Ireland and the European Regional Development Fund for providing the financial resources that made this research possible. This work was supported under grant number 12/RC/2289-P2 (The Insight Research Centre for Data Analytics) and aspects of this research have been supported by 16/RC/3918 (CONFIRM).

Finally, I want to thank my friends, family and partner, Oscar, for their encouragement and unwavering support. I would especially like to thank my Dad, who, through his calm and steady support, always nurtured my curiosity and creativity, and inspires me to live with motivation, purpose, and a lifelong love of learning.

Abbreviations

ACGIH	American Conference of Governmental Industrial Hygienists
AGREE II	Appraisal of Guidelines, Research and Evaluation
AI	Artificial intelligence
AR	Augmented reality
ART	Assessment of repetitive tasks of the upper limbs
ATP	Adenosine triphosphate
BMI	Body mass index
CDC	Centre for Disease Control and Prevention
CE	Consumed endurance
Cobot	Collaborative robot
CoM	Centre of mass
CoP	Centre of pressure
CREC	Clinical research ethics committee of the cork teaching hospitals
D25	Dynamic task at 25% SI
D45	Dynamic task at 45% SI
DV	Dependent variables
DWSM	Digital Workplace Stress Management
ECG	Electrocardiogram
EDA	Electrodermal activity
EMG	Electromyography
EN	European Norm
ESENER	European Survey of Enterprises on New and Emerging Risks
ET	Endurance time
EU-OSHA	European Agency for Safety and Health at Work
EWCS	European Working Conditions Survey
$Force_{max}$	Maximum force
GDP	Gross domestic products
GDPR	General data protection regulations
GSR	Galvanic skin response
GUI	Graphic user interface
H&S	Health and safety
HAL	Hand activity level
HAR	Human activity recognition
HMI	Human machine interface
HSA	Health and Safety Authority
HSE	Health and Safety Executive
ICT	Information and communication technologies
IMU	Inertial measurement unit
IoT	Internet of things
ISB	International Society of Biomechanics
ISO	International standards organisation
IV	Independent variables
JT-SJT	Joshi-ten and Shisei Juryo-ten system
LCS	Local coordinate system
LIME	Local interpretable model-agnostic explanation

MAC	Manual handling assessment chart
MEF	Maximum exertable force
MET	Maximum endurance time
ML	Machine learning
MoCap	Motion capture
MSD	Musculoskeletal disorder
MVC	Maximum voluntary contraction
NIOSH	National Institute for Occupational Safety and Health
OCRA	Concise index for the assessment of exposure to repetitive hand movements of the upper limbs
OSHA	Occupational Safety and Health Administration
OWAS	Ovako Working Posture Analysing System
PATH	Posture, activity, tools and handling assessment
PLA	Polylactic acid
PPE	Personal protective equipment
PPG	Photoplethysmography
QEC	Quick exposure check
RAPP	Risk assessment of pushing and pulling
REBA	Rapid Entire Body Assessment
RF	Random forest
RPE	Rate of perceived exertion
RULA	Rapid Upper Limb Assessment
RWL	Recommended weight limit
S25	Static task at 25% SI
S45	Static task at 45% SI
SAFE	System for Activity-aware Fatigue Evaluation
SERA	Safety & Ergonomic Risk Assessment
SHAP	Shapley Additive explanation
SI	Standardised intensity
TLV	Threshold Limit Value
TLX	Task load index
$Torque_{max}$	Maximum torque
TT	True torque, relative torque, $\frac{Torque}{Torque_{max}}$
TT1	TT calculated using measured shoulder MVC for $Torque_{max}$
TT2	TT calculated using measured elbow MVC for $Torque_{max}$
TT3	TT calculated using gender-based MVC values for $Torque_{max}$
TTcal	TT determined using calibration task
VR	Virtual reality
WMSD	Work-related musculoskeletal disorder

List of Figures

FIGURE 1: TASKS THAT INVOLVE HIGH ERGONOMIC RISK (SUCH AS REPETITION, HEAVY LOADS, SUSTAINED CONTRACTIONS AND AWKWARD POSTURES) LEAD TO LOCALISED MUSCLE FATIGUE AND, OVER TIME, WMSDS. 4
FIGURE 2: NUMBER OF DOCUMENTS PER YEAR IN SCOPUS (AS OF 28/04/2025) 8
FIGURE 3: FATIGUE FORECASTING SYSTEM CONSISTING OF IMUS, PRESSURE INSOLES AND CUSTOM APPLICATION 11
FIGURE 4: THE KEY GAPS IDENTIFIED AND HOW THE THESIS ADDRESSES THEM 13
FIGURE 5: THESIS STRUCTURE 23
FIGURE 6: SAFE FRAMEWORK OVERVIEW. 24
FIGURE 7: THE RELATIONSHIP BETWEEN CONTRIBUTING FACTORS, FATIGUE AND WMSDS. FACTORS AND FATIGUE TYPES HIGHLIGHTED IN RED ARE ADDRESSED IN THE PRESENT WORK. 29
FIGURE 8: METHODS TO PHYSICAL FATIGUE MEASUREMENT AND THE ASSOCIATED DATA COLLECTION METHODS ACCORDING TO YU ET AL. (2019), EACH OF WHICH ARE DISCUSSED IN THIS SECTION. 33
FIGURE 9: MOST COMMONLY USED WEARABLE SENSORS IN THE FIELD, (A) ELECTROMYOHRAPHY (EMG), (B) PHOTOPLETHYSMOGRAPHY (PPG), (C) INERTIAL MEASUREMENT UNITS (IMU), (D) PRESSURE INSOLES, (E) ELECTRODERMAL ACTIVITY (EDA) OR GALVANIC SKIN RESPONSE (GSR), (F) EMPATICA SMART WATCH............... 43
FIGURE 10: ERGONOMIC TOOLS CURRENTLY USED IN OCCUPATIONAL SETTINGS, (A) JACK SIEMENS, AN EXAMPLE OF A SIMULATION TOOL, (B) ERGODROID MOBILE APPLICATION GUI, (C) SKELEX 360, (D) AIRFRAME, (E) SUITX, (F) NOONEE CHAIRLESS CHAIR, (G) KINETIC REFLEX, (H) STRONGARM SAFEWORK SENSOR WITH HARNESS AND TOUCHSCREEN DEVICE FOR ALERTS AND INSIGHTS, (I) HONEYWELL BIOHARNESS 3, (J) MOVELLA XSENS MT AWINDA, (K) USER INTERFACE WITH AN EXAMPLE OF A WARNING VISUALLY DISPLAYED 50
FIGURE 11: TESTING POSITIONS FOR (LEFT) SHOULDER AND (RIGHT) ELBOW 71
FIGURE 12: CLUSTERED BAR GRAPH OF THE MEANS AND STANDARD DEVIATIONS OF THE $Torquemax$ FOR THE SHOULDER AND ELBOW BY GENDER.. 72
FIGURE 13: RESIDUALS FOR (TOP LEFT) HEIGHT, (TOP RIGHT) MUSCLE %, AND (BOTTOM RIGHT) FOREARM CIRCUMFERENCE AGAINST SHOULDER $Torquemax$.. 73
FIGURE 14: RESIDUALS FOR (LEFT) HEIGHT AND (RIGHT) FOREARM CIRCUMFERENCE AGAINST ELBOW $Torquemax$ ... 73
FIGURE 15:NORMAL PROBABILITY PLOTS OF THE RESIDUALS FOR (LEFT) THE SHOULDER MAX TORQUE MODEL AND (RIGHT) THE ELBOW $Torquemax$ MODEL. 74
FIGURE 16: IMU PLACEMENT ON THE SHOULDER, UPPER ARM, FOREARM, HAND AND TORSO. 80
FIGURE 17: LOCATIONS OF THE CENTRE OF MASS OF THE ARM.. 81
FIGURE 18: EXPERIMENTAL AND PREDICTED ENDURANCE TIMES. 83
FIGURE 19:MEAN LENGTH OF TIME (S) PARTICIPANTS SPENT IN EACH BORG RPE CATEGORY.................................... 83
FIGURE 20: ALL SIX ENDURANCE MODELS THAT ARE ASSESSED IN THE STUDY, ALL ARE IN TERMS OF TORQUE/MAXIMUM TORQUE. 86

FIGURE 21: ARM POSITION AT (LEFT) 0 ° AND (RIGHT) 90 ° DURING THE TASKS. DURING THE STATIC TASK, THE 90 ° POSITION IS MAINTAINED WHILE THE ARM IS FLEXED BETWEEN 0-90 ° DURING THE DYNAMIC TASK AT 50 BEATS PER MIN. 90
FIGURE 22: PROCEDURE FOR CALCULATING PREDICTED ENDURANCE TIMES FOR EACH OF THE SIX ENDURANCE MODELS WITH FOUR METHODS OF OBTAINING MAXIMUM TORQUE, RESULTING IN 6×4=24 DIFFERENT RMSE VALUES. 91
FIGURE 23: MEAN AND STANDARD DEVIATION (BLACK LINES) OF THE EXPERIMENTAL ENDURANCE TIMES FOR ALL TASKS FOR ALL SUBJECTS, MALES AND FEMALES. 93
FIGURE 24: DIFFERENT METHODS OF DETERMINING MAXIMUM TORQUE RESULT IN DRAMATICALLY DIFFERENT TRUE TORQUES, THE VARIABLE USED TO CALCULATE ENDURANCE PREDICTION TIME, FOR BOTH (A) MALES AND (B) FEMALES. 95
FIGURE 25: CALIBRATION TRUE TORQUES PLOTTED AGAINST EXPERIMENTAL ENDURANCE TIMES FOR ALL MODELS. STATIC TASKS APPEAR ON THE MODEL CURVE WHILE DYNAMIC TASKS DEVIATE SLIGHTLY AS THEIR TRUE TORQUE WAS CALCULATED USING THE TORQUE MAX OF THE STATIC TASK AT THAT LOAD. 95
FIGURE 26: RMSES FOR EACH MODEL AND TRUE TORQUE COMBINATION FOR ALL TASKS, FOR (A) ALL SUBJECTS, (B) MALES, (C) FEMALES. FAP GEN = FREY LAW AND AVIN GENERAL POWER MODEL, FAEXP GEN = FREY LAW AND AVIN GENERAL EXPONENTIAL MODEL, FAP SH = FREY LAW AND AVIN SHOULDER POWER MODEL, FAEXP SH = FREY LAW AND AVIN SHOULDER EXPONENTIAL MODEL. 97
FIGURE 27: RECOMMENDED USE OF CALIBRATION METHOD TO DETERMINE AN INDIVIDUALISED MAXIMUM TORQUE VALUE FOR ENDURANCE PREDICTION. 100
FIGURE 28: DETAILS OF THE THREE APPROACHES USED IN THE METHODOLOGY 105
FIGURE 29: ET ERRORS OF THE THREE APPROACHES USED IN THE METHODOLOGY. 108
FIGURE 30: A SNAPSHOT OF RAW FORCE DATA FOR ONE SUBJECT'S LEFT FOOT DURING EACH OF THE FIVE TASKS. 116
FIGURE 31: THE SET UP OF THE COMPONENTS FOR THE ASSEMBLY TASK (LEFT) AND THE ASSEMBLED COMPONENTS (RIGHT) 116
FIGURE 32: ACCURACIES OF THE RANDOM FOREST CLASSIFIERS ACROSS ALL NINE OBSERVATION WINDOW SIZES (2, 3, 4, 5, 6, 8, 10, 12, AND 15 S). 120
FIGURE 33: CONFUSION MATRIX SHOWING THE PREDICTION ACCURACY FOR THE 5 S OBSERVATION WINDOW. 121
FIGURE 34: ANALYSIS OF FEATURE IMPORTANCE FOR THE 5 S OBSERVATION WINDOW. 121
FIGURE 35: SHAP ANALYSIS OF FEATURE IMPORTANCE FOR MANUAL HANDLING IN THE 5 S OBSERVATION WINDOW 122
FIGURE 36: SHAP ANALYSIS OF FEATURE IMPORTANCE FOR WALKING IN THE 5 S OBSERVATION WINDOW 122
FIGURE 37: SHAP ANALYSIS OF FEATURE IMPORTANCE FOR ASSEMBLY IN THE 5 S OBSERVATION WINDOW 123
FIGURE 38: EXAMPLE OF THE TRAJECTORY OF THE COP FOR EACH OF THE FIVE TASKS FOR ONE SUBJECT. 123
FIGURE 39: ACCURACY VALUES ACROSS ALL WINDOWS AFTER RE-ANALYSIS WITH THE FIVE MOST IMPACTFUL CLASSIFICATION FEATURES. 124
FIGURE 40: ANALYSIS OF FEATURE IMPORTANCE FOR THE 5 S OBSERVATION WINDOW AND THE HIGHEST PERFORMING FEATURES. 124
FIGURE 41: CONFUSION MATRIX SHOWING THE PREDICTION ACCURACY FOR THE TOP 5 FEATURES IN THE 5 S OBSERVATION WINDOW. 125

FIGURE 42: SAFE FRAMEWORK BLOCK DIAGRAM. INPUTS ARE NON-DYNAMIC PARAMETERS (BLUE BOXES) AND DYNAMIC (RED BOXES) DATA OBTAINED FROM MANUAL INPUT, AND STREAMED SENSOR DATA, WHILE ENDURANCE MODELLING AND TASK CLASSIFICATION (GREY BOXES) ARE USED TO GENERATE ENDURANCE METRICS AND CAN BE EXPORTED (GREEN BOXES) FOR FURTHER ANALYSIS. 133
FIGURE 43: TORQUE CALCULATION 134
FIGURE 44: SAFE FRAMEWORK AND METHOD FOR CALCULATING ENDURANCE METRICS 136
FIGURE 45: SENSOR PLACEMENT AND GLOBAL COORDINATES OF IMUS 139
FIGURE 46: THE FOUR PANELS PRESENT IN THE APPLICATION SHOWING THE SUBJECTIVE INFORMATION PANEL (TOP LEFT), CALIBRATION TASK PANEL (TOP RIGHT), TASK MEASUREMENT PARAMETERS PANEL (BOTTOM LEFT), AND TASK MEASUREMENT PANEL (BOTTOM RIGHT). 140
FIGURE 47: TASK CYCLE FOR MANUAL HANDLING (TOP) AND PICK AND PLACE (BOTTOM) TASKS 144
FIGURE 48: PICK-UP AND DROP-OFF POINTS FOR MANUAL HANDLING TASKS, WITH MHNONERGON LOCATIONS DEVIATING FROM MHERGON BY -49CM AND +39CM FOR PICK-UP AND DROP-OFF POINTS RESPECTIVELY. WALKING PATH WHILE HOLDING THE LOAD IS INDICATED BY THE BLUE ARROW. 146
FIGURE 49: PICK AND PLACE TASK INVOLVED REPEATEDLY LIFTING AND PLACING THE BOX LATERALLY FROM THE BLACK TABLE ON THE LEFT TO THE WHITE TABLE ON THE RIGHT AND VICE-VERSA. THE BLACK TABLE WAS 18CM HIGHER IN PPNONERGON COMPARED TO PPERGON TO INCREASE ERGONOMIC RISK. 146
FIGURE 50: MHERGON TASK FOR ONE SUBJECT SHOWING MOCAP AND IMU JOINT ANGLES (TOP), TASK CLASSIFICATION WITH PI AND IMU JOINT ANGLES DATA (MIDDLE) AND THE CALCAULTED TORQUE AND PREDICTED ENDURANCE TIMES (BOTTOM) 152
FIGURE 51: CE PLOTS FOR ALL TASKS FOR ONE SUBJECT 153
FIGURE 52: RELATIONSHIP BETWEEN TIME, BORG SCORES AND CE VALUES 154
FIGURE 53: PRODUCT DEVELOPMENT PROCESS 180

List of Tables

TABLE 1: WORK TO COMBAT ENDURANCE MODELLING DISADVANTAGES IN THE RESEARCH WORK DESCRIBED IN THE THESIS 14

TABLE 2: COMMERCIAL AND RESEARCH SYSTEMS INTEGRATING WEARABLES FOR ERGONOMIC RISK OR FATIGUE MONITORING, DETECTION OR PREDICTION OF THE UPPER BODY DURING MANUAL HANDLING ACTIVITIES,, INCLUDING THE PRESENT WORK. 16

TABLE 3: SUMMARY AND COMPARISON OF MEASUREMENT METHODS 34

TABLE 4: SUMMARY AND COMPARISON OF CURRENT INTERVENTIONS 47

TABLE 5: CURRENT ERGONOMIC TOOLS USED IN OCCUPATIONAL SETTINGS. 48

TABLE 6: SUBJECT INFORMATION 70

TABLE 7: COMPARING SUBJECT INFORMATION BETWEEN THE ORIGINAL ANALYSIS AND THE RE-ANALYSIS 75

TABLE 8: MINIMUM R^2 DETECTED WITH A POWER OF 80%, TYPE I ERROR OF 5% FOR VARYING NUMBERS OF INDEPENDENT VARIABLES AND SAMPLE SIZES 76

TABLE 9: SUBJECT INFORMATION 80

TABLE 10: ENDURANCE MEASUREMENTS AND PREDICTIONS. 82

TABLE 11: ANTHROPOMETRIC AND DEMOGRAPHIC DATA OF PARTICIPANTS 88

TABLE 12: IDEAL AND REAL STANDARDISED INTENSITIES (%) OF THE LOADS LIFTED IN THE STUDY. 88

TABLE 13: SUBJECT DETAILS. 105

TABLE 14: EXPERIMENTAL AND PREDICTED ENDURANCE TIMES FOR EACH SUBJECT AND TASK AND THE ASSOCIATED ERRORS. 107

TABLE 15: THE ACTUAL AND DETECTED DUMBBELL MASSES AND THE ASSOCIATED ERROR. 108

TABLE 16: DATASETS WITH PRESSURE INSOLES 112

TABLE 17: TOTAL DATA SIZE PER WINDOW = (TOTAL NO. OF SAMPLES ÷ NUMBER OF SAMPLES PER WINDOW) × NO. OF TASKS 119

TABLE 18: COMPARISON OF MOCAP AND IMU SHOULDER AND ELBOW JOINT ANGLES INDICTED BY MEAN ± STANDARD DEVIATION FOR RMSD, MAE, CMC 152

TABLE 19: WILCOXON SIGNED-RANK TEST Z-SCORES COMPARING THE MEANS BETWEEN ERGON AND NONERGON TASKS 155

TABLE 20: MEAN ± STANDARD DEVIATIONS OF TARGET CE VALUES (BASED ON BORG SCORES) AND CE VALUES WITH AND WITHOUT SCALING, AND THE ASSOCIATED NORMALISED RMSE 155

List of Appendices

Appendix 1: Linking Publications to Chapters 188

Appendix 2: DOIs for Thesis-Related Publications 189

Appendix 3: CRediT Author Statement for Publications 190

Appendix 4: Additional Peer-Reviewed Collaborative Publications During the PhD 191

Appendix 5: Linking Objectives with Experiments 192

Appendix 6: Detailed Overview of Measurement Methods 194

Appendix 7: Detailed Overview of Current Interventions 202

Appendix 8: Poster Presented at the EMBC Conference in Glasgow, July 2021 209

Appendix 9: Linearity Tests for All Independent Variables Against the Dependent Variable: Shoulder Maximum Torque 210

Appendix 10: Linearity Tests for All Independent Variables Against the Dependent Variable: Elbow Maximum Torque 213

Appendix 11: Regression Analysis Results - Shoulder Maximum Torque 216

Appendix 12: Regression Analysis Results - Elbow Maximum Torque 217

Appendix 13: Borg Rate of Perceived Exertion Scale 218

Appendix 14: Karolinska Sleepiness Scale 218

Appendix 15: Breakdown of Predicted ET RMSEs Based on Gender and Movement. RMSEs for Each Model and TT Combination for Female Subjects During (a) Static Tasks and (b) Dynamic Tasks, and for Males During (c) Static Tasks and (d) Dynamic Tasks. 219

Appendix 16: Breakdown of Predicted ET RMSEs Based on Gender and Load. RMSEs for Each Model and TT Combination for Female Subjects During (a) 25% SI tasks and (b) 45% SI tasks, and for Males During (c) 25% SI tasks and (d) 45% SI tasks. 219

Appendix 17: Predicted ET RMSEs Including Maximum Torque Regression Models. RMSEs for Each Model and TT Combination for (a) All Subjects and All Tasks, (b) Male Subjects and All Tasks (c) Female Subjects and All Tasks. 220

Appendix 18: Predicted ET RMSEs including maximum torque regression models, based on gender and movement. RMSEs for each model and TT combination for male subjects during (a) static tasks and (b) dynamic tasks and for females during (c) static tasks and (d) dynamic tasks. 220

Appendix 19: Predicted ET RMSEs including maximum torque regression models based on gender and load. RMSEs for each model and TT combination for male subjects during (a) 25% SI tasks and (b) 45% SI tasks and for females during (c) 25% SI tasks and (d) 45% SI tasks. 221

Appendix 20: Supplementary Material for Section 4.2 222

Appendix 21: Poster Presented at INSIGHT Plenary in Galway, October 2023. 229

Appendix 22: Supplementary Material for Chapter 5 230

Chapter 1 Introduction

In recent years, technological advancements have significantly transformed industrial operations which are reshaping the role of workers. In Chapter 1, the concept of the smart factory worker is explored as well as the key trends, risks and challenges in the rapidly evolving area of smart factories and Industry 5.0 scenarios. Here, the problem addressed in the thesis is identified: high ergonomic risk, physical fatigue and muscle fatigue. The gaps in the state-of-the-art are outlined and the research question, hypothesis, and objectives that address these gaps in the course of the thesis are stated. Finally, the thesis structure and scope are outlined.

1.1 Background

This section provides the context for the research presented in this thesis. It begins by outlining how technological advancements are changing the nature of industrial work, with a focus on the smart factory worker. The section then explores the central challenges of ergonomic risk, physical fatigue, and work-related musculoskeletal disorders (WMSDs).

1.1.1 The Smart Factory Workforce of the Future

Industry 4.0 is a broad term that encompasses societal and technological changes that are possible due to developments in information and communications technology (ICT) such as internet of things (IoT) [1], [2], [3], [4], big data analytics [2], [3], cloud computing [2], [3], artificial intelligence (AI) [3], [4], robotics [3], [4], and extended reality [4], [5]. Using these technologies, productivity can be improved in a holistic manner in manufacturing contexts by considering the environment, machinery and workforce [6]. In terms of workforce, a human-centric approach to prioritise sustainability and well-being is possible with such technologies which can better equip them to navigate obstacles and difficulties in occupational environments; this concept is called *Operator 4.0* [4], [7], or *Resilient Operator 4.0* [6], or the *smart factory worker of the future* [4], which was first presented by Romero *et al.* (2016) [7]. Operator 4.0 exists within the context of Industry 4.0 and focuses on leveraging the indispensable physical, cognitive and sensorial abilities of humans while also leveraging the strengths of automation and Industry 4.0 technologies [4], [7], [8].

However, alongside these technological advances, workers remain exposed to substantial physical demands, particularly during manual handling tasks, where WMSDs continue to be a leading cause of occupational ill-health.

Even though Industry 4.0 and Operator 4.0 are an active research area, a new concept of the fifth industrial revolution was established in 2017 and gained wider recognition in 2021 [9]. Building on the technologies and focus of Industry 4.0 and Operator 4.0, Industry 5.0 considers the entire industrial ecosystem, and the concept hones in on a "human-centric collaborative economy within a world facing population growth, resource constraints, and increasing interconnectedness" [1], [8]. There is a strong focus on resilience and sustainability, and operators can co-exist and work synergistically alongside machines in *human-automation symbiosis*, or in *human cyber-physical systems*, as opposed to machines replacing humans in work environments [1], [3], [4], [6], [7], [8].

Areas of research in terms of monitoring manufacturing workers' activities in these industrial revolutions include the *super-strength operator* (increasing strength and resistance), the *virtual and augmented operator* (using augmented and virtual reality tools), the *healthy operator* (using wearable devices to ascertain their state), the *smart and analytical operator* (using intelligent assistants, AI and big data tools), the *collaborative operator* (in tandem with robots), and the *social operator* (using social networks to quickly adapt to challenges) [10]. According to a systematic review [4], studies relating to Operator 4.0 tend to focus on worker augmentation, smart manufacturing, and even super-strength workers through the use of exoskeletons, and a shift in perspective to health prioritisation is key for the operator, as opposed to technology or productivity prioritisation. While these technological advances promise much, they also introduce new health and safety (H&S) challenges, particularly in the realm of ergonomic risk.

1.1.2 Ergonomic Risk, Fatigue and WMSDs

The Occupational Safety and Health Administration (OSHA) [11] and European Agency for Safety and Health at Work (EU-OSHA) [12] websites outline five categories of hazards to workers: s*afety* (such as falls, electrical hazards, dangerous machinery), *chemical* (hazardous gases or liquids), *biological* (dangerous viruses, bacteria or moulds), *physical* (extreme noise, temperatures or light) and *ergonomic* (manual activities, body positions, or working conditions that cause strain), and EU-OSHA also includes *psychosocial risks*. Psychosocial risks mainly arise due to the context in which the work is performed and can result in poor outcomes psychologically, physically or socially [13]. These risks result from poor work design (excessive loads, conflicting work demands), poor organisational management (ineffective communication, poorly managed organisational change, lack of support from management, job insecurity), or a poor social context (harassment, difficult colleagues/customers, lack of support from colleagues). A 'hazard' has the potential to cause harm while 'risk' considers the possible extent of harm and its likelihood [14], both will be used interchangeably since 'hazard' is mainly used by OSHA and 'risk' is mainly used by EU-OSHA. Various European surveys [15], [16] indicate that ergonomic risks are the most commonly reported by workers, therefore, ergonomic risk is the focus of the thesis.

Ergonomic Risks and WMSD Prevalence

An EU-OSHA report, the European Survey of Enterprises on New and Emerging Risks (ESENER) [15], surveyed more than 45,000 workplaces in 33 European countries in 2019 and found risk factors that resulted in WMSDs were most frequently identified. Related survey questions and the percentage of respondents who experienced these risks included "prolonged sitting" (61%), "repetitive hand or arm movements" (65%), and "lifting or moving heavy loads" (52%). These factors are linked to ergonomic risks and the latter two risks saw notable increases compared to the 2014 ESENER report [15]. Psychosocial risks such as "long or irregular working hours" (21%) were reported less than other risks in this category such as "difficult interactions with customers" (59%) and "time pressure" (45%). Large organisations were more likely to report higher risks and tended to focus on safety risks more than WMSD prevention or psychosocial risks, although small organisations also tended towards the latter [15]. The 2019 ESENER report also revealed that 90% of injuries and absenteeism were caused by WMSDs [15].

Furthermore, according to the 6th European Working Conditions Survey (EWCS) [16] which surveyed 44,000 workers in 35 European countries, 33% of workers feel exhausted "most of the time" or "always" at the end of the workday and are more likely to say their H&S is at risk as a result, although long working hours and shift

Figure 1: Tasks that involve high ergonomic risk (such as repetition, heavy loads, sustained contractions and awkward postures) lead to localised muscle fatigue and, over time, WMSDs.

work greatly affected this response. The most reported health problems were backache (43%) and muscular pains in the neck and upper limbs (42%), followed by headaches (35%), overall fatigue (35%), muscular pain in lower limbs (29%), anxiety (15%), skin problems (8%) and hearing problems (6%). These values are in alignment with other studies that assess WMSD prevalence in industry [17]. Similar to the most prevalent risks in European workers today from the ESENER [15] and EWCS [16] reports, a systematic review [4] found that ergonomic, psychosocial, and safety (in terms of injury and accidents) risks are most pertinent to the smart factory worker of the future. Since the most prevalent risks are ergonomic in nature (ESENER [15], systematic review [4]), and the majority of the most common health issues can be classified as WMSDs (EWCS [16]), it can be concluded that ergonomic risk and WMSDs are the most pressing factors affecting operator health; therefore, these interrelated issues are addressed in the thesis.

Fatigue-Failure Theory and Impact of WMSDs

Perhaps the term musculoskeletal disorders (MSDs) was best described by Lind *et al.* (2023) [18]: "MSDs is an umbrella term for injuries and illnesses of the locomotor apparatus (i.e., tendons, ligaments joints, nerves, vessels, and other supporting structures involved in locomotion)" and disorders acquired as a result of or advanced by work activities are referred to as WMSDs. MSDs and WMSDs related to repetitive motion, overuse and sustained stress can also be called cumulative trauma disorders which mainly affect soft tissues [19]. They are broadly divisible into two categories: traumatic (where WMSD is associated with an event or action) and idiopathic (where WMSD is brought about through gradual mechanical degradation and is influenced by confounding factors) - regardless, the cause is primarily biomechanical [20].

There are many different theories to explain the presence of MSDs, as discussed by Kumar (2002) [20], such as the *multivariate interaction theory* (injury is caused by a combination of biomechanical, psychosocial and individual differences), the *differential fatigue theory* (injury is caused by asymmetry and imbalance during tasks), the *cumulative load theory* (injury is caused by certain thresholds of load and repetition being met) and the *overexertion theory* (injury is caused by exertion exceeding the tolerance of the individual). All theories agree that the source of such disorders is biomechanical and, realistically, they are all at play to differing extents and interact with one another to cause an acute or cumulative injury [20]. The *fatigue failure theory* [21] and cumulative trauma theories [19], [22], account for these interactions and state that mid-air, repetitive tasks (even with low loads) [15], [16], [18], [19], [21], [23], [24], [25], [26], working with heavy loads [15], [19], [22], [25], sustained contractions [18], [22], [27], [28] and working in awkward postures [16], [18], [19], [29] increase ergonomic risk and lead to localised muscle fatigue [30], [31], [32], compounding in WMSDs over time, Figure 1. Manual handling tasks, defined as "any transporting or supporting of a load, by one or more workers, including lifting, putting down, pushing, pulling, carrying or moving of a load", are major contributors to such disorders [33], [34]. Such tasks are prevalent in industry contexts [35], thus contributing to a high prevalence of WMSDs in this field [17].

This occurs because when these biomechanical factors exceed an individual's ability and there is not adequate time for recovery [18], [19] the exposures cause residual strain, inflammation, and pain which in turn affect the tissue's ability to recover from and adapt to stresses [20]. More specifically, the exposures may cause muscles to fatigue at differing rates, resulting in altered kinetics and kinematics that are not optimal (such as redistributed loading, co-contraction and altered muscle synergies), especially when the loading is not proportional to the individual capabilities (i.e., *differential fatigue* and *overexertion* theories). This results in reduced ability to recover from and adapt to stresses. It is also important to consider the visco-elastic properties of many tissues in the locomotor apparatus which exhibit time-dependent deformation and may undergo permanent structural changes once stress thresholds are exceeded. Importantly, such thresholds are lowered over time as a result of reduced load-bearing capacity due to cumulative fatigue (i.e., *cumulative load* and *overexertion* theories). The exposures may also lead to microstructural damage to the locomotor apparatus, and even though biological tissues are capable of healing, complete tissue repair is not possible without sufficient rest and recovery, further elevating injury risk. When repeated over time, these conditions "set the stage for injury even if the stress does not rise extraordinarily" [20]. Unfortunately, many occupations require these movements, postures and loads for long durations or high intensity without sufficient rest time [18], resulting in a high incidence of WMSDs.

According to the Health and Safety Executive (HSE) in the UK [36], WMSDs typically begin with symptoms such as "aches and pains, tenderness, weakness, tingling, numbness, cramp, burning, redness and swelling" as well as "stiffness, pain or reduced movement in [the] joints" and overtime lead to conditions such as gorilla hand syndrome [37], trigger thumb [38], carpal tunnel syndrome [24], [25], [36], [38], tendonitis [24], [36], [38] and osteoarthritis [36]. As reported by the EWCS [16], WMSDs relating to the back and upper limbs are most common. A large proportion of employees (70%) reported engaging in work that entailed tiring or painful postures and 13% of these respondents experienced this work more than three quarters of the time [16]. Similarly, approximately 70% of respondents' work comprised of repetitive hand movements, and 31% of this was present in over three quarters of their work [16]. Women and older age groups suffer from WMSDs most often [39]. Workers in physically demanding industries such as construction, warehousing, agriculture, healthcare, and manufacturing are particularly susceptible to fatigue and WMSDs [15], [17], [24], [38], [40], [41], thus, the focus on WMSDs in the context of smart factories in the thesis. The prevention of WMSDs is the responsibility of many parties, including the employer, employee, ergonomists and occupational health professionals, regulatory bodies and unions. Responsibilities include training, workload management, reporting issues, research and developing solutions, compliance with and enforcement of regulations.

In terms of impact, WMSDs are a leading cause of workplace absences, disability, and economic burdens globally [15], [40], [42], [43]. People with WMSDs have poorer health outcomes, decreased quality of life, and WMSDs can lead to early retirement [40]. The cost of WMSDs, including direct costs for treatment and indirect costs due to productivity and absences, result in 2% of the gross domestic products (GDP) in Europe [3], [40], [44], and financial burdens due to medical costs are also present on an individual level [40]. Besides from costs, fatigue and WMSDs can have detrimental impacts on the worker with regard to physical and psychological wellbeing [40]; there are also impacts on the organisation in terms of reduced quality [45], [46] and productivity [47], [48], [49], [50], process interruptions [46], [51] and high staff turnover rates [49]. Fatigue also leads to increased mistakes [50], injuries [52], accidents [47] and negatively affects well-being [53].

It seems reasonable to expect that the growing trend of increased automation and use of ICT would lead to a reduction of manual activities and thus WMSDs, however this is not the case [54]. Mathiassen (2006) [55] discussed the state and trends in industry and the service sector, such as the focus on reducing time losses which leaves fewer tasks for workers to complete and fewer job rotation options, resulting in fewer opportunities for biomechanical variation and recovery [55]. The same can occur when temporary workers are hired during high production periods and are given simple tasks [55], [56]. This, combined with results from recent surveys indicating a high prevalence of WMSDs [15], [16], reviews stating that ergonomic risks are pertinent to smart factory workers in the future [4], and the extent of the negative impact of WMSDs on workers and organisations alike [40], highlight that WMSDs are a persistent, growing issue that must be curtailed.

The mechanistic relationship between ergonomic exposure, neuromuscular fatigue, altered load distribution, and cumulative tissue damage underscores the importance of monitoring fatigue as an early indicator of WMSD risk, and serves to benefit the interests the entire industrial ecosystem [4], [48]. This thesis addresses these challenges by focusing on the mitigation of physical and muscular fatigue, as well as ergonomic risks in factory/manufacturing contexts using Industry 4.0 and 5.0 technologies, which offer new opportunities to enhance workforce health and wellbeing. This aligns with the previously identified recommendation to prioritise the health of the operator [4] and the goals of Operator 4.0 [4] and Industry 5.0 [1], [3], [4], [6], [7], [8].

Research Landscape

While risk factors for WMSDs are well-established, it is important to understand the trends in research topics, funding and investment in the research landscape surrounding fatigue monitoring. The area has significantly evolved over the past decade as publications in this domain have surged, bibliometric analysis shows a year-on-year increase in publications addressing muscle or physical fatigue and ergonomic risk. Between 2014 and 2024, documents in English with the terms muscle or physical

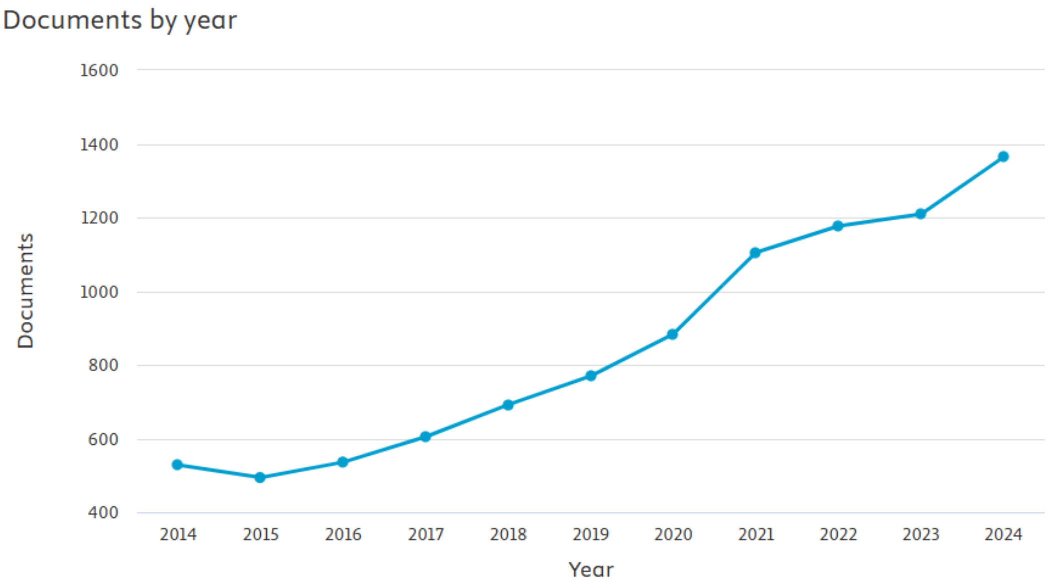

Figure 2: Number of documents per year in Scopus (as of 28/04/2025)

fatigue or ergonomic risk with monitoring, prediction, estimation or detection (and excluding keywords that relate to the fatigue of materials and fatigue in relation to the elderly and specific diseases) increased from 528 to 1364 per year (Figure 2). This growth is driven by advances in wearable technologies and data analytics, as notable keywords in the results were wearable sensors and wearable technology, surface electromyography (EMG), heart rate, biomechanics, endurance, questionnaires, algorithm, machine learning (ML), workload, muscle strength and workers.

This scientific momentum is mirrored in funding trends. Horizon Europe, among other initiatives, has substantially invested in research targeting occupational health. Projects that finished between 2022 and 2024 with budgets exceeding €4 million, such as those listed below highlight the EU's commitment to developing innovative preventive strategies. These investments underscore the socio-economic relevance of fatigue prediction systems in high-risk professions, especially for the smart factory.

- Smart glasses for multifacEted visual loss mitigation and chronic disEase prevention indicator for healthier, saFer, and more productive workplAce foR ageing population [57] (EU contribution ≈ €4 million).
- FlExible assembLy manufacturIng with human-robot Collaboration and digital twin modEls [58] (EU contribution ≈ €6.3 million).
- Smart environments for person-centered sustainable work and well-being [59] (EU contribution ≈ €4 million).

- Smart Working environments for all Ages [60] (EU contribution ≈ €4 million)
- Personalised Body Sensor Networks with Built-In Intelligence for Real-Time Risk Assessment and Coaching of Ageing workers, in all types of working and living environments [61] (EU contribution ≈ €4 million).
- Smart, Personalized and Adaptive ICT Solutions for Active, Healthy and Productive Ageing with enhanced Workability [62] (EU contribution ≈ €4 million).

1.2 Identified Gaps in the State-of-the-Art

A comprehensive review of existing literature (see Chapter 2) revealed several consistent limitations in current approaches to ergonomic risk, physical fatigue and WMSDs. These gaps are discussed in detail in 2.2.6 Identified Gaps in the State-of-the-Art but are summarised here to show the motivation for the research framework.

Despite an abundance of research in the field, there is a lack standardisation and generalisability. An array of measurement methods, such as, ergonomic risk assessments [63], [64], [65], [66], theoretical muscle models [30], [67], [68], [69], empirical endurance models (summarised in [70], [71]), subjective scales [72], [73], [74], etc., produce different outputs, each with its own limitations. This diversity of perspectives has led to poor comparability across studies, limited reproducibility, and inconsistent outcomes [3], [18], [75]. The lack of consensus in defining and quantifying fatigue, heterogeneous datasets, and limited real-world validation further constrain progress toward practical, generalisable solutions.

A number of reviews have highlighted the need for continuous, real-time systems capable of proactively mitigating WMSDs through wearable technologies aligned with Industry 4.0 and 5.0 developments [3], [4], [18], [76], [77], [78], [79]. However, persistent gaps remain. There is a lack of consideration of dynamic movements and varied arm configurations [3], [75], task generalisability while maintaining individualisation [70], [80], [81], or automated load input in such systems. From a user-centred standpoint, practical barriers such as comfort [75], [82], privacy [3], [18], [83], and data transparency [84], [85] also influence acceptance, leaving a gap between technological capability and workplace integration. In addition, while machine-learning methods show potential [3], [83], [86], there is a lack of explainability in classifier decisions [87], and there is a need for large, diverse datasets [76], [79] that have limited adoption in occupational contexts.

The present thesis addresses many of the aforementioned challenges through the development of a torque-based endurance modelling and task classification framework that enables proactive fatigue forecasting. Specific challenges (which are discussed in more detail in 1.3.2 Research Gaps Addressed and Novel Contributions) this work targets are the absence of: (i) consideration of dynamic arm movements and configurations; (ii) task-generalised predictive models; (iii) inclusion of individualised parameters and strength measurement; (iv) automated load input; (v) explainable task classification; and (vi) predictive forecasting methods for WMSD prevention. By integrating wearable sensors, task classification, and endurance modelling within an interpretable software application, the framework contributes toward methodological standardisation and practical translation of ergonomic monitoring in the smart factory workforce of the future.

1.3 Research Framework

Building on the background and gaps in the state-of-the-art, this section introduces the research hypothesis and objectives of the thesis. It outlines the overall structure and scope of the research and identifies specific research gaps that the thesis aims to address. These gaps highlight the limitations of current fatigue and ergonomic risk management and establish the need for the novel methods proposed in this thesis.

1.3.1 Research Hypothesis and Objectives

The prevalence of WMSDs and the indication that they are not declining reveal that current established workplace measures are not effective at reducing the pervasiveness of this issue. Additionally, these areas continue to attract substantial interest and ongoing investment, as reflected in recent bibliometric trends and European funding initiatives, Figure 2. In response to this, the thesis proposes a framework that leverages Industry 4.0 and 5.0 technologies and embodies the principles of the healthy operator, offering a more effective way to reduce WMSD risk and improve workplace health outcomes compared to existing interventions. The framework developed in this thesis presents a methodology for physical fatigue prediction using wearable sensor data from inertial measurement units (IMUs) and pressure insoles, accounting for both

Figure 3: Fatigue forecasting system consisting of IMUs, pressure insoles and custom application

individual and task-related parameters, Figure 3. It is hypothesised that an individualised, task-specific fatigue forecasting model, integrating motion monitoring with automated load input, will improve the accuracy and reliability of physical fatigue predictions compared to existing methods. Moreover, implementing these models in a wearable system with a graphical user interface (GUI) enables proactive fatigue forecasting, helping to mitigate ergonomic risks, reduce localised muscle fatigue, and lower the prevalence of WMSDs. The overarching research question is therefore: **Can a wearables-based system for physical fatigue prediction be developed that accounts for individual abilities and generalises across different tasks?**

To address this research question, the following objectives have been defined:

- Objective 1: To develop an individualised model for physical fatigue forecasting.
- Objective 2: To develop a model that accounts for task-related parameters during fatigue forecasting by continuously monitoring motion and by automating load input.
- Objective 3: To develop and test a physical fatigue forecasting system comprised of wearable sensors and a custom application implementing the individualised and task-specific models.

Objective 1 refers to the integration of individual parameters with a forecasting model. Thus far, the thesis has briefly explored how some interventions are more proactive than others, and for effective WMSD mitigation, forecasting approaches that allow timely intervention by producing predictions prior to the onset of fatigue are more impactful. This will be discussed in more detail in 2.1.2 Measurement and Prediction Methods. In this research work, endurance models that predict the time until fatigue are chosen as a proactive forecasting approach. These models already incorporate basic individual and task-specific parameters such as $Force_{max}$ and the external load, indicating a positive starting point to tackle this objective. However, there are many problems associated with these models, covered in detail in section 2.1.2 Measurement and Prediction Methods. The work carried out as part of Objective 1 aims to address the many limitations and concerns surrounding endurance models, including increased personalisation parameters to generate individualised endurance predictions. The model adopts a torque-based approach as opposed to a force-based approach which sees a change in the variable used to measure maximum strength, which was previously maximum force ($Force_{max}$) to now maximum torque ($Torque_{max}$). A novel approach to determine $Torque_{max}$ also aids in producing more individualised endurance predictions.

Objective 2 focuses on integrating the adjusted endurance model with wearable sensors to automate task-related inputs and contributing towards adaptability to different tasks. As mentioned in the thesis introduction, IMUs are commonly used for motion data tracking and pressure insoles present a lesser explored means of generating load data for fatigue and ergonomic risk applications as they are typically used to detect falls, awkward postures and activities in occupational studies. Task prediction via wearable sensors offers a way to achieve automated load input, as different tasks are associated with different components, loads and geometries. The torque-based model also sees the inclusion of new parameters that enable arm dynamics and therefore any upper body task to be accounted for, contributing to Objective 2. This, combined with automatic load input from pressure insoles means that the model can perform predictions for any upper extremity task that is performed.

Objective 3 aims to develop a physical fatigue forecasting framework and system that integrates the endurance model from the work on Objective 1 with the task-specific motion and load data from wearables from the work on Objective 2. This is facilitated by a custom application that enables the input of individual and task information and the display of endurance metrics and is validated during simulated industry tasks in a laboratory setting.

1.3.2 Research Gaps Addressed and Novel Contributions

While a detailed summary of the state-of-the-art methods that are used to address WMSDs is provided in the next chapter, this section details the novelty and specific gaps that are addressed with the proposed framework. This research addresses key gaps (Figure 4) in current physical fatigue prediction methods, including limited consideration of dynamic movements, insufficient individualisation, and lack of task-adaptive prediction. By integrating wearable sensors, torque-based endurance modelling, and automated task classification, the proposed framework lays the groundwork for proactive, real-time fatigue forecasting. Explainable elements enhance model interpretability, while implementation as a wearable application ensures practical deployment in occupational environments. Together, these contributions advance both methodological rigor and real-world applicability, providing a foundation for safer, ergonomically informed workplaces.

While disadvantages exist for wearable sensing technologies, they also present great opportunity for continuous worker monitoring and to create more proactive prediction methods of prevention WMSDs [3], [75], thus wearable sensors are utilised in the research work in the thesis. However, solely relying on objective metrics may present issues as the individuals' perception is also an important consideration. For this reason,

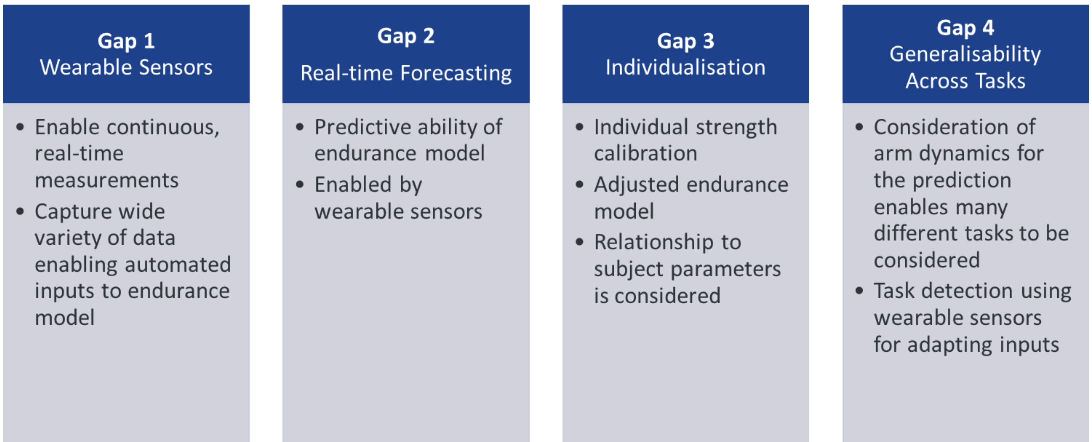

Figure 4: The key gaps identified and how the thesis addresses them

Table 1: Work to combat endurance modelling disadvantages in the research work described in the thesis

Problem	Solution	Section
Lack of standardised methods to measure maximum strength.	Developing a novel method to determine maximum strength.	3.1, 3.3
Lack of consideration of dynamic tasks.	Introducing dynamic parameters via the consideration of torque as opposed to force.	3.2, 3.3
Disagreement on presence of endurance limit.	Comparing models with and without an endurance limit (asymptote).	3.3
Lack of comparisons between models and inputs.	Comparing multiple models and inputs. Open-access publication of dataset.	3.3
Lack of generalisability of models.	Comparing existing models instead of developing a new model for this dataset. Open-access publication of dataset.	3.3, 5
Lack of generalisability to different tasks.	Consideration of dynamic parameters during complex, industry-type tasks. Open-access publication of data.	3.2, 3.3, 5
Variability in muscle group and posture.	All arm configurations are accounted for with the adjusted endurance model.	3.2, 3.3, 5
Lack of consensus on the influence of individual differences.	Inclusion of additional individual parameters. Performance of statistical analyses for correlation. Open-access publication of dataset.	3.2, 3.3, 5

a subjective questionnaire that enables continuous self-reported fatigue measurement without task interference is also used in the present work.

Many disadvantages of endurance models are described in section 2.1.2 Measurement and Prediction Methods, and the thesis contributes to mitigating for these disadvantages, see Table 1, highlighting the novelty in the work on endurance models in the thesis. No torque-based endurance model has previously been used to predict physical fatigue for loaded, dynamic manual handling tasks, underscoring a key, original contribution of this work. In addition to dealing with many limitations of endurance models (Table 1), the application of the torque-based approach aids in dealing with gaps in the field in Figure 4, further justifying the selection of this modelling methodology in the thesis. For example, alterations made to the endurance model in the process of this work sees the inclusion of additional individualised parameters into the endurance model for calculation of the predicted ET, such as arm segment lengths and masses. The integration of wearables with the adjusted endurance models enables these parameters to be considered on a continuous, dynamic basis, supporting future real-world deployment. The projected time to fatigue output presents proactive, predictive capabilities, and aligns with the goal of delivering a forecasting solution, which is a significant gap in the current literature. In addition, this output represents a move towards increased standardisation, allowing it to easily be compared to other work with the same output (time to fatigue). In terms of generalisability, which is a key concern relating to endurance models and fatigue in the literature, the system considers arm configuration for the prediction calculation (via wearable sensors and the modified endurance model for dynamic tasks), therefore predictions are specific to the movements of the task. Generalisability of the SAFE framework is taken a step further in the research work by the development of a task detection algorithm using pressure insoles that dynamically adapts the load and task-related endurance coefficients inputted to the endurance model based on the detected task type and alters the predictions by detecting activity/rest phases. These features underscore the significant contribution of the thesis work as they are required in real working environments where tasks change throughout a shift period.

Overall, the predictive capabilities of endurance modelling presents a promising approach for the research in the thesis, considering the Hajifar *et al*. (2021) [77] call for proactive, predictive approaches, especially when deployed with wearable sensors as this enables continuous monitoring. To date, endurance modelling has been tested using vision-based detection systems in human machine interface (HMI) research under unloaded conditions and for a 2 s static "dwell time", not for loaded manual handling tasks [37], [88]. Therefore, the use of wearable sensors with endurance modelling and task classification for manual handling applications presents a novel, objective and direct approach for predicting fatigue, allowing timely intervention, and thus the potential reduction of WMSDs.

In order to highlight the gaps addressed and novel contributions of the thesis research work, Table 2 compares the proposed system to current systems existing in commercial and research domains that pertain to upper body WMSD intervention using wearables in the context of manual handling tasks. While the next chapter explores the state-of-the-art in more detail, a comparison of the thesis system to systems that have been deployed in real-time or demonstrate strong potential for real-time implementation is a key starting point to establish the contributions of the present work. The beginning of the table lists commercial systems which are very basic in nature, typically consisting of one or two sensors, with the exception of the XSens

Table 2: Commercial and research systems integrating wearables for ergonomic risk or fatigue monitoring, detection or prediction of the upper body during manual handling activities,, including the present work.

Solution/ Author	**Types of sensors**	**Commercial or Research**	**Measurement/ Algorithm**	**Comments**	**Automatic load input?**	**Feedback?**
Kinetic Reflex [89]	IMU (1)	Commercial	Detects high risk bending, reaching and twisting, posture correction.	Worn on worker's belt.	No	Vibrotactile
SafeWork Sensor [90]	IMU (1)	Commercial	Detects awkward postures, posture correction.	Work vest with platform with analytics for workers, managers and safety leader.	No	Vibrotactile
Honeywell Bioharness [91]	PPG, temperature, IMU (1), GPS	Commercial	Fatigue monitoring using physiological indicators related to heart and breath rate, temperature, activity and posture in real-time as well as location.	Chest-worn device.	No	Visual
Ergo Live and Ergo Expert [92]	IMU (up to 17)	Commercial	Produces standardised ergonomic reporting based on posture and loads.	Wearable data inputted to simulation software (XSens and third party).	No	Visual
Vignais *et al.* (2013) [93]	IMU (7) and goniometer	Research	Produces standardised ergonomic reporting based on posture and loads (RULA), posture correction.	Assessed the upper body during MH tasks in industrial environment.	No	Visual (via AR) and Auditory
Peppoloni *et. al* (2016) [94]	IMU (3), EMG (3)	Research	Produces standardised ergonomic reporting based on posture and loads (RULA, SI), muscle effort and fatigue estimation.	Assessed the upper body during pick and place task.	No	No
Arroyave-Tobon and Osorio-Gomez (2017) [95]	Markerless MoCap	Research	Produces standardised ergonomic reporting based on posture and	Assessed the upper body during "air-modelling" manufacturing	No	Visual (via AR)

Solution/ Author	Types of sensors	Commercial or Research	Measurement/ Algorithm	Comments	Automatic load input?	Feedback?
			loads (RULA), posture correction.	tasks, i.e. the components exist in a virtual space.		
Mengoni *et al.* (2018) [96]	Markerless MoCap	Research	Produces standardised ergonomic reporting based on posture and loads (RULA), posture correction.	Assessed the upper body during manufacturing tasks and uses AR for object recognition.	No	Visual
Lins *et al.* (2018) [97]	IMU (15),	Research	Produces standardised ergonomic reporting based on posture and loads (OWAS), posture correction.	Experiment evaluated the optimal vibrotactile pulse length and repetition while standing.	No	Vibrotactile
Kim *et al.* (2018) [98]	IMU (17), EMG (5), Force plate	Research	Estimates joint overloading based on load and posture.	Full body assessment during manufacturing tasks.	Yes	Vibrotactile
Yu *et al.* (2019) [99]	Markerless MoCap, PI	Research	Estimates current joint capabilities and fatigue index using a muscle model.	Full body assessment during construction tasks.	No	No
Manghisi *et al.* (2020) [100]	Markerless MoCap	Research	Produces standardised ergonomic reporting based on posture and loads (RULA), posture correction.	Assessed the upper body during manufacturing tasks and training.	No	Auditory and Vibrotactile
Cerqueira *et al.* (2020) [101]	IMU (4)	Research	Produces standardised ergonomic reporting based on posture and loads (RULA, LUBA), posture correction.	Smart garment for assessment of the upper body during assembly tasks completed with a cobot.	No	Vibrotactile and Visual
Giannini *et al.* (2020) [102]	IMU (17), EMG (2)	Research	Produces standardised ergonomic reporting based on posture and loads (ISO 11228, NIOSH 94-110, Snook and Ciriello method,	Smart garment for assessment of the full body during MH tasks.	No	Visual

Solution/ Author	Types of sensors	Commercial or Research	Measurement/ Algorithm	Comments	Automatic load input?	Feedback?
			REBA, SI), fatigue monitoring via EMG.			
Battini *et al.* (2022) [80]	IMU (17 for the body, 14 for the hands and fingers), activity tracker (ECG, heart rate, temperature, respiration, microphone)	Research	Produces standardised ergonomic reporting based on posture and loads (OWAS, RULA, REBA, PERA), posture correction, fatigue monitoring via physiological indicators.	Assessed the body during manufacturing tasks and training. Cables are used to connect the hand/finger IMUs.	No	Visual
Trkov et al. (2022) [103]	Accelerometer (3), PI	Research	Continuously outputs NIOSH score based on detected task	Full body assessment during MH tasks. ML used to detect tasks and load, with NIOSH lifting index compute from classified task and pre-recorded inputs.	Yes	No
O'Sullivan *et al.* (Present work)	IMU (3), PI	Research	Fatigue prediction using torque-based endurance modelling.	Upper body assessment during MH tasks. Explainable ML used to classify tasks and continuous, endurance metrics are generated.	Yes	Visual

Abbreviations: IMU = Inertial measurement unit; PPG = Photoplethysmography; RULA = Rapid upper body limb assessment; AR = Augmented reality; MoCap = Motion capture; OWAS = Ovako working posture analysing system; REBA = Rapid entire body assessment; PERA = Postural ergonomic risk assessment; EMG = Electromyography; LUBA = Loading on the Upper Body Assessment; ISO = International Standards Organisation; NIOSH = National Institute for Occupational Safety and Health; SI = Strain index; MH = Manual handling; PI = Pressure insoles; Cobot = Collaborative robot; ML = Machine learning.

systems (Ergo Live, Ergo Expert) [92] that integrate motion data into simulation software. The basic commercial systems [89], [90], [91] focus on posture correction, however, the algorithmic specifics or scientific basis of the thresholds are not apparent due to the proprietary nature of the technology and lack of publicly available information. The Honeywell Bioharness [91] also assesses fatigue by analysing physiological indicators. The XSens systems [92] produce standard ergonomic reporting, there are multiple assessments that output non-standardised risk scores indicating the level of ergonomic risk. There are also custom systems in research that provide this reporting, which account for the majority of solutions (10/17) in Table 2 [80], [93], [94], [95], [96], [97], [100], [101], [102], [103]. Ergonomic risk scores are not a proactive means of preventing WMSDs in the context of continuous operator monitoring, as high risk needs to be exhibited over an extended period of time before intervention can take place but this method can be effective when combined with feedback for posture correction [104].

Other algorithms used in wearable systems in research include joint loading estimation [98], muscle fatigue estimation [99], and the present work, which adopts a torque-based endurance model for a predictive solution. This work is the only solution in Table 2 that proactively forecasts the presence of physical fatigue based on kinetic upper extremity data from wearable sensors using an endurance model, allowing timely intervention prior to fatigue onset.

Regarding external load, a key component of fatigue and ergonomic risk calculation, some studies [93], [96] assumed the components were below a load of 2 kg which does not impact the risk score in those cases, while other studies [100], [101] don't mention how load data is inputted to the ergonomic assessments, but it can be assumed that the load is assumed to be less than 2 kg, or loads are manually inputted, similar to Battini *et al.* (2022) [80] and Giannini *et al.* (2020) [102]. This is a significant disadvantage as it is not possible to ascertain the risk score without manual input, which interferes with the operator's work. In other words, while many of the solutions listed in Table 2 operate in real-time, not all of them are producing outputs in real-time without manual input, in which case they are simply streaming sensor data without meaningful, actionable outputs. In a real work environment, operators' tasks are continuously changing throughout a work period, many tasks comprise of multiple subtasks, and pausing work to input component parameters is not a realistic solution.

Vignais *et al.* (2013) [93] recommended that task adaptability must be integrated into such systems via object recognition, this can enable component parameters such as load to be automatically generated without manual input, but a wearable system other than the present work has not implemented this to date. Other task- or object-related work in Table 2 includes Mengoni *et al.* (2018) [96] who employs object recognition with augmented reality (AR), not to automatically input load, but to check the assembly progress and provide instructions to aid the operator throughout the task. Activity recognition takes place in the system by Giannini *et al*. (2020) [102] but for the purpose of determining the optimal risk assessment for the task being performed, since different risk assessments are generally better suited to a particular set of activities. Kim *et al.* (2018) [98] used force plates to obtain load and centre of pressure (CoP), however, force plates are not suitable for a real working environment as force plates do not allow for mobility. Trkov *et al.* (2022) [103] is the only system, aside from the present work, with the potential to consider load in real-time as tasks change throughout a work shift. That study involved manually calculating National Institute for Occupational Safety and Health (NIOSH) lifting index scores for each task and task classification was used to identify the current risk score due to its association with that task. Similarly, the present work uses task classification, but to generate the required external load input (and other component parameters) using pressure insoles, since specific components are associated with each task, negating the need for manual input and allowing for mobility during tasks. Explainable ML methods are used in the present work as this is an important factor in the context of occupational H&S. Moreover, the endurance modelling in the present work predicts endurance metrics for any upper arm positioning based on arm dynamics, unlike the Trkov *et al.* (2022) [103] set-up which remains limited to predefined tasks for which risk assessment has already taken place and is constrained by the typical limitations of ergonomic risk assessments.

The use of feedback to correct and train posture to result in lower ergonomic risk is a common practice, with visual, including the present work, (8/16) [80], [92], [93], [95], [96], [101], [102] and vibrotactile (6/16) [89], [90], [97], [98], [100], [101] methods most commonly used. AR has been used for feedback purposes [93], [95], where operators can simultaneously interact with the real and virtual worlds, the latter of which acts as a visual feedback mechanism. However, in the case of Arroyave-Tobon and Osorio-Gomez (2017) [95], AR was also used for "air-modelling", where the ergonomics of assembling virtual objects was examined. The system in the thesis uses a GUI to provide visual feedback to users to display warnings and current fatigue status on a continuous basis.

A key novelty of the research work presented in the thesis is that it provides a unified framework for WMSD prevention. The most common approaches can be broadly divided into operator monitoring or ergonomic risk assessment, as is evident in Table 2 and will be made clear in the next chapter, Chapter 2 State-of-the-Art in Workplace Fatigue, Wearables, and WMSD Prevention. Therefore, this work represents a convergence of these two originally separate approaches to WMSD prevention into a unified framework with potentially multiple uses, the relevancy of which depend on the user. Firstly, for the worker, visual feedback via the application can inform the individual when to take a break, and fatiguing movements or postures can be easily identified which may help with self-directed training to avoid awkward positions in future work. The system can aid with prioritising operator health in the smart factory of the future by the addressing the persistent ergonomic risks that workers face on a daily basis while being adaptable to different tasks without interference. For the manager and ergonomist professional, the identification of fatiguing movements can inform the delivery of training programs to workers, assessments of tasks and workstations can be carried out, and the impact of ergonomic improvements to tasks and workstations can be tracked. In addition, the effect of tasks on different individuals can be monitored in order to contribute to individualised scheduling, work targets and task rotations. The wide range of potential uses and relevancy to multiple user types denotes a meaningful contribution to the field.

While Balkin *et al.* (2011) [105] only considered physiological indicators as a means of online operator monitoring, the research work described in the thesis combines online operator monitoring with a biomechanical model to provide fatigue forecasting information to users, enabling action to be taken to prevent fatigue thus WMSDs prior to its onset. This represents a more proactive, streamlined approach to upper body WMSD prevention for manual handling tasks using Industry 4.0 and 5.0 technologies than existing commercial and research solutions in Table 2.

Finally, the pipeline proposed in this thesis introduces a novel method for fatigue prediction that integrates wearable sensing, biomechanical modelling, and task classification to dynamically predict endurance during manual handling tasks. Unlike existing approaches that rely on manual input during offline analysis and mostly ergonomic risk assessments, this system computes shoulder joint-level endurance metrics using IMU-derived kinematics, pressure insole-derived task classification, and subject-specific predictions via endurance modelling. By integrating joint angle and task computation with biomechanical endurance predictions tailored to the individual's body dimensions and movement patterns, the SAFE framework offers a unique and practical solution for proactive injury prevention in physically demanding professions that is applicable to numerous dynamic tasks. This integrated approach marks a significant step forward in bridging the gap between lab-based biomechanical analysis and field-deployable real-time ergonomic monitoring tools.

1.3.3 Thesis Structure and Scope

Figure 5 outlines the structure of the thesis. Chapter 2 provides a more detailed exploration of the state-of-the-art that informed the thesis hypothesis under investigation. The research work undertaken can be divided into endurance modelling, task classification and demonstration of the fatigue forecasting framework and are described in Chapters 3 to 5 respectively (based on peer reviewed publications), each with subchapters associated with peer-reviewed publications describing the experimental work. Implications and limitations of the results and future work are deliberated in the thesis discussion in Chapter 6.

The structure of the thesis follows section 3, 'Thesis Based on Publication', of the UCC Thesis Policy document[1]. The research conducted during this PhD has been disseminated through peer-reviewed publications and conference presentations and was recognised with the Wrixon Research Excellence Award (a prestigious Tyndall student award) in November 2024. The relevant publications are linked to thesis chapters in Appendix 1, with DOIs listed in Appendix 2 and author contributions specified using CRediT author statements in Appendix 3. Additional publications outside the scope of the thesis, published during the PhD, are listed in Appendix 4. Technical chapters correspond to three conference papers in tier-one conference proceedings, three journal papers, one of which is under review at the time of thesis

[1] https://www.ucc.ie/en/academicgov/policies/gs-policies/phd_regs/

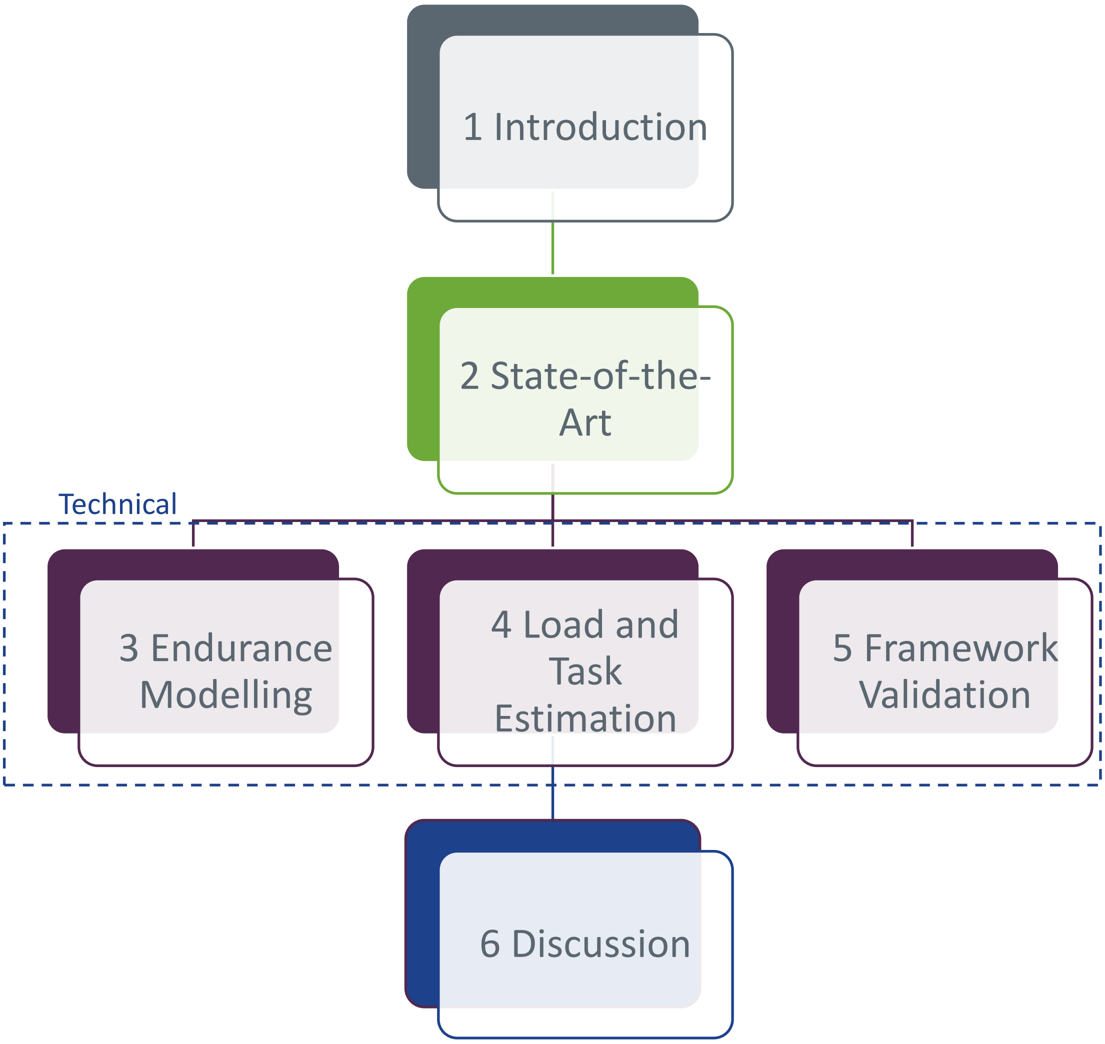

Figure 5: Thesis structure

submissions, and two open-access datasets [106], [107]. Minor changes to the published research work, as permitted by the UCC Thesis Policy, are noted at the beginning of each thesis section. Such changes typically include additional analyses, extended literature overview, or omission of repetitive background information that is presented in Chapters 1 and 2 of the thesis.

This research adopts a quantitative approach to achieve the project objectives and utilises both subjective and objective measurement methods. Anthropometrics, wearable sensor data, time until fatigue failure, maximum voluntary contraction (MVC) force, subjective questionnaires and task specific data are collected throughout

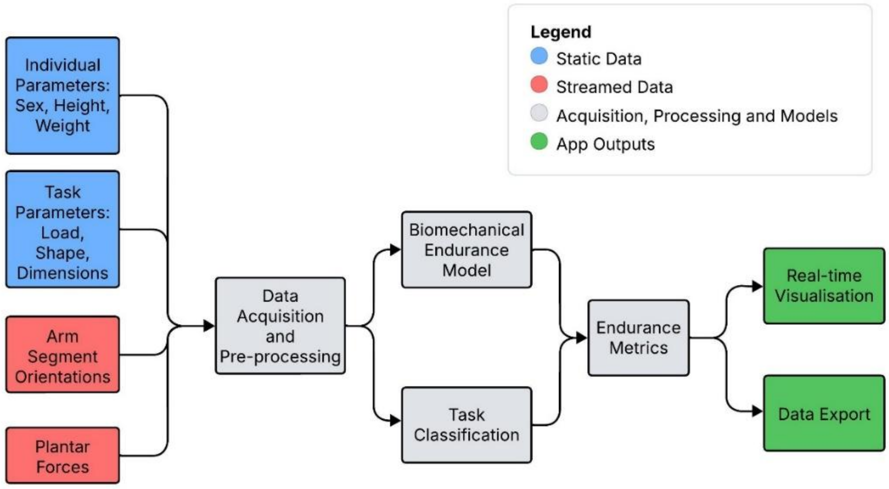

Figure 6: SAFE framework overview.

the research work described in the thesis. While subjective scales can be used as a qualitative approach, the ordinal scales that describe the participants' exertion is used for quantitative analysis in this research. Statistical and ML modelling methods are used to address the research question. This approach entails rigorous data collection and analysis, enabling a holistic view of physical fatigue that accounts for diverse tasks, individual differences and confounding factors.

Figure 6 shows the proposed SAFE framework. The inputs to the endurance model include manually inputted individual and task-related parameters (blue boxes) and streamed data for measuring plantar pressure and arm segment orientations (red boxes). These data are acquired and processed (grey boxes) using the application to calculate torque and $Torque_{max}$ (inputs to the endurance model), the former changes over time for dynamic tasks and the latter remains static for each load level (%MVC). Task classification is used to tune the endurance prediction based on activity status and determine the task-related parameters and task-related endurance coefficients that are inputted to the endurance model. Thus, endurance metrics are calculated using the models developed in the course of the thesis (grey boxes), data are visualised and exported using the application (green boxes).

The experiments conducted, variables measured and outputs that are associated with each objective and thesis chapter are described and summarised in Appendix 5.The first endurance modelling technical chapter, 3.1 Estimation of Maximum Shoulder and Elbow Joint Torque Based on Demographics and Anthropometrics, describes the development of regression models that use individual demographic and anthropometric data to estimate $Torque_{max}$ for the shoulder and elbow joints that can inputted to the endurance model. Instead of manual maximum strength measurement using a dynamometer being required from individuals when the system is being used in an occupational setting (which can be time consuming and requires specialised equipment and thus are not suitable for deployment in a real working environment), this model requires quick and easy to measure inputs while also providing individualised values. To achieve this, the first experiment gathered anthropometrics, demographics and $Torque_{max}$ data from participants, followed by multiple linear regression to generate the models. However, the regression models were compared to other methods of calculating $Torque_{max}$ in section 3.3 Improving Dynamic Endurance Time Predictions for Shoulder Fatigue: A Comparative Evaluation and it was found that a different novel approach more accurately predicted endurance in an individualised, cheap manner that does not required specialised equipment such as a dynamometer. The novel method, using a 'calibration task', required joint angles, individual data (anthropometrics and experimental ET) and external load parameters to determine the maximum strength inputs.

Continuing with Objectives 1 and 2, a second experiment was conducted to analyse how the torque-based model, which was originally designed for unloaded conditions in HMI research, predicted endurance for manual lifting tasks, described in section 3.2 Validation of Endurance Model for Manual Tasks. Lifting tasks were performed until fatigue (validated using maximum holding time and a subjective questionnaire) at 30 to 45% of the individuals' maximum producible force in a static and dynamic manner, both of which were conducted with the dominant hand and the latter of which was also conducted with both hands. The accuracy of the predictions from the endurance model suggested that more refinements to the model were required, and alternative means of generating the inputs should be considered. This led to the third experiment described in 3.3 Improving Dynamic Endurance Time Predictions for Shoulder Fatigue: A Comparative Evaluation in which fatiguing shoulder elevation tasks were conducted at two standardised intensities (25% and 45%) using torque inputs. Time to fatigue was recorded and additional wearable sensors collected physiological data while motion capture was used to generate joint angles, and the load was manually inputted to the model. Different models using the torque-based approach and different methods of generating $Torque_{max}$ (including the regression models from the first experiment) were compared to see which approach minimised the error. The relationship of individual parameters to experimental and predicted ET were also assessed. This work showed that the regression models generated from the first experiment did not minimise the prediction error, instead a new novel method to determine $Torque_{max}$ proved to reduce the errors significantly. Torque and experimental time to fatigue during the calibration task are required to determine $Torque_{max}$ at each load level. An important aspect of this work is that fatigue data were not used to generate a new model in the thesis but were compared to existing models in an effort to enhance model generalisability as many researchers generate a new model that suit their own data.

The data from this experiment were also used in a preliminary analysis for Objective 2 which is described in section 4.1 Evaluating Wearable Sensor Technologies for Predicting Shoulder Endurance, where data from different sensors were used to generate endurance predictions. Three different combinations of manual inputs and sensors, moving from a non-wearable lab-based approach to a wearable approach, were used to generate the joint angles and load inputs. Comparing these methods enabled assessment of how sensor type and data source affect model accuracy. Method 1 served as the non-wearable lab-based reference ("best-case") scenario, while Methods 2 and 3 represented increasingly wearable but potentially less precise measurement configurations. This comparison quantifies the trade-off between model performance and measurement feasibility, offering insight into the potential for real-world implementation of the approach. The results showed that near real-time prediction was feasible but only if efforts were made to counteract drift and bias associated with pressure insoles as this alone could not be used to determine the external load. This research work aided in determining the method of inputting the task-related parameters to the endurance model, i.e. task classification.

To achieve Objective 2 and to deal with the pressure insole issues established in section 4.1 Evaluating Wearable Sensor Technologies for Predicting Shoulder Endurance, a new experiment was conducted which saw participants wear pressure insoles and carry out industry-type tasks. Explainable ML methods were used to predict the task type based on force data alone (most studies utilise IMU sensors in the pressure insoles), detailed in section 4.2 AI-based Task Classification Using Pressure Insoles for Occupational Safety. The explainable approach employed in this analysis, using random forest (RF) and Shapley Additive explanation (SHAP), which is the explainability analysis used, denotes a move away from the ‘black box’ approach that is usually associated with ML techniques which is of utmost importance as transparency in decision making is crucial in occupational H&S issues. Through these results, it was evident that task classification could be used to determine what tasks are being performed so that (i) task-related external load parameters (e.g., mass and dimensions) can be automatically inputted to the model, (ii) task-related endurance coefficients can be applied to adjust predictions based on task type, and (iii) drift and bias regarding acquired force values to determine external load mass can be avoided.

To achieve Objective 3 and validate the SAFE framework, the final experiment, described in Chapter 5, involved subjects wearing a custom system composing of IMUs, pressure insoles and application while performing industry-type tasks. Tasks that exhibited high and low ergonomic risk were performed and subjective and objective exertion data were gathered to validate the subjects’ state. Workstation set-ups were assessed using ergonomic risk assessments to validate the level of ergonomic improvements. Repeated measures correlation and Wilcoxon signed-rank tests found that the endurance metrics calculated using the SAFE framework successfully distinguished low- from high-risk tasks and were highly correlated with time and subjective fatigue scores. Task-dependent endurance coefficients were calculated to tune endurance predictions based on self-reported exertion scores. This work contributed to the finalised SAFE framework shown in Figure 6.

Ethical approval is a key methodological consideration since the studies required the participation of human subjects, and was granted by the university’s ethics committee, the clinical research ethics committee of the cork teaching hospitals (CREC), under the reference numbers ECM 4 (p) 6/7/2021 and ECM 3 (i) 09/08/2022 and ECM 4 (h) 22/10/2024 & ECM 5 (3) 12/11/2024 & ECM 3 (xxxx) 11/03/2025. All participants were healthy individuals with no neurological or cardiovascular disorders and provided written, informed consent. They were recruited through word of mouth and UCC email cascades. Approved documentation included the participant information leaflet which was provided to participants regarding the purpose of the research, equipment used, and any potential risks associated with the research, and the consent form and data protection form which outlines the consent of the individual to participate and for their data to be used in accordance with general data protection regulations (GDPR).

Chapter 2 State-of-the-Art in Workplace Fatigue, Wearables, and WMSD Prevention

This chapter reviews existing research and developments relevant to fatigue assessment, ergonomics, and wearable technologies. Section 2.1 outlines fundamental concepts of muscle fatigue, including its definitions, classifications, underlying physiological mechanisms, and current measurement and intervention methods. Section 2.2 examines the broader landscape of related studies, focusing on key reviews in ergonomics, wearable systems, and fatigue management, with particular emphasis on upper-body applications. Finally, Section 2.3 synthesises the insights drawn from these works to identify current research gaps and inform the direction of the thesis.

2.1. Understanding and Assessing Fatigue in the Workplace

This section provides an overview of how fatigue is defined, classified, and influenced by various factors and what occurs on a physiological level during localised muscle fatigue. Then, current measurement methods and intervention strategies are reviewed which highlight the need for improved solutions.

2.1.1 Fatigue: Definitions, Classifications, and Contributing Factors

As discussed in section 1.1.2 Ergonomic Risk, Fatigue and WMSDs , high ergonomic risk leads to localised muscle fatigue in the short term and can lead to WMSDs overtime. The thesis focuses on fatigue prediction to proactively mitigate upper body WMSDs for manufacturing smart factory workers. Therefore, an overview of fatigue, and more specifically muscle and physical fatigue, is provided in this section prior to outlining measurement methods.

Definition and Complexity of Fatigue

Fatigue is a complex phenomenon with "physical, neuromuscular, psychological, mental and emotional aspects" [23], [27], [108] and has many accepted definitions [27], [83], [109], [110]. It has been described as a "hypothetical construct" linking causal factors to safety-related outcomes [47], a "non-specific symptom" that takes the form of exhaustion and reduced capacity for voluntary tasks [111], a reduction in muscle force-generating capacity [112], and even a “biological drive for recuperative rest” [47]. These varied descriptions underscore the ambiguity surrounding fatigue, often explicitly acknowledged through terms such as “non-specific.” Beyond WMSDs, fatigue is also associated with cardiovascular diseases, cancer, gastrointestinal disorders, and obesity [83].

Figure 7 shows that contributing factors (*work*, *lifestyle*, *individual* [40]) that have been found to affect fatigue (*sleepiness*, *mental fatigue*, *muscle fatigue* and *physical fatigue* [47]), and safe recovery is possible once the decision is made to rest. However, if the operator decides, or is required, to continue working (green decision point in Figure 7), this can lead to impaired performance capabilities in the short term (and cause accidents [47], mistakes [50] and injuries [52]), and over time lead to WMSDs [35] and the associated knock-on effects of absences, disability and financial burdens [15], [40], [42], [43], Figure 7.

Contributing and Confounding Factors

Confounding factors associated with work include loading and recovery time and the ratio between them [19], [27], heavy loads [40], task complexity and variability versus mental stimulation and monotony [47], i.e. ergonomic risk. Factors relating to lifestyle choices include smoking and high body mass index (BMI) [40]; and individual

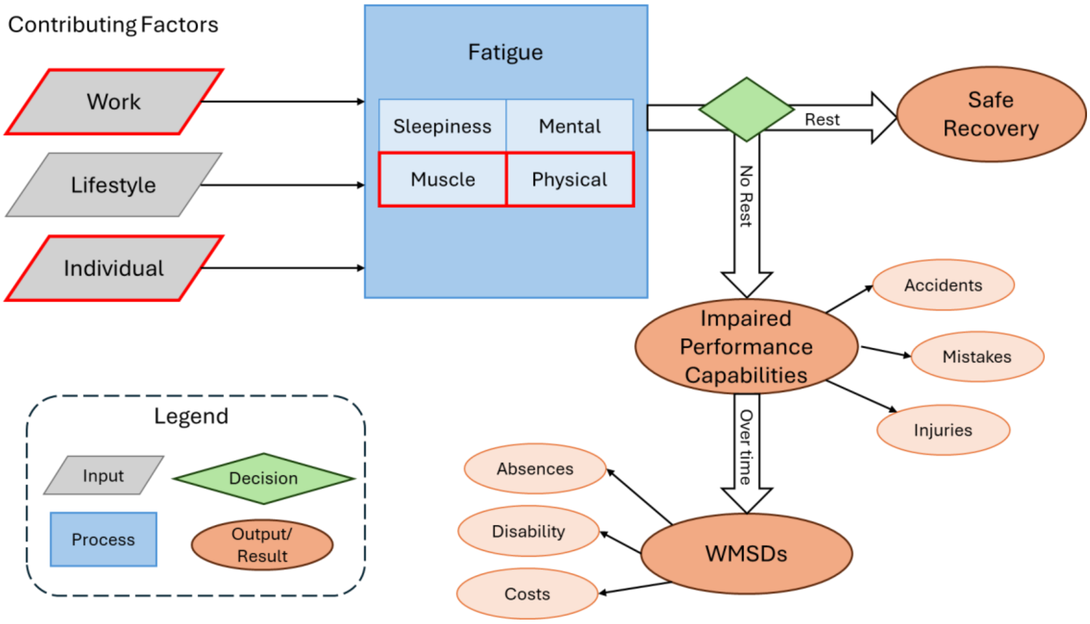

Figure 7: The relationship between contributing factors, fatigue and WMSDs. Factors and fatigue types highlighted in red are addressed in the present work.

differences relate to gender, age, general health [40], and sleep homeostasis [47], [109]. The array of contributing factors results in difficulties quantifying, predicting, and thus, preventing fatigue. For instance, while a worker's fatigue may stem mainly from physical exertion, factors such as demographics, emotions, and time of day also influence its onset. Moreover, studies show that tasks are perceived as more physically demanding when psychological demands are higher and control over the work environment is lower [82]. These examples illustrate the multifactorial nature of fatigue and the difficulty in isolating specific causes or predicting distinct fatigue types due to the interrelation of contributing variables.

Categorisations of Fatigue

Fatigue is often classified as acute or chronic, depending on whether rest can restore performance [83], [111]. It may also be grouped into central, peripheral, and psychological types [111], which dynamically interact and make isolating single causes difficult. However, in occupational H&S research, alternative frameworks are commonly applied. Fatigue categorisations considered in the present work include the four types of fatigue identified by Williamson *et al.* (2011) [47] in the context of occupational H&S: *sleepiness*, *mental fatigue, physical fatigue,* and *muscle fatigue*, Figure 7.

Mental fatigue is defined as "a general sensation of weariness, a disinclination for any effort, feelings of inhibition and impaired mental performance, and reduced efficiency and alertness" [113] and a strong focus of mental fatigue and sleepiness is present in the context of transport occupations and shift work in the literature [47], [86]. On the other hand, physical fatigue is defined as a decline in overall performance caused by physical exertion [114] and muscle fatigue is a decrease in the ability to produce maximum force ($Force_{max}$) [111], or the required or expected force [115]. While mental fatigue and sleepiness can be present in shift work and excessive workload scenarios in manufacturing occupations, muscle and physical fatigue are strongly associated with manufacturing occupations and manual handling in general.

The physical, repetitive and complex nature of manual handling tasks in industry contexts considered in the thesis encourages a shift in focus to physical and muscle fatigue in an acute context and are thus highlighted in red in Figure 7. Furthermore, since it was found that "upper limbs are more prone to fatigue than lower limbs" [110] which aligns with the increased prevalence of WMSDs of the upper extremities compared to the lower extremities (EWCS [16]), justifying the focus on the upper extremities in the thesis. Work and individual factors are highlighted in Figure 7 as these contributing factors are addressed in the course of the thesis.

Ambiguous and varied definitions of fatigue, alternative methods of categorising fatigue (acute/chronic; central/peripheral/psychological; sleepiness/mental/physical/muscle) and the array of confounding factors result in a lack of standardised and generalised approaches in the field (discussed in section 2.1.2 Measurement and Prediction Methods).

Physiological Mechanisms of Muscle Fatigue

From a physiological perspective, the decreased ability to produce force during muscle fatigue is caused by any failures upstream of the *cross-bridge*, which can constitute metabolic or vascular systems, or ionic components [111], [116]. Muscular contraction occurs via a process called *cross-bridge cycling*, where myosin and actin molecules attach within the muscle cell using chemical energy from the breakdown of adenosine triphosphate (ATP), and the onset of muscle fatigue can be attributed to failures in the systems that contribute to the functioning of this process or the accumulation of muscle by-products, for example lactic acid and phosphates [111], [116], [117]. The mechanisms that cause fatigue can vary with sex due to anatomical and physiological differences [118].

Recovery occurs when these metabolites are removed via blood flow through the muscle [110], [116]. In addition, Frey Law and Avin (2010) [71] discussed how endurance time (ET), the period of time a task can be maintained until fatigue, depends on "variations in fibre type …, motor unit distribution/activation …, neural activation …, task specificity …, and/or absolute force/muscle cross-sectional area". Within a muscle, a single motor neuron activates the muscle fibres in its motor unit and Ma *et al.* (2015) [119] described the two types of motor units: slow-twitch (type I) and fast-twitch (type II). Fast-twitch motor units are capable of producing a higher force more rapidly than slow-twitch fibres but are less resistant to fatigue [99], [119]. Due to this, force and torque generation capacity decrease more rapidly under higher workloads and full recovery after fatigue can only take place until all motor units are recovered [99], [119]. Intensity, duration, environmental conditions and the type of contraction also influence muscle fatigue [23], [120]. More specifically on contraction type, blood flow begins to be restricted (also called ischemia) at approximately 20% of MVC force by intramuscular pressure [121], causing a reduced oxygen supply, a build-up of metabolites and pH decrease, and thus muscle fatigue. Meanwhile, dynamic contractions cause a pumping effect of blood flow, increasing oxygen supply to the muscle and the rate of metabolite removal [120], thus a lower rate of fatigue progression is typically observed during dynamic compared to isometric tasks. In practice, MVC force, measured using a dynamometer, is often treated interchangeably with $Force_{max}$ and is widely used as the reference for normalisation (i.e., %MVC), as is the case in the thesis. Strictly speaking, however, MVC represents the highest force a subject can voluntarily produce, whereas the true maximal force capacity, $Force_{max}$, of the muscle is typically greater and can only be estimated through methods such as electrical stimulation or biomechanical modelling. Visser and van Dieen (2006) [28] proposed mechanisms through which upper-extremity muscle disorders can arise from a biochemical and physiological point of view, which include impaired blood flow, calcium ion accumulation, and overloading of type I motor units, among others.

Summary and Relevance to Thesis

To conclude, fatigue is a complex occurrence with multiple interrelated contributing factors. Muscle and physical fatigue are the focus of the thesis and the endurance modelling work in Chapters 3 and 5 incorporates both individual demographics and task characteristics to account for these interrelated factors. Analyses are also performed to uncover relationships between fatigue and these factors. The overall aim of the system utilising the SAFE framework in the thesis is to intervene on workers at the correct moment to help them decide if they should rest or continue working (see the green decision point in Figure 7) and thereby reduce the negative impacts of fatigue both in the short term (due to performance impairment) and long term (due to WMSDs), Figure 7. Different methods of measuring fatigue and ergonomic risk focus on different contributing factors to varying extents and will be explored next.

2.1.2 Measurement and Prediction Methods

This section provides an overview of the various methods used to assess and predict ergonomic risk and fatigue. It first outlines the general categories of available approaches, followed by a summary of how these methods have been integrated into computational and sensor-based techniques in recent years. Finally, it evaluates the strengths and limitations of existing measurement and prediction methods within this context.

Overview of Methods

Yu *et al.* (2019) [99] categorised physical fatigue measurement into subjective and objective methods, and mentioned there are self-report, observational and direct methods of collecting data in these categories, Figure 8. These methods are presently used in workplaces and in research to measure or predict fatigue and ergonomic risk. Figure 8 summarises the subcategories of physical fatigue measurement, where *subjective* is subjective questionnaires and *objective* includes *muscle development models*, *physiological indicators* and *biomechanical* methods (which includes *ergonomic risk assessments* and *endurance models*). Each of these methods used to assess fatigue and ergonomic risk to reduce the risks of WMSDs are summarised and compared in Table 3 (key examples of each method are discussed in more detail in Appendix 6).

The biomechanical category includes methods that assign high-risk scores for awkward postures or set a threshold that cannot be exceeded, as well as posture- and exerted force-based methods that consider both postures and loads, such as, ergonomic

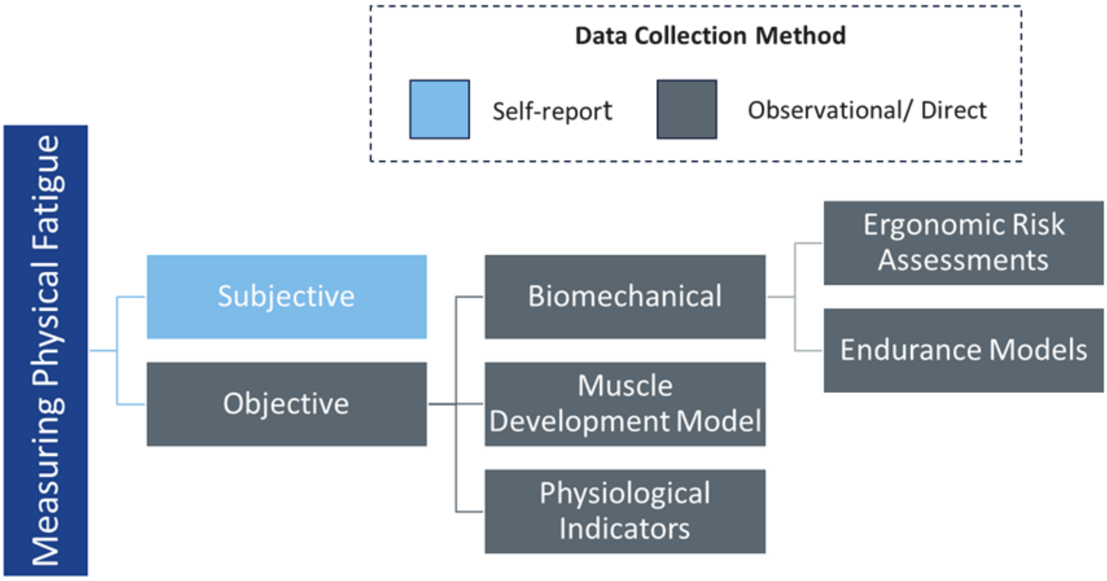

Figure 8: Methods to physical fatigue measurement and the associated data collection methods according to Yu et al. (2019), each of which are discussed in this section.

Table 3: Summary and comparison of measurement methods

Method	Description	Pros	Cons	Method Type		Data Collection Type			Examples
				Sub.	Obj.	S	O	D	
Subjective Questionnaires	Worker perceptions of fatigue, pain, psychosocial factors, task difficulty, effort and complexity.	• Quick, easy and cheap to deploy • Often used as gold-standard fatigue reference measure • Some have been correlated to physiological indicators (not all) • Effective for low load levels	• Subjective – affected by dishonesty, emotions, motivation, individual pain perception, situational factors • Ability to self-detect fatigue is impeded while in a fatigued state • Can interfere with tasks • Difficult to achieve precise values • Inconsistent classification of fatigue levels	X		X			Borg Rate of Perceived Exertion (RPE) and Borg CR10 scales [72], Need for Recovery Scale [122], NASA task load index (TLX) [73], Karolinska Sleepiness Scale (KSS) [74]
Ergonomic Risk Assessments	Assessing ergonomic risk due to task parameters such as load, repetition, asymmetry and duration.	• Can be used to assess the ergonomics of different workstations, tools and individuals carrying out tasks • Scores can account for individual percentiles	• Semi-subjective • Affected by between- and within-observer variance • Intervention takes place after high-risk movements are performed (potentially for extended periods) • Assesses several static snapshots, not entire task • Gross categorisations which are often inconsistent with other assessments • Anthropometry often not considered	X	X		X	X[2]	NIOSH Lifting Equation [65], Rapid Entire Body Assessment (REBA) [64], Rapid Upper Limb Assessment (RULA) [63], Threshold Limit Value (TLV) by the ACGIH for Lifting and Hand Activity [66]

[2] Ergonomic risk assessments can be considered a direct approach when direct sensing technologies (either wearables, simulation or camera-based systems) are used to generate risk scores.

Method	Description	Pros	Cons	Method Type		Data Collection Type			Examples
				Sub.	Obj.	S	O	D	
Endurance Models	Predicting time to physical fatigue using empirical models.	• Models for different tasks, range of joint angles, individual factors, principle joint or muscle group • Proactive method as it predicts ET, allowing for intervention to take place prior to the onset of fatigue	• Not applicable to dynamic tasks as they assume constant force, isometric conditions • Models often developed using unskilled workers • Endurance limit[3] is contested • Lack of generalisability to different tasks, range of joint angles • Affected by individual variability, especially at low %MVCs • Influence of individual differences is unclear • Lack of standardisation regarding the methods that are used to calculate $Force_{max}$ and $Torque_{max}$		X			X[4]	Rohmert's MET model [123], summaries provided by Frey-Law and Avin (2010) [71], El ahrache (2006) [70], Consumed endurance [37], New improved consumed endurance model [88]
Muscle Models	Estimating fatigue using fatigue development mechanisms.	• Theoretically developed based on physiological fatigue mechanisms • Consider differences between muscle groups, postures, recovery, diffusion rate of muscle by-products	• Often lacks experimental validation • Often difficult for real-time deployment due to presence of multiple complex parameters • Struggle to account for submaximal contractions • Estimations are not adjusted based on joint configurations.		X			X	Models based on the cross-bridge [30], relationships between muscle force-pH and accumulation of muscle by-products [69], [110], motor unit principles [68], [108], [124], [125]

[3] Endurance limit is the relative force that can be produced without fatigue

[4] Endurance models can be considered a direct approach when direct sensing technologies (either wearables, simulation or camera-based systems) are used to generate predictions. This has only been done in human machine interface research in unloaded conditions, not for manual handling tasks under dynamic, loaded conditions.

Method	Description	Pros	Cons	Method Type		Data Collection Type			Examples
				Sub.	Obj.	S	O	D	
		• Further research required for prediction capabilities • Can be applicable to dynamic conditions	• Lack of standardisation regarding the methods that are used to calculate $Force_{max}$ and $Torque_{max}$						
Physiological Indicators	Detecting physiological changes, such as cardiovascular and electromyographic, due to fatigue.	• Can measure physiological response in real-time • Wearables for physiological measurement are compact, portable, wireless	• Can be uncomfortable, especially with direct skin attachment • Impacted by lack of defined fatigue thresholds (regarding subjective scores and physiological thresholds) • Impacted by noise, bias, drift					X	Subjective scores mapped to physiological signals [86], [126], [127], [128], [129], [130], [131].

Abbreviations: Sub. = Subjective; Obj. Objective; S = Self-report; O = Observational; D = Direct; ACGIH = American Conference of Governmental Industrial Hygienists.

risk assessments. Biomechanical methods (i.e. ergonomic risk assessments and endurance models, Figure 8 and Table 3) also include models that measure physical fatigue due to workload in terms of force or torque at a joint or muscle level through simulation software such as 3DSSPP [132], OpenSim [133] and AnyBody Modelling System [134]. Endurance models are included in this category as these models estimate the time to fatigue based on force or torque parameters. Some muscle development models also consider force and torque, but they have a distinct category within objective measurement, Figure 8, as they model physiological changes that occur during fatigue.

Additionally, Figure 8 details the data collection methods associated with each category, where self-report methods are associated with the subjective category and observational and direct data collection methods are associated with objective physical fatigue measurement. Self-report entails diary entries, interviews and, most frequently, subjective questionnaires [135], [136], where the opinion of the worker is taken into account regarding their exertion level or the complexity or difficulty level of a task. This method is cost-effective and relatively easy to deploy to a large cohort but can be time consuming and distracting to the task at hand.

Observational methods involve an ergonomics professional reviewing video footage or shadowing a worker while completing their tasks, usually to generate risk scores associated with postures or loads via ergonomic risk assessments. They are not considered to be entirely objective as results are influenced by the ability of the assessor [99], [137], and can lack repeatability, accuracy and reliability [18], [138]. This method is time consuming since multiple days of footage are often required to understand the risk associated with all tasks in a particular job [99]. While ergonomic risk assessments are still referred to as an observational data collection method [139], direct approaches using wearable sensor technologies are increasingly being used in research, using tools such as computer vision, IMUs or optical motion capture (MoCap).

Direct methods involve using goniometers (angle measurement), dynamometers (force measurement), tape measures, distance measuring wheels, stop watches and wearable sensors to monitor risks and workers' state. Wearable sensors can measure aspects of physical work such as intensity (load magnitude, extent of non-neutral postures), repetition (frequency of force exertions and motions), and duration (length of activity, sustained non-neutral postures) [140], [141] as these have been found to affect H&S, and physical and mental health [41]. Wearables are also used to measure the posture of workers for input to muscle models and ergonomic risk assessments in research. In addition, wearables are used to measure physiological indicators which are related to fatigue directly, such as increased heart rate measured using photoplethysmography (PPG) or measuring increased sweat using galvanic skin response (GSR) or electrodermal activity (EDA). Simulation programmes are considered an observational approach by some authors [139] and a direct approach by others [99], and direct measurements from cameras and wearables can be combined with simulation programmes that integrate muscle models or ergonomic risk assessments.

Methods of measuring fatigue are often used in conjunction with one another, for example, a subjective questionnaire can be used to gain insight into an individual's perception during a fatiguing task or act as a validation tool for the presence or absence of fatigue where fatigue monitoring/estimation is taking place through physiological indicators, endurance or muscle models [86], [142]. This marks the introduction of the *fatigue reference measure* which is a significant component to any fatigue study, where the state of the individual is ascertained prior to the fatiguing task, and it verifies that the task did in fact induce fatigue and some methods can be used to identify the point at which fatigue occurs, and is typically done using a subjective questionnaire [68], [86], although EMG [120] and PPG [143] have also been used.

Computational and Sensor-Based Methods

In the pursuit of more effective strategies to evaluate and mitigate WMSDs, technology-driven methods have become increasingly valuable. Two key approaches in this domain are wearable sensor technologies and computational simulations. Simulations allow for the modelling of ergonomic scenarios, enabling researchers to predict injury risks and assess intervention strategies without direct human testing. Meanwhile, wearable sensors provide objective data on workers' movements, postures, and physiological responses, offering insights into biomechanical strain and potential risk factors.

In ergonomic simulation tools, human body models are generated and the model's activities are simulated, resulting in ergonomic evaluation indices [136]. Lowe *et al.* (2019) found that biomechanical modelling through simulation software was the fifth most used ergonomic assessment tool. Examples of such software include Siemens Jack [144], BoB [145], RAMSIS [146], and 3DSSPP [132], and they calculate parameters such as spinal compression and shear forces, forces, torques and cumulative parameters. These tools are suitable for planning and use in early task and workstation design phase, however, they are not suitable for real-time [147], and they require high experience in 3D modelling and the included ergonomic evaluation indices can be limited [136].

According to Lind *et al.* (2023) [18], wearables can be referred to as both devices or systems as they can consist of many sensors (to detect a physical input) that make up an instrument (to measure or manipulate variables), and many instruments can make a device (electronic or mechanical system that performs tasks) and a system is a set of devices or instruments. This section uncovers the fundamental features of wearable technologies and the opportunities they present, how they can be applied in the field, and the most common wearables in the field.

Wearable sensors are a direct method of data collection and have been used for physiological monitoring or integrated with ergonomic risk assessments or muscle fatigue models [138], [148]. Wearable sensors negate the disadvantages of observational methods in terms of repeatability and observer differences, they are small, portable, compact, and relatively cheap they can easily be worn by an individual while they are operating in a working environment [75], [80], [138], also, they are suitable for continuous, long-term monitoring [86]. The non-invasive aspect of the devices also aids in protecting a user's privacy [126] compared to methods such as blood lactate monitoring, and wireless connectivity facilitate timely interventions without interference during work activities [3], [75], [138]. Wearables are not dependent on the location of the individual as is the case with other imaging tools, such as computer vision, but is dependent on the placement of the sensor on the body of the operator [41]. These features mean that wearables are suitable candidates for use in fatigue and ergonomic risk management in industry environments for worker wellbeing improvement, WMSD reduction and increased efficiency [126], [137], however they are also prone to problems such as noise, magnetic interference, incorrect placement, repeatability issues, risk of moving/dislodging the sensor if a vigorous movement is involved [75], [110]. Other important considerations include the fact they need to be charged [99] and the desired metric needs to be greater than the noise of the signal which can occur due to motion artefacts [41].

Wearables can be used to monitor an individual's movements and physiological state as well as assessing the effectiveness of WMSD prevention measures, such as assistive devices or systems developed for automated ergonomic risk, or new H&S protocols [18], [148]. In research, they can enable collaborative robots (cobots) to more effectively match an operator's movements or state [10], [149] and help with training [10], [18] or task allocation [150]. Dornelles *et al.* (2022) [10] systematically reviewed Industry 4.0 technologies related to workers in manufacturing (for example, virtual reality, digital twin, environment and machine sensors, etc.) and only wearable devices were found to relate to monitoring health and ergonomics of workers, which is aligned with the goal of the thesis.

Balkin *et al.* (2011) [105] identified the manner in which wearable technology can be utilised for work H&S in occupational environments. Firstly, *fitness for duty* detects the alertness of an individual prior to beginning their workday. Secondly, *online operator monitoring* takes place throughout an entire work period and attempts to use *physiological indicators* to detect the onset of fatigue. Finally, *performance monitoring* with wearable sensors can identify if the rate of work or output has decreased, it can measure the accuracy of movements to detect tiredness and lack of concentration, which may denote mental or physical fatigue. It must be noted that if a failure is found using performance monitoring methods, fatigue has already occurred, rendering it too late for preventative measures to be put in place. Balkin *et al.* (2011) [105], did not include ergonomic risk tools, endurance models, or muscle-development models in these classifications, although they have been used in conjunction with one another in research (described in more detail later in the thesis) and the SAFE framework achieves online operator monitoring with predictive endurance modelling.

The five ergonomic modelling frameworks of Hajifar *et al.* (2021) [77] were reordered from least to most proactive in [3]: *descriptive modelling* (identifying associations between variables and outcomes), *explanatory modelling* (identifying one or more factors that lead to or produce an outcome), *cross-sectional predictive modelling* (using statistical or machine learning models to predict an outcome based on independent variables), *real-time monitoring* (detecting statistically significant changes in measured outcomes), and *forecasting* (predicting future values of a dependent variable). Forecasting is considered the most proactive, as it enables timely interventions by leveraging data from sensors and wearable technologies.

Rather surprisingly, Lowe *et al.* (2019) [139] noted no difference in the use of direct measurement methods, including goniometers, dynamometers and wearable sensors (namely EMG, optical and non-optical MoCap), between their 2019 survey and an almost identical survey by Dempsey *et al.* (2005) [151]. This slow uptake may be attributed to organisational structures (which are discussed further in the thesis discussion) or to factors assessed in a 2018 survey [152], also assessing the views of ergonomists. The researchers believed that slow uptake of wearables was affected by "employee data privacy and compliance, sensor durability, information validity and efficacy" [75]. Regardless, there is a growing trend in the use of wearables in ergonomic interventions in current research [137] and they are set to play a large role in occupational H&S in the future [10]. Additionally, the discussion details how uptake can be improved with a device deploying the framework presented in the thesis in terms of simplified calibration and increased comfort by using a minimal number of sensors, exploring who should have access to user data, getting feedback from workers, among many other methods.

A systematic review by Martins *et al.* (2021) [86] explored wearables used for fatigue monitoring with ML approaches, and the main inputs for physical and muscle fatigue were motion (using optical MoCap technology and IMUs), muscle activity data from EMG, heart and breath rate features from PPG and electrocardiogram (ECG) sensors, GSR from on-skin electrodes, and skin temperature from temperature sensors. Reviews by Lim and D'Souza (2020) [75] and Stefana *et al.* (2021) [137] found that pressure insoles are also used in ergonomic studies. IMU, MoCap, EMG, PPG, GSR, and pressure insole sensors are now briefly discussed and shown in Figure 9.

Inertial sensors include accelerometers, which range from uniaxial to triaxial and measure linear acceleration, and gyroscopes which measure angular velocity, and IMUs which include both a triaxial accelerometer, gyroscope, and triaxial magnetometer [75]. IMUs use both an accelerometer and a gyroscope to measure 3D rotations, and the accelerometer can be used to deal with the limitations of gyroscope data (which suffer from drift) and vice-versa, as gyroscope data are used to correct orientation errors from accelerometer caused by gravity [75]. Magnetometers measure magnetic fields and the magnetometer in an IMU enables the sensor's orientation in terms of earth's geomagnetic field to be found, although it can be affected by local magnetic field disturbances. IMUs are considered a non-optical method of motion capture [153].

In the context of reducing ergonomic risk and fatigue, IMUs provide data on the rate of movement and an indirect estimation of joint angles, although there is a lack of standardised methods using such sensors for joint angle estimation [41], [75]. A narrative review by Lim and D'Souza (2020) [75] note their use in real work settings is not common but conclude that inertial sensing is a "viable tool for online biomechanical exposure assessment and real-time feedback towards proactively identifying and mitigating the risk of work-relevant MSDs".

MoCap refers to optical systems being used to convert real movements into digital data, generally in combination with markers placed on bony prominences of the body [153]. Markers can be active (reflective) or passive (infrared LEDs), but optical MoCap does not necessarily need to include markers, for example, computer vision-based methods. Optical MoCap is considered the gold-standard for motion analysis and different analyses or biomechanical software packages can be used to generate biomechanical statistics from MoCap data to validate motion-related features generated from IMU [75]. In terms of analysing movements during physical fatigue and ergonomic risk in real work environments, MoCap faces difficulties regarding dependence on the location of the individual [147] and the markers attached to clothing or skin may interfere with work to a greater extent than other wearable devices such as IMU which feature fewer attachments.

EMG measures muscle activity, primarily due to changes in calcium ions during cross-bridge cycling during contraction [41]. Surface EMG, henceforth referred to as EMG, is non-invasive and enables researchers to study the onset of fatigue by means of analysing the physiological and biochemical changes in the lead up to failure [120], and EMG-related features have shown correlation to the Rapid Upper Limb Assessment (RULA, [63]) ergonomic risk assessment [154] and Borg [37], [155],

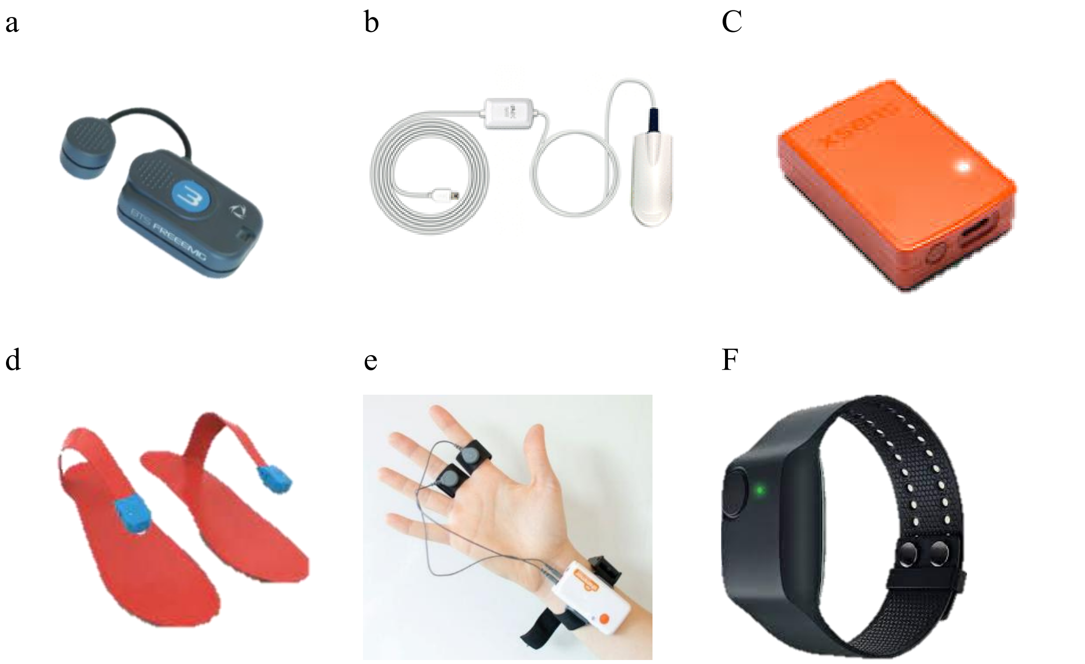

Figure 9: Most commonly used wearable sensors in the field, (a) electromyohraphy (EMG), (b) photoplethysmography (PPG), (c) inertial measurement units (IMU), (d) pressure insoles, (e) electrodermal activity (EDA) or galvanic skin response (GSR), (f) Empatica smart watch

especially at higher loads [23], [156]. The use of EMG as an objective fatigue reference measure bypasses the pitfalls presented by subjective questionnaires, such as influence of emotional state and motivation on scores, and some researchers view it as the gold-standard [127], but EMG is not without limitation. No generalised standard exists for muscle fatigue detection via EMG [120], [157], there is no consensus on the indicators to use for specific tasks [120], [157], and some indicators are not valid at low levels of exertion [37]. EMG poses issues in terms of repeatability due to placement, cross-talk [37], [138], [157], differing anatomies (such as high BMI), and increased muscle temperature during the onset of fatigue [148], [158]. It is not suitable for long-term monitoring [127], for example throughout a work shift, and is often viewed as a semi-invasive sensor as it requires direct attachment to the skin.

PPG is an optical technique to measure changes in blood volume and features from PPG sensors, such as heart rate, heart rate variability, and respiration rate, have been used to detect both physical and mental fatigue [86]. Although the accuracy of this sensor is sensitive to motion, skin colour and ambient lighting. GSR, also called EDA, refers to measuring the electrical conductance of the skin which can change when sweat is produced from glands as a result of emotional or psychological factors. Features from temporal and frequency spectrums of GSR data have been used to predict fatigue and stress, and they have been placed on neck, shoulders, hands and fingers [86]. Pressure insoles are specialised shoe inserts embedded with sensors to measure the distribution and intensity of pressure across the foot, they can be used to estimate total ground reaction forces and the CoP of ambulation. In terms of fatigue and ergonomic risk management, pressure insoles provide valuable data regarding movement, posture, coordination and activity classification [137], [159].

In the thesis, data from IMUs and pressure insoles were used to generate the required inputs to the fatigue prediction models relating to kinematics, task and load, and in line with minimising the number of sensors (for comfort and suitability real-time applications in the future), additional sensors such as EMG, GSR and PPG were not included. MoCap was used in experiments to validate the IMU-derived joint angles.

Evaluation of Measurement and Prediction Methods

It was mentioned that "[a]mbiguous and varied definitions of fatigue, alternative methods of categorising fatigue… and the array of confounding factors result in a lack of standardised and generalised approaches in the field" and the diverse range of fatigue and ergonomic risk measurement methods explored in this section demonstrate this. The overview of methods in this section is important to outline the diverse landscape of approaches used in the field, along with advantages and disadvantages. It provides a solid basis from which to justify the chosen methodology in the thesis which, as mentioned, utilises an endurance modelling approach due to its predictive capabilities, and extensive work is completed to address the disadvantages of endurance models mentioned earlier.

In this section, it was shown that different methods of measurement produce different outputs and this can result in difficulties comparing the accuracy and effectiveness of alternative approaches in the field; subjective questionnaire scores can represent exertion, difficulty, fatigue or task complexity level on scales of varying ranges, ergonomic risk assessment scores do not consider fatigue *per se* and generate values associated with particular postures, loads, frequencies and other individualisation or task considerations, endurance models output predicted ET, while muscle development models and methods based on physiological indictors often output an estimated fatigue level, subjective questionnaire score, or MEF. In addition, the goal can differ greatly between studies, for example, some focus on detecting fatigue so that the worker can be notified to rest or adjust their posture, while others focus on adjusting tasks, targets, tools or the environment in such a way that exertion levels are reduced, and the information can also be used for worker selection [75].

Muscle models are theoretically developed from a physiological perspective, while endurance models primarily adopt a mechanical approach, incorporating factors such as force and $Force_{max}$. Endurance models are derived empirically and have been tested in real world scenarios, although they are only valid for the specific conditions under which they were developed [110]. Furthermore, endurance models output ET predictions which is valuable since it can be considered a forecasting approach that predicts fatigue prior to its onset, enabling timely intervention to take place, which is more effective for WMSD prevention than less proactive approaches that detect or estimate the current fatigue level or MEF [3], [77]. The predictive capabilities of endurance models is a key reason for utilising this approach in the thesis.

Endurance models and some muscle models utilise $Force_{max}$ or $Torque_{max}$ information to determine the strength of the individual. However, there is a lack of standardisation regarding the methods that are used to calculate this input. One endurance model [37] calculated $Torque_{max}$ using one $Force_{max}$ value for males and another for females taken from $Force_{max}$ tables [160]. One muscle model [68] used a $Torque_{max}$ model based on gender and elbow and shoulder joint angles [161]. An endurance model designed using subject data [162] found MVC force using $Force_{max}$ values from a dynamometer, and models that included arm length and weight [161]. Chaffin provided guidelines for consistent strength measurement using force meters [163], and some studies used their own measured MVC values for inclusion in their models or to validate recovery or fatigue [27], [88], [119], but pushing directions varied and did not always align with the direction of movement during the task performed in the study. In addition, they did not always mention enough details for replication and did not refer to specific guidelines, such as Chaffin *et al.* (1975) [163]. Thus, the lack of a standardise methods for generating this important variable is assessed in the thesis.

There are other methods of measuring fatigue such as analysing blood lactate levels at prescribed intervals [120] and blood oxygen levels [164], using performance related measures with neuro-behavioural tasks that intermittently test abilities like reaction time [86], [109], detecting behavioural-based methods via yawning and eye closures [86], measuring the change in maximum producible force or torque at prescribed intervals [119], [165], [166], [167] or simply observing the participant and recording the time to which the task position can no longer be maintained [71], [120]. While they are often easily standardised, these methods only “detect” fatigue after it has occurred meaning timely intervention is not enabled and they significantly interfere with the work being performed. Neuro-behavioural tasks and behavioural-based methods also experience these disadvantages while focussing on mental fatigue, and the blood lactate approach is invasive.

Studies using other measurement methods outside endurance modelling will continue to be discussed throughout the thesis because other methods (namely questionnaires and ergonomic risk assessments) are used as fatigue reference measures, and the studies provide valuable insights in terms of placement and processing of wearables, experimental protocols, and analysis techniques. The methods discussed in this section provides a basis to discuss the implementation of WMSD prevention strategies in current workplaces (next section) and the literature (2.2 Literature Review).

2.1.3 Current Fatigue and WMSD Interventions

In this section, the policies, standards and systems in place to assuage WMSDs in occupational settings today are discussed. It is important to understand the context in which the proposed system will operate and the policies and standards it will be subject to. Interventions to reduce ergonomic risk, fatigue and WMSDs are implemented in the form of legislation, ergonomic interventions, international standards organisation (ISO) standards, guidelines, best practices and health promotion [40]. Standards are influenced by tables of maximum allowable weights [168] and ergonomic risk assessments [139], [151] and endurance models [162]. However, there is disagreement regarding the generalisability and reliability of these standards. According to some researchers [42], [138], [162], [169], [170], ISO standards should be used with caution. While ISO standards are voluntary, this section will also look at mandatory policies in place for WMSD prevention. In addition, many commercially available wearable sensor systems integrate such standards and perform ergonomic risk assessments or monitoring physiological indicators. Table 4 provides an overview of these interventions, including mandatory policies, ISO/EN standards, and commercial

Table 4: Summary and comparison of current interventions

Intervention Method	**Description**	**Examples**	**Mandatory?**	**Comment**
Occupational H&S Policies	European directives outline how employers are required to address risks and integrate ergonomics and human factors into workplace; these are translated into policies in member states which recommend specific tools.	MAC [171], ART [172], RAPP [173][5]	Yes	European directives are vague and don't recommend specific tools, and the scientific basis for tools recommended by UK and Ireland H&S bodies is not provided. H&S bodies enforce these regulations and provide information to employers regarding risk management.
ISO and EN Standards	Standards that define principles, risk assessment methods, and design recommendations to minimize physical strain and reduce the risk of WMSDs.	ISO 11226 recommends the OWAS [174], RULA [63], REBA [64]; ISO 11228-1 recommends NIOSH Lifting Equation [65]; ISO 1228-2 recommends the Snook and Ciriello tables [168]; and ISO 11228-3 recommends the OCRA [175].	No	No transparency provided on how the MH ISO standards were developed, scientific basis for the standards is not clear. ISO standards influence EN and member state standards and mandatory policies. Lack of attention given by the scientific community to the ISO standards.
Commercial Systems	Wearable systems that are used to assist workers, or monitor workers' postures or physiological parameters, oftentimes providing real-time alarms to alert when rest or posture changes are required.	Exoskeletons [176], [177], [178], [179], Wearable systems [89], [90], [91], [92].	No	Many devices operate in real-time to improve ergonomics or assist workers carrying out MH tasks. No guidance provided to employers from H&S governing bodies regarding recommended and tested products.

Abbreviations: MAC = Manual handling assessment chart; ART = Assessment of repetitive tasks of the upper limbs; RAPP = Risk assessment of pushing and pulling; H&S = Health and safety ; ISO = International Standards Organisation; EN = European norm standards; WMSDs = Work-related musculoskeletal disorders; OWAS = Ovako working posture analysing system; RULA = Rapid upper limb assessment; REBA = Rapid entire body assessment; NIOSH = National Institute for Occupational Safety and Health; OCRA = Concise index for the assessment of exposure to repetitive hand movements of the upper limbs; MH = Manual handling.

[5] These tools are recommended by the H&S governing bodies in Ireland and the UK that align with the EU directive for occupational H&S

Table 5: Current ergonomic tools used in occupational settings.

Product	Description	Examples	Standard	Sensor/ Mechanism	Comment
Pen and Paper, Software Tools	Ergonomic risk assessments completed using observational data collection methods, final risk scores are calculated using a template using pen and paper or software tools.	Paper templates, excel worksheets, or programmes that help to calculate scores based on observations.	Ergonomic risk assessments.	None.	Most commonly used method for completion of observational ergonomic risk assessments [139].
Simulation Tools	Simulates workstation parameters and generates ergonomic risk assessment scores, force or torques using human body models.	Siemens Jack [170] (Figure 10a), BoB [178], RAMSIS [179], and 3DSSPP [107].	Ergonomic risk scores, spinal compression, shear forces.	None, IMU, MoCap or EMG.	Not suitable for real-time, typically used in early task design [147], available ergonomic indices can be limited [136]. Wearable sensor data can be integrated into simulations for post-task analysis.
Mobile Applications	Wide variety of application, can be used as a software tool to perform ergonomic risk assessments, or for distribution of training information, or to connect sensors and monitor workers in real-time and provide warnings based on different measurement approaches, for example, endurance modelling, muscle models or physiological monitoring.	Ergodroid (software tool for ergonomic risk assessments, Figure 10b) [180], Apecs: Body Posture Evaluation (markerless posture estimation) [181].	Ergonomic risk assessments.	None.	Use is relatively low as it is in the early adoption phase, but has high potential for impact [139], especially for integration of endurance models, muscle models physiological monitoring through direct data collection means.

Product	Description	Examples	Standard	Sensor/ Mechanism	Comment
Commercial Exoskeletons	Transfer load from the upper body to the legs, in some cases using a purely mechanical system that operates by means of pulleys and cables. This can help to reduce strain and fatigue and switch between tasks.	Skelex 360 from Skelex, (Figure 10c) [176], AirFrame by Levitate Technologies (Figure 10d) [177], SuitX by Ottobock (Figure 10e) [178], Noonee Chairless Chair (Figure 10f) [179]	None	Spring-loaded mechanism with pulleys and cables (Skelex, AirFrame, SuitX,), Mechanical locking and load-bearing frame	Battery-less systems that focus on the super-strength worker, not necessarily health prioritisation. Very expensive, for example Skelex 360 costs €2995, Chairless Chair costs €2190.
Commercial Wearable Sensor Systems	Sensor-based devices that monitor posture, movement, and muscle activity in real time to detect risky motions and provide feedback or alerts to reduce the risk of musculoskeletal injuries.	Kinetic Reflex (Figure 10g) [89]	Not publicly available, likely uses a posture threshold limit	IMU (around the belt).	Often operate in real-time to alert operators regarding dangerous postures (except forXSens Ergo) which allow for proactive WMSD management. Many systems based on ISO standards, the scientific basis of which are unclear [169], [170]. Ergo Expert allows for integration to third party simulation software and the input of custom models. Wearable systems, such as EMG, IMU and MoCap, can be used by ergonomists. Battery life, trust issues with AI, lack of consideration of force are limitations.
		SafeWork Sensor by StrongArm (Figure 10h) [90]	Not publicly available, likely uses a posture threshold limit	IMU (vest).	
		Honeywell Bioharness (Figure 10i) [91]	Not publicly available, monitors fatigue using kinetic and physiological sensing	PPG, temperature, IMU, GPS (worn on chest).	
		Xsens Ergo [92] (Figure 10j,k)	RULA [63], REBA [64], UNE 1005-4	IMU (up to 17 for full body).	
		Xsens Ergo Live [92] (Figure 10j,k)	DIN, EN and NIOSH standards		
		Xsens Ergo Expert [92] (Figure 10j,k)	DIN (German), EN (European) and NIOSH standards		

Abbreviations: IMU = Inertial measurement units; MoCap = Motion capture; EMG= Electromyography; WMSD = Work-related musculoskeletal disorder; IMU = Inertial measurement units; RULA = Rapid upper limb assessment; REBA = Rapid entire body assessment; DIN = German norm; EN = European norm; NIOSH = National Institute for Occupational Safety and Health, AI = Artificial intelligence.

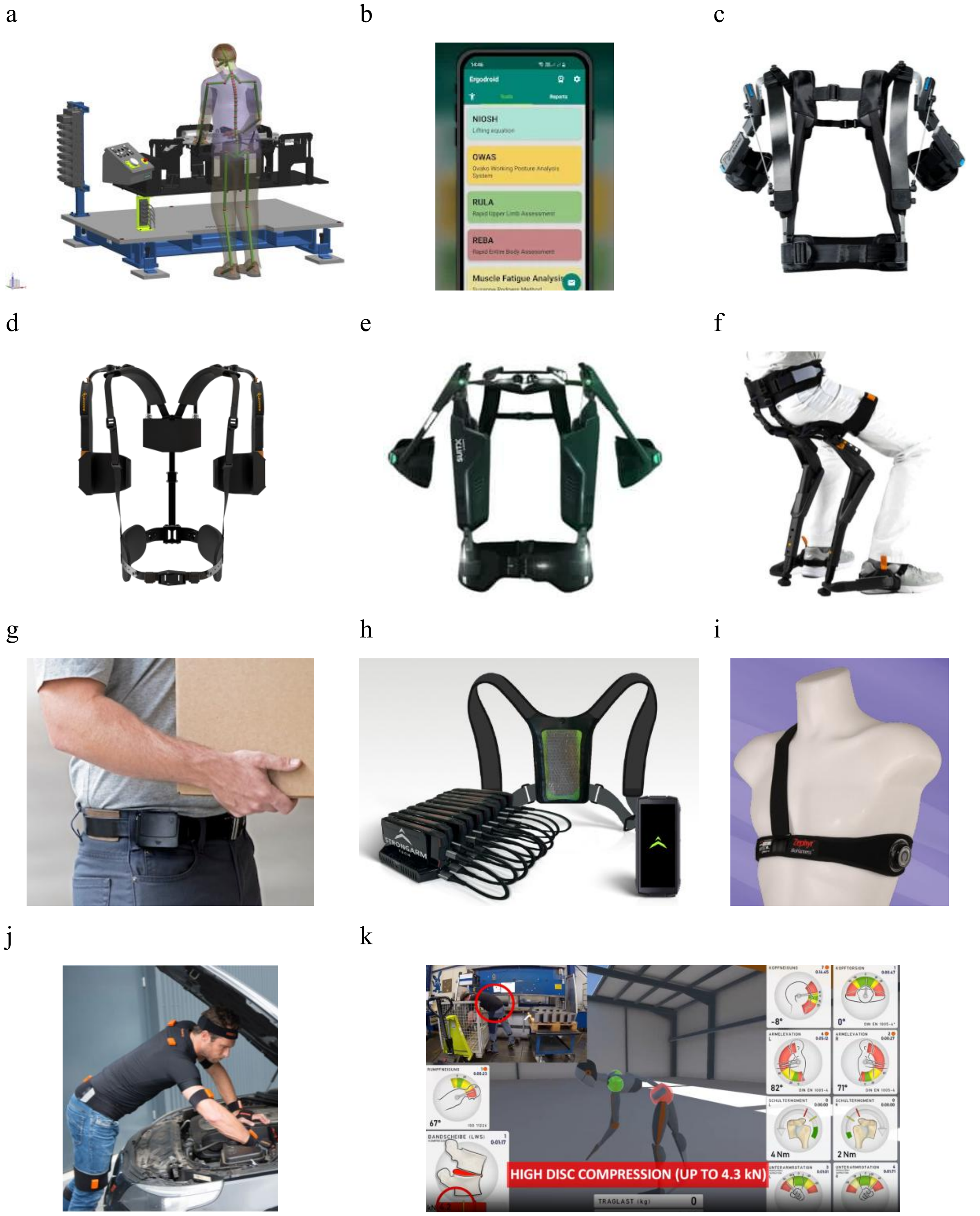

Figure 10: Ergonomic tools currently used in occupational settings, (a) Jack Siemens, an example of a simulation tool, (b) Ergodroid mobile application GUI, (c) Skelex 360, (d) AirFrame, (e) SuitX, (f) Noonee Chairless Chair, (g) Kinetic Reflex, (h) StrongArm SafeWork Sensor with harness and touchscreen device for alerts and insights, (i) HoneyWell BioHarness 3, (j) Movella XSens MT Awinda, (k) user interface with an example of a warning visually displayed

systems used in practice. Full details of the directives, standards and current commercial systems are provided in Appendix 7.

The focus now shifts to the practical tools employed in workplaces to ensure compliance with ergonomic and safety regulations and to carry out risk assessments accordingly. These tools include software and pen-and-paper methods, simulation tools, mobile applications, exoskeletons, and specific commercial wearable sensor systems on the market. Table 5 summarise these tools, their applications, and relevant standards, while Figure 10 shows the tools in the order they are discussed in the table. Note that the detailed description of current commercial devices listed in Table 5 is provided in Appendix 7. Finally, an assessment of current interventions in place to assuage WMSDs is provided next in this section.

Assessment of Current Interventions

There is no clear indication that assessment methods recommended by standards (such as ISO and EN) are based on scientific evidence, and even seem to be based on "personal opinion" according to some researchers [169], [170]. According to Armstrong *et al.* (2018) [169], it was unclear if ergonomic ISO standards are generally accepted by the research community and they suggested that they are not as very few articles in the literature have paid attention to the standards [169], however, the standards were referred to with some current systems (Table 5). This includes XSens Ergo (Figure 10j,k) which utilises European standards to set thresholds, and Scale Fit with Ergo Live which provides ergonomic reports based on DIN, EN and NIOSH standards; as previously mentioned, German and European standards are heavily influenced by ISO standards. While these standards are voluntary guidelines, the concerning reality is that researchers and manufacturers are designing new systems around these guidelines.

Unlike ergonomic ISO standards, which seem to have very little transparency regarding the authors and the process undertaken to develop them [169], EU directives, which have ultimately been rolled out as laws in member states, have a clear process and undergo thorough debates, external reviews and revisions. 90/269/EEC is most relevant EU directive for reducing WMSDs and specifically mentions its goal is to reduce WMSDs of the back, although shoulder and upper limb are the most common type of WMSDs [15], [16], and no other directive within 89/391/EEC specifically relates to these. Additionally, 90/269/EEC was drafted in 1990 and is still in force[6]. While much research in ergonomics has taken place since 1990, it is not

[6] The specific directive for minimum safety and health requirements for the manual handling of loads where there is a risk of back injury to workers, 90/269/EEC, was drafted in 1990 and consolidated in 2007 and 2019, meaning it is still in place but with additional amendments added to the bottom of the directive, amendments from those years relate to how directives are developed and changed.

necessary to change the directives as the statements therein are quite broad and thus are still applicable, and they do not recommend specific risk assessments as the standards do.

The Health and Safety Authority (HSA) in Ireland recommends the manual handling assessment chart (MAC tool) [171], risk assessment of pushing and pulling (RAPP tool) [173], and assessment of repetitive tasks of the upper limbs (ART tool) [172] because they are used by the Health and Safety Executive (HSE) UK. However, neither organisation provides a scientific justification for selecting these tools over the many others available in the field. There are no recommendations for specific wearable device systems for physiological monitoring or ergonomic risk assessments, which should be provided to employers or ergonomists who require guidance on choosing between systems on the market. Nevertheless, it is important to mention that work completed by national occupational H&S organisations such as the HSA and HSE UK, like conducting inspections and providing online tools for risk assessment and manual handling training, is imperative to WMSD risk reduction in workplaces today.

A review by Valero *et al.* (2016) [81] compared multiple assessment methods including ergonomic assessment tools: RULA [63], Rapid Entire Body Assessment (REBA) [64], Ovako Working Posture Analysing System (OWAS) [174], quick exposure check (QEC) [182], and the posture, activity, tools and handling assessment (PATH) [183] and some recommended by the UK HSE and HSA: MAC [171], ART [172], in terms of their ability to measure amplitude, duration and frequency of tasks. All methods assess amplitude, only ART and QEC consider duration, and all methods except REBA assess frequency. These results show that the recommended ART tool in Ireland and the UK succeeds in capturing all of the essential aspects of work, supporting the recommendation, although the tool does not appear on the ergonomic survey [139], indicating its use is not widespread.

Exoskeletons potentially reduce WMSDs in a manner that offers assistance and reduces strain on the worker and is oftentimes battery-less. However, exoskeletons often claim to enable workers to lift heavier loads which repeats the emphasis on creating super-strength operator as opposed to the emphasis on worker health as recommended by Ciccarelli *et al.* (2023) [4].

Most of the wearable devices on the market include an IMU, often incorporated as just a single sensor which is a positive point from a comfortability perspective for the wearer but can be a significant drawback in terms of accuracy and reliability [75], for example the SafeWorker Sensor [90], (Figure 10h), is placed on the back and the Reflex [89], (Figure 10g) , is placed at the pelvis. The number and placement of sensors depend on the parameters that are being measured and the movements being monitored [75] but it is unclear what exact parameters and models are used to initiate an alarm/vibrotactile feedback in these devices as this is proprietary information to the manufacturer. These systems also face weaknesses such as limited operation time before requiring charging, for example, the Honeywell Bioharness [91], (Figure 10i), operates for 12-28 hours and has a 3-hour charge time. The lack of available rigorous validation studies and consensus on how raw data are integrated is a notable limitation as are compatibility issues across operating systems and the risks of device fatigue (physical and mental fatigue arising from prolonged digital device use or continuous information processing) and over-dependency [184]. In addition, it is not clear who owns user data and how the data will be used making it vulnerable to security breaches and may foster prejudice against certain user groups, also, individuals may have issues trusting the decision made by AI algorithms posing issues for acceptance of the technology [184].

A key strength of current systems is the inclusion of multiple ergonomic risk assessments (as seen in all Movella Xsens Ergo products) and real-time analytics tools (such as SafeWorker Sensor, Ergo Live, Ergo Expert) which enhance their effectiveness. On the downside, a key concern is the reliance on EN and ISO standards for setting thresholds (all Movella Xsens Ergo products). Additionally, such systems do not automatically measure external loads or forces as they rely solely on IMUs, requiring manual input instead. This creates a gap in real-time risk evaluation, highlighting the need to estimate external load based on task type or use pressure insoles for load estimation.

In conclusion, there are structures and authorities in place to ensure measures are taken to reduce ergonomic risk, fatigue and WMSDs in occupational settings. However, WMSDs remain a significant global issue, indicating the need for further research into new methods and systems to better address their prevention. The system developed in the present research focuses on operator health and builds upon the strengths of current ergonomic interventions (Table 4 and Table 5), such as the use of wearable sensors for measuring kinetic data, monitoring and alerts. The system has notable improvements compared to current commercial tools (Table 5) such as estimating load and task and focussing on fatigue prediction rather than current risk estimation, which represents a more proactive approach. The reliance on ISO and EN standards, along with the numerous limitations associated with current systems (Table 5), suggests considerable room for improvement in both guidelines and systems is needed and the present work aims to counteract the disadvantages by moving away from ergonomic risk assessments and towards a solution that is suitable for dynamic conditions and can adapt to different upper body tasks in an automated manner.

2.2 Literature Review

While 2.1. Understanding and Assessing Fatigue in the Workplace defined fatigue and key methods, this subsection explores how those methods are applied in research and identifies gaps in the research. This section analyses the key reviews, research and studies in the areas of wearable technologies, ergonomics and fatigue management and provides a comprehensive overview of current state-of-the-art in these fields. These can be used to understand general research directions and trends, as well as methodologies employed and modelling approaches. Despite differences in scope, ranging from shoulder-specific reviews to broader analyses of fatigue studies employing ML, the reviews presented in this chapter consistently highlight similar research gaps and propose comparable recommendations. This chapter begins with general ergonomics and Industry 4.0 topics, then narrow the focus to reviews that specifically relate to the upper body, as these were found to be amongst the most pressing WMSDs [15], [16]. However, reviews that focussed on the whole body noted that most studies address the upper body regardless [80], [137].

2.2.1 Wearable Technologies for Occupational Well-Being

Some reviews touch on research streams and gaps in the area of developing human centric workplaces. Recommendations relating to human aspects identified by a review on Industry 4.0 in general [78] include the use of wearable devices to continuously monitor the worker, workload and ergonomic issues, the use of personal protective equipment (PPE) to improve worker H&S, and further investigation into stress and psychosocial risks. In addition, findings from a working group on “Human factors and ergonomics in industrial and logistic system design and management” [185] suggest a focus on individualised and age-friendly solutions. An Operator 4.0 review [4] also suggests a focus on addressing the ageing population as well as predictive and proactive approaches as opposed to approaches that are reactive or exclusively preventative. Gaps identified by this review [4] include addressing magnetic disturbances in inertial sensing, real-time monitoring that the operator has access to (not just managers and ergonomists), inclusion of multiple sensors, consideration of mental fatigue and emotional responses and the use of data fusion.

Bavaresco *et al.* (2021) [186] highlighted studies that use IoT technology (most commonly wearables) for occupational well-being monitoring. Many studies measure motion data alongside other physiological indicators such as heart rate [187] and EMG [188]. These studies and systems usually aim to generate warnings when physiological parameters are outside the normal range [187], [189]. Other interesting applications of wearables in the context of Industry 4.0 includes examples where access to specific work areas was enabled depending on the workers state [190], and another where environmental sensors alerted the individual to unsafe conditions [191]. The use of wearables for psychological monitoring are another avenue of research, where a common goal is to ascertain the mental state of the individual by detecting drowsiness, lack of attention and stress [189], [190]. The authors found that ML is commonly integrated into studies that involve wearables and IoT for occupational wellbeing, occasionally with data fusion techniques, to detect and classify unsafe movements, falls, and work activities, to count repetitive actions, to estimate mental state, and to activate a safety lock depending on facial recognition [186].

2.2.2 Ergonomic Applications of Wearables

Stefana *et al.* (2021) [137] performed a systematic literature review on wearable devices for all aspects of ergonomics, although all of the devices were found to relate to physical ergonomics, one to cognitive ergonomics, and none to organisational ergonomics. Devices included a smart watch, pressure insoles, smart glasses, body-mounted smart phone and sensor systems. Sensor systems accounted for the majority of the devices reviewed and are considered advantageous as different sensors at different points on the body mean that a diverse set of measured variables are used in the risk assessment and the setup is not "bulky", saying this, there was a lack of attention to the lower extremities. Almost all of the sensor systems included IMUs, ranging from two to 17 sensors, yet there is no established protocol for the placement of these sensors and sensor systems were occasionally complimented by EMG and heart rate sensors. For some authors [101], the work focussed on maintaining the minimum number of sensors without sacrificing performance.

From the 24 papers reviewed, it was established that the main purpose of the devices was for ergonomic assessment (16/24), ergonomic improvement (3/24) or both (5/24). For assessment, most devices considered postures during different tasks measured using IMUs or pressure insoles, sometimes in conjunction with EMG, while other studies analysed biomechanical loads and overexposure risks. Studies that focused on reducing the risk factor used a smart watch, smart glasses, and a robot, while the remaining studies aimed to assess and improve risks in real-time via GUIs, vibrotactile feedback and alarms. In some cases, ML was used to recognise dangerous situations, and the authors recommended this integration in the analysis of ergonomics, especially with the use of feedback. Most devices (21/24) were proposed for workers, mainly construction and industrial, and referred to at least one standard, either ergonomic risk assessments (such as RULA or NIOSH), or ISO standards (ISO 11226, 11228-1 or 11228-3). The authors recommended demonstration in real contexts as only 4/24 studies did so, another four studies described both real contexts and simulations or experimental tests, while the remaining studies were completed in only simulations or experimental tests.

Lind *et al.* (2023) [18] focused more specifically on wearable motion capture devices (specifically accelerometer and IMU) in ergonomics for the prevention of WMSDs of the trunk and upper limbs in real-work settings. The authors mentioned that motion capture with ergonomic risk assessment is in its early stages but show great potential in increasing the quality of risk assessments typically performed by self-report and observational methods which are considered subjective and semi-subjective. Additionally, these tools do not feature a continuous scale and often categorise risk into broad categories. Emerging advantages include continuous measurement, real-time assessment and feedback, and tracking improvements in technique as a result of feedback. The use of AI and ML with this technology shows promise, such as performing risk assessments using computer vision, reducing signal noise, analysis with other wearables and the potential for ergonomic assistants. Virtual reality technology can also be used for feedback or training.

Several factors relating to the usability and feasibility of wearable ergonomic systems need to be improved, such as, long-term wearer comfort, battery life, time needed to don and doff, stability of wireless connection, analysis and reporting software for practitioners, researchers and workers. The needs can depend on the customer, for instance, researchers are willing to deal with high costs, longer calibration and data collection time if accuracy and precision are high, whereas practitioners in the field generally do not have access to such resources and ease of use is preferred. Other areas to improve on include dealing with magnetic interference on IMUs, developing standardised methods for joint angle measurement using IMU (especially for the wrist), using angular velocity for the difficult measurement of task repetitions (it has been unclear what amplitude thresholds were required to count a repetition), and ensure privacy for the wearer. There is a need for standardised protocols in sensor placement, data analysis, hardware used and reference postures, meaning the neutral or baseline position used to measure and evaluate the angles of body segments relative to each other.

Lind *et al.* (2023) [18] made reference to the 2018 European joint research project report that provides research-based guidance for practitioners, researchers and policy makers on 'Assessing Arm Elevation at Work with Technical Systems' [192]. The report acknowledges that excessive arm elevations are linked to WMSDs, particularly in the shoulder and neck, and it recommends using technical systems such as accelerometers and IMUs for measurements over self-reports, it also highlights the need for accurate data and standardised measurement with the technical systems. Nevertheless, there is no presence of the report findings in standards or policies, there are no recommendations for employers regarding specific systems, and the report is only referred to in a research context.

Ranavolo *et al.* (2018) [138] assessed the use of wearables for risk assessment at work. IMU, EMG (both are most frequently used) and dynamometers were used to generate risk classifications through standardised ergonomic risk assessments or instrument-based approaches. Instrument-based approaches classified lifting tasks into low/high levels of risk, and in some cases, they rely entirely on objective data from wearables (relating to trunk inclination, joint angles, and muscle activity) and have been found to correlate to standardised ergonomic risk assessments. The most frequently assessed tasks were lifting and manual handling with low loads and high frequency, and a small portion of the studies assessed real working tasks. The authors believe the instrument-based approach for direct risk assessments and evaluating new standardised tools is favourable in light of the concerns regarding ISO standards raised by Armstrong *et al.* (2018) [169], see section 2.1.3 Current Fatigue and WMSD Interventions, and the lack of accuracy, repeatability and reliability of ergonomic risk assessments. In terms of the ideal system, they recommend the use of IMU and EMG "without doubt", preferably embedded in "plastic suits" that also act as assistive devices [193]. Pressure insoles may provide valuable information regarding ground reaction forces, and visual tracking may be useful for ergonomic risk assessments. They suggest future work should address the critical limitation of the inability to determine lifting frequency using instrumental methods. In addition, the sensor number trade-off was discussed as a high number of IMUs, while providing accuracy and reliability, will lead to a long data transfer time, potentially limiting real-time use.

2.2.3 Fatigue Assessment and Modelling

Santos *et al.* (2016) [23] performed a systematic review to assess the influence of task design on upper limb fatigue. This review mainly looks at assembly tasks which are relevant to factory workers and are highly repetitive low-load tasks (<20% MVC). The authors assessed job rotation, cycle time (time to complete a task from start to finish), duty cycle (percentage of active time compared to total cycle time), work pace and work-rest schemes on upper limb fatigue. While rest breaks had some positive effects on subjective ratings, no consistent results were observed for the effects of job rotation on subjective and objective ratings, and personal factors and study duration were found to affect results the most. The authors also echoed the need for studies to be conducted in real work environments.

Kheiri *et al.* (2023) [3] delved into forecasting applications in upper limb fatigue modelling, which is of primary interest in the thesis since WMSDs relating to the upper extremities are the most common [15], [16]. This review aimed to extend the adjacent area of *human reliability modelling* (which refers to using historical data to make predictions about future outcomes) to ergonomics practices as it is traditionally employed to reduce human errors when working with machines through cognitive, task and environmental modelling. The review offers a comprehensive overview of existing fatigue management approaches for the shoulder and provides valuable recommendations for future research.

ET and features extracted from wearable sensors (mainly from EMG) were utilised as both dependent (the outcome, measured value) and independent (the value causing or influencing outcome) variables, while task factors (load, frequency, duration, intensity, working angles and distances, etc.) and participant-related parameters (gender, age, height, etc.) were typically independent variables, and muscle strength, fatigue and Borg rate of perceived exertion (RPE) score were dependent variables.

The main modelling techniques of the reviewed studies were statistical or biomechanical, or a combination of both. Statistical models included were used to compare the effect of task factors, muscle groups on fatigue, or to develop prediction models for fatigue, recovery or heart rate. Statistical modelling methods "fall short of capturing deeper levels of association among the different aspects involved in fatigue development" and the authors mention it is important to use methods beyond the classical statistical methods if the goal is generalised models. The authors also mention that classical methods cannot account for confounding factors. Biomechanical models, according to the authors of this review, refer to theoretical muscle models and this method enabled the identification of fatigue indicators and the relationship between them. However, the differences in biomechanical modelling approaches and outputs (for example, pH, force, subjective exertion) makes it difficult to compare them.

According to this review, the main gaps and opportunities in the field of upper limb fatigue modelling are as follows: *Lack of consideration of dynamic tasks* (most studies considered static tasks) and *task dynamics,* meaning "past kinematic sequences"; *Lack of real-time update to human conditions* (few models had the capability to adapt predictions in real-time due to lack of wearable sensors and lack of adaptive models); *Lack of fully considering multi-modal information for analysis* (data fusion techniques can aggregate data from multiple sources); *Lack of considering entire shift or continuous working over days* (shorter experiments may not provide results that are representative of fatigue throughout an entire work shift); *Lack of addressing data heterogeneity* (this can relate to worker information or measurement devices and is important for ML approaches); *Lack of addressing data privacy* (this was considered in none of the reviewed studies, and individualised models are a contentious topic); *Lack of recruiting actual workers* (students from universities made up the majority of the subjects in these studies and there can be significant difference between skilled and unskilled workers during manual handling tasks in terms of muscle fibre activation, posture, and feet stability, and a lack of female participants was also noted).

2.2.4 Machine Learning and Artifical Intelligence in Ergonomics and Fatigue Modelling

Moshawrab *et al.* (2022) [83] details the AI algorithms used for physical fatigue detection, estimation, forecasting and classification with physiological indicators and details the challenges in the field. Main challenges include the lack of a standard and unified fatigue classification scale, lack of knowledge about clear thresholds of vital signs for severe fatigue, user technology adoption and engagement, as well as privacy, noise, artefacts and links to diseases. This is consistent with other literature reviews concerning ML with physiological monitoring via wearables, such as **Martins *et al.*** (2021) [86] who also discussed the lack of tasks with a long duration in real work environments, the lack of validated data acquisition systems, classification differences in subjective scales, lack of addressing data imbalances (when one data label is more common than the others), the importance of the fatigue reference measure, and selecting an experimentation task that resembles the target application. **Imran *et al.*** (2024) [194] built on the review by Martins *et al.* (2021) [86] but excluded some screening criteria and focused more on the use of physiological signals and associated analyses. This review recommended modelling multiple aspects of fatigue through multiple synchronised sensors, and to study the interaction between physical and mental fatigue.

Chan *et al.* (2022) [76] identified three areas of research for ML with WMSD prevention in general: understanding the incidence and severity of WMSDs, the risk factors of WMSDs, the underlying mechanisms of WMSDs, and to develop and evaluate interventions for WMSD prevention. Future recommendations for the research field include access to code and data, personalisation of models, and intervention implementation. In terms of using ML in manufacturing ergonomics, **Lee *et al.*** (2021) [79] found that data availability and small, incomplete datasets pose a challenge for future research, and warns that correlation may not be enough to develop models or policies as it does not always mean causation and the change of fatigue level over time needs to be considered. The author echoed the need for studying the interaction between physical and mental fatigue. In addition, a review by **Adelino *et al.*** (2024) [195] found that integration of ML and AI into human factors and ergonomics research is still limited.

2.2.5 Innovative Approaches for Upper Limb WMSD Prevention

1.3.2 Research Gaps Addressed and Novel Contributions highlighted and summarised key wearable ergonomic systems in the literature which form an important portion of the state-of-the-art landscape. A detailed comparison between these methods and the framework presented in the thesis was explored in that section and informed the thesis hypothesis and objectives. Other key studies include **Hincapie-Ramos *et al.*** (2014) [37] and **Li *et al.*** (2023) [88] who employed a torque-based approach to endurance modelling, substituting force terms with torque terms, in HMI research with virtual reality (VR) systems. This approach generated a metric to assess the ergonomics of brief, unloaded mid-air hand positions as such movements are common in VR interactions.

2.2.6 Identified Gaps in the State-of-the-Art

There is an extensive range of views on how WMSDs can be prevented, from biofeedback posture training to systems integrating ergonomic assessment tools and theoretical models to methods relying solely on pre-set posture thresholds from disputed international standards or physiological indicators with undefined thresholds. The array of alternative approaches in practice and in research and differing perspectives on WMSD prevention has led to a lack of standardisation in the field and difficulties in comparing accuracy, repeatability and reliability of approaches due to differing outputs, lack of task generalisability, and lack of standards when it comes to wearables. Regardless of these issues that need to be overcome, there are also valuable lessons that can be learned from this diverse array of perspectives that can be applied to the system in the thesis.

Consistent themes are raised by the reviews which can inform the direction of the research in the thesis. Many of the reviews align with the recommendation for **real-time** systems for **proactive** WMSD mitigation via continuous, real-time monitoring and acknowledge the role **wearables** play in this and their alignment with the industrial revolutions underway [3], [4], [18], [76], [77], [78], [79]. Wearables also present the ability to continuously map biomechanical exposures and arm **dynamics** which was also called for by reviews [3], [75]. There are common problems associated with approaches that solely rely on **physiological indicators**, such as data heterogeneity [3], lack of defined thresholds to define exertion states [83], the lack of a standardised fatigue scales [76] and inconsistent fatigue classifications [86] to relate these thresholds to, and the presence of data imbalances in such datasets [86].

In addition to the **standardisation** problem with fatigue scales [83], standardisation problems exist with the use of wearable sensors: there are no standard placements [75], [137], or standard methods for joint angle extraction [18], [41], [75], or standard analysis methods [3], [18], [192], hardware used [18], [192] or reference postures [18], or the method of determining $Force_{max}$ or $Torque_{max}$. Other problems include dealing with magnetic disturbances [4], [18] and balancing the trade-off between number of sensors with performance and accuracy [4], [75], [137], [138], transfer time [138] and comfort [75]. Other standardisation issues include the differences in outputs produced by different modelling approaches depending on the method of dealing with WMSDs [3], for example ergonomic risk assessments have their own unique scale of risk scores in gross categories [18], [80], ML models output binary or multilevel fatigue categories [86], and biomechanical models output ET [70], [71], [119] or predicted Borg RPE score [68], [196] or maximum exertable force (MEF) [124].

In terms of the **goal of the wearable systems**, some focussed on assessment and others on improvement and training, or both [137], and prediction/forecasting are much less common [3]. A form of **feedback** was present across most systems in the literature, regardless of the goal, including visual feedback via a GUI, or auditory or haptic feedback [18], [80], [137]. The main features assessed related to posture [137] where cut-off points, based on custom, ISO or

NIOSH standards [80], [137], [138], initiated a visual, auditory or vibrotactile response, in a few cases ergonomic risk indices were calculated in real-time and initiated a warning [80]. **Training** and feedback were found to be an effective approach to reducing ergonomic risk, although visual feedback was found to be more invasive than auditory or vibrotactile feedback in terms of interference with work [75], [81]. In addition to training, integration of ergonomics with **risk or accident detection** has also been suggested [137], [186].

Some studies were conducted in a laboratory **setting** and others in work settings, and researchers are calling for more models and devices to be tested in real-work scenarios with real workers [3], [18], [23], [86], [137], [138], [197], and over more realistic work periods [3], [86]. Moreover, the **type of work** is also important to consider, tasks at lower loads have not shown consistent findings [23] and if work is cyclical, it is possible to extrapolate work exposures from a short sample to an entire day, but this is more difficult to do in situations where work is not cyclical (for example where loads, frequency and duration vary throughout the day) and different assessments need to be carried out over multiple individuals over a long period of time which can be very expensive and time consuming [75], [198]. Lifting tasks, either via pick and place or heavy manual handling lifting, were most common [86], however there is difficulty measuring the number of repetitions in a consistent and effective manner [18], [138]. There are also problems with **generalisability** of ergonomic risk assessments and biomechanical models for different tasks [70], [80], [81].

Many of the research devices show alignment with **ISO and EN standards** [80], [137], [138], and existing ergonomic risk assessments [18], [80], [137], [138], similar to devices that are currently on the market [184]. Furthermore, substantial differences have been found between these standards and other models in research [199]. As previously discussed, the reliance on such standards is a cause for concern [138] but the integration of these standards into European legislation makes it difficult for researchers to avoid them. In terms of the ergonomic risk assessments, there are positives in terms of wearables addressing their semi-subjectivity and lack of repeatability compared of the observational approach, but they face limitations in terms of generalisability and classification due to lack of continuous scale and broad categorisations [18], [80]. Some reviews [18], [138] highlighted new risk assessments that utilised sensor data for risk score generation on a **continuous scale** which can help to avoid classification problems and provide more precise scores than the traditional ergonomic risk assessments, and the two types of assessment were found to correlate in some cases.

The reviews detail that the use of **ML** in the field shows promise but it is still relatively unexplored and it may be successful in uncovering underlying relationships with confounding factors since classical analysis has limitations in this regard [3], [4], [18], [195]. It may also prove useful if data fusion approaches are used [3], [4], [18], [186]. However, there are some serious drawbacks to the use of ML that have not been adequately addressed in the literature, such as the correlation-causation issue [79], and differences in the classification of subjective scales [86]. The lack of explainability in classifier decisions [87] is also a cause for concern, especially since H&S is concerned. There is a requirement for complete, large, diverse datasets which are not currently available [79] and these should be made open access [76], however, participation, privacy and user acceptance are obstacles to this [184]. ML studies are usually combined with physiological indicator data from wearable sensors [86], [194], meaning the issues associated with this data (such as standardisation, lack of experienced workers and real work settings, etc.) are also present in such studies.

Many reviews [3], [18], [83] touch on **privacy issues** of ergonomic and fatigue devices. Privacy concerns have potential to affect user acceptance and compliance and it leaves the field in a difficult position when combined with the recommendations for consideration of personal factors in endurance, fatigue and risk assessments [3], [200]. While individuals should have the choice to opt in or out of wearables, large diverse datasets are required to generate systems that are not biased [41]. Surveys have been carried out on ergonomist practitioners regarding barriers to uptake of wearable devices in work environments and privacy is consistently a primary concern [75], [152]. In a case of working with cobots and chatbots [200], it was found that demographic and work-related data were seen as non-sensitive, thus shareable, by the workers and they were more willing to share personal data when the system was more fun and trustworthy (in terms of speed of the cobot, etc.), and there were personal benefits in terms of their health. According to these surveys, **other concerns** include worker compliance, sensor durability, cost/benefit ratio of using wearables, and information validity and efficacy [18], [75]. More specifically on worker compliance, there seems to be a paradoxical relationship in the literature between workers reacting negatively to being monitored and welcoming the employer taking an interest in their health [152]. Therefore, a key part of deploying such systems is giving the worker access to their own information, which is echoed by other authors [4], [136].

The main concerns mentioned affect **user acceptance** of these devices in work places [83], in addition to competitor actions [201] and technology readiness affects adoption and acceptance

[18]. Stefana *et al.* (2021) [137] touch on this topic as the inclusion criteria included a *ready to wear* category, which comprised of smart glasses, watches and pressure insoles, while sensor systems usually did not fall under this category and accounted for the majority of studies. Other areas mentioned by Lind *et al.* (2023) [18] that affect user acceptance and the deployment of these devices include long term wearer comfort, battery life, time needed to take on and take off, and stability of wireless connection. A study on IMU comfort [82] found that they were comfortable to wear for long working shifts, although this can depend on sensor location [75] and gender (females reported lower discomfort than males) [82]. Ultimately, the workforce needs to be involved in choosing technologies for a successful adoption of such technology [201].

Finally, some of the reviews called for the development of **personalised models** and a more in-depth analysis into **individual parameters** [3], [4], [23], [76], [185], especially age due to the trend of an aging workforce [4], [185]. Other suggestions include examining the **association between physical and mental fatigue** [4], [79], [194], consideration of **emotions** [4], [79], and **psychosocial risks** [78].

2.3 Thesis Rational and Research Direction

The state-of-the-art in the preceding sections highlights the complexity of physical fatigue and its implications for musculoskeletal health in occupational settings. While fatigue has been explored from multiple perspectives, including physiological, biomechanical, and perceptual, its assessment and estimation remain diverse. Current methods vary widely in scope and applicability and tend to focus on either the detection of fatigue once it has occurred or the evaluation of ergonomic risk factors, rather than enabling proactive management or prevention. Assessments such as RULA, REBA, and ART, though widely adopted, assess only partial dimensions of work and are often unsuited to fast-changing or non-standardised industrial tasks. Although endurance models present predictive capabilities, they traditionally rely on simplified, static inputs that limit generalisability. More recent wearable technologies offer objective data and show promise for continuous assessment, but challenges persist in load estimation accuracy, algorithm validation, and generalising models across diverse tasks and populations. Workplace standards and assessment tools derived from ISO and EU directives remain constrained by limited transparency, inconsistent scientific grounding, and outdated task representations.

Collectively, these findings reveal a clear need for systems that are predictive, individualised, task-generalisable and have the potential to operate in real-time moving beyond risk detection toward active prevention of WMSDs. A notable gap exists regarding predictive modelling and practical monitoring of workers under dynamic task conditions.

The design of the system in the thesis takes key gaps identified in the state-of-the-art as it acknowledges the importance of the need for a cohort of participants with gender balance, generalised models that are applicable to different tasks, and open access datasets. The work also deals with recommendations, such as consideration of arm dynamics, and predictive and proactive forecasting solutions and actionable insights for users through a GUI. While the inclusion of subject information is a concern from a privacy perspective, some researchers believe it can provide more meaningful insights, thus individualised fatigue management by means of wearables, GUI and subject-specific information is presented in the thesis. Additionally, in terms of the opportunities that applications present, Lowe *et al.* (2019) [139] stated "[g]iven the ubiquity of smartphones and mobile apps … this seems to be an opportunity for development and an enhancement of existing approaches" when specifically referring to the completion of ergonomic assessments in the workplace today. This is also pertinent to online monitoring and providing feedback as applications provide a cheap, accessible means of delivering practical and actionable information to users.

In conclusion, through the use of wearable sensors, torque-based endurance modelling, explainable task classification, the research work in the thesis addresses the following main gaps and lays a strong foundation for real-time application:

- Lack of consideration of dynamic movements and different arm configurations (Chapter 3 and 5)
- Limited generalisability across tasks (Chapter 4 and 5)
- Lack of consideration of individual parameters (Chapter 3 and 5)
- Absence of automated load input (Chapter 4 and 5)
- Lack of explainability in classifier decisions (Chapter 4)
- Lack of proactive, predictive methods (Chapter 3 and 5)

Chapter 3 Endurance Modelling

This chapter focuses on working towards achieving Objective 1 (aiming for forecasting and individualisation) and Objective 2 (aiming for task generalisability and automatic input of model parameters by continuously extracting data from wearables) due to:

1. the forecasting nature and increased individualisation of torque-based endurance models compared to traditional endurance models,
2. working towards more accessible and accurate measures of individual maximum strength for input into endurance models,
3. consideration of any static and dynamic tasks with the upper extremities and the adjustment of ET predictions based on these movements,
4. testing the models during lifting activities, a movement which is involved in a variety of manual handling tasks such as load-bearing walking, pick and place and assembly,
5. using wearable sensors for inputting parameters into the endurance model.

The studies presented in this chapter are based on the following manuscripts:

- [202]: P. O'Sullivan, M. Menolotto, B. O'Flynn, and D. S. Komaris, 'Estimation of Maximum Shoulder and Elbow Joint Torques Based on Demographics and Anthropometrics', in 2022 44th Annual International Conference of the IEEE Engineering in Medicine & Biology Society (EMBC), Glasgow, Scotland, United Kingdom: IEEE, Jul. 2022, pp. 4346–4349. doi: 10.1109/EMBC48229.2022.9870906.
- [203]: P. O'Sullivan, M. Menolotto, B. O'Flynn, and D.-S. Komaris, 'Validation of Endurance Model for Manual Tasks', in 2023 45th Annual International Conference of the IEEE Engineering in Medicine & Biology Society (EMBC), Sydney, Australia: IEEE, Jul. 2023, pp. 1–5. doi: 10.1109/EMBC40787.2023.10341139.
- [204]: P. O'Sullivan, M. Menolotto, B. O'Flynn, and D.-S. Komaris, 'Improving dynamic endurance time predictions for shoulder fatigue: A comparative evaluation', Appl. Ergon., vol. 125, p. 104480, May 2025, doi: 10.1016/j.apergo.2025.104480.

This chapter focuses on the investigation of the empirical biomechanical modelling portion of the SAFE framework through a series of studies. The first experiment, described in section 3.1 Estimation of Maximum Shoulder and Elbow Joint Torque Based on Demographics and Anthropometrics, examines how anthropometric and demographic data can be used to predict maximum shoulder and elbow joint torque for the development of a method of calculating

$Torque_{max}$. In terms of novelty, the models allowing for cheap, quick and individualised determination of $Torque_{max}$ using basic anthropometric measurements and does not require specialised equipment. The second experiment detailed in section 3.2 Validation of Endurance Model for Manual Tasks investigates how a torque-based endurance model predicts fatigue during manual tasks. This is the first case of deploying a torque-based endurance model to static, dynamic and two-handed loaded conditions for manual handling applications. The third endurance modelling experiment, described in section 3.3 Improving Dynamic Endurance Time Predictions for Shoulder Fatigue: A Comparative Evaluation, involves comparing different torque-based endurance models with different methods of generating $Torque_{max}$ to determine which methods are best suited to predicting ET for shoulder elevation tasks across sex, load level (%MVC) and movement type, i.e. static or dynamic.

This work represents a key contribution of the thesis, where the endurance modelling and $Torque_{max}$ calibration method was shown to accurately predict fatigue for loaded static and dynamic tasks. Through the torque-based endurance modelling, individualisation is achieved via inclusion of anthropometric parameters such as arm segment lengths and masses, and the novel calibration approach that results in load-specific strength measurement for an individual. Furthermore, task generalisation is achieved via the continuous adjustment of endurance predictions based on joint angles, upper extremity CoM with respect to the shoulder and hand-held item parameters, which in combination with application to dynamic tasks, results to applicability of the model to any upper extremity task in the sagittal plane. In this way, the present approach goes beyond traditional force-based endurance models that account for isometric conditions and a specific task or muscle group, as well as the methods to measure strength which vary from study to study. Additionally, the dataset was made publicly available to aid with addressing the lack of publicly available open access sensor data in the field. This work forms the basis of future work (described in Chapter 5 System for Activity-aware Fatigue Evaluation (SAFE) Framework: Predictive Fatigue Modelling for Occupational Tasks) that applies this method of endurance modelling to industry-type tasks.

3.1 Estimation of Maximum Shoulder and Elbow Joint Torque Based on Demographics and Anthropometrics

This section is based on work published in the proceedings of the 44th IEEE Engineering in Medicine and Biology Conference [202] and was presented in Glasgow, UK in July 2022, Appendix 8.

In the original conference article, the data of 19 subjects (nine females) were analysed, however since then, additional $Torque_{max}$ data and participant demographics and anthropometrics were collected in the experiments that proceeded. Consequently, the analysis was repeated with a sample size of 53 subjects (24 females) to further strengthen the models. While the original analysis produced strong correlations for the prediction of $Torque_{max}$ of both the shoulder and elbow joint models, with R^2 values of .6 and .7 respectively ($P<.005$), there are numerous benefits of a repeat analysis in this case, including increased sample size, the use of adjusted R^2 instead of R^2 to account for the number of independent variables more effectively, and the inclusion of results from statistical tests that address many statistical assumptions and considerations associated with multiple linear regression, some of which were omitted from the original conference paper for brevity. More detailed justification for repeating the analysis can be found in 3.1.4 Discussion.

3.1.1 Introduction

Human joint torque is relevant to a wide variety of contexts, such as sports performance, health, ergonomics, and robotics. For example, in robotics, human joint motion and torque were analysed to replicate natural joint movements and to improve ergonomics for collaborative human-machine tasks in industry [205], [206]. Research shows there is a link between high rotational torques in baseball pitching and overuse injuries of the shoulder [207], and the $Torque_{max}$, sometimes referred to as strength [162], [208], affects the fatigue an individual experiences when carrying out manual tasks [37], [68].

In terms of modelling torque, Otis *et al.* (1990) [209] explored the effects of direction on the shoulder joint torques of dominant and non-dominant arms and Günzkofer *et al.* (2011) [210] completed similar work to model elbow joint torques in various directions. Other research investigated the impact of handle orientation on MVC force measurement which can be used to design assistive equipment for workers [211], and found that handles positioned 90° from the force direction maximised strength. Chaffin *et al.* (1999) [161] developed a model to summarise the effect of flexion angles and gender on $Torque_{max}$, while Coury *et al.* (1998) [212] did so for adduction-flexion posture combinations and included weight and gender in the final models. On the other hand, some studies requiring $Torque_{max}$ data use a set $Force_{max}$ value for males and females to calculate $Torque_{max}$, for example one endurance model [37] utilised 87.2 N for females and 101.6 N for males produced at the elbow joint from tables by Tan *et al.* (1994) [160]. $Torque_{max}$ can also change with ethnicity, age and sex [213], [214].

Other research showed that position, direction of movement, and grip affect the maximum elbow joint torque a person can produce [215]. Testing involved individuals pushing against a dynamometer at various joint angles, hand positions (supination/pronation), with and without a handle (to test the influence of grip), and the $Torque_{max}$ was recorded in flexion. Some of the same conditions that the $Torque_{max}$ was reported by this research (flexion in sagittal plane, supination, with handle) was implemented in the present study since flexion movements in the sagittal plane is particularly relevant to industry type manual handling tasks. MVC measurement guidelines from Chaffin (1975) [163] were also adhered to in the present study. Furthermore, forearm circumference, volume and muscle thickness have an effect on the $Torque_{max}$ [215], [216], thus these factors were considered in the present work. In addition, joint torque predictions have been made from muscle response data using EMG techniques with success [217], [218]. However, the methods employed to measure such parameters were time consuming, i.e., water tank for measuring forearm volume [215], or required specialized equipment, i.e., magnetic resonance imaging or EMG for muscle thickness and activity [216]. Therefore, a compromised approach to simplify the process involved measuring forearm circumference using a measuring tape, and a weighing scale that measures body composition parameters to obtain muscle %.

This study aimed to develop models for the prediction of $Torque_{max}$ of the shoulder and elbow joints that can be used to obtain a measure of maximum strength for input to endurance models for application in occupational settings. The models can significantly simplify and accelerate measurement processes and negate the need for specialised equipment. The existing research described above provided the grounds for the variables chosen as inputs for the estimation models, with a preference for easily and quickly measured parameters. The research can also be applied to sporting, clinical and industrial domains to help reduce the frequency of injuries.

3.1.2 Methodology

Demographic and anthropometric data of 53 participants (24 females) were recorded (Table 6). The clinically validated OMRON BF511 Body Composition Monitor [219] was used to measure the body's composition parameters, and a measuring tape to measure the forearm girth of the dominant arm (self-reported). Three measurements of forearm circumference were taken while the arm was in supination, at the proximal, middle, and distal end of the forearm, and the mean value was found.

The MVC produced at the shoulder joint was tested with the arm outstretched straight ahead (shoulder flexed to 90°) with the palm supinated causing the shoulder, wrist, and elbow joints to be in alignment, Figure 11 (left). The $Force_{max}$ produced at the elbow joint was tested with the elbow joint flexed 90° relative to the upper arm in the sagittal plane, and the palm in supination, Figure 11 (right). Participants were seated to minimize the influence of the participant's body mass and size on the measurements; the thighs were horizontal, the feet rested on a footrest attached to the adjustable seat, and the back was upright [163], [215]. The participant assumed a seated position that allowed the handle of a Walfront NK-500 push/pull dynamometer to touch their palm during testing. The plastic handle and clamp for the dynamometer were custom designed, and 3D printed using polylactic acid (PLA) and a fused filament modelling printer. The settings of the dynamometer were adjusted to record the peak force produced. The participants were asked to perform a MVC as they pressed against the dynamometer in the shoulder testing position, Figure 11 (left). Three MVC measurements were recorded with a rest of 1-min between measurements [163]. After the appropriate seat adjustments were made for the elbow testing position, Figure 11 (right), three force values were recorded in the elbow testing position while locking the shoulder joint and bending the elbow joint only. Again, there was a 1-min rest between recordings.

The $Torque_{max}$ was calculated with:

$$T = F \times d \qquad \textit{(Equation 3.1.1)}$$

where T is torque (Nm), F is the force (N) measured by the dynamometer and d is the length (m) from the acromion to mid-palm (d1, Table 6), measured with a measuring tape. Similar was done for the maximum elbow joint torque, using the distance from the elbow to mid-palm

Table 6: Subject information

Parameter	Mean $\pm$ Standard Deviation	Range [min max]
Age (years)	31 $\pm$ 8	[21 62]
Height (m)	1.73 $\pm$ .08	[1.58 1.95]
BMI (kg/m2)	24.4 $\pm$ 3.4	[18.4 31.6]
Muscle %	33.5 $\pm$ 6.2	[18.6 45.2]
Fat %	27.0 $\pm$ 9.0	[10.1 52.5]
Visceral Fat	5.9 $\pm$ 2.8	[2 13]
Mean forearm circumference (cm)	22.6 $\pm$ 3.5	[17.5 31.0]
Acromion to mid-palm, d1 (cm)	66.4 $\pm$ 5.4	[56.2 86.0]
Olecranon to mid-palm, d2 (cm)	32.5 $\pm$ 3.2	[27.5 45.5]
Shoulder Maximum Force (N)	67.6 $\pm$ 27.9	[24.5 141.7]
Elbow Maximum Force (N)	120.6 $\pm$ 53.9	[45.6 281.2]
Shoulder Maximum Joint Torque (Nm)	45.6 $\pm$ 20.6	[16.1 99.5]
Elbow Maximum Joint Torque (Nm)	40.1 $\pm$ 20.3	[13.0 102.3]

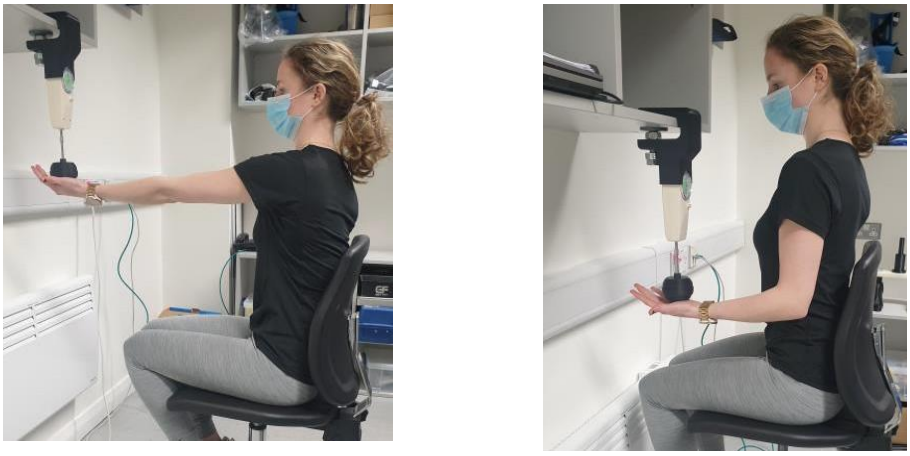

Figure 11: Testing positions for (left) shoulder and (right) elbow

(d2, Table 6). Arm length measurements from published anthropometric tables [220] were, on average, .3% and 7.7% higher than the manual measurements for the arm segments, indicating that the measurements were aligned with recorded anthropometrics in the literature.

Scatter plots mapped the relationship between the independent variables (IVs) and the dependent variables (DVs) to check for linearity. Following this, the variables with the highest correlations were run through multiple linear regression analysis with each DV separately and three different types of variable selection methods were applied: stepwise, backward, and forward; each of these methods either add or delete variables from the model based on their statistical significance and provide the input IVs to the model. This was required as it is important to achieve a balance between having too many and too few IVs in the model - a high number of IVs will explain a high proportion of the DV but will also increase the variance of prediction. The variable selection methods help to narrow down to the best IVs.

3.1.3 Results

No non-linear relationships were found in the scatter plots between the IVs and the DVs, see Appendix 9 for the shoulder $Torque_{max}$ and Appendix 10 for the elbow $Torque_{max}$ relationships, therefore, no transformations were required. Moderate to strong linear relationships were found between height, weight, fat %, muscle %, and average forearm circumference and both DVs.

For each variable selection method and each DV, the coefficients of the multiple linear regression equation were statistically significant (P<.05) for only the forward and stepwise variable selection methods, which in fact produced the same coefficients – indicating the best models were achieved. The stepwise results tables are shown in Appendix 11 and Appendix 12 for shoulder and elbow models respectively. The highest adjusted R^2 were .634 and .597 for each DV respectively, and a significance of P<.001 in the ANOVA tables indicate that at least one of the IVs have a statistically significant relationship with the DVs. The following IVs (and the statistical significance of their coefficients) produced the highest adjusted R^2 value for the shoulder $Torque_{max}$ model: height (P<.001), average forearm circumference (P=.009), muscle % (P=.011), with a statistical significance of P<.001 for the constant term, Appendix 11. The following IVs (and the statistical significance of their coefficients) produced the highest adjusted R^2 value for the elbow $Torque_{max}$ model: height (P<.001), average forearm circumference (P=.023), with a statistical significance of P<.001 for the constant term, Appendix 12. The models are shown in *Equation 3.1.2 and Equation 3.1.3* below. It must be noted that the models are only valid for the ranges of IVs shown in Table 6. Height is in meters, forearm circumference in cm.

$$Sh\_T_{max} = 108.76(Height) + 1.56(ForearmCirc.) + .98(Muscle\%) - 210.25 \qquad \textit{(Equation 3.1.2)}$$

$$El\_T_{max} = 157.82(Height) + 1.36(ForearmCirc.) - 262.93 \qquad \textit{(Equation 3.1.3)}$$

The analysis was repeated for males and females separately because a large difference was noted between males and females for the $Torque_{max}$ of both joints (Figure 12), however the analysis produced no statistical significance, meaning there was no justification for separate male and female models.

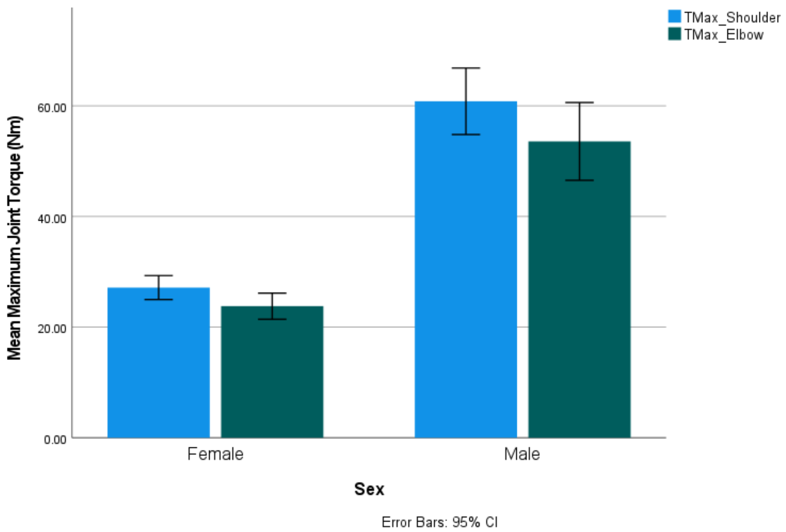

Figure 12: Clustered bar graph of the means and standard deviations of the $Torque_{max}$ for the shoulder and elbow by gender.

Several assumptions exist for multiple linear regression to be valid; these are linearity, equal variances of residuals and normality of residuals. Linearity was checked (Appendix 9 and Appendix 10) and variances were checked by plotting the independent variables against the residuals, Figure 13 and Figure 14, which are deemed constant if the plot is homoscedastic, that is, there is no trend in the data and it is dispersed randomly in a horizontal band with no outliers, which can be observed in the plots. Normality was checked via normal probability plots of the residuals, Figure 15, where large deviations from the line denote deviation from normality, which was not the case for the residuals in this study. Other considerations exist such

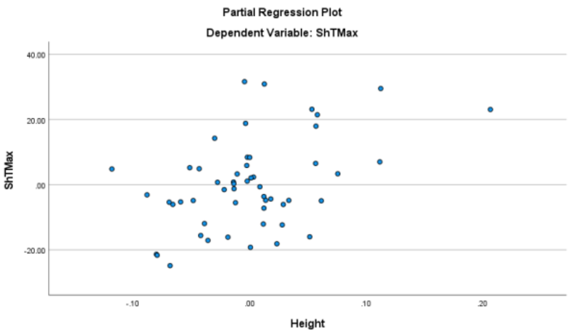

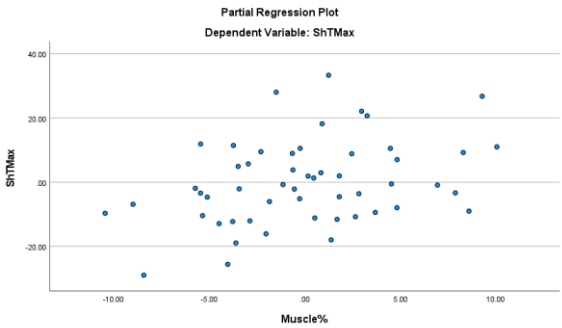

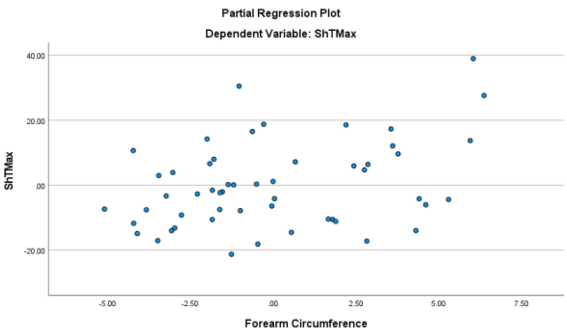

Figure 13: Residuals for (top left) height, (top right) muscle %, and (bottom right) forearm circumference against shoulder $Torque_{max}$

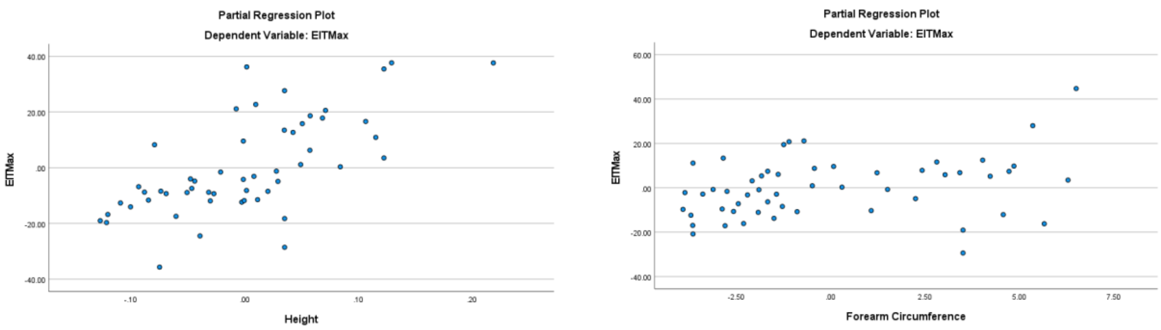

Figure 14: Residuals for (left) height and (right) forearm circumference against elbow $Torque_{max}$

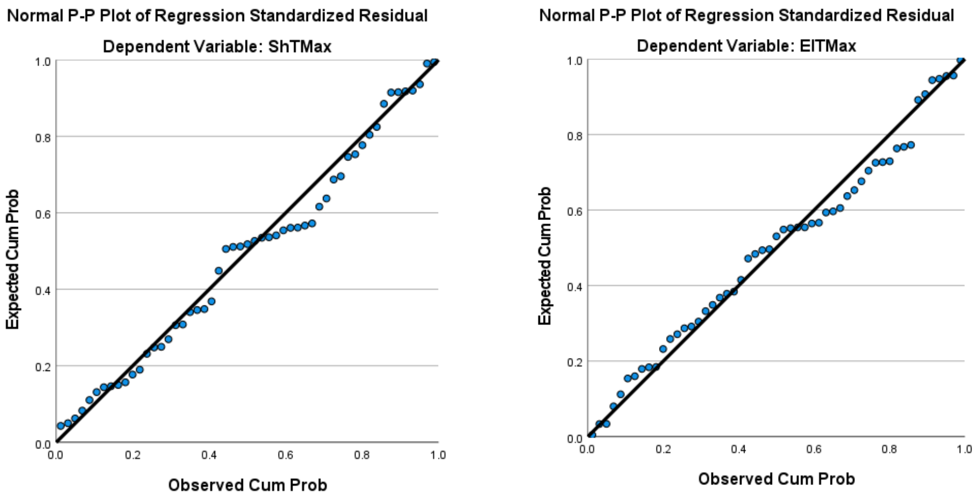

Figure 15:Normal probability plots of the residuals for (left) the shoulder max torque model and (right) the elbow $Torque_{max}$ model.

as multicollinearity (when one IV is a linear combination of the other IVs), which poses an issue as it increases the variances of the regression coefficients and makes the regression model less stable. Multicollinearity can be tested with the variance inflation factor (VIF), which is not desirable if greater than ten, and the highest VIFs are 2.24 and 1.28 for each of the models (Appendix 11 and Appendix 12). Influential cases must also be examined, these are data that appear to have a large influence on the calculation of regression coefficients, this does not pose an issue when Cook's distance is less than 1, and the highest Cook's Distances are .23 and .42 for each of the models.

3.1.4 Discussion

In this work, demographic and anthropometric parameters were linked to the maximum shoulder and elbow joint torque of 53 individuals. Multiple linear regression analysis identified height and forearm circumference as strongly influencing joint torques of both males and females, but muscle % was also significant for the shoulder model. In contrast, to other models [161], [212] that deemed weight a significant parameter. Two separate regression models described the combined effects of these parameters on shoulder and elbow $Torque_{max}$. Adjusted R^2 values were approximately .6, indicating strong relationships between the IVs and DVs. The results in this study are in alignment with the literature since there is a notable difference between the $Torque_{max}$ of males and females, however separate models were not developed or a gender term was not added, unlike other models [161], [212]. That being said, females occupied lower ranges of height, forearm circumference and, in some case, muscle %,

Table 7: Comparing subject information between the original analysis and the re-analysis

	Original analysis (19 subjects)		Re-analysis (53 subjects)	
Parameter	Mean $\pm$ Standard Deviation	Range [min max]	Mean $\pm$ Standard Deviation	Range [min max]
Height (m)	1.73 $\pm$ .08	[1.62 1.87]	1.73 $\pm$ .08	[1.58 1.95]
Muscle %	31.9 $\pm$ 6.4	[18.6 44.9]	33.5 $\pm$ 6.2	[18.6 45.2]
Average forearm circumference (cm)	26.4 $\pm$ 2.4	[22.0 31.0]	22.6 $\pm$ 3.5	[17.5 31.0]

with males occupying higher ranges of the variables in general, thereby generating models (*Equation 3.1.2* and *Equation 3.1.3*) that intrinsically account for gender differences. Papers utilising elbow MVC forces from Tan *et al.* (1994) [160] use force values of 87.2 N and 101.6 N for females and males respectively, while the present study found mean MVC forces of 77.4 N and 156.3 N respectively. This indicates moderate agreeability, especially for females, that may be accounted for in equipment differences, slight posture deviations and cohort characteristics. The mean joint torque for the shoulder in flexion were lower than values reported in Otis *et al.* [209] which only included male participants between 21 and 35 years, approximately 70.0 Nm compared to 45.6 Nm for all subjects, and 60.8 Nm for males only. Günzkofer *et al.* (2011) [210] showed elbow $Torque_{max}$ between 30 to 60 Nm for young males and females in flexion [210] which is in agreement with the values reported in the present study, albeit the range is much larger (Table 6). The number of subjects is in alignment with, or greater than, similar studies in the literature, for example, thirty subjects were used to develop $Torque_{max}$ models [212].

In terms of performing the re-analysis after the original conference paper publication, an increase in the sample size has multiple benefits, such as increasing the diversity of the cohort and increasing the ranges of IVs. In linear regression, the model can only predict outcomes for the ranges of IVs that were inputted to the model and extrapolating beyond the measured ranges of the IVs is outside the scope of the model. With the larger, more diverse cohort, those ranges were increased (highlighted in green in Table 7), thereby improving the applicability of the model. There are additional impacts of sample size on linear regression models [221], [222], [223]; a general guideline regarding sample size for linear regression suggests that the ratio of sample cases to IVs should not fall below 5:1. Another guideline states that samples of up to 20 subjects are only suitable for simple regression, that is, with only one IV. While the first guideline was adhered to in the model in the original conference article, with two IVs and 19 subjects, the second was not as more than one IV was included in the model generated with a small sample size. The repeated analysis in this chapter adheres to both sample size guidelines. Sample size also affects practical significance [221], [222], [223], which was achieved in the

Table 8: Minimum R^2 detected with a power of 80%, Type I error of 5% for varying numbers of independent variables and sample sizes

	Number of Independent Variables (α=.05)			
Sample Size	**2**	**5**	**10**	**20**
20	39	48	64	NA
50	19	23	29	42
100	10	12	15	21

original model - Table 8 shows that approximately 39% is the minimum R^2 to be found statistically significant with a sample size of 20, two IVs, alpha level of .05 and power of 80%, the latter of which denotes practical significance. While the number of subjects was increased with the repeated analysis, a model with too many independent variables reduces the power of the model. However, the minimum R^2 required to denote statistical significance with 53 subjects, and two or three IVs are between approximately 19% and 23%, indicating that practical significance was achieved with the re-analysis work as the R^2 were above this.

In the original analysis, forearm volume was determined using the method detailed in [224], however, the forearm volume method requires the distances between forearm measurements and this information was not collected in the newer cohorts. Nevertheless, measurements of the upper, middle and lower forearm were gathered in the initial cohort, thereby making it appropriate for use in the new analysis. Girth measurements were also utilised by [212] and multiplication of the circumference measurements in the forearm volume method may lead to amplified measurement error since they were multiplied and squared on the numerator of the equation, further justifying the new forearm measurement approach.

The novelty of this study not only lies in understanding the relationship between numerous individual parameters and $Torque_{max}$ and developing a model accordingly, but also in the identification of the most relevant factors to produce a model that estimates maximum joint torque. Using variable selection methods aided in identifying the minimum number of parameters needed for a reliable $Torque_{max}$ estimation. The work in this publication means a force gauge is not required for each subject in workplace settings; instead, basic anthropometric measurements are sufficient for $Torque_{max}$ estimations for input to the fatigue forecasting system being developed in this research work. Additionally, when considering the practicalities of deploying such a system by an ergonomist in an occupational setting, minimising the measurements required and the use of quick and easy to measure parameters would help to streamline their work process.

The mean and standard deviations of the age of the cohort remains a limitation of the study and other planes such as shoulder axial rotation and elbow varus/valgus torques, which are commonly used in sports and some occupational tasks, were not considered and neither were submaximal contractions. Although postures and arm configurations were visually inspected, restraints similar to those used in other similar studies and guidelines [163], [215] could have been used to ensure correction positioning or wearable sensors such as IMU could have been used to measure the positions. The models herein useful for the endurance models later in the thesis, and for applications that utilise biomechanical data for health, safety and rehabilitation purposes, and can be used to reduce the time for processing subjects in studies that require joint torque information.

3.1.5 Conclusion

Height, forearm circumference and muscle % were found to influence maximum shoulder and elbow joint torques and models to describe these relationships were generated using regression analysis. The models enable $Torque_{max}$ estimation for individuals using basic anthropometric measurements in an individualised manner and do not require testing with a dynamometer which is useful for the deployment of the fatigue forecasting system concerned in the thesis. Thus, the models are used in the comparative analysis that appears in 3.3 Improving Dynamic Endurance Time Predictions for Shoulder Fatigue: A Comparative Evaluation.

3.2 Validation of Endurance Model for Manual Tasks

This section is based on work published in the proceedings of the 45th IEEE Engineering in Medicine and Biology Conference (EMBC) [203] and was presented in Sydney, Australia in July 2023.

3.2.1 Introduction

MET models have been developed for differing conditions, for example, there are models focussed on modelling ET of different muscle groups and joints [70], [71], [225], and specific manual handling tasks such as two-handed truck pulling [226], push and pull tasks [227] and one-handed carrying tasks [228]. MET models are only applicable to the specific experimental conditions under which the data were gathered [70], meaning they are not generalisable to different tasks, making them unsuitable for assessing smart factory workers as their tasks typically change throughout a shift. In addition, these empirical models assume constant force and sustained isometric contractions [229] and differences have been found between ETs of static and dynamic tasks [230], meaning such models are not applicable to dynamic tasks, which is often the case in the work performed by smart factory workers. Individual differences such as sex [231], [232], and age [225], [231], [233] have shown to impact ET, although this has be disputed by other research [233], [234].

A torque-based endurance model [37], called the consumed endurance (CE) model, predicted ET during mid-air repetitive interactions based on the $Torque_{max}$ produced by an individual around the shoulder joint and the torque at a given moment. While the previous section focused on one of the inputs of this modelling approach, i.e., $Torque_{max}$, the present section focusses on applying the torque-based modelling approach to manual tasks. The CE model (*Equation 3.2.1*), derived from Rohmert's model [123] for static tasks, which describes the decline in endurance with increased relative torque, replaces $\frac{Force}{Force_{max}}$ with $\frac{Torque}{Torque_{max}}$ to capture changes in the moment arm, offering fatigue assessment for dynamic conditions.

$$ET\_CE = \frac{1236.5}{\left(\frac{Torque}{Torque_{max}} \times 100 - 15\right)^{.618}} - 72.5$$ *(Equation 3.2.1)*

The model continuously adjusts ET predictions based on arm configuration, load, acceleration of the centre of mass (CoM) of the arm segments and inertia of the arm, and the component being held. Replacing force terms with torque terms is commonly done in research with muscle models [68], [119], [208], for example, for the same model, one study used the force version [119] and another study used the torque version [99], but was not completed with endurance modelling up to this point. While the model was applied to simple unloaded hand interactions for HMI research, it may allow for the complexity and workload of manual tasks to be accounted for by considering these additional parameters compared to traditional endurance models that consider $\frac{Force}{Force_{max}}$. The model also considers anthropometrics such as arm segment lengths and arm masses based on the individual's height and body mass, meaning there is increased individualisation in the outputted predictions compared to other MET models that only consider $Force_{max}$ as an individualised measure. Consequently, by validating the CE model for industry tasks and, if necessary, by adapting the model for industry applications, a time to fatigue can be predicted for industry workers.

This study aimed to validate the CE model for manual lifting tasks in the sagittal plane under loaded conditions. As previously mentioned, the rate of fatigue development differs between isometric and dynamic contractions, therefore participants performed both static and dynamic tasks to understand the ability of the model under both conditions. Twelve subjects completed three lifting tasks with weights, static (one-handed) and dynamic (one-handed and two-handed), while wearable sensors were used to collect physiological data, and the Borg RPE scale [72] acted as a reference measure. It is hypothesised that the model predicts the time to fatigue for each subject, for both static and dynamic tasks, and therefore is suitable for use in the fatigue forecasting system development described in the thesis. It is important that the model is validated for simple lifting movements under static and dynamic conditions before it is applied to complex and intricate industry-type tasks.

3.2.2 Methodology

Twelve healthy participants (seven females, Table 9) took part in the study. The mean age of the cohort was 30 years in the range of [23 62] and weight ranged between [56.3 102.7] with a mean of 72.2 kg. Anthropometric measurements were recorded, and the force of MVCs for flexion of the shoulder was measured by means of a Walfront NK-500 push/pull dynamometer. During the measurement, the arm was outstretched straight ahead in supination with the shoulder, wrist and elbow joints in alignment. Participants were seated to minimise influence from the lower body, with their back upright, thighs horizontal to the floor and feet on a footrest attached to the seat. The seat height was adjustable to enable the participant's shoulder to be at the same height as the force gauge handle which was at the centre of their palm as they pushed upwards, moving their shoulder in flexion. MVCs and anthropometric data were used to calculate shoulder $Torque_{max}$ in flexion. Subjects were divided into two groups, A and B, depending on the order they completed the tasks in order to study the influence of task order on results. Subjects' details within each group are shown in Table 9.

Participants wore the XSENS Awinda shirt, glove and straps to adhere the IMUs (XSENS MTw Awinda, Movella, Enshede, Netherlands), sampling at 100 Hz. IMUs were placed on the dominant (self-reported) side of the body, to the sternum, shoulder, upper arm, forearm and the palm, according to the manufacturer's recommendations, Figure 16.

Participants performed three tasks. A static task with the shoulder of the dominant arm held at 90 ° in flexion, that is, in the same position as the MVC exercise, while holding a weight (*Static Task*); a dynamic task with the dominant hand, moving the shoulder joint from 0 to 90 ° in flexion while holding a weight (*Dynamic Task*); and finally, the *Dynamic Task* with both hands holding the weight (*Two-handed Task*). The MVC force was used to calculate the weight a subject lifted during the tasks, with participants approximately 30% to 45% of their MVC force.

Table 9: Subject information

Parameters	All Subjects	Group A	Group B
Sex	7 females, 5 males	4 females, 2 males	3 females, 3 males
Age (years)	30 ± 10	33 ± 14	26 ± 3
Weight (kg)	72.23 ± 13.18	71.52 ± 12.30	72.95 ± 13.96
Height (cm)	1.72 ± .06	1.70 ± .07	1.74 ± .05
Upper arm Length (m)	.33 ± .02	.34 ± .02	.33 ± .02
Forearm Length (m)	.26 ± .02	.27 ± .02	.26 ± .02
Hand Length (m)	.20 ± .01	.19 ± .01	.20 ± .02
Upper arm Radius (m)	.05 ± .01	.05 ± .01	.05 ± .01
Forearm Radius (m)	.04 ± .00	.04 ± .00	.04 ± .00
Hand Radius (m)	.03 ± .00	.03 ± .00	.04 ± .00
Maximum Shoulder Joint Torque (Nm)	49.61 ± 19.86	45.97 ± 20.52	53.25 ± 18.47

Figure 16: IMU placement on the shoulder, upper arm, forearm, hand and torso.

The hand was in pronation for the tasks in the study, this was done to isolate the shoulder muscles and reduce the influence of the biceps for the shoulder tasks. During the study, the exertion of subjects was tracked throughout the task by means of the subjective Borg RPE scale [72], Appendix 13.

The Borg RPE score was recorded before the task, and 10 s and 20 s after starting the tasks, and every 20 s thereafter [127], [235]. The tasks were completed until the subject was fatigued, verbally reporting they were maximally exerted on the Borg RPE scale (17≤), or when they were unable to maintain the target task position, or when they were unable to maintain the prescribed rate of movement (i.e., 60 beats per min played on a metronome) for the dynamic tasks [86], [88], and the experimental ET was recorded. Measuring maximum holding time is a common method used to generate endurance curves [70], [71], [88]. The final Borg rating was also noted at the end of each recording. Individuals took 10 mins of rest before they began the subsequent task; according to upper extremity recovery models [27], [119], [236] no more than 6 mins is required for recovery after a fatiguing interaction, and 10 mins was sufficient to reduce subject's Borg rating to 6 or 7, demonstrating that they were rested. Fatigue is highly task-dependent; therefore, subjects were divided into two groups with different task orders: Group A's task order was *Static Task*, *Dynamic Task*, *Two-handed Task*, while Group B's task order was the reverse.

$Torque_{max}$ was calculated using MVC forces and *Equation 3.1.1* in the previous section while $Torque_{shoulder}$ is the sum of the torques acting on the frontal axis of the shoulder joint, calculated for each frame based on the IMU-derived joint angles (relative orientation between quaternions of adjacent body segments) and the CoM position, using *Equation 3.2.2* in static conditions and *Equation 3.2.3* in dynamic conditions [37]. The torque was calculated for each frame based on the joint angles and the CoM position.

$$\|\vec{T}_{shoulder}\| = \|\vec{r} \times m\vec{g}\| \qquad \textit{(Equation 3.2.2)}$$

$$\|\vec{T}_{shoulder,t}\| = \|\vec{r} \times \overrightarrow{acc}_t \times m - (\vec{r} \times m\vec{g} + I_t\vec{\alpha}_t)\| \qquad \textit{(Equation 3.2.3)}$$

Where m is the mass of the arm and weight, $\overrightarrow{acc}$ is the acceleration of the CoM, found by double differentiation of the distance CoM from the shoulder, $\vec{r}$, found with *Equation 3.2.4* and *Equation 3.2.5*. $\overrightarrow{acc}$ is the acceleration of the CoM and angular acceleration α was found using $\frac{\overrightarrow{acc}}{\|\vec{r}\|}$ [37]. The mass of the weight was halved for the *Two-handed* task [208].

$$D = B + \frac{WrHaWe_{mass}}{EbWr_{mass} + WrHaWe_{mass}}\overrightarrow{BC} \qquad \textit{(Equation 3.2.4)}$$

$$CoM = A + \frac{EbWr_{mass} + WrHaWe_{mass}}{ArmWe_{mass}}\overrightarrow{AD} \qquad \textit{(Equation 3.2.5)}$$

Where A, B and C are the CoMs of the upper arm, forearm and hand respectively, D is the CoM

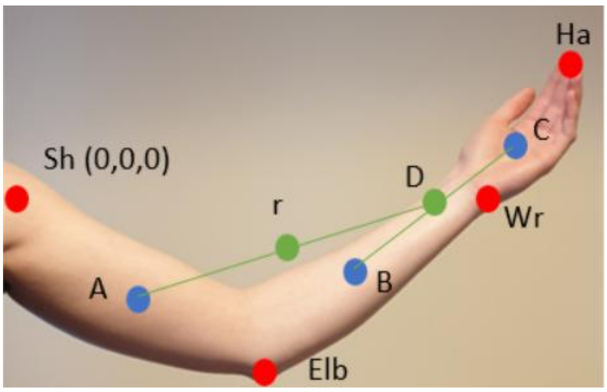

Figure 17: Locations of the centre of mass of the arm.

of the forearm (EbWr) and hand and weight (WrHaWe), Figure 17. The dumbbell was assumed to act at the CoM of the hand (C). Anthropometric tables were used to determine the mass, length and CoM of the arm segments [237], [238]. I denotes the inertia, which was found for each frame using the Parallel-Axis Theorem, as described in [220], see *Equation 3.2.6.* The inertia of the segments was summed with the inertia of the dumbbell, which is approximated as a sphere in this case. Since the torque varied throughout the dynamic movements, the mean predicted ET was extracted as the predicted ET for the task.

$$\sum I = m{\rho_0}^2 + mx^2 \qquad \textit{(Equation 3.2.6)}$$

Where m is the mass of the segment, ρ_0 is the radius of gyration around the centre of gravity and x is the distance from the shoulder joint.

3.2.3 Results

Table 10 shows the experimental and predicted ETs and the ET error. Measured ETs for *Dynamic Task* were slightly longer than those of the *Static Task*, likely due to the reduced torque as the shoulder angle decreased throughout the repetitive movement, however, this was not reflected in the mean predicted ET with the model in *Equation 3.2.1*. The *Dynamic Task* showed the highest errors, regardless of task order and gender, and the ET was consistently overestimated.

Sex affected measured ET, with the average measured ET greater for males in *Static* and *Two-handed* tasks and only slightly less than females for the *Dynamic* task, however, greater variability was observed for females in this task. Predicted ETs for males and females were all relatively close, indicating the model did not take the greater variability and generally lower MVC forces (Table 9) of females into account. These results indicate that the relative torques

Table 10: Endurance measurements and predictions.

		Static Task	**Dynamic Task**	**Two-handed Task**
Measured Endurance Time (s) (mean ± std)	All Subjects	63.25 ± 21.13	87.75 ± 34.67	138.42 ± 49.28
	Females	59.14 ± 19.79	93.86 ± 40.40	125.43 ± 39.71
	Males	69.00 ± 21.60	79.20 ± 21.79	156.60 ± 55.27
Predicted Endurance Time (s) (mean ± std)	All Subjects	56.01 ± 6.78	165.12 ± 4.47	172.30 ± 3.02
	Females	54.40 ± 3.25	165.61 ± 5.61	171.56 ± 1.86
	Males	58.27 ± 9.32	164.43 ± 1.74	173.35 ± 3.89
Endurance Time Absolute Error (%)	All Subjects	28.62 ± 23.27	115.45 ± 70.42	49.42 ± 38.72
	Females	35.74 ± 25.85	111.26 ± 81.23	54.98 ± 45.55
	Males	18.66 ± 13.91	121.32 ± 51.03	41.13 ± 24.13

for males and females were the same, i.e. the lower $Torque_{max}$ values were balanced with lower torque generated during the tasks, likely due to anthropometrics as tasks were performed identically by all subjects. However, the model successfully predicted higher ETs for *Static* and *Two-Handed* tasks for males, and for *Dynamic* tasks for females, which aligns with the experimental data (Table 10).

Figure 18 shows the *Dynamic* predicted ET was consistently higher than the measured ET and while the measured ETs of *Dynamic* and *Two-Handed* tasks varied between individuals, the predicted ET remained similar. There was no such pattern for the *Static* task. It is possible that group, therefore task order, affected the measured ETs. Group A completed the *Two-handed Task* last, and Group B completed *Static* first, resulting in lower measured ETs for these group-task combinations. Group A's mean experimental ET for the *Static* task was 77 s as opposed to Group B's 50 s, while Group A and B's mean experimental ET for the *Two-handed* task were 126 s and 151 s, respectively. This is also demonstrated in Figure 19 which shows the mean time spent in each Borg RPE exertion zone. Group A participants tended to be more exhausted

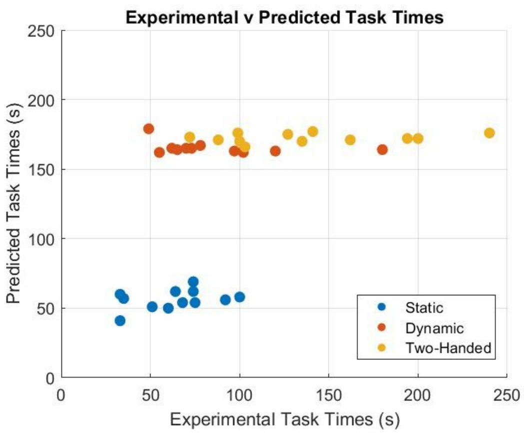

Figure 18: Experimental and predicted endurance times.

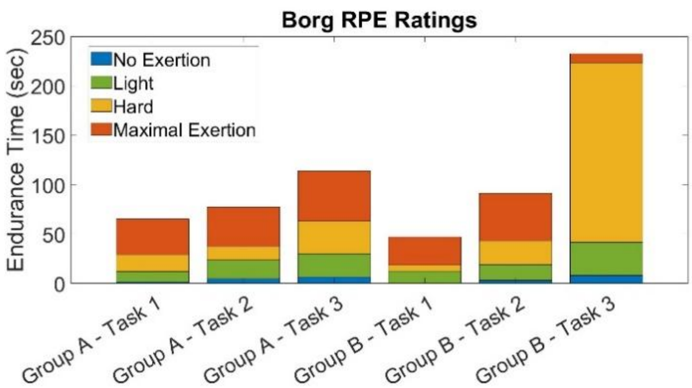

Figure 19:Mean length of time (s) participants spent in each Borg RPE category.

by the final task than Group B, spending most of their time in the maximally exerted zone. Likewise, Group B spent most of the *Static Task* maximally exerted.

3.2.4 Discussion

The preliminary work described in this section provided the basis for further experimental studies assessing the torque-based CE model. Task order and sex were found to affect the measured ETs of subjects, indicating that gender, previous tasks, their workloads, and duration must be taken into account in fatigue prediction, even if the individual reported that they were fully rested from previous activity. Errors for *Dynamic Task* were highest across all participants, regardless of sex or task order. The number of subjects limits the applicability of the study as studies studying ET ranged from ten to 40 [162], [226], [232], [234], [239], [240], and even a few over 80 participants [231], [233], although most MET studies consisted of fewer than ten participants, as discussed by Mathiassen and Ahsberg (1999) [162]. The narrow age range of the cohort, Table 9, was also a limitation and individuals were tested between 30-45% of their MVC, however, a range of intensities (i.e. 10 to 20%, 20 to 30%, etc.) in different directions should be tested to gain a full understanding of how the model performs under these conditions, which is applied in the next study described in section 3.3 Improving Dynamic Endurance Time Predictions for Shoulder Fatigue: A Comparative Evaluation.

Males had longer measured ETs than females in two of the tasks (*Static* and *Two-Handed*), Table 10, which is not in alignment with some literature [118], [234], [234], [239]. However, some results are aligned with other studies, such as [231], [241] who found women's strength was significantly less than men (similar to Table 9), and the difference increased with age, but, in one study [231], at the same level of %MVC (40%) women's endurance was greater than men (123%), this is similar to the *Dynamic* task (Table 10).

The results of the present study illustrated that the CE model can provide a valuable tool for estimating ET for static and dynamic lifting tasks about the shoulder joint under specific conditions. The choice of using torque instead of force, like in Romhert's model [123], better reflects the change of CoM during the movement, but makes any error in the anthropometric data (length and radius of the body segments of the arm) to propagate faster. On the other hand, Rohmert's model has been questioned, especially the presence of an endurance limit at 15% indicating that tasks at this exertion level can be maintained indefinitely [70], [162], [235] and it was found to overestimate ET for lower SIs, i.e. up to 20% MVC [235]. Due to these criticisms, it may be beneficial to assess any other torque-based endurance models in the literature, if present, or to develop a new endurance model. This approach will be performed in section 3.3 Improving Dynamic Endurance Time Predictions for Shoulder Fatigue: A Comparative Evaluation, especially since the errors indicate that this method of ET prediction is not suitable for deployment in the fatigue forecasting system. In addition, the method of determining $Torque_{max}$ described in section 3.1 Estimation of Maximum Shoulder and Elbow Joint Torque Based on Demographics and Anthropometrics [202] should be assessed with the CE model and any other torque-based endurance model in future work.

Future work can involve the reduction of errors and modification of the model to deal with the aforementioned shortcomings. For example, modifications may comprise of testing under different joint configurations (e.g. by flexing elbow and wrist to differing extents), other directions (e.g. internal and external rotation or abduction and adduction) while using one or two hands at a range of standardised intensity (SI) levels, i.e. %MVC, and considering the joint angles in more than one plane. Figure 18 showed that the model did not account for individual differences as much as initially expected since similar ET predictions provided for all subjects and they were not in alignment with the measured ET for *Dynamic* and *Two-Handed* tasks, suggesting that other considerations, such as the influence of body composition parameters and exercise level can be investigated in future work. In addition, the influence of task type and task order can be assessed in future work. The CE model was used to design more user-friendly fatigue reducing user interfaces in VR [37], similarly, this work may provide the basis for a more individualised approach to worker-specific target levels and workloads, tool selection and fatigue reduction in occupational settings.

3.2.5 Conclusion

The torque-based CE model was found to predict the ETs of a loaded and flexed shoulder joint, in one-handed static conditions and two-handed dynamic conditions with errors of 28.62% and 49.21% respectively. Gender was found to affect the predicted ET, especially for the *Static* task, the error 18.66% for males and 35.74% for females. The model significantly overestimated one-handed dynamic tasks across the cohort, regardless of task order.

More subjects and a wider range of abilities and ages are required for future work which may involve the integration of wearable sensors to gain unbiased physical exertion measurements and the modification of the CE endurance model to adjust different joints under load during static and dynamic conditions, with one and both hands and at a range of intensities and directions.

3.3 Improving Dynamic Endurance Time Predictions for Shoulder Fatigue: A Comparative Evaluation

This section is based on work published in Applied Ergonomics in May 2025. Additional analyses that were not included in the original publication are included in the thesis; these pertain to the inclusion of the regression models for $Torque_{max}$ from section 3.1 Estimation of Maximum Shoulder and Elbow Joint Torque Based on Demographics and Anthropometrics.

3.3.1 Introduction

Figure 20 shows different endurance models considered in this section and how the increase in relative torque results in differing reductions in endurance capacity, depending on the model. As previously mentioned, the CE model (*Equation 3.2.1*, orange line in Figure 20), derived from Rohmert's model [123] for static tasks, replaces $\frac{Force}{Force_{max}}$ with $\frac{Torque}{Torque_{max}}$ to account for changes in the moment arm, offering fatigue assessment for dynamic conditions. The CE model was applied in unloaded conditions [37] and in loaded conditions with high errors [203], and there are disagreements regarding the fixed asymptote (minus 15 in the denominator) not reflected in recent empirical findings [70], [88], [162]. The new improved consumed endurance (NICE) model (*Equation 3.3.1,* blue solid line in Figure 20), addressed these limitations by removing the asymptote and fitting a power curve to experimental data [88].

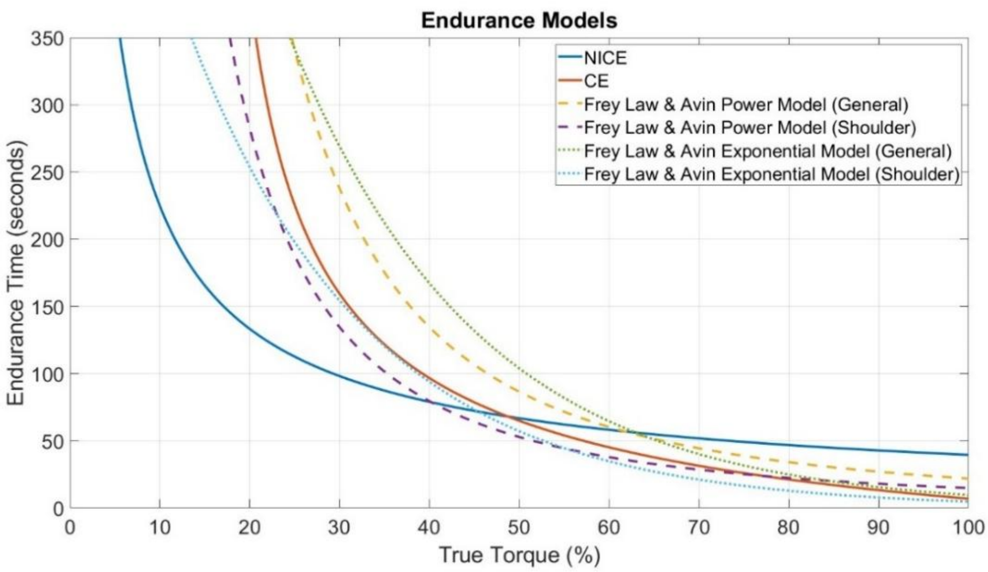

Figure 20: All six endurance models that are assessed in the study, all are in terms of torque/maximum torque.

$$ET\_CE = \frac{1236.5}{\left(\frac{Torque}{Torque_{max}} \times 100 - 15\right)^{.618}} - 72.5 \qquad \textit{(Equation 3.2.1)}$$

$$ET\_NICE = \frac{1277.9066}{\left(\frac{Torque}{Torque_{max}} \times 100\right)^{.7546}} \qquad \textit{(Equation 3.3.1)}$$

Frey Law and Avin [71] offered a comprehensive meta-analysis of MET models by fitting power and exponential curves to empirical endurance data from multiple studies. The Frey Law & Avin power ($ET = b0 * (MVC)^{b1}$) and exponential ($ET = b0 * exp^{(MVC*b1)}$) models contain coefficients ($b0$ and $b1$) that describe endurance for different joints as well as generalised curves for the whole body in terms of MVC%, also called SI. For example, the general power model was expressed as $ET = 21.92 * MVC^{-1.98}$ and similar to the CE model (*Equation 3.2.1*) which replaced force inputs in Rohmert's model [123] with torque inputs, the force inputs were replaced with torque inputs in these general and shoulder power models (*Equations 3.3.2* and *3.3.3*) and general and shoulder exponential models (*Equations 3.3.4 to 3.3.5*) in this work.

$$ET\_FA\_Power_{General} = \frac{21.92}{\left(\frac{Torque}{Torque_{max}}\right)^{1.98}} \qquad \textit{(Equation 3.3.2)}$$

$$ET\_FA\_Power_{Shoulder} = \frac{14.86}{\left(\frac{Torque}{Torque_{max}}\right)^{1.83}} \qquad \textit{(Equation 3.3.3)}$$

$$ET\_FA\_Exp_{General} = \frac{1122.32}{e^{\left(\frac{Torque}{Torque_{max}}\right) \times 4.76}} \qquad \textit{(Equation 3.3.4)}$$

$$ET\_FA\_Exp_{Shoulder} = \frac{685.46}{e^{\left(\frac{Torque}{Torque_{max}}\right) \times 4.97}} \qquad \textit{(Equation 3.3.5)}$$

This study built on previous research in section 3.2 Validation of Endurance Model for Manual Tasks [203] and compared torque-based endurance models (*Equation 3.2.1 and Equation 3.3.1* to *Equation 3.3.5,* curves in Figure 20) and four methods of obtaining $Torque_{max}$ to assess their predictive accuracy for fatiguing static and dynamic tasks. The goal was to determine the most effective models and inputs for predicting ET and to address the limitations of current methods by developing a more individualised approach. By focusing on fundamental tasks, this research aimed to lay the groundwork for applying these models to more complex industrial tasks.

3.3.2 Material and Methods

Subject parameters, ET and MoCap data for shoulder tasks were extracted from an open-access dataset [242] which also includes additional tasks and sensor data.

Participants

Twenty-nine participants (14 females) were asked to attend the session fully rested and completed a 5-min upper body warm-up prior to data capture. Demographics and anthropometrics were gathered (Table 11) using the clinically validated OMRON BF511 Body Composition Monitor (Omron Corporation, Kyoto, Japan) [219] and anthropometric measuring tape following measurement guidelines [243], [244].

Maximum Forces and Sensor Set-up

MVCs of the shoulder and elbow joints in flexion (Table 11) were measured using a loadcell (range=30 kg; accuracy=.02%; non-linearity=.02% F.S.) in the same manner previously described in section 3.1 Estimation of Maximum Shoulder and Elbow Joint Torque Based on Demographics and Anthropometrics. MVCs and tasks were completed with the dominant arm which was defined as the arm used to perform daily tasks. Participants pushed upwards against the loadcell using maximum effort for 3 s while maintaining a straight posture three times [67], firstly for a practice test, and forces were recorded on the second and third attempts with a 2-min break in between [196], [245], the mean of which was used to determine MVC. The closest weights to 25% and 45% SI, determined the dumbbell weight lifted during tasks in the study,

Table 11: Anthropometric and demographic data of participants

Parameters	All Subjects	Males	Females
Age (years)	27.7 ± 4.3	28.5 ± 3.6	26.9 ± 4.8
Height (m)	1.72 ± .09	1.78 ± .07	1.65 ± .04
Body Mass (kg)	70.48 ± 13.13	78.41 ± 11.11	61.99 ± 9.25
Body Mass Index (kg/m^2)	23.70 ± 3.13	24.55 ± 2.77	22.81 ± 3.25
Fat %	26.95 ± 7.82	22.64 ± 6.54	31.56 ± 6.28
Muscle %	33.27 ± 5.71	37.66 ± 3.82	28.56 ± 3.01
Upper Arm Length (m)	.34 ± .04	.36 ± .04	.33 ± .03
Forearm Length (m)	.26 ± .03	.28 ± .04	.25 ± .02
Hand Length (m)	.18 ± .01	.18 ± .01	.18 ± .01
Shoulder MVC (N)	62.88 ± 23.81	82.78 ± 15.15	41.55 ± 7.04
Elbow MVC (N)	112.23 ± 53.17	152.69 ± 43.37	68.88 ± 14.43

Table 12: Ideal and real standardised intensities (%) of the loads lifted in the study.

Standardised Intensities (%)			
Ideal SI	**All Subjects**	**Males**	**Females**
25	24.5 ± 3.8	27.1 ± 3.4	21.9 ± 2.0
45	44.5 ± 4.5	45.8 ± 4.6	43.7 ± 4.0

available weights (in kg,) were .5, 1, 2, 3, 4, 5, 6, 7.5, 10, corresponding closely to the desired SI, and actual SIs are shown in Table 12. The closest dumbbell load was typically below the desired SI for females (for example, 25% SI corresponded to 1.17 kg for one subject, and this was rounded down to the available 1kg load, resulting in an actual SI of 21.33%) and the opposite was true for males, explaining the differences in actual and desired SI between sexes.

Ten Prime 13 and 2 Prime 13X OptiTrack cameras (NaturalPoint, Inc., Corvallis, OR, USA), sampling at 180 Hz, obtained motion data required for calculating torque. The highest mean calibration ray error was .6mm and mean calibration wand error was .1mm. A 27-marker set by Optitrack [246] was utilised, enabling tracking of the upper body. Markers were attached to the participant using double sided sticky tape and Velcro.

Tasks

Subjects completed four tasks, Figure 21:

- Static at 25% (S25); the shoulder joint was flexed 90° to the trunk with the arm outstretched, dumbbell was hand-held in a supinated position, posture was upright.
- Dynamic at 25% (D25); the shoulder joint was continuously flexed between 0° and 90°, where the arm was down by the individual's side at 0°, and in the static task position at 90°.
- Tasks were repeated at 45% load intensity, called S45 and D45.

Other tasks are included in the dataset [242], and were completed in two different orders, refer to the dataset for more information. Furthermore, these tasks involve minimal complexity, providing a basic platform to test and compare the models, and a lifting action such as this is relevant to manual handling and assembly tasks. SIs of 25% and 45% were chosen as there is a rapid decrease in endurance curves around 15-20% SI due to the ischemic effect as a result of intramuscular pressure [247], and there is much disagreement about ETs in this range, as previously mentioned. Thus, 25% was chosen as the first SI to attain an idea of ETs after this rapid decrease, and 45% was chosen as ETs reduce significantly beyond 50% SI.

For the 25% SI tasks, Borg RPE [72] scores (Appendix 13) were attained before the task, 5 s into the task, at 15 s, and every 15 s thereafter [248]. For 45% SI tasks, Borg RPE score was acquired before the task, at 5 s, 10 s and every 10 s thereafter [127], [235]. Experimental ET was recorded as the time taken to reach a fatigued state, indicated by Borg RPE score ≥ 17 [86] or when the correct form could no longer be maintained [88]. As previously mentioned, measuring maximum holding time is a common method used to generate endurance curves [70], [71], [88]. Since endurance models were valid for slow isokinetic cycles lasting 2 s in other research [247], a slightly faster rate (50 beats per min) which still encouraged controlled movement was maintained using a metronome, as quicker movements more closely resemble the rate of real-world occupational tasks. Regarding rest breaks, 7.5- and 10-min were provided for tasks at 25% and 45% SI [27], [67], [119], [236], and tasks could only begin when Borg RPE was 6 or 7, indicating a rested state.

Analysis

Predicted ET was found using six models (*Equation 3.2.1* and *Equations 3.3.1* to *Equation 3.3.5*) and four methods of obtaining $Torque_{max}$, Figure 22. $True\ Torque\ (TT)$ is the required input to all models and is expressed as $\frac{Torque}{Torque_{max}}$, where torque is the sum of the torques acting on the frontal axis of the shoulder (*Equation 3.2.3*, [37], described in the previous section in more detail) and was calculated using joint angles extracted from MoCap data, anthropometric data (Table 11 and [220]), inertia, angular acceleration and dumbbell load, see grey in Figure 22. $Torque_{max}$ is the maximum torque produced by the individual (*Equations 3.3.6* and *3.3.7*), see orange and blue boxes in Figure 22.

Gaps in the position tracking of markers smaller than 90 samples (~.5 s) were filled using cubic interpolation via Motive software (NaturalPoint, Inc., Corvallis, OR, USA); larger gaps were filled with pattern interpolation using surrounding markers as reference. A 4th degree Butterworth filter with a 6 Hz cut-off was used for filtering, takes were exported and run through a MATLAB script to extract joint angles. A simplified approach entailed creating vectors for arm segments using shoulder, elbow, wrist and finger markers and the angle

Figure 21: Arm position at (left) 0 ° and (right) 90 ° during the tasks. During the static task, the 90 ° position is maintained while the arm is flexed between 0-90 ° during the dynamic task at 50 beats per min.

between them were found in sagittal plane.

While torque can be calculated from MoCap data, this method of calculating torque takes the hand-held load into account and can be used with wearables, such as IMUs, which future work aims to incorporate. Torque remains approximately constant throughout the static tasks (as rotational equilibrium is maintained) and it fluctuates throughout each cycle in the dynamic tasks as CoM changes. Since $Torque_{max}$ is a constant, predicted ET remains fairly constant for static tasks and fluctuates throughout dynamic tasks.

$$\|\vec{T}_{shoulder,t}\| = \|\vec{r} \times \overrightarrow{acc}_t \times m - (\vec{r} \times m\vec{g} + I_t \vec{\alpha}_t)\| \qquad \textit{(Equation 3.2.3)}$$

$$Torque_{max} = \frac{Torque \times 100}{\sqrt[0.7546]{\dfrac{1277.9066}{Exp\_ET}}} \qquad \textit{(Equation 3.3.6)}$$

$$Torque_{max} = MVC \times l \qquad \textit{(Equation 3.3.7)}$$

Since the calculation of torque remains consistent, TT varies depending on the method to determine $Torque_{max}$. For TT_1, TT_2 and TT_3, $Torque_{max}$ was approximated by multiplying MVC by arm length, the latter of which was the distance from the relevant joint to mid-palm, *Equation 3.3.7*, Figure 22. However, different methods of quantifying MVC exist among endurance studies. MVC was measured from the shoulder joint in the NICE study [88], while the CE study [37] used 101.6 N for males and 87.2 N for females from elbow MVC tables

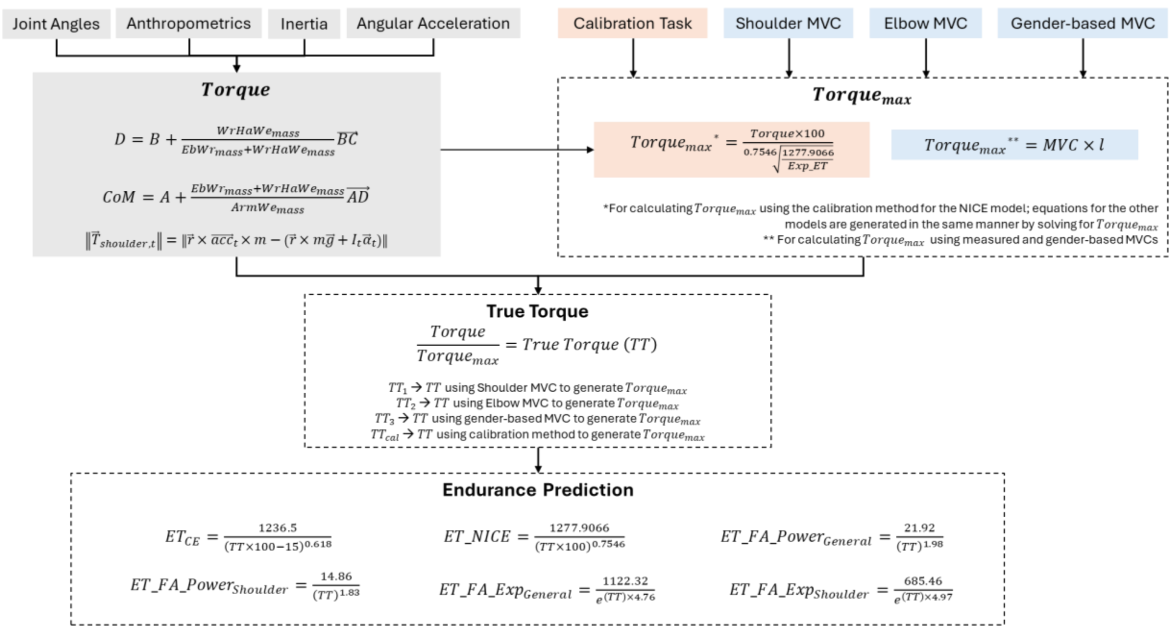

Figure 22: Procedure for calculating predicted endurance times for each of the six endurance models with four methods of obtaining maximum torque, resulting in 6×4=24 different RMSE values.

[160]. Measured MVC from the shoulder (TT_1) and elbow (TT_2) and sex-based tables (TT_3) were used to generate three sets of TTs. Although tasks in this study focussed on shoulder elevation, elbow MVC was included as this joint was used in the HMI-related CE study [37] which included similar tasks.

A new method of obtaining TT using a calibration task, which is called TT_{cal}, was compared to the aforementioned TTs (TT_1, TT_2, TT_3). Instead of measuring MVC, generating TT_{cal} used a calibration task to determine the $Torque_{max}$ that resulted in the correct ET prediction for the calibration task conditions; this $Torque_{max}$ was then used to predict the ET for all other tasks, see orange section in Figure 22. In other words, the torque and experimental ET of the calibration task were inputted into the models that were rearranged to solve for $Torque_{max}$, Figure 22 shows an example with the NICE model (*Equation 3.3.6*). The process was completed using all models resulting in six TT_{cal} per calibration task.

All tasks were assessed on their ability to perform as a calibration task; mean and absolute mean ET errors (%) were used to compare the predictive ability of the tasks to determine which ones perform most effectively as calibration tasks. The TTs (TT_1, TT_2, TT_3 and TT_{cal}) were then inputted into each of the six models (*Equation 3.2.1* and *Equations 3.3.1* to *3.3.5*) and the ability of different models and TTs to predict the experimental ETs of the participants were compared. In this way, the impact of $Torque_{max}$ on ET prediction of the models can be ascertained, and the optimal TT and model can be selected.

MATLAB Curve Fitter was used to assess the fit of experimental data to the curves. All subjects were analysed, then males and females were analysed separately, firstly for all tasks, then in the following groups: static and dynamic tasks, and tasks at 25% and 45% SI. Root mean squared errors (RMSEs) of the TTs with all six models were examined to understand the impact of $Torque_{max}$ on ET predictions and to identify which models, TTs and model-TT combinations (e.g. CE-TT_1 meaning TT_1 was inputted to the CE model) resulted in the lowest error for each sex, movement, and load category. This information may be used to inform which models and TTs are best suited to a specific cohort of individuals under specific movement or load conditions. Experimental data from the NICE study [88] were shared with the authors, to enable RMSE comparisons to be made with the present work.

3.3.3 Results

This section presents the key findings of the study, structured around the primary variables and factors under investigation. First, the influence of personal factors on fatigue and performance metrics was examined, followed by an evaluation of how the choice of calibration task may impact model outputs. Finally, the effects of TT, sex, and task type on the outcomes were explored, highlighting significant interactions and trends observed across participant groups.

Personal Factors

Mean experimental ETs across all tasks were slightly higher for females (Figure 22). At best, moderate Pearson correlation coefficients were achieved when analysing the relationship between personal factors and experimental ETs, showing moderate negative relationships between muscle % and S25, D25 or D45 (>-.394, $P<.05$), and moderate positive relationships between fat % and D25 or D45 (>.427, $P<.05$).

Calibration Task Selection

To determine which tasks performed best as calibration tasks, each task (S25, S45, D25, D45) was analysed to determine which returned the TT_{cal} that yielded the lowest error in the predicted ETs for all other tasks. This was tested on all six models to compare how models perform with a calibration task. Overall, D45 performed best across all models, producing absolute mean ET errors between 20.6% and 22.2%. Following this, tasks were grouped based on load, meaning only 25% SI tasks were used to predict ET of 25% SI tasks and the same for 45% SI tasks, this approach reduced errors compared to using D45 as the calibration task. For 25% SI tasks, NICE with D25 claimed the lowest mean absolute error (9.5%), while NICE

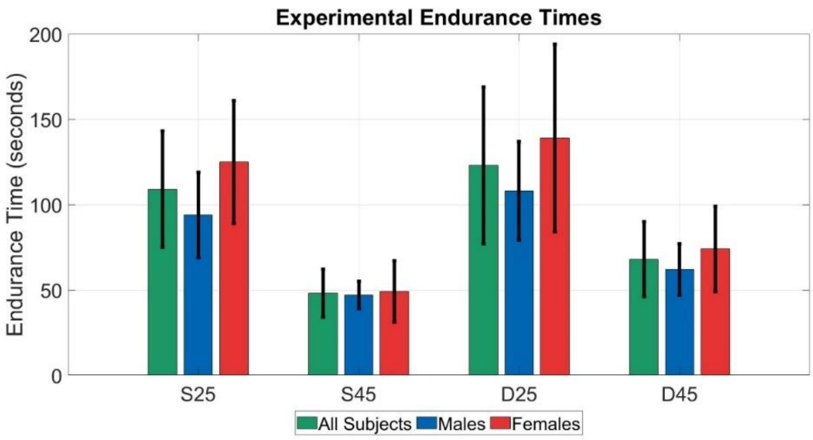

Figure 23: Mean and standard deviation (black lines) of the experimental endurance times for all tasks for all subjects, males and females.

with S25 was at 11.7%; S25 performed better than D25 across all other models but with higher mean absolute errors than the NICE model. For the 45% SI group: D45 performed better than S45 in all models except for NICE, where NICE achieved the lowest error across all models in this load group with an absolute mean error of 9.8% for S45 and 11.8% for D45. Based on this information and the ease of replication of static compared to dynamic tasks, S25 and S45 were selected as calibration tasks for their respective load groups. This means that the $Torque_{max}$ generated for each model using tasks S25 and S45 were used to generate TT_{cal}, as per Figure 22, to predict ETs for all tasks at that load.

Influence of TT, Sex and Task Type

TTs were plotted against experimental ET (Figure 24 for TT_1 to TT_3 and Figure 25 for TT_{cal}), firstly, to show the difference between experimental ETs (data points) and predicted ETs according to the endurance models (solid and dashed lines, [37], [71], [88]); secondly, to show how TT influenced predictions; and finally, to show load, movement and sex differences. TT_{cal} results are in a separate figure (Figure 25) to the other TTs (Figure 24) since TT_{cal} changes with load level and the equation used, this is not the case for TTs 1 to 3, thus TTs 1 to 3 appear in the same figure. Mean predicted ET was plotted in Figure 24 and Figure 25 and since the mean torque resulted in the mean predicted ET for both tasks, mean torque was divided by $Torque_{max}$ to generate TT for these figures. For Figure 24, TTs were labelled depending on MVC, where TTs from measured shoulder and elbow MVCs were TT_1 (red) and TT_2 (purple), respectively, and TT_3 (blue) were calculated using literature-reported sex-based MVCs [160]. It is evident that TT and sex, males in (a) and females in (b), greatly impacted predicted ET; for example, TT_3 resulted in a worse fit to the models than TT_1 and TT_2 for males. The wide range of female experimental ETs made it difficult to determine which model and TT, if any, were best suited to predicting ET; saying this, TT_3 fitted the models for females better than males. Even though the real SIs were within 5% of the target SIs (Table 12), the TT range was much greater than this due to the influence of parameters that were used to calculate torque, such as arm mass and arm length.

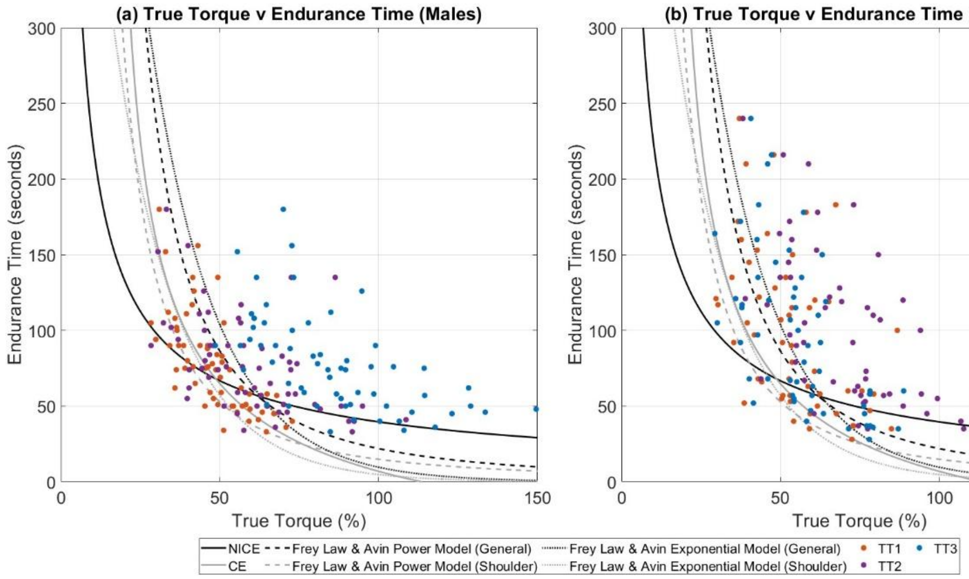

Figure 24: Different methods of determining maximum torque result in dramatically different true torques, the variable used to calculate endurance prediction time, for both (a) males and (b) females.

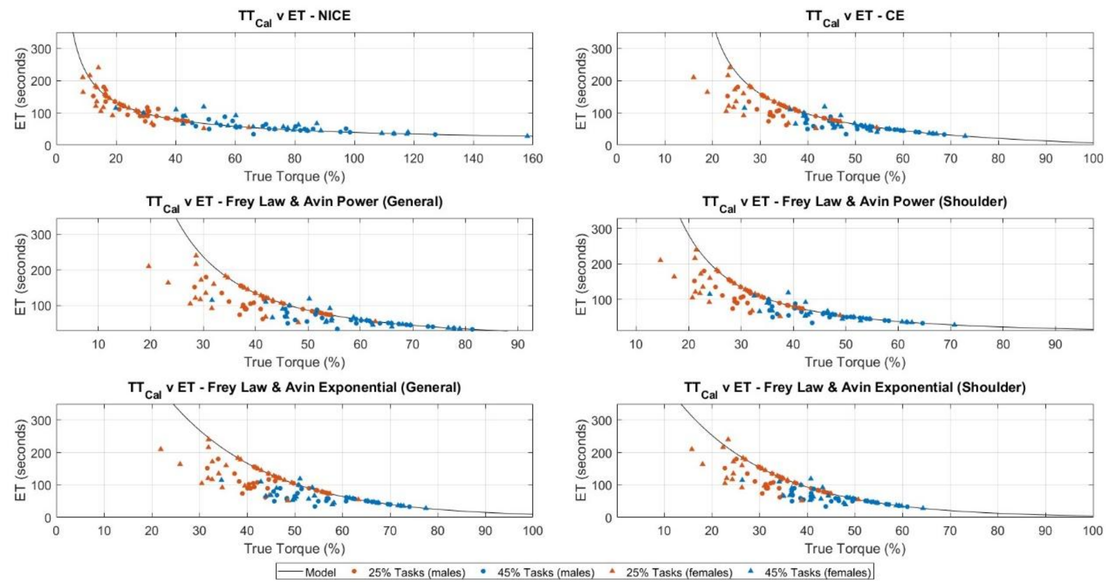

Figure 25: Calibration true torques plotted against experimental endurance times for all models. Static tasks appear on the model curve while dynamic tasks deviate slightly as their true torque was calculated using the torque max of the static task at that load.

In Figure 25, each model is shown individually because a different $Torque_{max}$ depending on the model in question; a sex breakdown is also provided (circles for males, triangles for females). Static tasks appear on the model curve since these tasks were used to generate the $Torque_{max}$ that delivered 0% error, while dynamic tasks appear close to the curves, often following a consistent trajectory, with females deviating further from the curve in general than males with D25. Models typically overestimated the ET of dynamic tasks with this method because experimental ET of dynamic tasks (represented by data points) mostly fall under the predicted ET values (represented by curves), except for the NICE model where there seems to be a more even distribution of data points. This is the opposite for TT_1, TT_2 and TT_3 as they frequently underestimated ETs (Figure 24), particularly for TT_3 with males and for TT_2 with females.

The fit of experimental data (using TT_1, TT_2, TT_3, TT_{cal}) to each of the models resulted in 24 RMSEs each for the following categories: all tasks, static tasks, dynamic tasks, tasks at 25% and 45% SI, for all subjects, males and females. Figure 26, Appendix 15 and Appendix 16 show the RMSEs across all categories, highlighting the models, TTs, and model–TT combinations that resulted in the lowest errors. Across all tasks and subjects (Figure 26), NICE-TT_{cal} performed the best and lowest RMSEs were generated with this model-TT combination (RMSE is 19.11 s for all subjects, 12.16 s for males and 24.45 s for females). The TT_{cal} column in Figure 26 includes the combined RMSE of static and dynamic task, note the 0s RMSE for static tasks using TT_{cal}, as shown in Appendix 15 (a) and (c) which gives a breakdown of static and dynamic tasks by sex. For dynamic tasks, Appendix 15 (b) and (d), NICE-TT_{cal} remains the best performing model-TT combination, where the best RMSE for females was reduced from 56.20 s (best model-TT without TT_{cal}) to 34.58 s (best model-TT with TT_{cal}) and for males from 25.21 s (best model-TT without TT_{cal}) to 17.19 s (best model-TT with TT_{cal}).

Appendix 16 shows a breakdown of SI and sex, where $NICE$-TT_{cal} resulted in the lowest RMSEs for males (14.31 s) and females (31.07 s) for both tasks at 25% SI (S25 and D25), and the remaining model-TT combinations span the following ranges: 32.41 s ($FA\_Exp_{Shoulder}$-TT_{cal}) to 85.81 s ($FA\_Exp_{General}$-TT_1) for males and 52.44 s ($FA\_Exp_{Shoulder}$-TT_{cal}) to 187.50 s (CE-TT_{cal}) for females. Similar to 25% SI tasks, $NICE$-TT_{cal} resulted in the lowest RMSEs for males (9.53 s) and females (15.18 s) for 45% SI tasks, Appendix 16. Remaining model-TT combinations for 45% SI tasks ranged from 12.26 s ($NICE$-TT_2) to 49.05 s ($FA\_Exp_{Shoulder}$-TT_3) for males and 21.50 s (CE-TT_{cal}) to 52.37 s ($FA\_Exp_{Shoulder}$-TT_2) for females. The introduction of TT_{cal} led to significant reductions of RMSEs across all load levels and subjects. There were consistently higher RMSEs for females at both load levels, however, TT_{cal} narrowed the gap between male and female errors, especially at 25% SI for females, 67.31 s (best model-TT without TT_{cal}) to 31.07 s (best model-TT with TT_{cal}). R^2 for $NICE$-TT_{cal} were .459 for D25 and .314 for D45, denoting a weak explanation of the variability in the data.

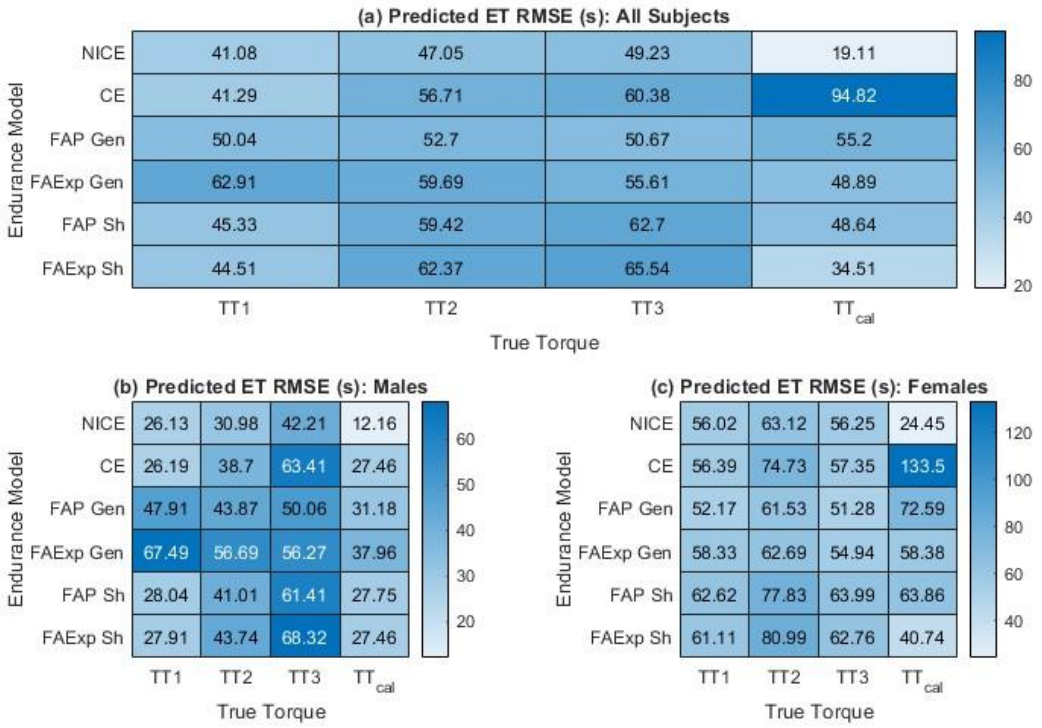

Figure 26: RMSEs for each model and true torque combination for all tasks, for (a) all subjects, (b) males, (c) females. FAP Gen = Frey Law and Avin general power model, FAExp Gen = Frey Law and Avin general exponential model, FAP Sh = Frey Law and Avin shoulder power model, FAExp Sh = Frey Law and Avin shoulder exponential model.

3.3.4 Discussion

This section begins with a summary of the key outcomes, followed by a discussion of how the method to calculate $Torque_{max}$ can influence fatigue estimates. The implications of task type (static versus dynamic) are considered, alongside an evaluation of model fit and prediction accuracy and the influence of personal factors. Limitations of the study are acknowledged, and practical recommendations are offered based on the results. Finally, directions for future research are proposed to further advance the field.

Summary of Findings

This study built on previous research [203] and used six torque-based endurance models to predict ET during lifting and highlighted the impact of $Torque_{max}$ measurement. Unlike traditional models that rely on force inputs and focus on one joint or task [70], [71], [227], [235], [249], the described approach accounted for changes in $Torque$ and considered three joints in the upper extremities, widening the applicability to tasks with different arm configurations. The study's findings offer practical recommendations for improving ET predictions. By conducting static calibration tasks at multiple load levels researchers can determine the optimal $Torque_{max}$ for lifting tasks in a standardised and easily reproducible manner. Future work will focus on assessing the generalisability of this method to other manual tasks. This approach provides a repeatable method for reducing ET prediction errors and presents potential for improving fatigue management in real-world settings. Furthermore, the predictive output supports the move towards proactive fatigue prevention for dynamic tasks which is lacking in the literature [3], [75], and previously mentioned methods in current research, such as [63], [71], [123], [124], [168], [196], do not directly provide.

Influence of $Torque_{max}$

Results highlighted variations in ET predictions based on the method used to quantify $Torque_{max}$. The $NICE$ model, when combined with the calibration approach, demonstrated the lowest prediction errors. The $Torque_{max}$ used to generate TT_1, TT_2, TT_3 with *Equation 3.3.7* may have faced error propagation while $Torque_{max}$ achieved by the calibration method did not. Calibration tasks resulted in reduced errors for both static and dynamic tasks, as mean errors (mean absolute errors) were 7.63% (11.65%) for both 25% SI tasks and -4.69% (9.8%) for both 45% SI tasks, where positive values indicate overprediction and negative to underprediction of ET. ET errors were reduced compared to previous work [203] which used the CE model to predict ET of fatiguing static and dynamic shoulder elevation using only measured shoulder forces for $Torque_{max}$; mean absolute ET errors (and standard deviations) were 28.62% $\pm$ 23.27% for static and 115.45% $\pm$ 70.42% for dynamic tasks.

Static versus Dynamic Tasks

Figure 25 revealed that dynamic tasks exhibited a different endurance trajectory compared to static tasks, with lower mean TT for dynamic tasks at the same SI, due to torque fluctuating during movement. When the arm is outstretched at 90 ° from the trunk, torque is at its peak, but torque decreases as the arm moves closer to 0 °, primarily because r decreases. Meanwhile, the high torque position was maintained during static tasks, resulting in a shift of the dynamic data points to the left (to this lower TT) compared to the static data points completed at the same SI, leading to models generally overpredicting dynamic tasks with TT_{cal} (Figure 25) which can lead to H&S concerns in real-world applications (i.e. endurance limit has been reached before the model predicts). However, $NICE\text{-}TT_{cal}$, with its lower RMSE, showed a more even distribution of dynamic data points, suggesting a better fit and reduced errors compared to other models, Figure 25(a). It was found that endurance models can predict ET for quicker, more realistically paced tasks for workers compared to force-based models that were valid for static tasks and slow movements with sustained contractions [247].

Model Fit and Accuracy

Frey Law and Avin models [71] showed R^2 values between .784 and .897 (using force inputs), while the $NICE$ model [88] had an R^2 of .572. In the present study, the best-performing model, $NICE\text{-}TT_{cal}$ showed lower R^2 values (.459 for D25 and .314 for D45, P<.01), although these were for dynamic movements as opposed to static movements in the aforementioned studies. Interestingly, D25 had a better R^2 than D45, although D45 performed better in terms of RMSE. Despite lower R^2, the RMSE of the $NICE\text{-}TT_{cal}$ model (19.11s) was significantly lower than the $NICE$ model's RMSE (65.23s) [88], indicating improved predictive accuracy.

Personal Factors

Mean experimental ETs across all tasks were slightly higher for females (Figure 23), which is in alignment with studies that found females generally exhibit lower fatiguability than males during isometric tasks at the same SI [118], [239], [250] - similar trends were found during some dynamic tasks [118]. Higher sex-based fatiguability differences were observed for lower velocities and SIs, particularly with elbow flexors [118], [250], and similar effects may apply to shoulder tasks in the present study. Importantly, muscle group and contraction type affect sex differences, where recovery is slower for females in lengthening activations of some muscle groups [250], which can be explored in future research. Additionally, lower actual SIs for females compared to males (Table 12) may have impacted differences. The inclusion of torque denoted increased individualisation compared to force-based models due to the inclusion of arm segment lengths and masses in *Equations 3.3.5, 3.3.8,* and *3.3.9*. Contrary to expectations, fat % showed a positive relationship with experimental ET, while muscle % had a negative relationship. These findings highlight the need for further research to explore the impact of personal factors on endurance.

Limitations

The number of subjects was in alignment with the literature, but this can vary significantly, ranging from 9 [247] and 12 [88], [235] to 40 [162] and 60 [251] participants. A larger dataset could achieve a more representative view of the population, and the narrow age range of subjects (Table 11) does not represent the working population. Measured arm segment lengths could have been considered from the shoulder joint centre [252] instead of the acromion. Additional dumbbells, such as a 1.5 kg dumbbell, may have resulted in actual and desired SIs matching more closely (Table 12) and may impact sex-based differences. Despite participants feeling rested before tasks, there may be a cumulative effect of fatigue that potentially resulted

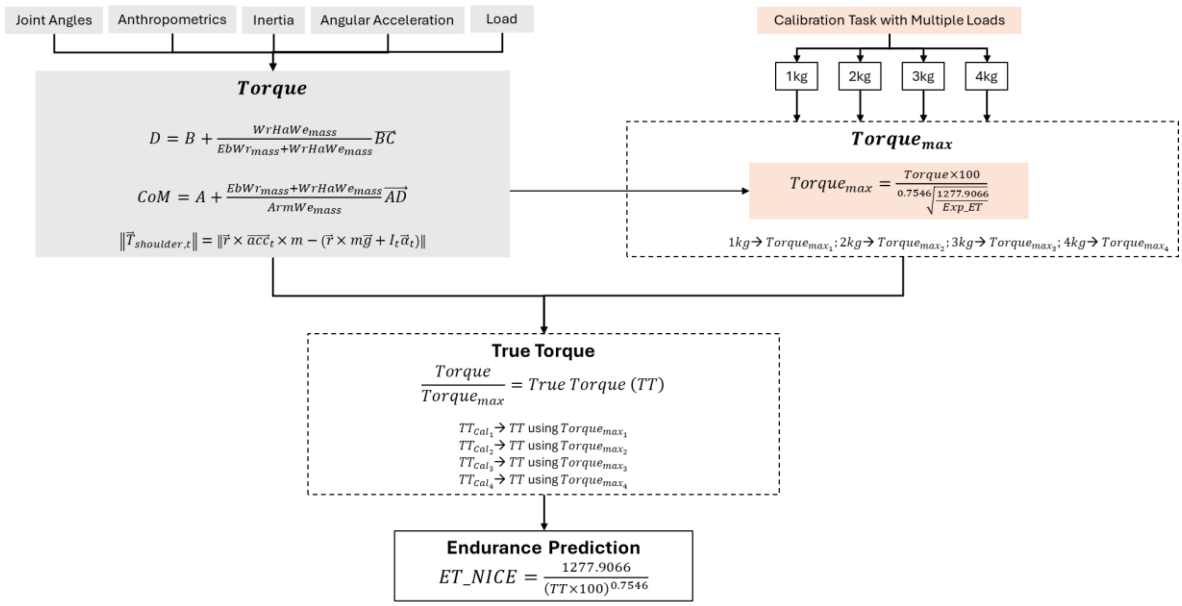

Figure 27: Recommended use of calibration method to determine an individualised maximum torque value for endurance prediction.

in underperformance in final tasks. Other methods of $Torque_{max}$ measurement exist, for example, [161] determines MVC from loadcell, mass and anthropometrics, and [202] uses height and upper forearm volume. These methods and other maximum ET models, listed in [124], were not considered. A straight-arm configuration was maintained in all tasks without consideration of abduction and bent-arm conditions as was done in the CE and $NICE$ studies [37], [88].

Practical Recommendations

New ET models were not developed, instead, alternative inputs and models were compared to reduce ET prediction errors. Static calibration tasks should be completed with multiple loads and the $Torque_{max}$ corresponding to the load in a manual handling task should be used to predict ET, Figure 27. This work established an easily reproducible approach to achieve reduced ET errors that take an individual's fatigability at each SI into account. However, these results may not provide optimal $Torque_{max}$ for tasks other than lifting; different calibration tasks may be more appropriate depending on the specific type of task for which endurance is being estimated. This study offered a significant contribution when modelling endurance with torque for loaded dynamic tasks and provided an alternative approach to measuring $Torque_{max}$ leading to lower errors and potential to reduce errors in more complex tasks.

Future Research

The limitations can be addressed by exploring alternative calibration tasks and comparing the calibration approach to other $Torque_{max}$ measurement methods. Future research can consider posture, individual factors, measured distances to joint centres, applicability to tasks with increased complexity, one-handed versus two-handed tasks and cumulative fatigue using the dataset [242]. Wearables have been used with ergonomic risk assessments [80], [137] and muscle models [99], [196] and may aid in adapting the present work to real tasks and work environments. Although a system incorporating endurance models, IMUs for motion tracking, and pressure insoles for external load estimation could enable fatigue forecasting [3], [75], further research is needed. Thus, a focus on load and task estimation using pressure insoles is the focus of the coming chapters. The results contribute to proactive evaluation of work tasks and help refine endurance models for ergonomic assessment. By improving fatigue predictions, this research supports future advancements in workplace safety and injury prevention, paving the way for more advanced risk assessments and fatigue monitoring solutions.

3.3.5 Conclusion

Six models and four methods of measuring $Torque_{max}$ were used to predict ET of 29 subjects under static and dynamic conditions at low and medium SIs. Predictions varied greatly depending on the $Torque_{max}$ employed. A calibration task which determined the optimal $Torque_{max}$ and the $NICE$ model produced the lowest RMSEs. For all tasks, the mean RMSE was reduced from 41.08 s for the best model without the calibration method to 19.11 s using the calibration method for all subjects, from 26.13 s to 12.16 s for males and 51.28 s to 24.45 s for females. Static tasks at a particular load can be used to calibrate an individual for personalised endurance prediction of dynamic tasks and presents opportunities for improved ergonomic risk assessment while laying the foundation for physical fatigue detection with wearables.

Chapter 4 Load and Task Estimation

This chapter focuses on working towards achieving Objectives 1 and 2 aiming for task generalisability and automatic input of model parameters by continuously extracting data from wearables:

1. assessing how the introduction of wearable sensors affects ET accuracies when input to the endurance model,
2. classifying common industry tasks (such as load-bearing walking, pick and place and assembly, as well as walking and standing) using pressure insoles to determine task-based load inputs to the endurance model.

The studies presented in this chapter are based on the following manuscripts:

- P. O'Sullivan, M. Menolotto, B. O'Flynn, and D.-S. Komaris, 'Evaluating Wearable Sensor Technologies for Predicting Shoulder Endurance', in 2025 47th Annual International Conference of the IEEE Engineering in Medicine & Biology Society (EMBC), Copenhagen, Denmark, doi: https://doi.org/10.1109/embc58623.2025.11253989.
- [253]: P. O'Sullivan, M. Menolotto, A. Visentin, B. O'Flynn, and D.-S. Komaris, 'AI-Based Task Classification With Pressure Insoles for Occupational Safety', IEEE Access, vol. 12, pp. 21347–21357, 2024, doi: 10.1109/ACCESS.2024.3361754.

The work described in this chapter lays the foundation for task generalisability in the SAFE framework and contributes towards the extension of the endurance models (developed in the previous chapter) to any upper extremity task with any load – a key novel contribution of the thesis. The first publication in this chapter, covered in section 4.1 Evaluating Wearable Sensor Technologies for Predicting Shoulder Endurance, analyses how ET prediction accuracies change depending on the methods used to input parameters into the endurance model, moving from a lab-based approach that requires manual input and MoCap data towards a fully wearable approach utilising IMUs and pressure insoles. The results served as a pivotal factor in shaping the final approach taken to meet the project's objectives, where automated load input to the endurance models in the SAFE framework is performed using task classification. More specifically, a load is assigned to a particular task, task classification is used to detect the task taking place and inputs the appropriate hand-held item parameters into the endurance model to ensure ET predictions are adjusted based on task type. This work also highlighted the importance of accurate joint angle measurement as this was shown to impact endurance predictions, and thus contributed to the methods for joint angle measurement and analysis in Chapter 5 System for Activity-aware Fatigue Evaluation (SAFE) Framework: Predictive Fatigue Modelling for Occupational Tasks. Subsequently, section 4.2 AI-based Task Classification Using Pressure Insoles for Occupational Safety describes the experiment (experiment number 4, Appendix 5) where pressure insoles alone were used to classify industry-type tasks using explainable methods, a key novelty of this work. As mentioned in Chapter 2 State-of-the-Art in Workplace Fatigue, Wearables, and WMSD Prevention, explainable AI methods are crucial for trusting classifier decision in the context of occupational H&S, and there is a lack of such methods in research and in the field. The dataset was made publicly available to aid with addressing the lack of open access public sensor data in the field.

The model developed in this chapter is deployed later in Chapter 5 System for Activity-aware Fatigue Evaluation (SAFE) Framework: Predictive Fatigue Modelling for Occupational Tasks where it is used to tune endurance predictions and assign task-specific endurance coefficients, which is discussed in more detail in Chapter 5 System for Activity-aware Fatigue Evaluation (SAFE) Framework: Predictive Fatigue Modelling for Occupational Tasks. In addition, this model showed strong potential for near real-time deployment which is important for future use of the SAFE framework. Overall, this chapter contributes towards expanding the torque-based endurance modelling through the use of wearables (Objective 1) and achieving the task generalisability related objective of the thesis (Objective 2) and bridges the SAFE framework closer to near real-time deployment.

4.1 Evaluating Wearable Sensor Technologies for Predicting Shoulder Endurance

This section is based on work published in the proceedings of the 47th IEEE Engineering in Medicine and Biology Conference and was presented in Copenhagen, Denmark in July 2025.

4.1.1 Introduction

This study presents a comparison of different sensors to see how predicted ET is affected for dynamic shoulder tasks when the NICE endurance modelling approach is used in conjunction with the calibration method defined in section 3.3. This work marks a preliminary step before using the established novel method for endurance prediction using wearable sensors (which is the goal of future work) and marks the introduction of pressure insoles into the experiments in the thesis. Pressure insoles measure the plantar pressure experienced between the foot and the sole of the shoe, and they can be used to estimate total ground reaction forces and the CoP in ambulation [254], [255], [256]. While force plates are considered the 'gold-standard' for load measurement in biomechanics, pressure insoles such as the loadsol® (Novel GmbH, Munich, Germany), F-Scan (Tekscan, Massachusetts, USA), and Moticon (Munich, Germany) allow the collection of pressure data inside and outside a laboratory setting with good accuracy. The present section is the first case of integrating an endurance model with a wearable system for loaded tasks to the authors' knowledge. Therefore, this study analyses offline endurance prediction and lays the groundwork for real-time endurance prediction with wearables, and the effect of alternative wearables on endurance predictions is assessed. The results will inform the design an endurance prediction framework and system for use with the NICE models and novel method of estimating $Torque_{max}$.

4.1.2 Methods

This section outlines the experimental procedures, modelling strategies, and evaluation techniques employed in this study. It begins with a description of the data collection process and experimental setup, followed by the methods used for torque estimation. Finally, the approach for predicting ET and the evaluation metrics used to assess model performance are presented.

Data Collection and Experimental Protocol

Anthropometric, demographic, and wearable sensor data of six subjects (Table 13) were extracted from a publicly available dataset [242]. MoCap data were collected using Optitrak (Natural Point, Inc., Corvallis, OR, USA) and IMUs from MTw Awinda (Xsens Technologies B.V., Enschede, The Netherlands) were both used to obtain kinematic information. Loadsol pressure insoles from Novel GmbH, Munich, Germany, were used to gather load information during the tasks. MoCap used a 27 upper body marker placement, and the system was calibrated using a calibration wand and T-pose. IMUs were calibrated on a level surface using a heading reset and were then placed on the torso, upper arm, forearm and hand according to the manufacturer's guidelines. Pressure insoles were calibrated using the subject's mass prior to each task and data were acquired using the loadsol application. Two tasks from the dataset are included in this study, relating to shoulder elevation movements from 0° to 90°, where a metronome at 50 beats per min guided participants' rate of movement. The task was completed with a dumbbell at 25% and 45% of the individuals' MVC force, measured with a force

Table 13: Subject details.

Subject Details				
Sub No.	**Sex**	**Age (years)**	**Body mass (kg)**	**Height (m)**
1	male	31	85.9	1.85
2	male	34	70.9	1.70
3	female	21	52.0	1.68
4	male	29	94.5	1.75
5	male	28	79.1	1.76
6	female	31	55.2	1.65

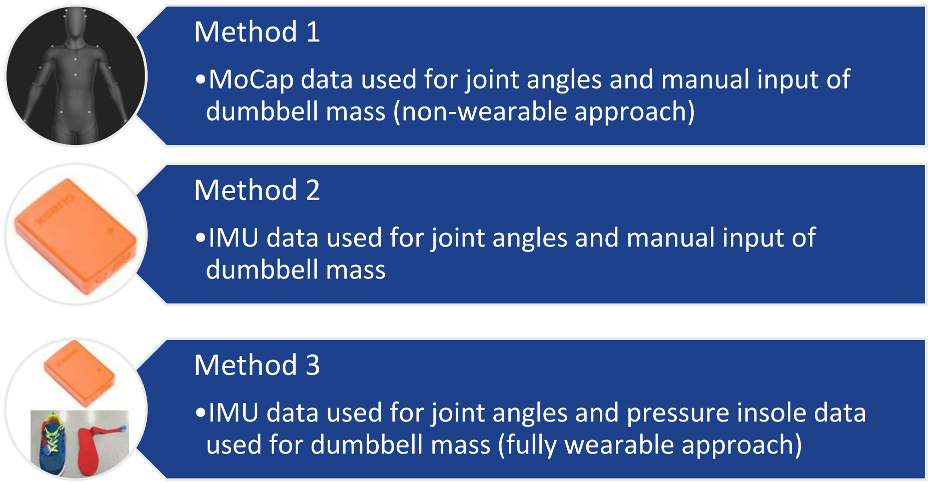

Figure 28: Details of the three approaches used in the methodology.

transducer in the measurement position, i.e. shoulder fully flexed and elbow fully extended. The dynamic shoulder tasks at 25% and 45% of MVC force are named D25 and D45 in the original dataset, and this naming convention changed to 25 and 45 in the present section. All tasks were completed until fatigue, the Borg RPE scale [72] was used to ascertain the subjective fatigue status of the participants throughout the trial and acted as the fatigue reference measure to ensure participants were fatigued at task cessation.

Torque Estimation Approaches

As mentioned, the method to determine the optimal $Torque_{max}$ was explored in section 3.3 and was used for this input. The present study looks at three methods of evaluating torque via wearable sensors (Figure 28). The methods employed are as follows: Method 1 (M1, non-wearable approach) used MoCap data to generate joint angles, and the dumbbell mass was inputted manually to the model; Method 2 (M2) used IMU data to generate joint angles and the dumbbell mass was inputted manually to the model; Method 3 (M3, fully wearable approach) used IMU data to generate joint angles and dumbbell mass was estimated from pressure insole data. A similar methodology has been employed in studies when investigating errors associated with the use of wearables compared to gold-standard technologies when estimating hand forces during manual handling activities [257].

As previously outlined in section 3.2 Validation of Endurance Model for Manual Tasks, the calculation of torque involved for each task required the following inputs: arm segment masses and lengths, CoM location and acceleration (deduced from joint angle data), dumbbell mass and dimensions [37]. Arm segment masses and lengths were taken from the anthropometric data in the dataset and were manually inputted to the equation; CoM was deduced from joint angle data (from MoCap for M1, IMU data for M2 and M3); dumbbell mass was manually inputted for M1 and M2 and determined from pressure insole data for M3. Dumbbell and arm inertia were respectively approximated as a sphere and determined using Winter (2009) [220].

Endurance Time Prediction and Evaluation

Joint angles determined from MoCap data signifies a non-wearable approach as it cannot be easily integrated into a work uniform or environment, but these joint angles act as the ground truth and a basis from which to compare the wearable approaches, as is commonly done in occupational ergonomic studies [18], [75]. The methods with IMU-enabled joint angle detection presents an increasingly wearable approach; the angular distance between the quaternions of the appropriate IMUs resulted in the shoulder (torso and upper arm IMUs), elbow (upper arm and forearm IMUs) and wrist (forearm and hand IMUs) determined the joint angles. For some subjects, an offset was applied to joint angle data from IMU to align with MoCap since this represented the ground truth of joint angles in the present study. For M3, *Equation 4.1.1* was used to determine the estimated dumbbell mass ($\widehat{m}_{dumbbell}$) using pressure insole data. The absolute value was used as, for some frames, the total force from each pressure insole ($Force_{PI}$) divided by 9.81 was less than total body mass according to the pressure insoles. With the inputs, torque and $Torque_{max}$ specified, predicted ET was calculated using *Equation 3.3.1* for each method and the associated errors were found.

$$\widehat{m}_{dumbbell} = \frac{Force_{PI}}{9.81} - Total\ body\ mass \qquad \textit{(Equation 4.1.1)}$$

4.1.3 Results

Three different ET predictions were obtained for the dynamic tasks of six subjects using the outlined method. Experimental and predicted ETs (named E_ET and P_ET) and associated errors are detailed in Figure 29 and Table 14, where the best performing approach for each subject is in bold green. Positive errors indicate overestimation of the predicted ETs compared to the measured experimental ETs and negative errors indicate underestimation.

Mean and absolute mean values for each load level are detailed at the bottom of Table 14, where M3 tended to underestimate values for both tasks (-23.8% for task 25 and -15.3% for task 45), while overestimation was evident in M1 and M2 for task 25 (29.7% and 24.0% respectively). On the other hand, mean errors for task 45 were very low for M1 and M2 (0.6% and -1.9% respectively). However, the mean absolute errors tell a different story with errors of 25.1% and 24.1% respectively, indicating an equal level of under and over estimation of P_ETs for task 45 with M1 and M2. Errors also show task dependency (Figure 29) with overestimation for task 25 and underestimation for task 45, especially for M1 and M2.

Across all tasks, M2 has the lowest errors (absolute mean error = 24.8%) and a mean error of 11.0% indicates general overestimation of ETs when joint angles from IMU data are used. Slightly higher errors are observed for M1(absolute mean error = 30.2%) and M3 (absolute mean error = 29.8%), with M1 generally overestimating ET (mean error = 15.1%) and M3 underestimating ET (mean error = -19.5%).

The IMU joint angles in M2 resulted in reduced errors compared to the MoCap joint angles in M1. While the mean absolute error for M3, where IMU are used for joint angles and pressure insoles are used for dumbbell mass estimation, is only 5% greater than the best performing method, a closer look is required. There is overestimation in ET predictions with IMU data

Table 14: Experimental and predicted endurance times for each subject and task and the associated errors.

Sub	**Task**	**E_ET(s)**	**Predicted Endurance Times**					
			Method 1		**Method 2**		**Method 3**	
			P_ET (s)[a]	***Error (%)***	**P_ET (s)**	***Error (%)***	**P_ET (s)**	***Error (%)***
1	25	90	103	*14.5*	92	*2.5*	101	*12.6*
	45	55	61	*11.1*	57	*4.0*	49	*-10.8*
2	25	62	99	*59.1*	90	*45.3*	41	*-33.5*
	45	34	56	*63.9*	55	*62.5*	41	*21.6*
3	25	135	188	*39.3*	172	*27.7*	58	*-57.2*
	45	92	*61*	*-34.0*	59	*-35.4*	36	*-60.4*
4	25	117	99	*-15.0*	121	*3.7*	110	*-5.8*
	45	88	62	*-29.5*	67	*-24.2*	67	*-23.4*
5	25	105	103	*-1.7*	100	*-4.6*	48	*-54.0*
	45	80	72	*-10.2*	73	*-8.9*	43	*-46.2*
6	25	88	160	*82.2*	149	*69.1*	84	*-4.8*
	45	57	58	*2.0*	52	*-9.6*	73	*27.4*
$\bar{x}$	25	99.5	125.3	*29.7*	120.7	*24.0*	73.7	*-23.8*
	45	67.7	61.7	*0.6*	60.5	*-1.9*	51.5	*-15.3*
$\lvert\bar{x}\rvert$	25	99.5	125.3	*35.3*	120.7	*25.5*	73.7	*28.0*
	45	67.7	61.7	*25.1*	60.5	*24.1*	51.5	*31.6*

Abbreviations: E_ET = Experimental endurance time, P_ET = Predicted endurance time

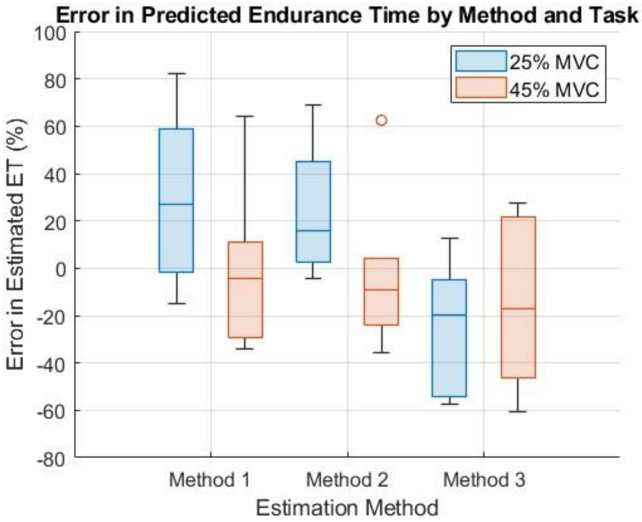

Figure 29: ET errors of the three approaches used in the methodology.

Table 15: The actual and detected dumbbell masses and the associated error.

Sub	Task	Real mass (kg)	Detected mass with pressure insoles (kg)	Error (%)
1	25	3.0	2.4	-20.0
	45	5.0	6.6	32.0
2	25	3.0	11.4	280.0
	45	5.0	8.1	62.0
3	25	1.0	7.9	690.0
	45	2.0	4.8	140.0
4	25	2.0	2.5	25.0
	45	3.0	2.9	-3.3
5	25	2.0	8.1	305.0
	45	4.0	9.8	145.0
6	25	1.0	3.3	230.0
	45	2.0	0.8	-60.0
$\bar{x}$	25	2.0	5.9	251.7
	45	3.5	5.5	52.6
$\lvert\bar{x}\rvert$	25	2.0	5.9	258.3
	45	3.5	5.5	73.7

(M2), but when pressure insole data is included, the predictions seem to lead to ET underestimation (negative error values in M3, Table 14). Looking at Table 15, this ET underestimation is due to the dumbbell masses perceived by the pressure insoles, which are greater than the actual mass due to sensor drift and bias. In the endurance model, the heavier the load, the shorter the predicted ET, which makes logical and practical sense. However, when the detected is heavier than the actual mass, as is the case with M3 (Table 15), this leads to underestimation of ET.

4.1.4 Discussion

The results presented enable the following questions to be answered: (a) Does the use of wearable sensors affect endurance predictions? (b) Is a fully wearable approach to endurance prediction feasible, and if it is not, what changes need to take place to make this feasible?

Figure 29 and Table 14 aids with answering question (a), where differences can be seen across the predicted ETs and errors of the methods. M2 presents the lowest ET errors across the results, likely due to differences in joint angle ranges/values detected by the sensors. Due to the nature of the NICE model, flexion movements that approach 90° result in lower predicted ETs, as this position involves a higher torque resulting in the endurance limit being reached more quickly. For this reason, higher shoulder flexion angles lead to lower predicted ETs, which may be the case for IMU and MoCap in this study as the mean error of 11.0% for M2 indicated less over estimation than the mean error of M1 (15.1%).

Regardless, the implications of a system with such errors would have negative consequences in an occupational setting with real users. The general overestimation of errors in M2 means that a notification would alert the user after the endurance limit has been reached, whereas in an ideal scenario this would happen before fatigue is reached. The high errors in dumbbell mass detection (Table 15) result in higher predicted ET errors (M3, Table 14), therefore the dumbbell mass detection methods require improvement before a fully wearable approach is employed. This leads us to answer question (b), where the results in this study do not reflect that a fully wearable approach is feasible in this manner and adjustments are required to the design of future studies to make this approach more effective.

Improvements to IMU analysis and dumbbell mass estimation may be done via thorough periodic calibration and filters for drift correction. Perhaps lifting load estimation based on upper body joint kinematics using ML [258] or task classification using pressure insoles can be used to input load information as certain loads may be associated with certain tasks. While this section showed high errors with insole data, the next section of the thesis proceeds with task classification using pressure insole data to explore whether task-specific patterns can still yield high classification accuracy. Additional wearable sensors may improve predictions, by considering physiological indicators and additional statistical analyses would provide deeper insights into the performance of the methods with the model.

From a WMSD prevention perspective, the results demonstrate that a wearable sensor system utilising an endurance modelling approach may be effective for predicting physical fatigue in occupational settings (once refinements are made), allowing intervention to take place prior to fatigue onset. According to reviews in the field [11], [13] such proactivity and real-time capabilities are lacking in the literature. A physical fatigue forecasting system based on endurance modelling presents an alternative to online operator monitoring via physiological indicators which face the aforementioned issues with undefined thresholds and inconsistencies with fatigue scales [76], [83], [86]. It also presents an alternative to the ergonomic risk assessments that are currently observationally conducted in workplaces [139], and face criticisms relating to repeatability, reliability and accuracy [18], [138]. Such a system can provide organisations with direct and objective WMSD prevention (typically very expensive due to resource demands) thanks to the compact, portable and accessible nature of IMUs and pressure insoles, especially compared to lab-based optical MoCap systems and force plates.

Future work would take the above considerations into account, as well as testing the models on work tasks in real-time, in accordance with the gaps identified by Kheiri *et al.* (2023) [3]. Some level of manual input would be required, such as body mass and height where arm segment masses and lengths can be found using anthropometric tables [220], [237], and the remaining model inputs would be determined automatically via wearable sensors. Initially, pressure insole data were expected to contribute to both automated load input and task classification in the real-time system, however the results in this section show that significant work is required before automated load detection is possible. Therefore, a focus on task detection via pressure insoles, explored in the next section, may provide valuable information which enable near real-time ET predictions with automated load input based on task type. This work acts as a preliminary step between lab-based endurance modelling with MoCap data (from section 3.3 Improving Dynamic Endurance Time Predictions for Shoulder Fatigue: A Comparative Evaluation) and task specific fatigue prediction in a fully wearable manner which will be explored in Chapter 5.

4.1.5 Conclusion

Three approaches, progressing from non-wearable to wearable, were employed to predict ETs of dynamic shoulder elevation tasks in conjunction with a torque-based biomechanical endurance model. The work demonstrates that including alternative wearable sensors result in different predicted ETs. The use of IMU to generate joint angles resulted in the lowest endurance prediction errors (absolute mean error = 24.8%) compared to errors with MoCap data (absolute mean error = 30.2%). Including pressure insole data for dumbbell mass estimation showed absolute mean error of 29.8%, although this resulted in frequently underpredicted ETs due to dumbbell mass overestimation. Future work will aim to reduce the error margins presented in this work using task classification and deployment of a fatigue prediction system using the torque-based endurance model.

4.2 AI-based Task Classification Using Pressure Insoles for Occupational Safety

This section is based on work published in IEEE Access in February 2024 [253]. Supplementary materials that were published alongside the manuscript are in Appendix 20. This work was presented at the INSIGHT plenary in October 2023, Appendix 21. Changes to this chapter from the published version include more details on the operation of SHAP, which is the explainability analysis used, and the relevance of this work in the context of the thesis as a whole.

4.2.1 Introduction

Research pertaining to pressure insoles extends from sporting to rehabilitation contexts, with studies assessing injuries and patients' recovery [259], [260] and aiding in sports performance [261], [262], [263]. The detection of activities of daily living via plantar pressure mapping has been investigated [264] and shows potential to monitor exercise technique and detect unhealthy posture. In clinical settings, the devices have been used to develop footwear to prevent ulcer recurrence in diabetic patients [265] and to detect freezing of gait in patients with Parkinson's disease [266].

In occupational H&S research, pressure insoles were used to detect loss of balance events [267], indirectly monitor loads on the lower back during manual handling [268], and design insoles that redistribute and reduce pressure on the workers' feet [269]. Specifically in the construction industry, the devices were used to reduce the possibility of back pain [270], quantify physical intensity [271] and workload with the assistance of computer vision [272], identify safety hazards [273], assess fall risk [274] and activity recognition [275], and classify fatigue levels from gait [276].

Task detection is important for both the worker and the employer in the context of Industry 5.0 and can be used to achieve an appropriate trade-off between work targets and the worker's wellbeing. Pressure insoles can be used to detect the CoP and distribution of force throughout the foot while an activity is performed, all of which give an indication of the type of task and the overall workload. Additionally, task detection and the weight assessment of the manipulated object or tool are crucial elements in biomechanical models for human endurance, which are also related to fatigue prevention research. Pressure insoles can be included in the personal protective equipment of smart workers and be fully integrated within a wireless sensing framework of smart manufacturing, leading to the comprehensive overview and monitoring of the safety status of the worker.

In terms of accompanying computational algorithms, ML has long been used in conjunction with wearable sensors to identify the state and activities of the user [153], including gait events [277], common daily activities [278], and even cooking [279]. Classification is important for the monitoring of ergonomic risks and physical activity for health and wellness purposes. De Pinho *et al.* (2017) [280] outlines three categories of activity classification using pressure insoles: gait phases and patterns, common daily activities, and specific activities. A literature review was conducted on studies involving ML algorithms and pressure insoles in line with the three aforementioned categories, and the search strategy and important elements extracted from each paper are presented in Appendix 20. Additional information on open access databases containing raw pressure insole data is provided (Table 16). Most existing datasets focus on

Table 16: Datasets with pressure insoles

Author	Description	Sub	Equipment and Sensors	Associated publication
Chatzaki *et al.* [286]	Parkinson's disease gait with neurologist evaluation	29	PI	[286]
Hora *et al.* [287]	Body size and lower limb posture during walking in humans	49	MC, PI (Pedar)	[287]
Howcroft *et al.* [288]	Fall risk prediction for older adults	75	Accelerometer, PI (F-Scan 3000E)	[289]
Losing and Hasenjager [290]	Three different walking courses in urban settings	20	Gaze, IMU, PI (IEE S.A., Luxembourg)	[291]
O'Sullivan and Menolotto [107]	5 industry tasks	20	loadsol®	Current paper
Wang [292], [293]	6 walking trials, 3 running trials, 4 non-locomotion trials	12	IMU, MC, IT, VC, EMG, PI (Moticon)	-
Yuzhu Guo *et al.* [294]	2 outdoor walking tasks in non-laboratory settings	9	IMUs, PI (F-Scan 3000E)	[295]

Abbreviations: MC = Motion capture, PI = Pressure insoles, IMU = Inertial measurement units, IT = Instrumented treadmill, VC = Video cameras, EMG = Electromyography. All listed datasets are publicly available.

clinical or outdoor scenarios, while the present dataset captures raw force data during industrial tasks (Table 16).

In summary (Tables 1 to 3 in Appendix 20), it was observed that many research groups have used their own custom designed insoles [281], [282], where ML-based classification is often used for validation purposes. It was also evident that there is little consistency in the classification techniques employed, as well as the validation and assessment methods [283], [284], [285]. A high degree of variability in terms of segmentation methods was also apparent, ranging from gait cycle [283] to step [296] to fractions of a second [280], while time windows of different lengths were often used for activity classification, sometimes with an overlapping or sliding window. The majority of activity recognition studies utilise pressure insoles with built-in IMUs [297], [298] and MoCap [299], [300], [301]. The use of additional sensors allows tasks to be distinguished easily, often with higher accuracy, for example [268]. However, in terms of real-world deployment of human activity recognition (HAR) systems, a task classification system based on force data alone has benefits in reducing cost and computing power and minimising the impact of wearables on an individual's daily activities.

Therefore, the present study aimed to use a supervised ML classifier for the task classification of industry-related work activities, using ad-hoc features evaluated on three specific pressure sensor areas in each insole. The features extracted consider both statistical and morphological aspects of force data; force data alone has yet to be considered in HAR research with pressure sensors alone as studies generally benefit from the assistance of accelerometers and/or additional sensors (Tables 1 to 3 in Appendix 20). The explored method of classification was random forest (RF) and the feature analysis method was the SHAP analysis library [302].

SHAP provides a way to interpret model predictions by fairly distributing credit among features, based on principles from cooperative game theory. In this framework, the prediction task is viewed as a "game," where each feature is a "player" contributing to the final output, or "reward." The SHAP value quantifies each feature's average contribution by considering all possible combinations of features and the change in prediction when that feature is added. Therefore, it allows a thorough understanding of the impact each feature has on the overall classification and a within class evaluation provides insights into the impact feature values have on individual classes. While other explainability methods (for example, feature importance, permutation importance, partial dependence plots, etc.) evaluate the influence of a feature on a model's overall performance, only SHAP and local interpretable model-agnostic explanations

(LIME) methods can identify individual feature contributions. While SHAP and LIME are model-agnostic, SHAP is more efficient for tree-based models (i.e., RF) as it traces the tree paths and using the structure of the trees to calculate each feature's contribution efficiently.

RF is commonly used in HAR studies, for example, [280], [303], [304], (Table 2 in Appendix 20), but is utilised in only a few specific recognition studies, such as [267] and [305]. An explainable approach through RF and SHAP enables transparency, and therefore trust, in the decisions made by the classifier, which is essential in a H&S context. This is important since ML models will be used to make decisions that ultimately affect the health of workers and it is imperative to understand how and why decisions are made, furthermore, trust is required for device uptake and worker acceptance. Additionally, important features required for task identification can provide insights into how insole-based sensing systems can be optimised for real-time task classification.

The collection of insole pressure data created in this study has been made openly accessible through the publication of the open access database on Zenodo [107]. While the focus of the study was the industry sector, the present research is relevant to all areas of occupational H&S research since manual handling, assembly and pick and place tasks are required in almost all professions to varying extents; and as such, manual handling training is a requirement in most workplaces.

The contributions of this work include the use of explainable ML methods for the task detection of five common occupational tasks; analysis of the most significant features highlighted by the SHAP analysis which give rise to recommendations for the future design and optimisation of pressure insoles for occupational H&S specifically, as well as an open access dataset of pressure insole data included in the study. Overall, the sensors, the features extracted from these sensors and their analyses for enhanced explainability, and the creation of a new open-source database of pressure insole data for task classification present valuable contributions to the development of accurate, cost-effective and streamlined real-time HAR systems for smart manufacturing. Task recognition of common work activities, such as those presented in this study, can aid in the real-time detection and prevention of WMSDs. Different tasks are associated with different levels of fatigability, depending on factors such as load [40] and task complexity [47], and using the methods described in this paper, the operator's state can be monitored with information from pressure insoles such as task type, duration, and load.

4.2.2 Methodology

In this section, the participants and data collection methods are described as well as the features extracted, and analyses employed to achieve explainable work task classification.

Participants

Twenty subjects (ten females) were recruited by word of mouth and email advertisement to take part in the study. The mean age of the subjects was 29 years and ranged between [20 64] while their weight ranged between [53.5 102.7] with a mean of 71.6 kg. Participants completed a brief warm-up routine for 5 mins and were given manual handling training prior to data capture.

Data Collection

Subjects all wore the same type of trainers containing loadsol® pressure insoles (i.e., the same insoles used in section 4.1 and later in Chapter 5), which sample at 100 Hz, in a choice of three sizes (EU 39, 43 and 45). Subjects with different shoe size did not qualify for participation in the study. Each insole samples force data from three areas: heel, midfoot and forefoot. The heel and midfoot sensors each occupy 30% of the insole length, and the forefoot takes up 40% of the insole length.

Each participant carried out five tasks for at least 1 min each, of which 55 s were analysed for data balancing purposes. The first was standing still in static posture (Task 1); the second was level walking (Task 2), where, prior to the task, subjects were advised to change the direction and speed of their ambulation. The next three tasks were industry-related; they were assembly (Task 3), pick and place (Task 4) and manual handling (Task 5).

Figure 30 shows 3 s of force data for all tasks. All subjects changed their walking direction and speed throughout Task 2, at a self-elected time and speed. The assembly task involved piecing together 3d printed bolts and nuts and taking them apart repeatedly until 1 min of data were acquired; the parts were laid out in a semicircular arrangement on the workbench within arm's reach (approximately 25 cm) of the participant (Figure 31). The pick and place task involved moving light weights (.5 kg and 1 kg) from one corner of the table to the other in a self-selected manner and speed; more than one weight could be moved at a time, and weight(s) could move diagonally, side-to-side, or straight ahead. Finally, the manual handling task required the subject to lift a box containing a 10 kg weight from the floor to a chair (height of 48cm) to a table (75cm); again, at a rate subjects chose, and the order of lifting was not prescribed (for

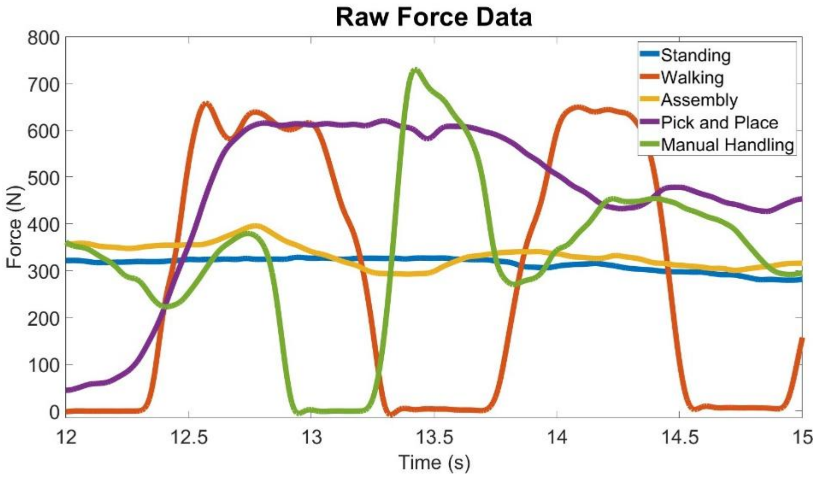

Figure 30: A snapshot of raw force data for one subject's left foot during each of the five tasks.

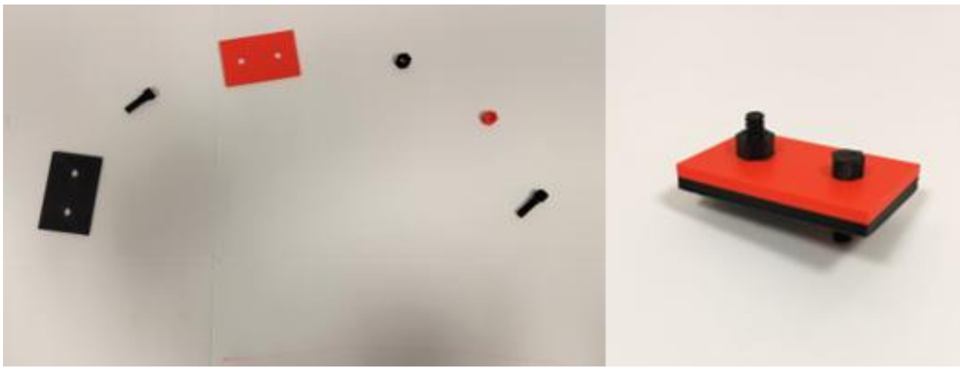

Figure 31: The set up of the components for the assembly task (left) and the assembled components (right).

example, from the floor to the table and finally to the chair). Participants were instructed to carry out the tasks continuously at a self-selected rate for at least 1 min and in the order they chose (for manual handling, assembly and pick and place tasks), thus enabling the classifier to also take into account the individual differences that take place during the completion of tasks.

Feature Extraction

Space-temporal and morphological information were extracted from raw data provided in force (N) from the commercial software accompanying the pressure insoles (loadsol-s), to create the training and testing datasets for the ML classifier. Features from force data, CoP and morphology of the peaks were obtained over different time windows (2, 3, 4, 5, 6, 8, 10, 12 and 15 s). By evaluating these varied time windows, we aimed to address model performance across different temporal resolutions, aligning with the needs of real-time applications. A total of 24 features (explained below) that provided a detailed representation of the peaks and pressure dynamics of the force signal were extracted from the data; where the number of features related to force, CoP and peaks morphology were 11, six and seven, respectively. The total number of data points per feature was calculated by: (total no. of samples ÷ number of samples per window) × no. of tasks. Table 17 details the total number of data points for each of the windows considered. For example, for 55 s of data acquisition at 100 Hz and considering an observation window of 2 s, for five tasks: 5500÷200=27.5, rounding down and multiplying by the number of tasks there are 27×5=135 data points for the 2 s window and total data size of 24 features ×135 data points.

1) Force-related values: Force-related features (all in N) were calculated for the total force of the insole and included mean value, standard deviation, range, median value, mode, interquartile range, skewness, covariance, and kurtosis, as well as the ratio of the forefoot force to the heel force (mean and standard deviation), which were calculated using only forefoot and heel sensors.
2) CoP values: The CoP coordinates on the ground plane were evaluated considering fixed distances between the three pressure sensors of each insole during foot flexion/extension, and a constant distance between participants' feet. The X and Y position of CoP in cm considering the origin on the axis (0,0) between the feet, was evaluated as follows:

$$X_{CoP} = \frac{\sum_{t=1}^{n}\left(\frac{D_f}{2}F_t^L + \frac{-D_f}{2}F_t^R\right)}{\sum_{t=1}^{n}\left(F_t^L + F_t^R\right)} \quad Y_{CoP} = \frac{\sum_{t=1}^{n}\left(\frac{S_f}{2}F_t^F + \frac{-S_f}{2}F_t^H + F_t^M\right)}{\sum_{t=1}^{n}\left(F_t^F + F_t^H + F_t^M\right)}, \qquad \textit{(Equation 4.2.1)}$$

where t is the data sample that goes from 1 to 5500 (55 s of acquisition at 100 Hz), D_f is the mean distance in cm between the feet, evaluated on the basis of the body segments length based on the average height of the cohort (as per [220]), as $D_f = 171 \times .191$. S_f is the weighted mean size in mm of the shoe used by the cohort, evaluated as $S_f = \{[(39 \times 9) + (43 \times 9) + (45 \times 2)] \div 20\} \times .6658$, where the last value is the conversion between European shoe size to cm. ${F_t}^L$, ${F_t}^R$, ${F_t}^F$, ${F_t}^M$ and ${F_t}^H$ are respectively the contribution in Newton of the sensors of the left insole, the right insole, the front pressure sensors of both insoles, the middle sensors of both sensors and the heel pressure sensors of both insoles. From the value of the CoP, three statistical values were evaluated per each coordinate (X and Y): mean value, standard deviation, and range (in cm).

3) Peak morphology values: The dynamic behaviour of the pressure values can vary according to the task being performed. The static task might produce uniform pressure

on the overall insole over time; while activities where the body weight moves from one foot to the other or goes across different areas of the same foot produce peaks and valleys in the data. To capture such behaviour, time-domain and frequency-domain features related to the morphology of the pressure values were evaluated for each window per total insole force value:

a) Shaper factor – gives an indication of peak profile:

$$SF = \frac{\left(\frac{1}{N}\sum_{i=1}^{N} {D_i}^2\right)^{\frac{1}{2}}}{\frac{1}{N}\sum_{i=D}^{N}|D_i|} \qquad \textit{(Equation 4.2.2)}$$

where N is the number of data sample per time window of observation and D is the sample data.

b) Peak to peak value – difference between the minimum and the maximum value of the pressure within the time window in Newton.
c) Number of peaks per time window – number of peaks that exceed 60% of the maximum value of pressure, within the time window.
d) Mean distance between peaks that exceed a 60% threshold of the maximum value of force within the time window in seconds.
e) Mean amplitude of peaks within the time window in Newton.
f) Standard deviation of the spectral power distribution (discrete Fourier transform) within the time window.
g) Main frequency within the spectral power distribution (discrete Fourier transform) – excluding the peak at 0 Hz, the main frequency was extracted per each time window.

Training and Assessment of Supervised Machine Learning Classifier

The features extracted per each time window were labelled according to the task being performed and were used for the training process of the RF classifier. Note, due to varied movement rates of participants, key activity phases (for example, lifts) were executed at different points within the time windows. Support Vector Machine, k-Nearest Neighbour and Naïve Bayes were evaluated; they all offered considerably worse performance. These classifiers were omitted for brevity, however, the code for all classifiers and the associated database of extracted features can be accessed online at https://github.com/patricia-o-sullivan/PID4TC_Analysis.

Table 17: Total data size per window = (total no. of samples ÷ number of samples per window) × no. of tasks

Time window	Frame per window	Data points per feature	Data points per window
2	200	27.50	135
3	300	18.33	90
4	400	13.75	65
5	500	11.00	55
6	600	9.17	45
8	800	6.88	30
10	1000	5.50	25
12	1200	4.58	20
15	1500	3.67	15

[a]Total data size per time window of observation, where the number of data points per feature is the total no. of frames ÷ no. of frames per time window, and the rounded down no. of data points × no. of tasks gives the total data points per window per subject.

A 10-fold cross-validation was employed to train and test the data, where each fold contains all the measurements for two subjects. This split guarantees the model is learning patterns that can generalise to unseen subjects. For each fold and time window, accuracies were computed from the confusion matrices, and the classifier was assessed using SHAP to evaluate feature importance. SHAP values are assigned to each feature, representing its influence on the predicted outcome relative to the other features in the dataset, where high SHAP values indicate a high influence. The analysis also provides insights into the influence of features on each task individually by indicating if a high or low feature value influences the classification of a particular task. Cross-validation and SHAP results for the folds were aggregated for each window.

The highest performing features, based on the SHAP analysis, were rerun through the classifier in the same way as described for the first iteration of the analysis to gain an understanding of how fewer features impact on accuracy.

4.2.3 Results

This section details the dataset associated with this work and describes the classification results, including the features that most strongly influenced classifier outputs.

Pressure Insoles Data for Task Classification (PID4TC)

Pressure insole data used in this work are available at doi: 10.5281/zenodo.7755802 under CC.BY.40 license [107]. The dataset is composed of .csv files and is accompanied by relevant metadata (.txt files) for database description and navigation. PID4TC is organised by subjects, where each .csv contains 55 s of acquisition at 100 Hz, organised by task.

Industry Task Classification

The accuracy of the classifier ranged from 80-86%, with a gradual improvement as the observation windows increased (Figure 32). The highest accuracy (≈ 86%) was observed for windows larger than 10 s (1,000 frames), while reaching a peak of 82% after 5 s before the value briefly declines. Task prediction that takes place within 5 s can be considered 'real-time' and offered good accuracy, thus prompting further analyses. The confusion matrix of the 5 s window iteration is presented in Figure 33, with the highest accuracies for manual handling and walking (dark shaded values), closely followed by assembly and standing tasks. Pick and place was incorrectly predicted as either assembly or standing tasks approximately 45% of the time.

Figure 34 highlights the features that have the most impact on the classifications shown in Figure 33, quantified by SHAP values. Higher positive values (visible in Figure 34-Figure 37 and Figure 40) indicate positive contribution to the prediction, i.e. it leads to the identification of that class, while lower negative values (evident in Figure 35-Figure 37) indicate negative contribution to the prediction, i.e., it helps to rule out that class. Overall, the features related to the CoP (SHAP impact values: range in y direction ≈ .25, range in x direction ≈ .21, mean in x direction ≈ .18, std in x direction ≈ .14, std in y direction ≈ .12), spectral entropy (≈ .10) and morphology of the peaks (distance between peaks in seconds ≈ .08) played a major role in the classification of all tasks. Furthermore, statistical features extracted from force data, such as covariance (≈ .09), standard deviation (≈ .09), and the ratio of the front of the foot to the heel (≈ .08) were also prominent. The SHAP analysis also gives a within task breakdown of feature

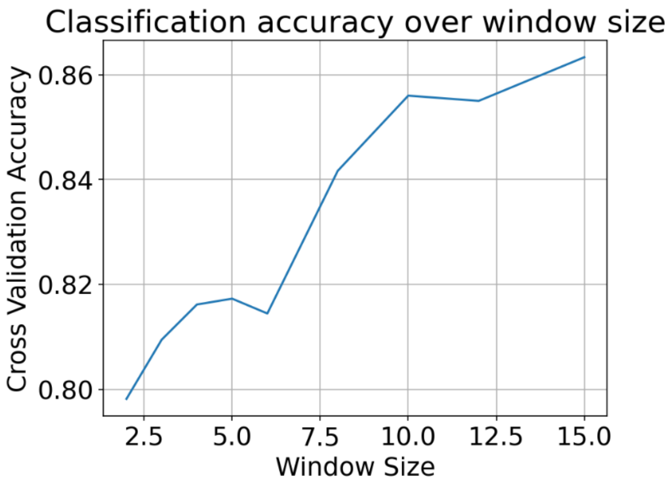

Figure 32: Accuracies of the random forest classifiers across all nine observation window sizes (2, 3, 4, 5, 6, 8, 10, 12, and 15 s).

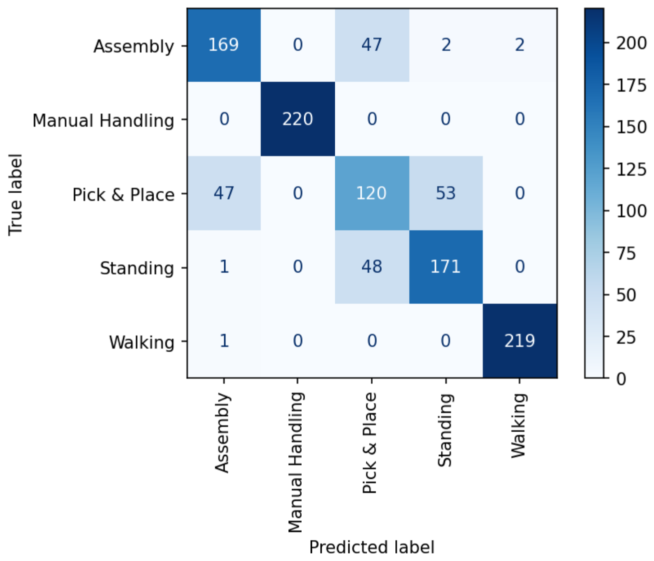

Figure 33: Confusion matrix showing the prediction accuracy for the 5 s observation window.

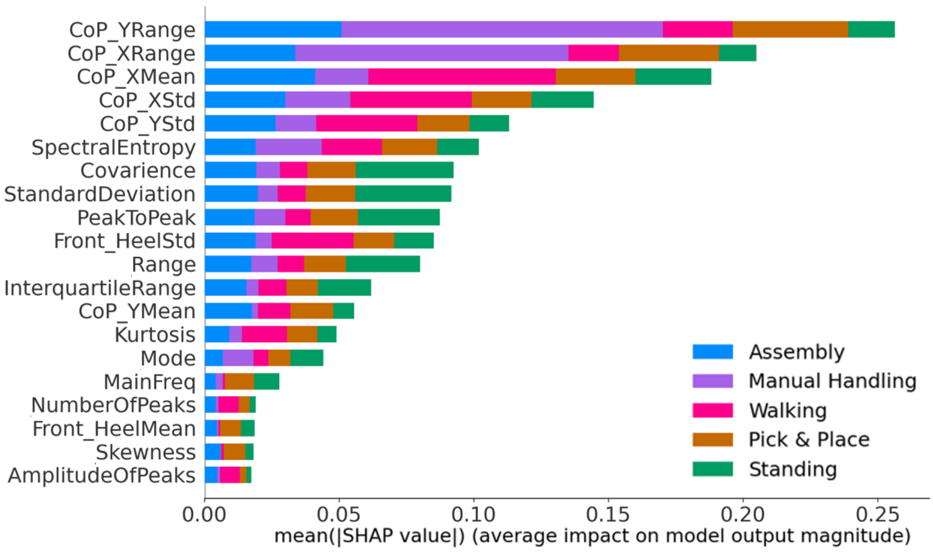

Figure 34: Analysis of feature importance for the 5 s observation window.

importance by calculating a score for all the input features for a given model, resulting in a range of SHAP values for the twenty highest scoring features in a class (coloured regions for each feature, Figure 34). Manual handling, walking and assembly tasks were misclassified the least (Figure 33) due to the strong influence of the feature values on the classification of these tasks; hence, in Figure 34, these tasks carry greater SHAP values (e.g., purple-shaded zone for the manual handling task in the CoP YRange feature).

Figure 35 to Figure 37 also provide insights into feature importance within tasks with the overall highest SHAP scores: manual handling, walking and assembly. A clear contrast in feature values is present in the highest impacting features (high SHAP values) which is evident from the high colour contrasts assigned to the ranges of SHAP values. This means the large magnitudinal differences in feature values, especially in CoP, aided in the identification of tasks. High values of the CoP range resulted in high SHAP values (≈ .2 to .3) for manual handling (Figure 35), while low CoP ranges were found to be impactful (up to ≈ .1) on the classification of walking (Figure 36) and assembly (Figure 37). High values of CoP standard deviations and mean in the x direction (up to ≈ .20) for walking and (up to ≈ .10) for assembly helped for their respective categorisations. In addition, a decreased classification accuracy was observed in the confusion matrix for tasks where the CoP is more confined (Figure 33 andFigure 38), for example, pick and place and standing. The natural shift of the weight along the sagittal and coronal axes (changes in CoP) varies depending on the task, to the greatest

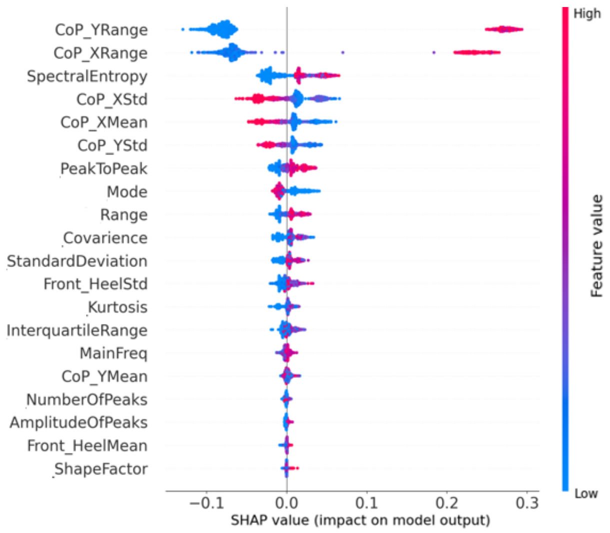

Figure 35: SHAP analysis of feature importance for manual handling in the 5 s observation window.

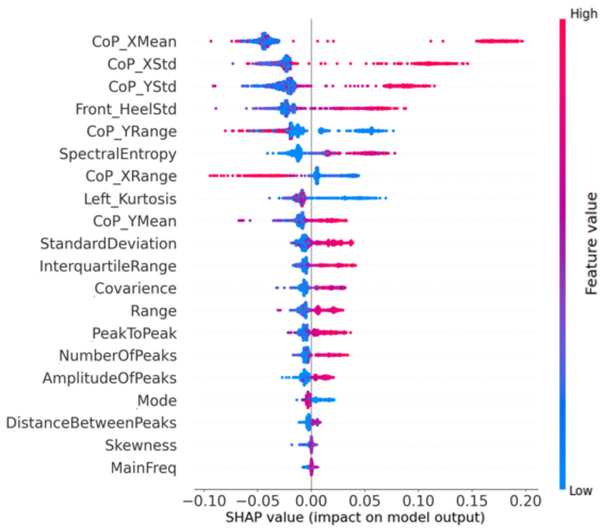

Figure 36: SHAP analysis of feature importance for walking in the 5 s observation window.

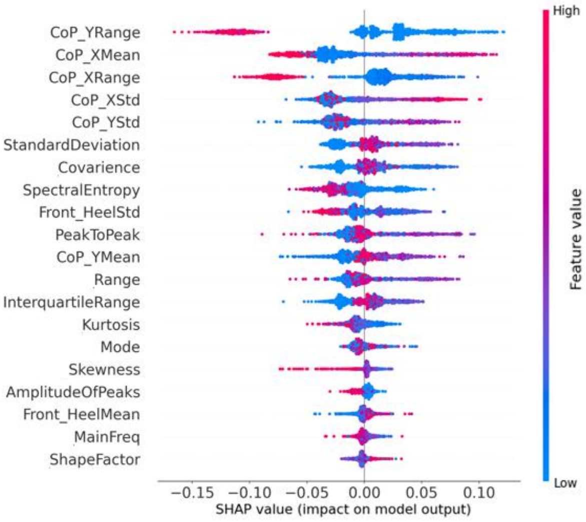

Figure 37: SHAP analysis of feature importance for assembly in the 5 s observation window.

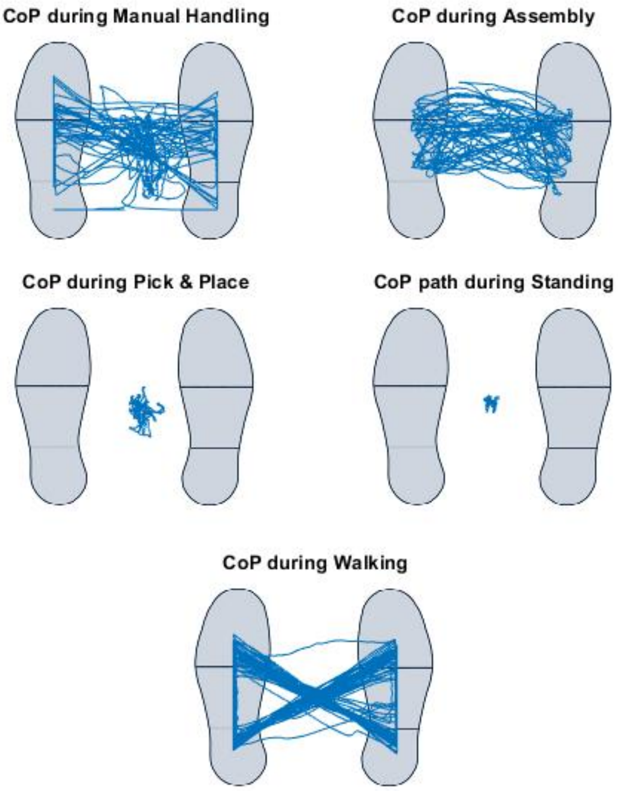

Figure 38: Example of the trajectory of the CoP for each of the five tasks for one subject.

extent during manual handling and walking and to a lesser extent when manipulating objects while both feet are stationary; this, results in a broader range of feature values with higher associated SHAP values as it is easier to distinguish features that vary depending on the task.

The analysis was repeated using only the top five features from Figure 34, all of which are CoP related features: range and standard deviation in both directions and mean in the x direction.

The second RF classification returned marginally better accuracies across almost all windows, including the 5 s window which increased by 1% to 83% (Figure 39). Figure 40 focusses on the SHAP analysis for the 5 s window, with highest SHAP values still associated to manual handling, walking and assembly. Interestingly, the mean CoP in the x direction became the most influential factor in the reanalysis, jumping up from third (Figure 34). Overall, higher SHAP values are present in the new analysis (Figure 40) compared to the analysis containing all features (Figure 34), as the mean CoP in the x direction attained a mean SHAP value of approximately .45, and all other features achieving a score higher than ≈.25, which was also the highest SHAP value in the initial analysis. In addition, the confusion matrix in Figure 41 shows fewer misclassifications for the updated analysis. The exclusion of lower impact features caused a small reduction in misclassifications, while there was no increased risk of over-fitting.

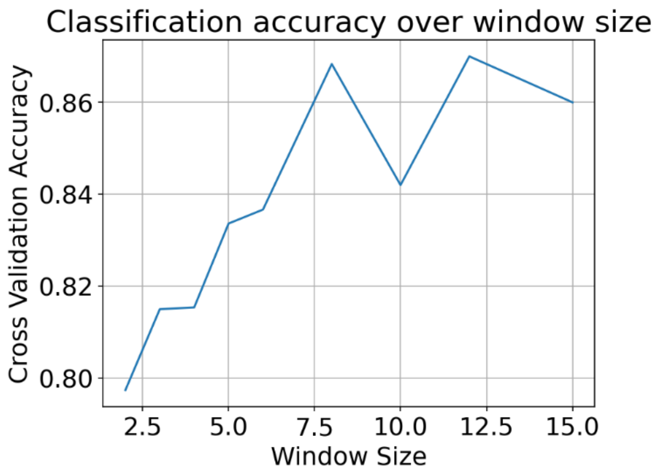

Figure 39: Accuracy values across all windows after re-analysis with the five most impactful classification features.

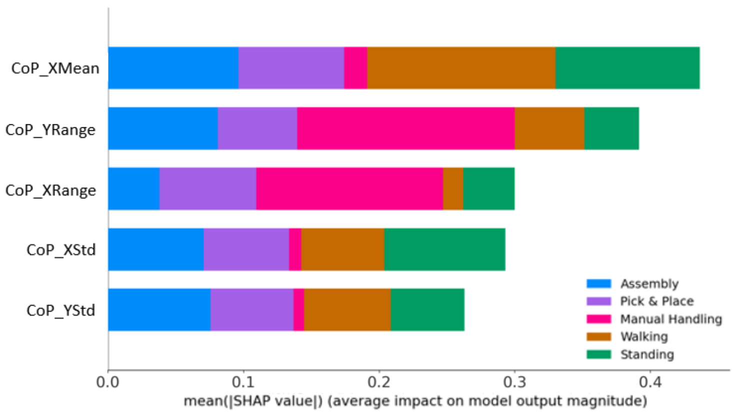

Figure 40: Analysis of feature importance for the 5 s observation window and the highest performing features.

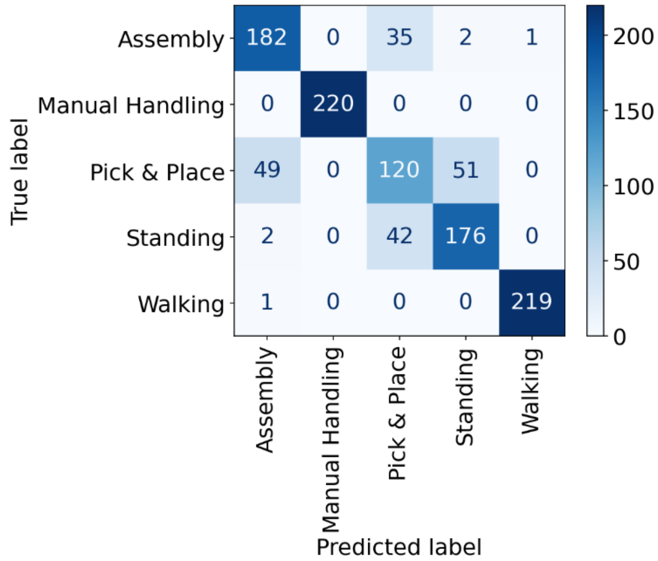

Figure 41: Confusion matrix showing the prediction accuracy for the top 5 features in the 5 s observation window.

4.2.4 Discussion

This study investigated the use of pressure insoles for human task classification in the context of occupational H&S. Pressure insole data were collected from 20 subjects while performing five industry-related tasks. From the raw data, 24 features were evaluated and labelled to form the training dataset for the RF classifier. The best classification accuracy produced a rate of 86% above 10 s of data observation. While the purpose of the study was to present a highly explainable classifier, and not necessarily to achieve the highest possible accuracy, the methods show an accuracy of 82% was reached after 4 to 5 s, which is in alignment with the accuracy levels achieved in the classification of other occupation-specific tasks [306], [307]. The 4 to 5 s time window is aligned with studies concerning activity recognition classification (Table 3 in Appendix 20, e.g., [276], [308]) and indicates potential for real-time classification in edge-AI capable devices. In a real work environment, 5 s is a realistic time frame to collect sufficient samples for classification that is robust to momentary changes in activity, for example, standing still for an instant before picking up an object and assembling. To further improve real-time predictions in working environments, a sliding or overlapped time window can be implemented in future applications, as was done in [308], [309], to take the previous activity prediction into account in combination with new data.

Occupation-specific studies generally feature a maximum of ten subjects (Table 3 in Appendix 20), making the number of subjects in the present study higher than other occupation-specific studies, but is on the middle to lower side when compared to all ML research involving pressure insoles (Tables 1-2 in Appendix 20), and therefore remains a limitation to the study.

Additionally, the cohort may not be representative of the population as they do not have industry work experience. Other limitations include the completion of tasks in a laboratory as opposed to an industry setting which typically features more noise, and the inclusion of a subset of possible industry tasks. Tasks had low complexity and were performed in an isolated manner, and no transitions were considered. Only one type of pressure insole with a three-sensor configuration was utilised in the study. Given that previous work showed high errors at lower loads (Table 15), it is likely that the present study, with a much greater load, would result in higher absolute force measurement during the loaded industry-type tasks. However, since CoP is a relative force measure, errors in absolute force measurement did not contribute as heavily to the classification. Regardless, absolute force measurement will need to be addressed in future work by improving sensor stability, calibration and drift.

The release of the raw data, database of extracted features, and classifier code encourages transparency in the analysis methods, and the use of 10-fold cross validation and accuracy as the main measure of prediction success enables pressure insoles and ML studies to be compared, since these are the most frequently occurring approaches in recent years (Appendix 20).

ML algorithms, such as the one employed in this study, use the labelled data to establish a function that can map the features' correlation to a specific label. Some ML techniques, for instance RF, allow a more direct evaluation of the importance of each feature in the classification process. Such characteristics related to interpretability [64], are particularly relevant to industrial applications. In fact, for safety and regulatory reasons, it is preferable to implement AI-based techniques that take decisions based on models that can be fully understood in human terms, while a black-box decision-making behaviour can lead to a lack of trust. While deep learning (DL) models showed high classification accuracies in Appendix 20, and a subset of DL models provide a certain degree of explainability, it was decided not to proceed with a DL approach for a number of reasons. Firstly, a relatively small dataset is concerned in this study, and a DL model is more likely to overfit. Secondly, while feature extraction in the present work requires computation inputs were reduced to 5 features, and DL models would be more computationally demanding due to multiple layers and operations which limits the ability to deploy low-cost embedded devices. In addition, DL model structure is strongly dependent on the domain and the dataset, while the current approach using standard ML techniques can be easily and quickly adapted to a different dataset and problem. Finally, while SHAP can be applied to any model, the fact that the Shapley values are computed using a TreeExplainer makes it more related to a RF classifier, making the provided explanation more reliable in this study.

RF was employed in this study since it is a non-linear ML technique that provides good classification performance and interpretability balance. Due to the limited dataset, it was decided to not proceed with the hyperparameters tuning as the result of the cross-validation process would likely cause overfitting, rather the default parameters were kept. A comparison with other models where the parameters have been kept as default is available in the accompanying GitHub repository. In general, RF performed better, which can be verified from the analysis script stored in the repository.

SHAP analysis is advantageous over other feature performance analyses because it provides a within class feature importance breakdown, and the impact feature values have on the class prediction. This information is valuable from the perspective of studying misclassifications and improving classifier performance as an understanding of what features are causing misclassifications is gained, and the most impactful features can be selected for modelling to reduce incorrect predictions and increase accuracy, as was the case in the present study. From the SHAP analysis, CoP features were identified as having the highest impact (Figure 34 to Figure 37), and included the ranges, standard deviations and the mean in the x (medio-lateral) direction. These features produced the highest accuracy (83%) and SHAP values (between ≈.25 to .45) for the 5 s window when classified alone (Figure 39 to Figure 41). This indicates that the number and disposition of the pressure sensors can be optimised for CoP, encouraging enhanced task classification in comparable set-ups. For example, a two-quadrant (front-back) or four quadrant sensing disposition (front-left, front-right, heel-left, heel-right) could offer more precise information in this regard. This will aid in keeping the number of sensors to a minimum, optimise wearability, data throughput and energy consumption, all of which are crucial factors in edge-AI devices, internet of things and smart manufacturing environments as a whole. Application-focused insoles may also aid in reducing the number of task misclassifications, which, with the current pressure sensor number and configuration of the insoles may affect productivity and pose H&S risks. For instance, a worker is engaged in a pick and place that is erroneously detected as assembly or rest may lead to a collaborative robot operating in the occupied workspace or there may be implications on task rotations, work scheduling and active work time registered.

To minimise computational requirements and power consumption, force data only were analysed from the pressure insoles, and no additional sensors were utilised in the classification. This represented a challenge compared with similar works, where the classification mostly involved diverse tasks with dynamic characteristics that are more easily distinguished from one another, and in some cases, a variety of sensors were utilised ([280], [284], [307], [310]). In this sense, the features selected for the classification played a crucial role. The general approach was to focus on describing the morphology of the pressure signal, especially the peaks' frequency, intensity, and distribution. The weak relevance of these features (peak to peak is only the tenth most significant feature) in the classification might indicate that different subjects may have different strategies for performing the same task. Nonetheless, the spectral entropy and especially the behaviour of the CoP (first six most significant features for classification, Figure 34) demonstrated a good task dependency and a sufficient agnostic level towards the subjects. CoP was extracted from force data of only two occupation-specific studies involving ML and pressure insoles [268], [276] (Table 3 in Appendix 20), one study of which conducted a feature importance analysis, where CoP-related features were among the ten most important features in the assessment of lower back loading during manual tasks [268].

The confusion matrices (Figure 33 and Figure 41) and SHAP values in all SHAP analysis figures have highlighted tasks with limited CoP variations throughout their execution, as shown in Figure 38, are more likely to be misclassified. This calls for further investigation, both in terms of feature selection, device design and AI classification strategy. For example, the images generated from CoP in Figure 38 may be utilised as inputs to the classifier instead of the averaged values across time windows. Exploring the behaviour of the pressure values in the frequency domain has generated useful information to distinguish manual handling from the remaining tasks. Similarly, other time-frequency domains, such as wavelet transform, may offer different indicators for task classification.

By associating a task with pre-defined component parameters, task classification can used to automatically generate component-related inputs to the endurance model without drift or bias potentially affecting endurance predictions. This also aids with real-time implementation of the SAFE framework in a wearable system for ergonomic risk and fatigue reduction since such systems require post-processing or make assumptions when considering load (as discussed in section 1.3.2 Research Gaps Addressed and Novel Contributions).

4.2.5 Conclusion

This section presents a transparent, non-invasive means of assessing worker tasks using pressure insoles. A lack of explainable methods was identified in the literature, and the present research exhibits comparable accuracies to such studies but with the benefit of increased explainability, meaning that industry-specific pressure insoles with optimised sensor configuration for the extraction of significant features, such as CoP can be achieved. This, in turn, can reduce data throughput and consumption, presenting potential for worker monitoring in smart manufacturing environments and integration into the SAFE framework developed in the course of the thesis.

Chapter 5 System for Activity-aware Fatigue Evaluation (SAFE) Framework: Predictive Fatigue Modelling for Occupational Tasks

This chapter focuses on achieving Objective 3 aiming to develop and test a physical fatigue forecasting system that delivers individualised and task-specific endurance predictions. This objective is achieved by:

1. outlining the novel framework that integrates torque-based endurance modelling and task classification,
2. developing the custom system (consisting of wearables) to acquire and stream data, deploy the models developed in the course of the thesis, and visualise and export outputs,
3. utilising the custom system to validate the framework and demonstrate its potential for use in online operator monitoring and ergonomic risk assessment.

This chapter is based on a manuscript of the same name that is under review at Applied Ergonomics. The SAFE framework integrates the torque-based biomechanical modelling work described in Chapter 3 Endurance Modelling, and the task detection work described in Chapter 4 Load and Task Estimation to form a singular framework. This framework can be used to predict the endurance of individuals carrying out upper extremity manual handling tasks while considering individual parameters (i.e., anthropometrics, strength) and task parameters (i.e., hand-held item load, geometry). While a variety of sensors may be used for framework deployment, IMUs, pressure insoles and a custom application were used to align with Objective 3, to capitalise on the advantages of wearable sensing (detailed in 2.2.1 Wearable Technologies for Occupational Well-Being), and to build on the work of Chapters 3 and 4.

Although this chapter extends previous work that addressed gaps in the state-of-the-art and proposed individual innovations (discussed in their respective chapters), it also introduces additional novel elements. Firstly, this is the first use of endurance modelling with task classification for individualised and task-specific endurance prediction, to the author's knowledge. Moreover, the present work goes beyond this to include torque-based endurance modelling that allows for prediction of any dynamic upper extremity task in the sagittal plane, significantly expanding its application, which is a notable contribution considering that traditional force-based endurance models are applicable to a narrow set of specific conditions (i.e., one task, joint, movement). Secondly, the task classification aspect allows for automated load input when certain tasks are associated with a given hand-held item, which goes beyond current methods that make assumptions regarding load or input this data in post-processing which is not conducive to real-time application. Furthermore, task classification is used to identify when an individual is at rest during the industry tasks and tunes the calculated torque (and thus endurance prediction) to align with real-world conditions. Thirdly, while the endurance model is generalisable across upper extremity tasks, task-specific endurance coefficients are determined at the validation stage, offering an approach to fine-tune the prediction to align CE with perceptive fatigue and exertion scores. Finally, a wearable system, such as the one developed in the present work, allows for predictions to be unaffected by movement across workstations, unlike other instrumentation used in ergonomic systems that require a fixed stationary position (such as force plates), or pose risk of obscuring camera field of view (such as markerless MoCap) which are commonly used in the field. Importantly, the use of wearables and the results in this chapter present strong potential for real-time use for online operator monitoring and ergonomic risk assessment – a key step towards proactive WMSD prevention.

5.1 Introduction

This work presents the System for Activity-aware Fatigue Evaluation (SAFE) framework for proactive WMSD prevention. This involves the application of a mechanistic approach to a wearable ergonomic system, combining endurance modelling and task classification to pave the way for proactive, real-time endurance predictions. Endurance models predict the time to physical fatigue (i.e., ET) using empirical methods [70]. Prior work (3.2 Validation of Endurance Model for Manual Tasks and 3.3 Improving Dynamic Endurance Time Predictions for Shoulder Fatigue: A Comparative Evaluation) advanced traditional force-based endurance models, which had been restricted to isometric conditions [70], [229] and required different models for different tasks [70], [71], [227], [228], [249], by applying a torque-based modelling approach under dynamic, loaded conditions. To date, such torque-based models have otherwise only been implemented for unloaded, mid-air pointing tasks in HMI research [37], [88].

Furthermore, plantar force data are used to classify tasks and detect rest in the SAFE framework, based on 4.2 AI-based Task Classification Using Pressure Insoles for Occupational Safety which also incorporated explainability analysis [253]. Task detection enables task adaptability [93] within the SAFE framework by automatically inputting task-related parameters (e.g., load, shape, size) for task-specific predictions. This improves upon current ergonomic systems that assume fixed loads or require manual input [80], [93], [96] or use force plates that limit mobility [98]. Thus, the SAFE introduced in this paper can deliver cumulative fatigue updates to predict an individual's physical state as tasks change during a work shift, with an appropriate endurance coefficient applied for each detected task.

The present work describes the modelling approach of the SAFE framework, a novel methodology incorporating biomechanical modelling and task classification that generates individualised and task-specific endurance metrics for proactive WMSD prevention. A system that adopts the SAFE framework, consisting of IMUs, pressure insoles and a custom application, was developed and is also described in the present work. Participants performed industry-type tasks while using the SAFE system to preliminarily validate that the SAFE framework can be used for online operator monitoring and ergonomic risk assessment. Specifically, the following were performed: (i) validate IMU-derived joint angles against gold-standard motion capture; (ii) implement the SAFE framework, i.e., compute endurance metrics from joint kinematics, anthropometrics, external load, and perform task classification; (iii) evaluate if the framework reflected the lower risk and perceived effort for ergonomically friendly tasks than non-ergonomic tasks; (iv) develop task-specific endurance coefficients to align outputted endurance metrics with perceived exertion. The approach in the thesis addresses common gaps in the field by incorporating dynamic tasks, improving task generalisability, and accounting for individual parameters.

5.2 SAFE Framework

The SAFE framework represents an integrated approach to operator monitoring and ergonomic risk assessment to capture, process, and interpret biomechanical data and predict endurance capacity. This section begins with an overview of the framework, followed by a detailed look at the modelling approach used.

5.2.1 Framework Overview

Figure 42 shows a block diagram of the SAFE framework. The framework inputs includes manually inputted data pertaining to the individual and tasks, and data streaming of arm segment orientations (e.g., using IMUs, optical or markerless MoCap) and plantar forces (e.g.,

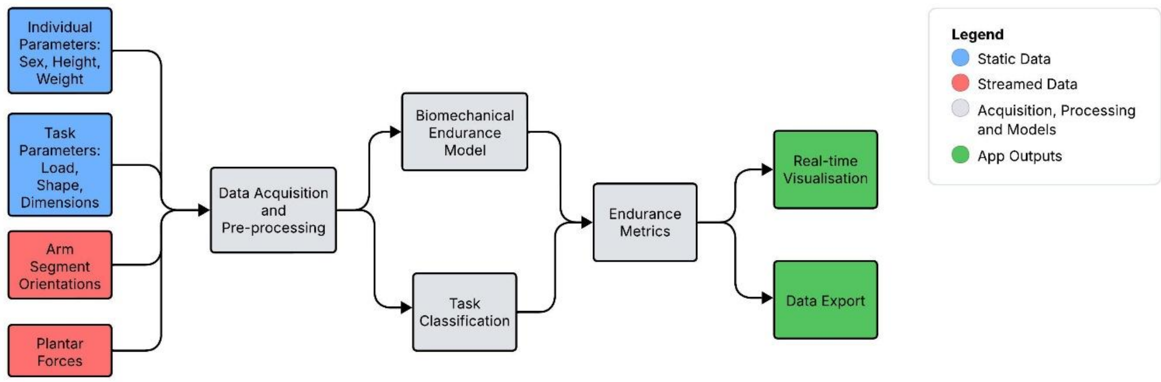

Figure 42: SAFE framework block diagram. Inputs are non-dynamic parameters (blue boxes) and dynamic (red boxes) data obtained from manual input, and streamed sensor data, while endurance modelling and task classification (grey boxes) are used to generate endurance metrics and can be exported (green boxes) for further analysis.

using force plates, or pressure insoles), and requires an application. The application supports the input of non-dynamic individual (i.e., sex, height, weight) and task (i.e., hand-held component load, shape, dimensions) parameters (see blue boxes, Figure 42); streaming of sensor data (see red boxes, Figure 42); task classification and endurance prediction (see grey boxes, Figure 42); display of endurance metrics using the GUI and data export in .xlsx format (green boxes, Figure 42). The endurance metrics outputted include predicted ET which estimates the remaining duration for which the current pose can be performed before fatigue, while CE quantifyies the cumulative endurance consumed, calculated by $CE = (Total\ Time\ /\ Predicted\ ET) \times 100$. Prior to use of the system for endurance estimation, the strength of the individual must be ascertained via the calibration task. This is used to determine the maximum producible torque of the individual at the appropriate load level [204] and impacts the calculated endurance metrics.

Overall, the SAFE framework aids in expanding the application of traditional force-based endurance models beyond static, isometric tasks [70], [204], [229] that require alternative equations for different tasks [227], [228], [249], joints (e.g., shoulder and elbow), muscle groups, and postures [70], [71] which are not common in industrial work [167] to a variety of dynamic tasks whose differing rates of fatigability can be accounted for using an appropriate endurance coefficient associated with the detected task. In particular, task classification can be used to determine which coefficient is best applied at a given moment and to determine when the individual is resting to ensure that CE is not accumulating when there is no activity. In this way, the SAFE framework provides a cumulative fatigue metric that describes individuals' physical state as tasks and activity levels change throughout a work shift. Parametrising the predictions based on subject and task data allows the torque-based endurance prediction and task classification to be individualised and task-specific. Therefore, in the future, a wearable system deploying the framework can be used, for example, by a worker for online operator monitoring and to receive feedback regarding current endurance capacity, rest breaks and task rotations using visualisation on the graphic user interface. The system can also be used by ergonomists to assess risk and inform task redesign with respect to loads, lifting distances, repetitions and indiviudal targets by assessing endurance metrics. The validity of the system for online operator monitoring and work station risk assessment is demonstrated in the present work by comparing predicted ET and CE to subjective self-report questionnaires and ergonomic risk assessments, detailed in 5.4 Validation.

5.2.2 Modelling Approach

The models used to calculate torque, maximum shoulder joint torque, predicted ET and CE have been described in detail in previous work [204], Figure 43 provides a summary. Individual and hand-held load parameters (blue in Figure 42, blue outline in Figure 43) and arm orientation data (red in Figure 42, red outline in Figure 43) are used to compute shoulder joint torque. Figure 43 shows these inputs aligned at the top of the flow chart. All elements

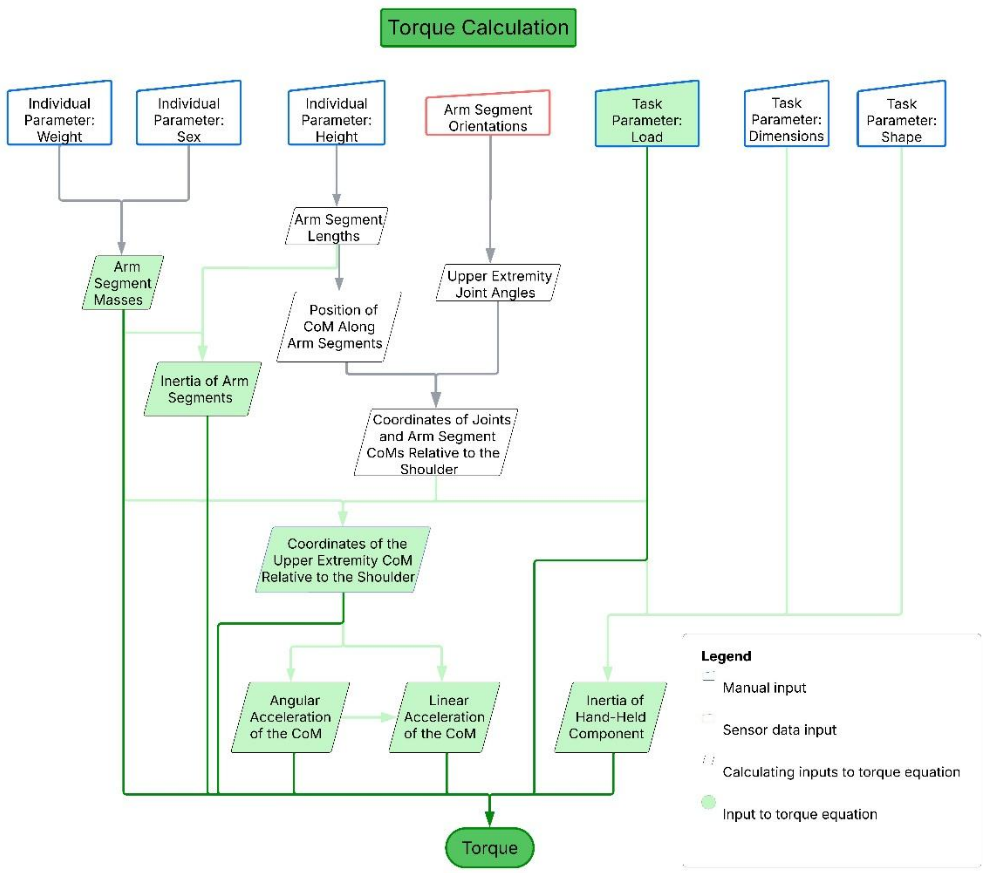

Figure 43: Torque calculation

filled in light green in Figure 43 are directly used in the calculation of torque, while those with no fill are used to calculate such inputs. Some parameters are used for both purposes; for example, load contributes to the calculation of hand-held component inertia and directly to torque.

Anthropometric tables [220] are used to determine arm segment (i.e., upper arm, forearm and hand) lengths, masses, and CoM position, Figure 43. Upper extremity joint angles are calculated from streamed arm segment orientation data. From there, the coordinates of the upper extremity joints and arm segment CoMs with respect to the shoulder are calculated. These data, along with the load of the hand-held item, are used to determine the coordinates of the CoM of the arm and load, again, with respect to the shoulder. The linear and angular acceleration of this upper extremity CoM is then calculated. Separately, the inertia of the upper extremity segments and the task-specific hand-held load are computed using arm segment lengths, masses, anthropometric tables and task parameters.

Torque calculated in the manner shown in Figure 43 is used in the calculation of maximum shoulder joint torque during the calibration task (left side of Figure 44) and in the calculation of endurance metrics (i.e., predicted ET and CE) during working tasks (right side of Figure 44). A simplified version of the torque calculation, showing only inputs and the torque output, is presented in Figure 44. The type of working tasks considered in the present work include typical industry-type manual handling tasks, such as pick and place and walking with a load, and are discussed in more detail in 5.4 Validation.

During the calibration task, the individual holds a load with one hand until complete fatigue with the shoulder flexed to 0° (where the arms down by the individual's side is -90°), elbow fully extended, i.e. flexed to 0°, and hand supinated, as per previous work [204]. The time to fatigue (i.e., experimental ET) and torque during the task are used to calculate the maximum shoulder joint torque with that specific load, Figure 44 (left). This maximum torque value is used, along with torque, to calculate endurance metrics during industry type tasks of the same load, Figure 44 (right). The hand-held items used in the calibration and industry tasks may differ (e.g., if a two-handed industry task uses a 5.0 kg load, then a calibration task load needs to be 2.5 kg since it is one-handed). Therefore, the calibration task related parameters are shown in

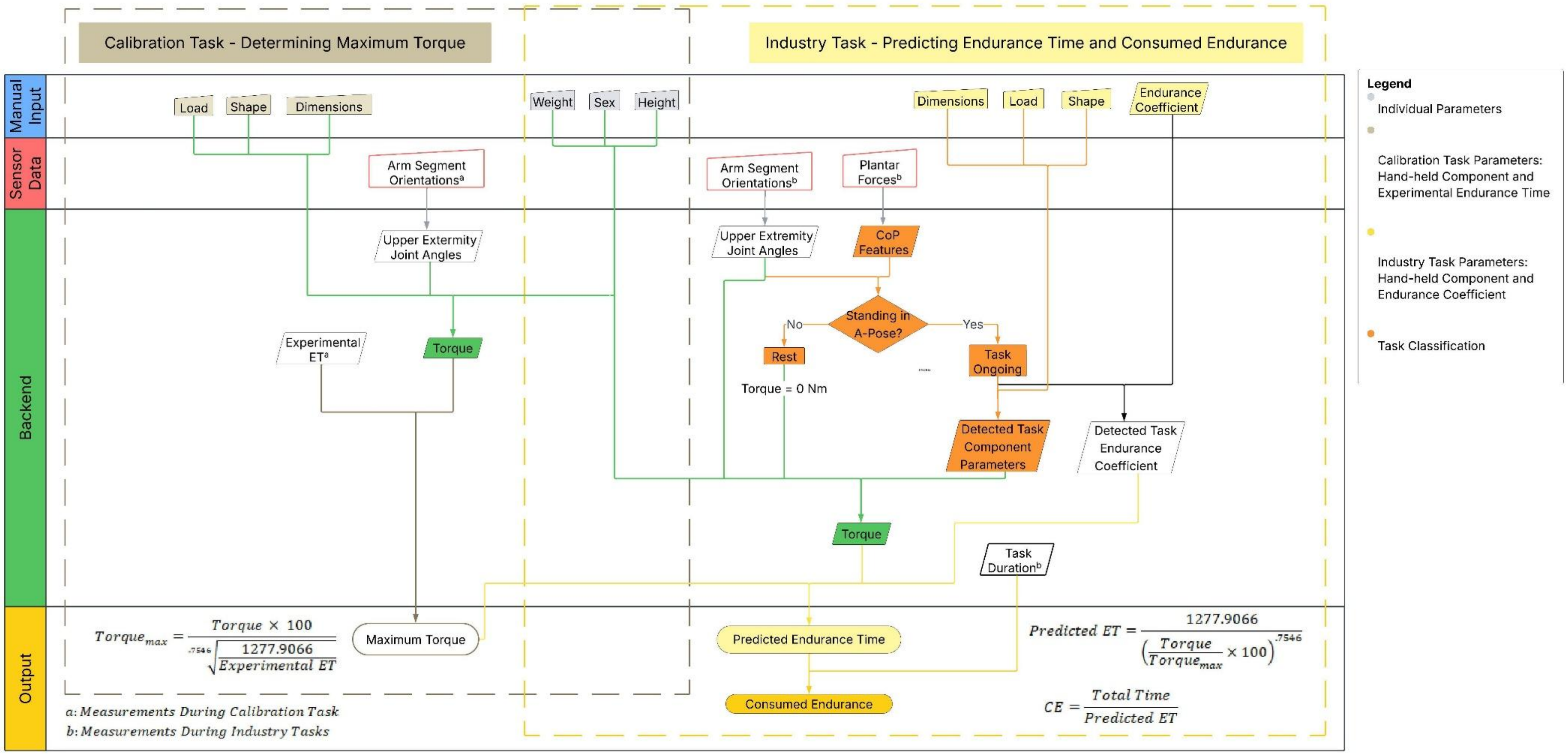

Figure 44: SAFE Framework and method for calculating endurance metrics

brown, Figure 44 (left), and the industry task related parameters are shown in yellow, Figure 44 (right), to indicate this potential difference.

The calculation of torque during the industry task requires the same inputs as the calibration task, i.e. individuals' height, sex, weight; hand-held load, shape and dimensions; arm segment orientation data for joint angle calculation. However, task classification using plantar force data are used to adjust torque depending on the activity level and to adjust endurance predictions depending on the task. 4.2 AI-based Task Classification Using Pressure Insoles for Occupational Safety involved using a RF classifier to estimate five industry-type tasks: 1: *manual handling* (i.e., pick up, walking with a load, and place); 2: *pick and place* (i.e. while standing); 3: *assembly* (i.e., piecing together components while standing); 4: *walking* (i.e., no hand-held load); 5: *standing* (i.e., no hand-held load) from publicly available pressure insole data [107] using CoP features. The SAFE framework uses the same features and classes to identify activities. If activity is detected, torque is calculated as normal (as shown in Figure 43) using the task-related parameters associated with the detected task. An additional rest-like state when participants maintained a neutral upper limb pose while standing is included in the present work, Figure 44 (right). Specifically, when arm segments are close to a neutral A-pose (standing upright with arms extended downwards), and the estimated task included standing, the window was relabelled as *rest*. Torque values are set to zero during *rest* to prevent fatigue accumulation in the absence of external loading. During activity phases, the appropriate task-specific endurance coefficient is applied to tune endurance predictions, depending on the classified task.

Torque is used to predict ET along with the $Torque_{max}$ determined from the calibration task, see equation in Figure 44 (right). To generate more realistic task-specific endurance predictions, a task-dependent endurance coefficient is introduced to scale the predicted ET. This coefficient accounts for differences in task difficulty and fatigue characteristics that align with subjective fatigue levels and are not fully represented by the model equations. The approach used to determine these coefficients is outlined in 5.4 Validation. Finally, CE is computed using the duration of the task and the ET prediction at a given moment, see equation in Figure 44 (right).

During industry tasks, torque remains at 0 Nm while the individual is at rest and increases as the CoM moves upwards and away from the shoulder joint, as the CoM changes more rapidly, and as tasks change, i.e., since some tasks may be associated with higher loads than others. Increased torque results in decreased predicted ET since higher torque postures cannot be maintained for an extended period, see equation in Figure 44 (right). High torque, low predicted ET postures result in higher CE compared to lower torque, higher predicted ET postures. Thus, higher torque postures increase CE more rapidly over time compared to lower torque positions, although the latter will eventually reach 100% CE, i.e., complete fatigue, if performed for enough time. These relationships demonstrate the SAFE framework's capability to generate individualised fatigue forecasts by integrating anthropometric characteristics and subject-specific strength derived from the calibration task with task-dependent joint loading. To enact this approach, the SAFE framework requires sensors and a centralised platform for collecting manually inputted and streamed data and implementing the endurance and task classification models required for fatigue forecasting. It is evident that a myriad of different sensors may be used to measure upper extremity movement and plantar forces, and the sensors and system features deploying the SAFE framework in the present work is described in the next section. This system was deployed during industry tasks, described in 5.4 Validation.

5.3 SAFE System

Due to the compact size, wireless transmission capabilities, allowance for mobility, and strong potential for fatigue forecasting, the present system utilises wearable sensors. A minimal number of off-the-shelf hardware were used to capture arm segment orientations and plantar forces: IMUs capture kinematic data (i.e., upper extremity joint angles) and pressure insoles stream plantar load distribution. A custom application was used to acquire, process and export data. This section describes the hardware and software elements of the system in more detail. The software discussion is divided into the front-end interface, which allows manual input and delivers feedback to users, and the back-end processes, which manage data acquisition, task classification, and endurance estimation.

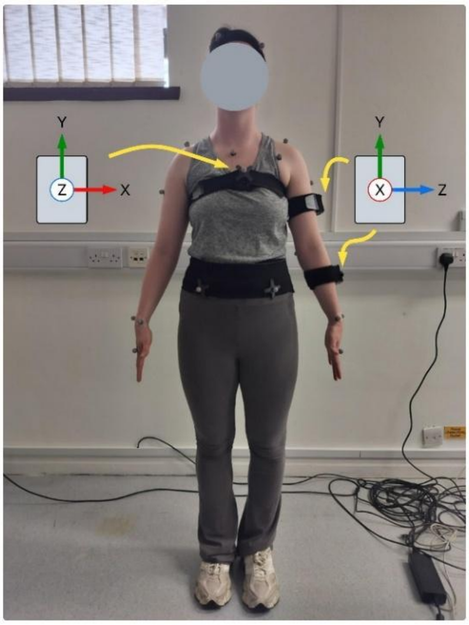

Figure 45: Sensor placement and global coordinates of IMUs

5.3.1 Hardware

The hardware component consists of three IMUs, which are mounted on the chest, upper arm, and forearm using velcro straps, Figure 45. IMUs, BMI270 (3-axis accelerometer + 3-axis gyroscope) + BMM150 (3-axis Magnetometer) from an Arduino Nano 33 BLE Rev2, streamed raw accelerometer and magnetometer readings to the application over Bluetooth with a target sampling rate of 50 Hz, effective sampling rate was ≈2.8 Hz, potentially due to hardware or BLE bandwidth limitations (implications of low effective sampling rate are discussed in 5.4.4 Data Analysis). Li-ion rechargeable batteries power the IMUs (1500mAh), with an embedded charging circuit utilising a type-C USB interface, and sensors were enclosed in 3d printed cases measuring 35 × 54 × 30 mm and weighing 40g. IMU orientation on each arm segment is shown in Figure 45. Pressure insoles, by loadsol (Novel GmbH, Munich, Germany), consisted of three sensors in a forefoot-midfoot-heel configuration and outputted force in Newtons at a rate of 100 Hz. Sensors are battery-powered and wirelessly connected to the data acquisition applications, i.e. to the custom application for IMUs and to a mobile phone app for pressure insoles.

5.3.2 Software

The software allows for online operator monitoring and risk assessment by facilitating sensor data streaming, manual input of non-dynamic subject and task specific parameters, calculation of endurance-related metrics, data visualisation, and export.

Frontend

There are four panels in the custom MATLAB application: 1. *subject information*; 2. *calibration task*; 3. *task component parameters*; 4. *task measurement*, see Figure 46 and supplementary material (Appendix 22) for a more detailed view.

The *subject information* panel enables manual input (white fields, top left of Figure 46, Appendix 22a) of subject identification number, sex, dominant hand, height (m), total body mass (kg) and MVC force (N) measured using a loadcell (range = 30 kg; accuracy = .02%; nonlinearity = .02% F.S.). Once mandatory information fields are filled in, generated information used in the endurance model are displayed (grey fields,

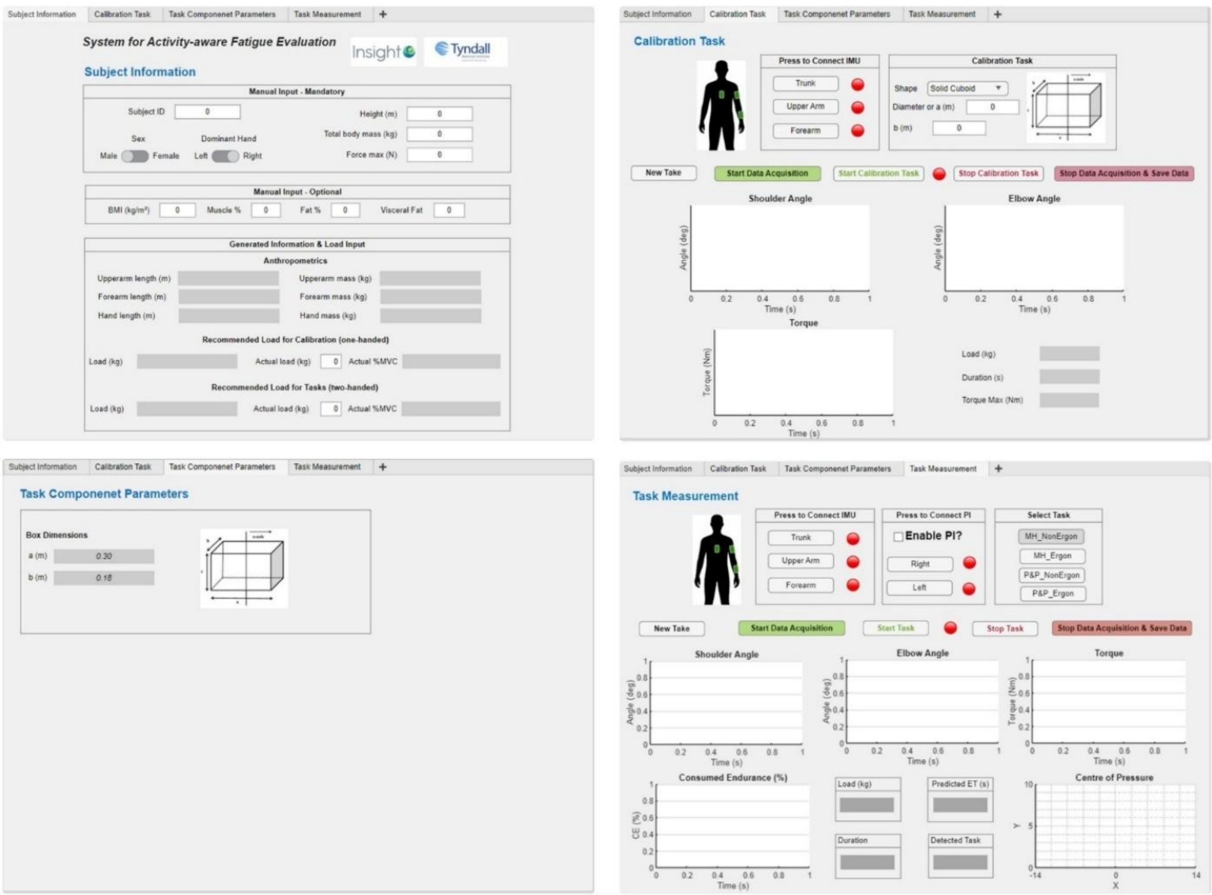

Figure 46: The four panels present in the application showing the subjective information panel (top left), calibration task panel (top right), task measurement parameters panel (bottom left), and task measurement panel (bottom right).

top left of Figure 46, Appendix 22a). For example, since the framework is later validated using loads at 50% MVC, the grey fields display recommended loads for the one-handed calibration and two-handed industry tasks based on the measured MVC (MVC force measurement is discussed in more detail in 5.4 Validation). Additional body composition parameters can be included, such as body mass index, muscle %, fat %, and visceral fat, although they are optional and not required for endurance metric calculation, with the system using default values if these parameters are not set.

The *calibration task* panel (top right of Figure 46, Appendix 22b) has three buttons to connect each IMU and a colour-coded indicator denoting connection status (red for disconnected and green for connected). To enable rotational inertia calculation of the hand-held load during the calibration task, a drop-down menu of component shapes includes solid cuboid and solid sphere and a space for manual input of dimensions is provided. If the shape is approximated as a cuboid, the sides perpendicular to the axis of the motion (lifting along the vertical axis in this case) are required. The load entered on the *subject information* panel (top left of Figure 46, Appendix 22a) is automatically displayed in the corresponding load field on the *calibration task* panel (top right of Figure 46, Appendix 22b), where it appears alongside metrics such as duration and maximum torque. The *calibration task* panel includes buttons to connect each IMU, colour-coded indicators showing connection status, and fields for entering or displaying load and shape parameters. After data acquisition using and prior to any additional data acquisition, the user clicks the 'new take' button to reset.

The *task component parameters* panel (bottom left of Figure 46, Appendix 22c) allows the manual entry of hand-held component characteristics during the task performed by the worker. Finally, the *task measurement* panel (bottom right of Figure 46, Appendix 22d) has similar features to the *calibration task* panel (plots for joint angles and torque, buttons to reset, connect IMUs, start and end data acquisition, etc.) but also includes a display of predicted ET and CE, and an option for pressure insole connectivity. If pressure insoles are enabled, CoP position and the detected task are displayed. A task selection tool on the top right of the panel (bottom right of Figure 46, Appendix 22d) is used to identify the tasks during the validation and is used in the filename when .xlsx files are saved.

Backend

The backend implements the SAFE framework described in section 5.2.2 Modelling Approach, processing IMU and manually inputting subject- and task-related inputs to compute shoulder joint torque, predicted ET, and CE. For the present study, calculations were simplified to focus on sagittal plane flexion-extension of the shoulder and elbow, with shoulder joint torque computed about the medio-lateral axis for a single arm. Wrist angles were fixed at 15° to reduce the number of sensors and interference on the participant and aid with comfort. Pressure insoles were not enabled in the validation and were acquired separately on a mobile application; thus, the validation was performed offline.

5.4 Validation

The validation protocol involved participants performing two pick and place (PP) tasks and two manual handling while walking (MH) tasks. MH and PP tasks had two ergonomic variants: ergonomically optimised (Ergon) and non-ergonomic (NonErgon); thus, the four tasks completed by all participants were: MHErgon, MHNonErgon, PPErgon, PPNonErgon. Ergonomic risk assessments and self-reported fatigue scores were collected to objectively and subjectively verify the differing ergonomic risk and perceived effort between Ergon and NonErgon conditions.

Optical MoCap was used to verify the flexion-extension shoulder and elbow joint angles acquired during the tasks to confirm that the endurance metrics derived from IMU data are within an acceptable range. Due to the acquisition of IMUs and pressure insoles using different applications, evaluation of the SAFE framework during the validation was performed in post-processing.

5.4.1 Subjects

Ten participants (six males, four females) were recruited by word of mouth and provided written, informed consent to take part in the study. Demographic data were recorded and body composition parameters were gathered using the clinically validated OMRON BF511 Body Composition Monitor (Omron Corporation, Kyoto, Japan) [219]. Average (standard deviation: range) of the age, height, weight and BMI of the cohort were 29.2 (6: 20-37) years, 1.72 (.06: 1.62-1.80) m, 73.1 (13.1: 54.7-97.3) kg, 24.7 (4.0: 19.6-30.7) kg/m^2, respectively. Similar to previous experiments, participants reported no musculoskeletal disorders and were asked to attend the session fully rested and completed a 5-minute upper body warm-up prior to data capture.

5.4.2 Validation Equipment

IMUs were placed on the chest and the self-reported dominant upper arm and forearm of participant (see Figure 45), similar to ergonomic studies that use unilateral IMU placement to generate shoulder and elbow joint angles [75], and as per 5.3.1 Hardware. Prior to every task during the data collection, pressure insoles were calibrated based on each individuals' weight as per the manufacturer's recommendations. Participants used available insole sizes EUR39 (n=6), EUR43 (n=3), EUR45 (n=1); no volunteers were excluded for size. A measuring tape and video camera were used to perform ergonomic risk assessments, and a loadcell (range = 30 kg; accuracy = .02%; nonlinearity = .02% F.S.) measured MVC force.

Ten Prime 13 and two Prime 13X OptiTrack cameras (NaturalPoint, Inc., Corvallis, OR, USA), sampling at 180 Hz and a 27-marker set by Optitrack (Conventional Upper Skeleton Marker Set) were utilised [246], enabled tracking of the upper body for system validation. The skeleton was modified to include additional markers required for shoulder and elbow joint angle calculation using International Society of Biomechanics (ISB) guidelines [311], such as the inferior, lateral and root of the scapula to form the scapula local coordinate system (LCS), and the medial epicondyle for the humerus and forearm LCS. Markers were attached to the participant using double sided sticky tape and velcro straps, Figure 45. The mean calibration ray error was $.74 \pm .04$ mm and mean calibration wand error was $.14 \pm .01$ mm.

5.4.3 Protocol

Personal information was inputted to the *subject information* panel (top left of Figure 46, Appendix 22a). MVC was recorded in the same position as the calibration task, ie. with the shoulder flexed to 0°, and the elbow fully extended using the loadcell [204]. Average (standard deviation: range) MVC force was 85 (15: 60-100) N and 53 (5:45-60) N for males and females respectively. The SAFE framework was validated using the available load closest to 50% MVC and the load from the one-handed calibration task was doubled for the two-handed industry tasks and placed in a box (30m × .20m

× .18m). Average (standard deviation: range) of the actual %MVCs of the loads used were 50.2 (1.6:49.0-52.7) % and 50.9 (3.3:49.46.4-54.5) % for males and females respectively. Participants performed the calibration task followed by four industry-type tasks in a randomised order for 5 mins each.

To acquire data for the calibration task using the software, the user clicked ‘start data acquisition’ (indicator went from red to yellow, top right of Figure 46, Appendix 22b). At this stage, the computed shoulder and elbow flexion-extension angles and corresponding joint torques in the sagittal plane were displayed in the plots. Once the user clicked ‘start calibration task’ (indicator turned green, top right of Figure 46, Appendix 22b) and the participant began the calibration task, the task duration and calculated maximum shoulder joint torque (Figure 44, left) were displayed in the grey fields (top right of Figure 46, Appendix 22b). The calibration task was complete once the individual reached fatigue, the user clicked ‘stop calibration task’ (indicator turned yellow, top right of Figure 46, Appendix 22b), and then ‘stop data acquisition & save data’ (indicator turned red, top right of Figure 46, Appendix 22b). The time between clicking ‘start calibration task’ and ‘stop calibration task’ was used as the experimental ET to calculate the maximum torque, Figure 44 (left).

For manual handling tasks, participants picked up the box containing the external load at the start position and walked to the end position at a steady and controlled pace over 12 s and placed the box at the end position, after which the participant performed an

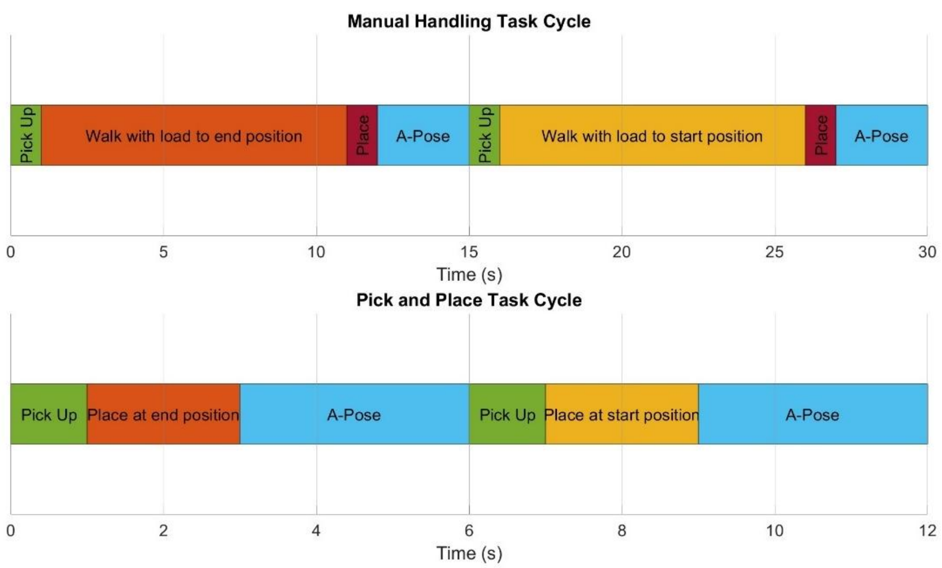

Figure 47: Task cycle for manual handling (top) and pick and place (bottom) tasks

A-pose and completed the course in reverse, see Figure 47 (top). One cycle took 30 s approximately, and subjects completed 10 cycles in the 5-minute duration of the tasks. A metronome was used to prescribe pick-up and drop-off times. For pick and place tasks, participants picked up the box from one table and moved it laterally to a different table while standing, see Figure 47 (bottom). Once the lift was complete, participants assumed an A-pose until the metronome sounded, when the box was placed back in the original position, meaning there were two lifts per cycle. Lifts were repeated every 6 s (Figure 47, bottom), for 5 minutes, resulting in 25 cycles over the task duration.

For manual handling (i.e., MH) and pick and place tasks (i.e., PP), the pick-up and drop-off locations differed between Ergon and NonErgon variants so that Ergon was more ergonomically friendly, meaning lifting distances and forward reaching and bending were reduced compared to NonErgon (see Figure 48 and Figure 49 for the laboratory's configuration). Load and pace can influence ergonomic risk scores and fatigue in the upper extremities during repetitive tasks [3], thus this was consistent between Ergon and NonErgon tasks. For MHNonErgon, the starting pick up location was 20 cm from the ground (49 cm lower than the MHErgon start point) and the drop-off location was 36 cm higher than the MHErgon drop-off location (Figure 48). For the PPNonErgon variant, the starting pick-up location was raised 18cm higher than PPErgon, Figure 49. Ergonomic risk assessments (NIOSH lifting index [65] for manual handling tasks and RULA (wrist and arm scores) [63] for pick and place tasks) were calculated for pick-up and drop-off positions for both tasks respectively to ensure higher risk levels for NonErgon tasks without incurring very high scores that posed a risk to participants. A measuring tape was used to generate data for the completion of NIOSH assessments and video footage was used to determine RULA scores observationally.

NIOSH lifting index scores are classified into very low (≤ 1), low (1.01-1.50), moderate (1.51-2.00), high (2.01-3.00) and very high (>3.00) risk, while RULA scores are classified into negligible (1-2), low (3-4), medium (5-6) and very high (>6) risk. Mean and standard deviation NIOSH scores were $.48 \pm .12$ and $1.07 \pm .30$ for MHErgon and MHNonErgon, respectively, while mean and standard deviation RULA scores were $5.3 \pm .3$ and $6.2 \pm .4$ for PPErgon and PPNonErgon, respectively.

Participants were asked to rate their subjective level of exertion and fatigue using the Borg RPE scale [72], before each task and at 1, 2, 3, 4 and 5 mins, where 6-7 in the scale indicates rest and very, very light exertion and 20 indicates maximal exertion. Participants rested between tasks for a minimum of 6 mins, consistent with previous literature [27], [110], [119], [236], until their Borg RPE scores returned to 6-7. Rest durations typically averaged around 7-8 mins. Final Borg scores were similar for both versions of manual handling and pick and place tasks (MHErgon ≈ 13 and MHNonErgon ≈ 15 versus PPErgon ≈ 12 and PPNonErgon ≈ 15).

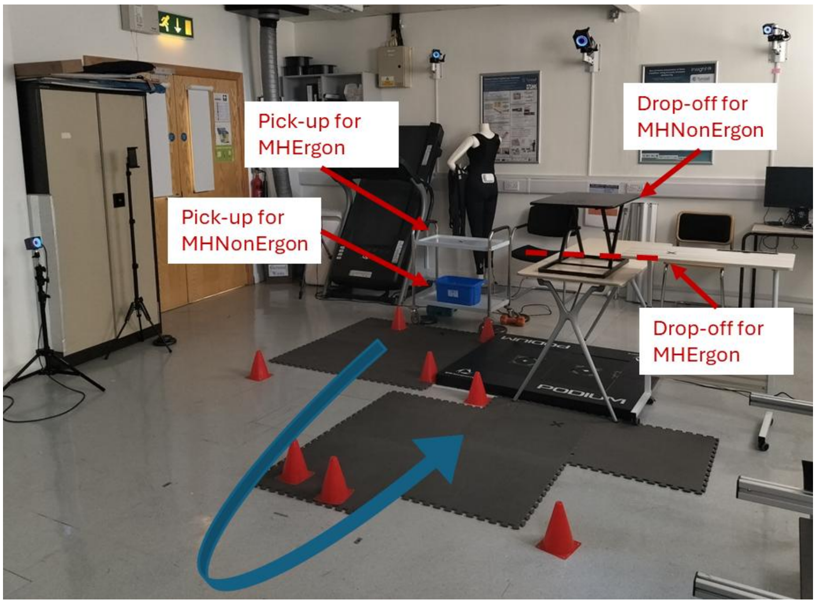

Figure 48: Pick-up and drop-off points for manual handling tasks, with MHNonErgon locations deviating from MHErgon by -49cm and +39cm for pick-up and drop-off points respectively. Walking path while holding the load is indicated by the blue arrow.

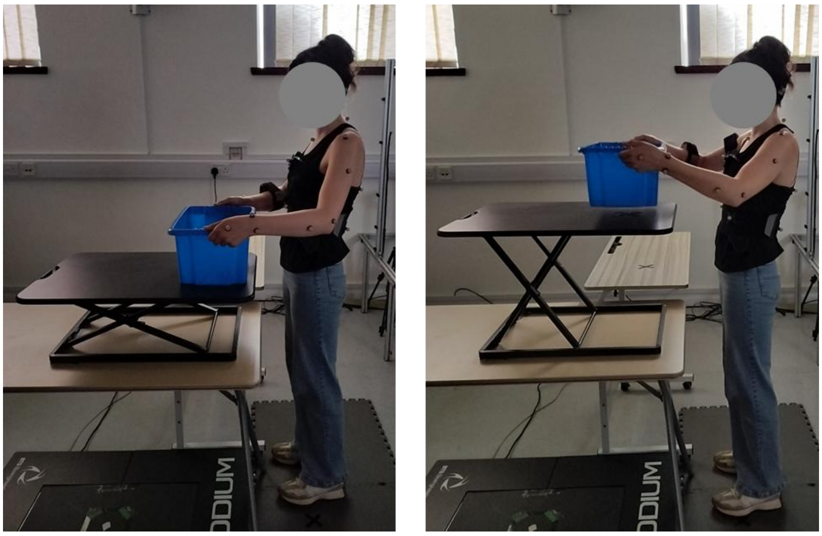

Figure 49: Pick and place task involved repeatedly lifting and placing the box laterally from the black table on the left to the white table on the right and vice-versa. The black table was 18cm higher in PPNonErgon compared to PPErgon to increase ergonomic risk.

The *task measurement* panel (bottom right of Figure 46, Appendix 22d) was used to acquire and visualise data during the industry tasks following the same operation as the buttons on the *calibration task* panel previously described, where CE accumulated between clicking ‘start task’ and ‘stop task’. The same box and load were used for all tasks, thus the task measurement parameters, shown in Figure 46 (bottom left) and Appendix 22c, remained unchanged throughout the data acquisition. Participants performed an A-pose for approximately 5 s prior to beginning the task, during which a distinct movement cue was executed to mark task onset, and then held an A-pose for approximately 5 s after task completion to aid with data synchronisation.

5.4.4 Data Analysis

Data Pre-Processing

For MoCap data, gaps in marker position tracking shorter than 90 samples (≈0.5 s) were filled using cubic interpolation in Motive software (NaturalPoint, Inc., Corvallis, OR, USA). For larger gaps, pattern-based interpolation was applied using nearby markers as references. The data were then filtered using a 4th order Butterworth filter with a 6 Hz cut-off frequency and zero-phase shift similar to studies in the literature that used MoCap data for joint angle calculation during quasi-static manual handling tasks [312], [313]. Processed takes were exported to .c3d and analysed in MATLAB to extract joint angles using ISB guidelines [311] which involved creating LCSs for the thorax, scapula, humerus and forearm. Virtual markers for the glenohumeral and elbow joint centres were determined by offsetting the marker on the acromioclavicular joint downwards by 7 cm [314] and finding the midpoint between the medial and lateral epicondyles, respectively. The Biomechanical ToolKit and Mokka [315] were used to append and visualise virtual markers. Only shoulder and elbow flexion-extension angles in the sagittal plane were extracted since the task movements mainly occurred about the medio-lateral axis and to allow comparison and validation with the generated IMU joint angles.

Since pressure insoles were not enabled during data acquisition with the software, IMU and pressure insole data captured using the custom and mobile applications respectively were exported post-task, and all processing took place offline. Thus, while this work demonstrates the efficacy of the SAFE framework using the validation system during industry-type tasks in a laboratory setting, it does not validate the real-time abilities of the framework. This will be tested in future work when it is possible to acquire pressure insole data on the developed application. One degree of freedom shoulder and elbow joint angles (flexion-extension in the sagittal plane) were determined from IMU data by forming directional cosines from the global coordinate system of the sensors, converting into quaternions and finding the relative angles between the chest and upper arm IMUs (after converting to Euler angles and using the roll to account for the 90° orientation offset) for shoulder angle, and between upper arm and forearm IMUs (using the local z-axis of each segment, Figure 45) for elbow angle. Although the effective sampling rate was low, the protocol involved slow, metronome-paced movements, ensuring that kinematic and torque variations of interest occurred within the resolvable frequency range and satisfied the Nyquist criterion [220]. Higher-frequency transients (which can occur due to sudden movements, impacts or short bursts of acceleration) were not captured due to the low sampling rate, but this was acceptable given the quasi-static, endurance-related dynamics under study. Spectral analysis of filtered 180 Hz MoCap joint angle data confirmed that the main movement peak occurred at .37 [.2-.8] Hz and 95% of the cumulative power was contained at .92 [.34-1.66] Hz, indicating that all meaningful motion fell within the bandwidth captured at the IMU sampling rate. IMU-derived joint angles were low-pass filtered using a 4th order zero-phase Butterworth filter, with the cutoff frequency adaptively set from the effective sampling rate: 6 Hz for ≥25 Hz sampling (capturing voluntary upper-limb motion, mostly <6 Hz), ~0.35×Nyquist (≤5 Hz) for 10–25 Hz, and .8–1.5 Hz for <10 Hz to preserve the relevant slow dynamics while attenuating noise. To attain a balance between noise reduction and preserving signal shape, linear/angular accelerations were obtained via Savitzky-Golay differentiation filter (3rd order, window set to ~0.2–0.4 s), following zero-phase low-pass filtering of joint angles.

Since data were acquired on different devices and were not synchronised, IMU, MoCap and pressure insole data were resampled and synchronised. MoCap joint angles and pressure insole data were down sampled and IMU joint angles were up sampled using cubic interpolation to 25 Hz. Using MATLAB, min-max normalisation was performed, and the cross-correlation function was used to determine the lag between MoCap and IMU data and then between pressure insoles data, and data were shifted accordingly. Appropriate offsets were applied in the calculation of the joint angles from the IMUs during each participant's A-pose at the start of the first task and applied as a fixed calibration to all tasks to bring the shoulder and elbow angles to -90° and 0°, respectively. To compare MoCap and IMU data, statistical features were extracted from MoCap- and IMU-derived joint angle data from each task: root mean squared difference (RMSD), mean absolute error (MAE), and coefficient of multiple correlation (CMC) [316].

Given the small, unbalanced groups (6 wore size EUR39, 3 wore size EUR42, 1 wore size EUR45), shoe size effects with pressure insoles were not tested. CoP features were extracted from pressure insole data and the model from previous work [253] was used to classify the tasks in the present work using a 1s window. Although the previous section, 4.2 AI-based Task Classification Using Pressure Insoles for Occupational Safety, suggested 5 s windows for near real-time classification [253], 1 s windows were required to capture short rest phases and transitions. In the present validation, task classification aided with distinguishing *rest* from activity phases to ensure no artificial fatigue accumulation while the participants were resting in A-pose position. For each trial, synchronised IMU, MoCap, and pressure insole data were trimmed to remove any data collected before the first rest phase and after the final rest phase.

Framework Implementation

Using manually inputted subject and task information, flexion-extension shoulder and elbow joint angles and task classification outputs, shoulder joint torque about the medio-lateral axis was calculated using the method shown in Figure 43 [204]. Since IMUs were placed on the dominant arm, shoulder joint torque is computed for one arm; thus, the task load was halved in the case of a two-handed task [208] and symmetrical loading was assumed. Torque exhibited a consistent non-zero baseline during A-pose rest periods, this likely arose from a combination of small errors in joint angle estimation and anthropometric approximations, which together resulted in systematically elevated torque values. Rather than applying a separate uniform offset correction, a task- and subject-relative torque floor ($\varepsilon = \max(1\ \text{Nm}, 2\% \cdot \max(\text{torque}))$) that both removes this baseline offset and ignores physiologically negligible loads was implemented, aligning rest-state torque to ≈0 Nm while ensuring robustness across tasks and participants. Using torque and experimental ET from the calibration task, maximum torque was calculated (Figure 44, left). This maximum torque, along with the torque acquired during each pick and place and manual handling task, was used to calculate predicted ET and CE for each task (Figure 44, right). CE was smoothed with a moving window covering 2–3 cycles (pick and place tasks: 24–36 s; manual handling tasks: 60–90 s) with edge padding.

Assessing the Framework

This step assesses the ability of the SAFE framework to predict fatigue and distinguish higher- from lower-risk conditions. To assess the validity of CE as a fatigue metric, CE values (using 2 cycle window lengths) at same time intervals that Borg values (i.e. at 0 s, 60 s, 120 s, 180 s, 240 s, 300 s) were noted and within-subject (repeated-measures) correlations [317] between time, Borg scores and CE was performed on a task-by-task basis. To confirm that the Ergon tasks were, in fact, more ergonomically friendly than their NonErgon counterparts and that the calculated endurance metrics reflected these differences, a one-tailed Wilcoxon-signed rank test was performed using NIOSH, RULA, endurance metrics and final Borg RPE scores, i.e. scores obtained at 5 mins.

Task-Related Coefficients

Observed CE values were initially higher than expected, therefore rescaling CE using task-specific endurance coefficients was required. Thus, the inclusion of the endurance coefficient for manual input in Figure 44 (right). Since the correlation analysis showed high positive correlation between CE and Borg scores, observed high CE values were rescaled using task-specific endurance coefficients to align with perceived exertion, ensuring the framework outputs reflected individual fatigue levels. This ensures the behaviour and relative pattern of the model is not altered and only rescaled.

To determine the task-specific endurance coefficients that reflected participants' fatigue levels, a new parameter called Target CE was calculated based on the Borg RPE score recorded for all participants at the end of each task. The Borg RPE scale is structured with linear increments [72], [318] and a linear relationship between Borg scales and muscle activation (%MVC) has been previously reported [319]. Jang *et al.* (2017) [196] extended this assumption to their model- that described the proportion of fatigued motor units, applying a linear mapping to the Borg scale. Following this rationale, the CE metric in the present study was linearly rescaled to the Borg RPE (6–20) scale, generating the Target CE parameter that provides a perceptual reference for

CE values. Since CE=0% and Borg=6 denote rested states and CE=100% and Borg=20 denote complete fatigue, Target CE values were generated based on reported Borg scores where each point on the Borg scale denoted a 7.14% increase of CE (i.e., if Borg=6 then Target CE=0%, if Borg=7 then Target CE=7.14%, if Borg=8 then Target CE=14.28%... if Borg=20 then Target CE≈100%). Since Target CE was based on self-reported fatigue, values were similar for both manual handling and pick and place tasks (MHErgon=47.6±16.8% and MHNonErgon=61.6±13.9% versus PPErgon=42.0±8.1% and PPNonErgon=60.9±16.5%). This resulted in 40 different Target CE values for each participant at the end of each task.

Coefficients that aligned observed CE values to Target CE were subsequently calculated using *k=TargetCE/observed CE* resulting in 40 different values for each subject and task. The coefficients were averaged across each task (*Equation 5.1*, i.e. four coefficients). To calculate the rescaled CE values that aligned the observed CE with perceived fatigue, the task-relevant endurance coefficients were multiplied by the observed CE values, i.e. $CE \times \bar{k}_{Task}$. RMSE values were calculated and normalised using the mean of the Target CE for each task to understand the deviation of rescaled CE from the Target CE.

$$\bar{k}_{Task} = \frac{1}{N}\sum_{i=1}^{N}\frac{TargetCE_{Task}}{OriginalCE_{Task}} \qquad \textit{(Equation 5.1)}$$

5.4.5 Results

Framework Implementation

This section covers the results from *data pre-processing* and *framework implementation* in 5.4.4 Data Analysis. Figure 50 shows MoCap- and IMU-derived joint angles (shoulder and elbow flexion-extension angles in degrees in orange and purple respectively for MoCap, and in blue and yellow respectively for IMU) at the top; total pressure insole load between two feet (in N, solid black line) and task classification (*assembly* in pink, *manual handling* in green, *pick and place* in purple, *standing* in blue, *walking* in yellow and *rest* in grey) in the middle; and torque (Nm, black solid line) and predicted ET (s, orange solid line) with rest/activity classification at the bottom during the MHErgon task for one subject. Similarities between IMU and MoCap joint angles are graphically evident in Figure 50 (top) and in the joint angle comparison metrics in Table 18. Results were not task dependent with comparable metrics across manual handling and pick and place task types. MAE and RMSD quantify overall agreement, with RMSD accounting for drift or spikes more sensitively, thus the larger range of 10.8°-15.1°, compared to MAE, 8.2°-11.3°. CMC evaluates waveform similarity and was high for elbow angles (CMC≥.91), indicating very similar patterns, and low for shoulder angles (CMC≈.52), indicating poorer shape agreement.

In Figure 50 (middle and bottom), rest phases are denoted by grey windows and were classified accurately and in alignment with the periods of time the subject held an A-pose (where shoulder and elbow angles were extended to ≈-90° and ≈0°, respectively)

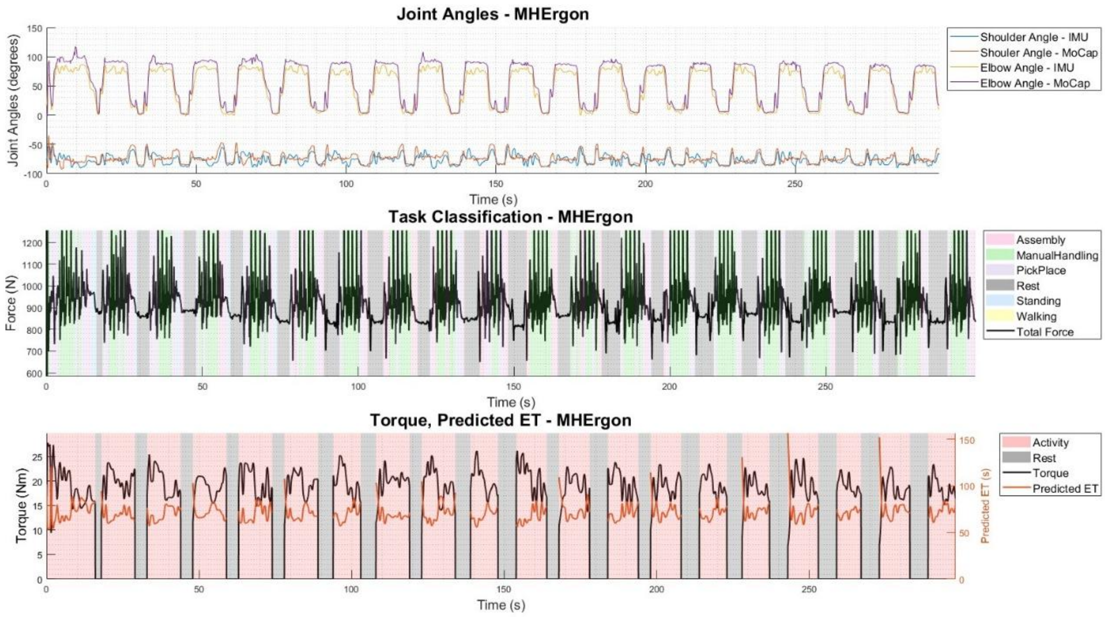

Figure 50: MHErgon task for one subject showing MoCap and IMU joint angles (top), task classification with PI and IMU joint angles data (middle) and the calcaulted torque and predicted endurance times (bottom)

Table 18: Comparison of MoCap and IMU shoulder and elbow joint angles indicted by mean ± standard deviation for RMSD, MAE, CMC

	RMSD (°)		**MAE (°)**		**CMC**	
	Shoulder Flexion	**Elbow Flexion**	**Shoulder Flexion**	**Elbow Flexion**	**Shoulder Flexion**	**Elbow Flexion**
Manual Handling Tasks	10.8±3.5	11.7±3.2	8.2±2.4	9.2±2.9	.56±.36	.95±.03
Pick and Place Tasks	15.1±5.2	14.2±2.9	11.3±4.3	10.7±2.2	.47±.36	.91±.04
All Tasks	13.0±4.9	13.0 ±3.3	9.8±3.8	10.0 ±2.7	.52±.36	.93±.04

RMSD = Root mean squared difference; MAE = Mean absolute error; CMC = Coefficient of multiple correlation and a relatively constant total pressure insole reading indicate standing still. The displayed task is accurately classified as *manual handling* (Figure 50, middle panel, green windows) for the majority of the recording, with a few phases marked as *standing* (blue windows) or *assembly* (pink windows). Task classification and IMU-derived joint angles were used to distinguish rest from activity to tune the torque calculations. Ground truth versus predicted classifications showed accuracy, F1 and specificity of .995%, .996% and .985% respectively across all data.

The impact of changes in arm segment positions, CoM position, and linear and angular acceleration on torque (Nm, black line in Figure 50, bottom), and thus predicted ET (s, orange line), are evident, i.e. as torque decreases, predicted ET increases since these reduced-torque configurations can be sustained for longer periods. Setting the torque to 0 Nm during *rest* (grey windows) results in infinite predicted ET in these phases, which is physiologically accurate, and ensures that additional endurance is not consumed during such phases when calculating CE. This is evident as CE goes to 0% during *rest* phases, blue lines in Figure 51 (i.e., between each lift) while smoothed CE shown in red and black in Figure 51 succeeds in capturing past kinematic sequences of the previous 2 and 3 cycles of activity. Changing smoothing duration from longer to shorter windows resulted in a median absolute difference of -13.9% (relative % median difference of -6%), indicating results were robust to window length. The shorter window length was used for remaining analyses.

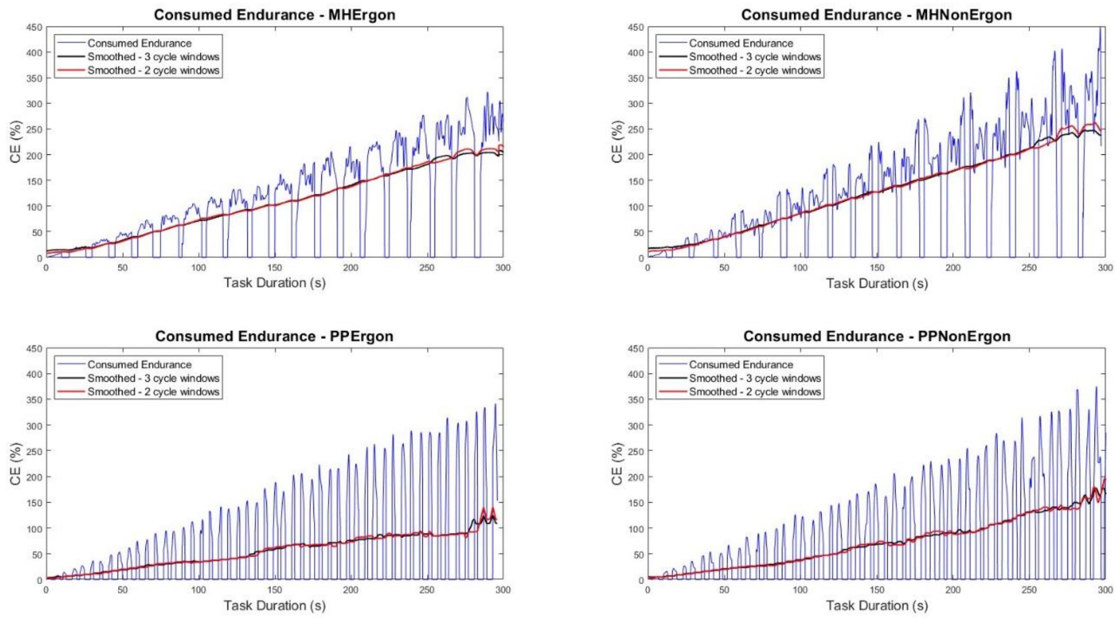

Figure 51: CE plots for all tasks for one subject

Assessing the Framework

This section presents the results corresponding to the similarly named subsection in 5.4.4 Data Analysis. The relationships between time, Borg RPE and CE values are shown in Figure 52. Pooled correlation coefficients (rrm) for time versus Borg was ≥.909 (P<.001), while time versus CE was slightly stronger ≥.962 (P<.001). CE showed strong correlation with Borg scores (rmm≥.878, P<.001), demonstrating its ability to predict fatigue levels.

Table 19 shows z-scores and one-tailed significance results from the Wilcoxon signed-rank test. Significant differences were detected between Ergon and NonErgon conditions for both task types using ergonomic risk assessments scores (P<.001 for manual handling tasks, P=.002 for pick and place tasks) and Borg RPE (P=.004 for manual handling tasks, P=.002 for pick and place tasks), where the NonErgon tasks induced both higher subjective fatigue ratings and risk. This validates that significant differences between higher- and lower risk task conditions were observed subjectively and objectively.

Importantly, to validate the SAFE framework during manual handling and pick and place tasks, the Wilcoxon signed-rank test results are also shown in Table 19. The significant difference in ergonomic risk assessments and Borg RPE scores at task completion is also reflected in the higher mean shoulder joint torque during NonErgon tasks (P<.001 for manual handling tasks, P=.014 for pick and place tasks), lower mean predicted ET throughout NonErgon tasks (P=.003 for manual handling tasks, P=.042 for pick and place tasks), and higher CE at the end of NonErgon tasks (P=.002 for

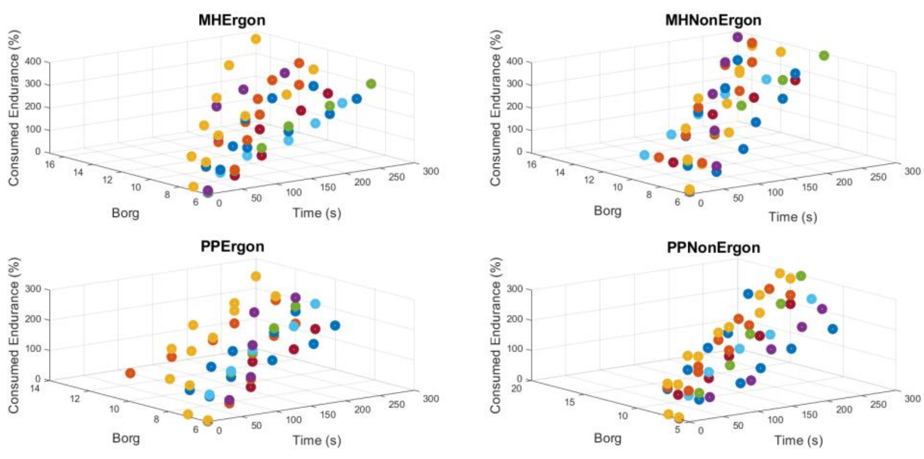

Figure 52: Relationship between Time, Borg scores and CE values

Table 19: Wilcoxon signed-rank test z-scores comparing the means between Ergon and NonErgon tasks

Tasks	**ERA**	**Borg**	**Mean Torque**	**Mean Predicted ET**	**CE**
Manual Handling	-2.807[a] (P<.001)	-2.625[a] (P =.004)	-2.803[a] (P <.001)	-2.599[b] (P =.003)	-2.701[a] (P =.002)
Pick and Place	-2.716[a] (P =.002)	-2.677[a] (P =.002)	-2.191[a] (P =.014)	-1.784[b] (P =.042)	-1.886[a] (P =.032)

a. Based on Negative ranks, i.e. NonErgon values higher than Ergon values
b. Based on positive ranks, i.e. Ergon values higher than NonErgon values

ERA = Ergonomic risk assessment; ET = Endurance time; CE = Consumed endurance

Table 20: Mean ± standard deviations of target CE values (based on Borg scores) and CE values with and without scaling, and the associated normalised rmse

Task	**CE without coefficients (%)**	***NRMSE***	**CE with coefficients (%)**	***NRMSE***
MHErgon	255.2±58.4	*4.49*	48.4±11.1	*.31*
MH NonErgon	313.0±60.4	*4.19*	63.9±12.3	*.30*
PPErgon	173.0±39.2	*3.22*	43.2±9.8	*.19*
PP NonErgon	228.2±47.38	*2.84*	62.4±13.0	*.29*

manual handling tasks, P=.032 for pick and place tasks) of NonErgon tasks using the SAFE framework.

Task-Related Coefficients

From lowest to highest, task coefficients were .1895 (MHErgon), .2042 (MHNonErgon), .2495 (PPErgon) and .2734 (PPNonErgon). Coefficients for manual handling tasks were lower than pick and place tasks, showing the former needed to be reduced by a greater extent to align with Borg ratings due to higher observed CE (i.e., without rescaling) calculated by the model.

Mean and standard deviation rescaled CE with coefficients ($\bar{k}_{Task}$) were compared to Target CE, Table 20. With coefficients applied, CE more closely resembled perceived fatigue, reducing errors to moderate levels (NRMSE=.19-.31), compared to the poor fit without coefficients (NRMSE=2.84-4.49). Thus, endurance coefficients effectively scaled CE values to within ≈30% of the Target CE and aligned the cumulative endurance metric with task-specific self-reported fatigue levels.

5.5 Discussion

5.5.1 SAFE Framework

The SAFE framework integrates wearable sensing, biomechanical modelling, and task-aware fatigue assessment to forecasting physical fatigue and shows strong potential for proactive WMSD prevention. The SAFE framework comprises of a torque-based endurance model which has been shown to accurately predict ET of loaded upper extremity dynamic tasks in combination with the calibration task to determine $Torque_{max}$ [204]. Torque-based endurance modelling has been tested during unloaded, mid-air pointing tasks for human machine interface research to date [37], [88] and during basic loaded static and dynamic high torque movements with the calibration approach [204]. The validation work demonstrated this framework can be applied to industry-type tasks with increased movement complexity and variability. Thus, the SAFE framework aids in expanding the application of traditional force-based endurance models beyond static, isometric tasks [70], [204], [229] that require alternative equations for different tasks [227], [228], [249] and joint, muscle groups, and postures [70], [71] (which are not common in industrial work [167]) to a variety of dynamic upper extremity tasks. Furthermore, the torque-based models and calibration task in the SAFE framework aid with generating individualised endurance metrics that align with the individuals' demographics, anthropometrics and strength at a specific %MVC.

While CE can be used to inform workers of their current endurance consumption, the endurance coefficients can also be used to rescale predicted ET, using $PredictedET_{Task} = \frac{Predicted\ ET}{k}$ This aligns with the need for forecasting approaches in the literature [3], [77] and this task-specific predicted ET can be used to calculate CE, Figure 44 (right).

The integration of task classification in the framework eliminates the need for manual load input during post-processing (although this feature was not demonstrated in the current validation due to sensor limitations and identical loads during tasks). The present work used task classification to distinguish rest from activity phases to reflect real conditions and prevent artificial CE accumulation during rest. Additionally, the validation showed that task classification accounted for slight variations in task timing, particularly during *rest* phases, preventing artificial CE accumulation and demonstrating robustness to inter- and intra-participant differences. This is a key requirement for real workplaces where individuals rarely perform tasks identically.

Future work can involve training ML models on specific work tasks and assign appropriate task-specific endurance coefficients in real-time. Furthermore, the previous work [253] on which the classification in the present work is based used explainability analysis to identify and utilise important features, which aligns with the need for explainability where ML is deployed in occupational contexts [87]. This aspect of the SAFE framework contributes to a cumulative fatigue metric that describes individuals' physical state as tasks change throughout a shift.

The framework was deployed on a system consisting of IMUs and pressure insoles with a custom application. However, the framework is not limited to such sensors and may also be deployed with an array of different equipment, e.g., force plate, markerless MoCap. The minimal number of sensors in the present work were selected to allow for mobility across the experiment set-up, something not achievable with force plates and a limited number of markerless MoCap cameras, and to minimise the interference of sensors with natural movement and comfort. This enables better simulation of real working conditions and minimises interference with the worker. Therefore, the SAFE framework exhibits versatility that allows for adaptation to different occupations, workplaces and worker needs depending on the sensors used, the tasks that the framework is trained on and inclusion of occupation-specific endurance coefficients.

The SAFE framework goes beyond current methods and wearable systems and it especially suitable for non-routinised work as it does not involve continuous interference on workers as is the case with questionnaires [187], [320], [321] and ergonomic risk assessments that require measurements like the NIOSH lifting index. It also avoids the need to observationally analyse hours of video footage [99] and is not affected by inter- and intra-observer differences similar to ergonomic risk assessments like RULA [18], [137]. Furthermore, the categorisation of some ergonomic risk assessments into gross categories, e.g. seven categories for RULA, has resulted in researchers questioning the risk classifications [322], [323] and calling for risk on a continuous scale [18], [138], which the present work achieves, i.e. CE ranges from 0-100%. The applicability of the framework to non-routinised work for any upper extremity task, calculation of risk on a continuous scale, and a GUI for visualisation of endurance metrics contributes to the potential of the SAFE framework to be deployed for continuous online operator monitoring. In this way, workers can manage their working schedules (e.g., when to rest, rotate task) using their smart phones in a manner that prioritises their safety, wellbeing and privacy. Additionally, the SAFE framework shows potential for use by workplace ergonomists, where the CE in given period may inform workstation or task redesign, similar to the changes that were observed between Ergon and NonErgon tasks in 5.4 Validation.

5.5.2 Framework Validation

Joint Angle Comparison

Pick and place tasks incurred slightly higher joint angle errors (RMSD ≈14.2-15.1°, MAE ≈10.7-11.3°) than manual handling tasks (RMSD ≈10.8-11.7°, MAE ≈8.2-9.2°), likely due to greater complexity and velocity [316], [324], [325]. Elbow angles showed excellent agreement [316] (CMC ≈.95 for manual handling, ≈.91 for pick and place), while shoulder angles showed poor agreement. These results align with Lebel *et al.* (2017) [316] and Kim and Nussbaum (2013) [324], and with MAE ranges for walking and daily activities (.6-25.6°) [326], [327], [328]. Higher shoulder errors may stem from offsets, reduced motion range (–35° to –90° vs. 0-144° at the elbow), or the estimation method, and alternative joint angle estimation methods (e.g., Lim & D'Souza, 2020 [22]) should be considered. Overall, IMU-derived joint angles fall within acceptable ranges, supporting the validity of the associated endurance metrics.

Assessing the Framework

Torque and predicted ET were, as expected, respectively higher ($P<.05$, Table 19) and lower ($P<.05$, Table 19) for NonErgon tasks since higher torque movements can be maintained for a shorter period of time. Significant differences between Ergon and NonErgon tasks were identified using ergonomic risk assessment and Borg scores ($P<.05$, Table 19). This difference was reflected in the increased CE ($P<.05$, Table 19), thus presenting CE's ability to distinguish between the two conditions. Ergonomic risk assessments are commonly used to assess the feasibility of wearable ergonomic systems [137] and similar to NOISH lifting index and RULA methods, the SAFE framework has the capability to distinguish ergonomically higher risk from lower risk tasks since significant differences in CE values were observed between Ergon and NonErgon tasks (Table 19). This portion of the validation supports the potential use of the SAFE framework for ergonomic risk assessment in the future.

The high correlations observed between CE and Borg scales support findings in the literature [37], [88], [196]. While observed CE (i.e., without rescaling) showed capabilities to distinguish higher- from lower- ergonomic risk conditions (Table 19), values were elevated. This outcome was expected because the torque-based endurance model was originally validated under extreme, high-torque conditions, i.e. shoulder flexion ≈-90° to 0° while elbow flexion ≈0° under static and dynamic conditions, where the arm's CoM is positioned far from the body and sustained until fatigue [204]. Real work tasks are less extreme, with the upper extremity CoM usually closer to the body and facing higher variability and high-torque postures rarely maintained for long periods, leading to overestimation when the model is applied directly.

Task-Related Coefficients

To achieve task-specific endurance metrics, the SAFE framework was rescaled using task-specific perceived fatigue (since Target CE was mapped from the Borg scores), similar to other studies in fatigue estimation employing machine learning [86] and muscle models [68], [196]. While subjective questionnaires have limitations, such as score classification inconsistencies [86] and susceptibility to environmental and emotional influences [155], they remain widely regarded as the gold-standard fatigue reference for fatigue assessment [86]. The rescaling resulted in CE values that reflected participants' state more accurately and resulted in significantly lower errors (NMRSE≈20-30%). While other endurance models have been developed for different tasks [227], [228], [249] and arm configurations [70], [71], here, this variability is captured within a single model through task-dependent coefficients. This provides a unified way to model endurance across diverse tasks involving the upper extremities and accounts for task- and joint-dependent differences in fatigue development [70], [71]. Task- and sex-specific coefficients were also explored in the course of the work and did not meaningfully improve performance.

5.5.3 Limitations and Future work

Regarding the SAFE framework, associating CE values with risk groups (e.g., low, medium, high) and using colour-coded interfaces can help workers quickly identify when they are nearing endurance limits. However, inconsistencies in the scores classifications of subjective fatigue scales (binary vs. multiclass with 3-5 levels [86]) highlight the need for more empirical evidence to establish accurate risk categories. Other areas for future work include investigation of additional personal factors, such as exercise type/frequency, when determining endurance coefficients. Alternatively, endurance coefficients could be tailored to the task by calculating a 'task difficulty index' that integrates CoM behaviour, posture, duty cycle and other task features.

While no negative impacts of misclassification (Figure 50, middle) were observed due to high accuracy of rest and activity detection, future implementations could risk applying incorrect CE scaling coefficients; thus, larger datasets will be required to improve task-type classification. In addition, in future deployment, coefficients will update only after stable classifications (e.g., ≥2 s persistence with a temporal smoother or Hidden Markov Model), which limits coefficient 'thrash' and reduces the impact of brief mislabels. While other studies have performed task classification to distinguish between the same task at multiple load levels to perform ergonomic risk assessments [103], direct estimation of hand-held loads along with task classification would further increase SAFE framework adaptability.

While the calibration task was optimal for static and dynamic shoulder flexion-extension movements in previous research [204], this task may not be generalisable to specific industry-type tasks. For example, Villaneuva *et al.* (2023) [68] continuously adjusted $Torque_{max}$ based on arm position in their model for unloaded HMI applications for their torque-based muscle model. Future work may look at dynamically adjusting $Torque_{max}$ based on task and arm position or considering alternative calibration tasks depending on the movements during a task. Further work should also explore post-task recommendations on task rotation and recovery [27], [68], and comparison with other fatigue models and frameworks [68], [99].

Regarding the SAFE system developed, future work should optimise Bluetooth and higher-rate acquisition (≥50 Hz) to enable dynamic analysis and broader deployment of the SAFE framework, while measuring full system latency during final implementation. Low IMU sampling rate likely caused decreased signal resolution and upsampled, interpolated data used in the present analysis introduce artifacts such as over smoothing or overshooting. Vibrotactile feedback has proven effective for training and posture correction [54], [75], [81], [137] and may serve as a low-interference method of delivering CE warnings. Previous work [204] found that $Torque_{max}$ varied depending on the load used. Future app versions should store $Torque_{max}$ values for multiple loads, so the appropriate strength value can be applied for each task. Integration of IMUs into a work vest may aid with comfort and progress the system towards being 'ready to wear' [137].

Regarding the framework validation experiment, although the number of participants is aligned with the number of participants in studies that assess sensor-based ergonomic systems [80], [94], [98], [99], [101], [102], [329], this number remains relatively small. A larger cohort of experienced workers would provide greater diversity and strengthen the generalisability of the findings. External validity remains to be established since tasks here were short, paced, and lab-based; future studies will deploy SAFE in uncontrolled settings with a wearable IMU vest, pressure insoles, and mobile app.

A 5 s window for task classification was recommended in the previous chapter [253]; however, 1 s windows were required to account for the rest breaks that were less than 5 s. Previous work [253] saw accuracy levels reduce with shorter windows; this may have led to misclassifications, however, it did not affect rest/activity classification as the accuracy was high. While the task classes in the present work (i.e., *manual handling*, *pick and place*, *assembly*, *walking* and *standing*) were used alongside IMU data to identify active and rest periods, future models can be trained on tasks as a whole (such as MHErgon, MHNonErgon, PPErgon, PPNonErgon) and account for all the transitions in those tasks. In this way, rest states and specific tasks can be detected so that the appropriate coefficient is applied during the detected activity.

Symmetrical loading was assumed in the present work; however, force production can be asymmetrical during bilateral dynamic tasks [330], and internal loading has been shown to vary with lifting direction and deviation from the sagittal plane centre during two-handed lifting tasks [331]. Therefore, adapting the model to better account for real-world loading conditions and the influence on fatigue and endurance metrics warrants further investigated. Additional planes of movement in joint angles, particularly those relevant to the three degrees of freedom shoulder joint, were not considered. IMUs on both arms and consideration of posture may aid with accounting for asymmetrical movements in future work. Although the tasks replicated high- and low-risk tasks (Table 19), participant safety constraints prevented us from including tasks with excessive risk, representing a limitation of the present work.

5.6 Conclusion

This study demonstrated that the SAFE framework can support online operator monitoring and ergonomic risk assessment in dynamic industrial tasks. By integrating wearable sensing, biomechanical modelling, and task classification, it delivers individualised and task-specific endurance metrics. Validation confirmed acceptable accuracy for IMU-derived joint angles, and task-specific CE metrics effectively distinguished ergonomic risk levels, aligning with subjective fatigue ratings. The inclusion of torque-based endurance modelling in the SAFE framework results in the framework results in individualised endurance predictions for a range of non-routinised work involving the upper extremities. Task classification enables adaptability of the framework to different tasks without continuous manual input, presenting potential for real-time application in future work. These findings establish the SAFE framework as a practical and adaptable foundation for operator monitoring, with future work targeting improved calibration, larger cohorts, and wearable systems with real-time deployment and feedback.

Chapter 6 Discussion, Conclusions and Future Directions

This chapter interprets key findings of the research, synthesising their significance and exploring their broader implications. The discussion considers how the SAFE framework can influence workplace practices, commercial opportunities, and the reduction of WMSDs. Additionally, the impact on employees, employers, and industry standards is examined. Following this, the limitations of the studies are acknowledged, highlighting areas where further research and refinement are needed. Finally, the chapter outlines future directions, including potential advancements in system development, further field research, and broader implications beyond the initial scope of this research.

6.1 Summary of Key Findings and Contributions

The hypothesis explored in this thesis was that a wearables-based system for physical fatigue prediction could account for individual abilities while generalising across different manual tasks. This was investigated by achieving the three thesis objectives, to summarise: Objective 1 for achieving accurate, individualised endurance predictions; Objective 2 for ensuring task generalisability, dynamic applicability, and automated load input; and Objective 3 for integrating the algorithms from Objectives 1 and 2 into a wearables-based ergonomic system. In terms of the mechanistic framework of fatigue-related tissue degradation described in 1.1.2 Ergonomic Risk, Fatigue and WMSDs, as fatigue alters load distribution and reduces tissue load-bearing capacity, cumulative exposure may accelerate microstructural damage when recovery is insufficient. The proposed monitoring approach therefore provides a means of identifying periods of elevated biomechanical vulnerability prior to the onset of clinically significant WMSDs.

6.1.1 Contribution 1: Torque-based Endurance Modelling and Calibration Method

The endurance modelling work in the thesis contributed towards the achievement of Objectives 1 and 2 and denotes a significant advancement in the prediction of endurance and fatigue in the field for a number of reasons. Firstly, this work represents the first application of a torque-based endurance model to manual handling tasks for WMSD prevention. The switch from force- to torque-based endurance modelling enabled prediction for dynamic tasks and any arm configuration, leading to generalisability across upper extremity tasks and addressing the limited, highly specific nature of traditional force-based MET models, where one model is suitable for a narrow set of isometric conditions. Secondly, the development of a novel standardised method for generating strength measurements represents a significant advancement in the field. The torque-based model and calibration method were validated across static and dynamic loaded tasks, achieving best-case RMSE of 19.11 s for ET prediction.

Thirdly, the torque-based approach resulted in individualised endurance predictions which cannot be achieved with traditional force-based models – a key contribution of the thesis work. This was achieved through the novel application of the torque-based approach to manual handling (due to the consideration of individual anthropometrics in the torque calculations) as well as the novel calibration task method developed in the work which determines an individual's strength at a specific load level. Finally, a lack of public datasets was identified and open access publication of the endurance dataset collected in the course of the thesis encourages further advancement in the field.

Overall, the endurance modelling work in the thesis contributed towards achieving Objectives 1 and 2 and addressed multiple gaps in the literature. These gaps were covered in detail in Chapters 1 and 2 and include lack predictive approaches for WMSD prevention; lack of consideration of dynamic tasks, a variety of arm configurations and task generalisability; lack of standardised methods to determine $Torque_{max}$; lack of investigation into personal factors and sex-based endurance differences; and lack of public datasets.

6.1.2 Contribution 2: Explainable Task Classification and Open Datasets

The work described in Chapter 4 Load and Task Estimation aided in achieving Objectives 2 and 3 and provided a strong basis for the load and task-related aspects of the SAFE framework. The preliminary testing in 4.1 Evaluating Wearable Sensor Technologies for Predicting Shoulder Endurance aided in establishing the unique approach used to deal with the automated load and task-specific elements of the SAFE framework, i.e. by using task classification. Meanwhile, 4.2 AI-based Task Classification Using Pressure Insoles for Occupational Safety saw the first use of explainable AI methods for industry-related task classification. The SHAP approach contributed towards transparent and informed feature reduction (top 5 CoP features), which is not the case with other task classification models in occupational H&S that adopt a “black box” approach. This novel model was deployed in the SAEF framework prototype in Chapter 5 System for Activity-aware Fatigue Evaluation (SAFE) Framework: Predictive Fatigue Modelling for Occupational Tasks. The task classification work also demonstrated the real-time capabilities of the task classification work, supporting its use in a real-time wearable ergonomic system with a high accuracy (83% for 5 s window). The data were also publicly released signifying a contribution towards the lack of datasets in the field and enables accessibility and transparency.

6.1.3 Contribution 3: SAFE Framework Integration and Prototype Deployment

While the endurance modelling and task classification work in the thesis present their own respective novelties and contributions to WMSD prevention research, the integration of these disparate areas to form the SAFE framework represents a significant step forward in the field. The framework does not rely on disputed standards in the ergonomics space, unlike real-time wearable ergonomic systems on the market and in research while addressing limitations of self-reports and traditional ergonomic assessments. For the first time, endurance modelling and task classification research were combined and deployed on a wearable system and its ability for online operator monitoring and ergonomic risk assessment was demonstrated.

The predictive, dynamic, task-generalisable and individualised aspects of the tuned torque-based endurance model represent a strong basis for a proactive, fatigue forecasting system, especially compared to existing approaches are largely reactive and comprise of detection or estimation of the current ergonomic risk or physiological state. The prototype application also integrates the novel calibration task method for determining $Torque_{max}$ and automatically feeds this into the endurance model during task measurement. Regarding the integration of task classification to the SAFE framework, this feature enables automated load input to the endurance model, which significantly improves on existing ergonomic systems that require load input during post-processing or make load-based assumptions. Task classification aspects of the framework also led to fine-tuning endurance predictions by accounting for rest phases and can be used to apply relevant task-specific endurance coefficients.

Specifically, the consideration of arm dynamics (through endurance modelling) and task changes (through task classification) of the SAFE framework represents a highly adaptive system that is capable of adjusting predictions based on real-world conditions over time that is otherwise not evident commercially or in the literature. The framework may be used to predict fatigue for any upper extremity task with any hand-held item (once the methods shown in the thesis are used to train the framework). These aspects of the system and technical results (from Chapters 3 to 5) demonstrate a strong potential for a real-time fatigue forecasting device in terms of online operator monitoring (as the output of the endurance model is predicted ET and CE) and ergonomic risk assessments (since the outputs were statistically significant between high- and low- ergonomic risk conditions).

Regarding use as an online operator monitoring tool, workers can monitor their current endurance capacity as task change throughout a working shift. Using this information, they can adjust accordingly by lowering the number of repetitions, taking a rest break or rotating tasks to introduce biomechanical variation. Regarding use as a tool for ergonomic risk assessment, this system could potentially complement or replace tools such as RULA and NIOSH during manual handling tasks in real working environments. In this way, the system can be used by ergonomists and managers assessing CE changes between tasks, tools and components, and assessing individual workers, contributing to improved operator training and technique that potentially reduces WMSDs. Therefore, this work brings these two previously distinct approaches to WMSD prevention together into a unified framework that supports multiple applications for the first time. Real-time deployment of the SAFE framework is feasible with targeted prototype improvements, discussed in more detail in 6.3 Future Directions, which has been discussed as a notable gap in the field.

Overall, the SAFE framework addressed many limitations that were outlined in the field (Chapter 2 State-of-the-Art in Workplace Fatigue, Wearables, and WMSD

Prevention) relating to lack of proactive and predictive approaches [3], [4], [18], [76], [77], [78], [79]; lack of assessment of dynamic tasks [3], [75]; standardisation issues [18], [41], [75]; lack of generalisability across tasks [70], [80], [81] while maintaining individualisation [3], [4], [23], [76], [185]; lack of explainability in classifier decisions [87] and generating outputs on a continuous scale that enable more precise risk classification [18], [80], [138]. At the same time, the work aligns with key foundational methods in the field, including implementing sensor placement norms [75], bench-marking against gold-standard systems, and employing recommended guidelines for kinematic analyses [41], [75], [311]. Additionally, the number of sensors was kept to a minimum to maintain comfort [75], to aid with user acceptance, and balance the trade-off between the number of sensors with performance and accuracy [4], [75], [137], [138].

6.2 Limitations

While the limitations of each study were individually covered in their respective sections of the thesis, a summary of the overall limitations of the research work is described here. The limitations discussed in this section mainly focus on experimental design and protocol, sample and generalisability, scope of measures, and deployment environment.

In terms of experimental design and protocol, the completion of all tasks on the same day was a limitation to the endurance studies, as one study found that self-reported recovery is not always reliable as fatigue symptoms were present in proceeding tasks in terms of reduced ET (i.e., needing more recovery time and increased subjective scores after the participant reported full recovery) [27]. This is in alignment with other studies [167] and the results shown in 3.2 Validation of Endurance Model for Manual Tasks (Figure 19), as perceived exertion was increased and there were impacts on ET of the last completed task in both groups. However, this was not assessed in subsequent studies (i.e., 3.3 Improving Dynamic Endurance Time Predictions for Shoulder Fatigue: A Comparative Evaluation) and during experiments where tasks were fully randomised (i.e., Chapter 5 System for Activity-aware Fatigue Evaluation (SAFE) Framework: Predictive Fatigue Modelling for Occupational Tasks), mainly due to the fact that task order fell outside the scope and the focus was optimisation of endurance modelling aspects of the work. However, the public release of the data [332] allow task order to be studied in future work and by other researchers.

While the time allocated for rest was in line with some studies [27], [67], [119], [236], Jebelli *et al.* (2020) [110] summarised research surrounding rest time, and some studies mention that 15 mins should be provided and another states that 90% MVC can recovered in 5 to 10 mins but about 30 mins is required for full recovery. Even though participants reported rested states (i.e., Borg RPE score $\leq$ 7) prior to commencing tasks, these studies may indicate that subjects who performed tasks to fatigue (i.e., Borg RPE score $\geq$ 17) may have required additional rest time between tasks. This is of less concern for the final experiment since tasks were not performed until fatigue and tasks were completed in a randomised order to negate the influence of cumulative fatigue related to task order.

The simplified manner in which joint angles were extracted from MoCap and IMU data in section 3.3 Improving Dynamic Endurance Time Predictions for Shoulder Fatigue: A Comparative Evaluation and 4.1 Evaluating Wearable Sensor Technologies for Predicting Shoulder Endurance meant that joint centres and joint constraints were not considered. Although, there is no consistency in the methods used in the literature to measure joint angles [41], the joint angle extraction from the custom IMUs was benchmarked against MoCap and ISB standards which considers these constraints [311]. The method of performing a static calibration to align the IMU to the skeleton is considered a typical alignment method [333] but can be affected by the ability of the person to carry out the calibration [41], [333] and other alignment methods such as those discussed by Stirling *et al.* (2024) [41] may be explored.

In terms of sample and generalisability limitations, the sample size of volunteers in the experiments, while on par with many studies (as mentioned in each individual discussion), is limited in terms of diversity (e.g., age, body composition parameters) and abilities, as participants consisted of students and researchers who lacked significant experience of assembly and manual handling tasks. Many researchers highlighted the need for performing tests on real workers in work environments [3], [18], [23], [86], [137], [138], [197], which this work did not address. Although, efforts were made to limit any other negative implications of the volunteers on the experiments, for example gender balance was maintained where the ratio of male:female subjects for experiments 1 to 5 (Appendix 5) were 29:24, 5:7, 15:14, 1:1, 3:2 and volunteers were given training for each task prior to data acquisition. However, the results of the cohort still may not be generalisable to experienced operators in the field. While relationships between $Torque_{max}$, ETs and gender were examined other studies have found that ET [118], [239], [334], $Torque_{max}$ and strength [213], [214], [241] can change with ethnicity, age and sex. A larger, more diverse cohort of volunteers would introduce more diversity into the study, thus generating a more representative view of the population and aid in studying these relationships more thoroughly.

In terms of limitations pertaining to the scope of measures in the thesis research work, physiological data from PPG and GSR were not gathered, which may prove useful in further tuning the present work by associating ET predictions with physiological symptoms of fatigue, or presenting an additional objective measure of fatigue, for example using EMG data. The thesis did not consider mental fatigue (suggested by [4], [79], [186], [194]) and psychological factors (suggested by [47], [78], [79]) which can have an effect on the rate of development of muscle fatigue [111]. There was no consideration of risk or accident detection [137], [186] or environmental factors [78], or in-depth consideration of privacy issues [3], [18], [83]. All possible confounding factors were not explored using ML [3], [4], [18], [195], for example, subjects' lifestyle factors, sleep homeostasis and psychological states. The system delivers visual feedback to the user via GUI but research suggests that auditory or vibrotactile feedback may be more effective, particularly for tasks that require relocation [75], [81].

There was a lack of consideration of posture, the lower extremities, both arms, arm rotations and movements in the frontal plane (i.e., abduction/adduction), and the effect of different work-rest schedules, such as job rotations, cycle time and duty cycle. The demonstration of the system in Chapter 5 involved tasks with bent elbow conditions, but these conditions were not considered in the analysis of different endurance models with various TTs in 3.3 Improving Dynamic Endurance Time Predictions for Shoulder Fatigue: A Comparative Evaluation. Additional calibration tasks can be considered in future work to ascertain if different configurations are better suited to predicting the endurance of different tasks.

The deployment environment denotes another limitation of the present work. Experiments in the thesis were performed in a laboratory environment which was identified by numerous reviews as a shortcoming of many studies in the field [3], [18], [23], [86], [137], [138], [197]. It is important to note, there is a trade-off between controlled, laboratory-based simulations of work activities that offer a high level of repeatability in experiments, and activities performed in a real-work environment over an entire shift which feature high degrees of variability and are less predictable but are true reflections of workplace tasks [75], [198], [335]. Thus, while the laboratory-based experiments in the thesis were necessary to ascertain the feasibility and accuracy of the system, testing the system in a real-world work environment over realistic working periods [3], [86] is the only way to understand its true efficacy.

6.3 Future Directions

Despite the limitations outlined in the previous section, the findings of this thesis provide a strong and novel foundation for future research. The endurance modelling, task classification, and their integration into the SAFE framework collectively address long-standing gaps in WMSD prevention research, including dynamic task generalisability, automated load estimation, and individualised fatigue prediction. This thesis contributes the first application of a torque-based endurance model to loaded manual handling tasks, a novel calibration method for determining load-specific strength, and the first integration of endurance modelling and explainable task classification into a wearable, real-time fatigue forecasting prototype. These advances represent a meaningful progression beyond traditional, reactive ergonomic tools and establish a robust platform upon which future developments can build. The following research directions therefore aim not to only resolve fundamental shortcomings, but to expand, refine, and translate an already rigorous and innovative framework into broader real-world contexts. Three future directions of research are discussed in this section:

- System and Framework Development
- Individual and Physiological Factors
- Generalisability

These future directions are enabled by the research work described in the thesis. In terms of system development, the system deploying the SAFE framework in the thesis consists of wearables, a MATLAB application and BLE data streaming. Future system development work may focus on improving the existing system (e.g., increasing IMU sampling rate, developing an Android mobile application, and improving comfort and wearability), adapting the system and framework to different occupations, or expanding the application of the system to integrate other areas of research (e.g., by including additional sensors for other assessments such as detecting environmental hazards). Key research questions in this area may include: What wearable ergonomic system characteristics support employee compliance, acceptance, comfort and privacy? How does long-term use of the SAFE framework in real work environments affect injury incidence, absenteeism, and perceived fatigue? What CE thresholds best support worker well-being and prevent WMSDs?

In terms of physiological and individual factors, future research may build upon the investigation into the influence of such factors on endurance that took place in 3.2 Validation of Endurance Model for Manual Tasks and 3.3 Improving Dynamic Endurance Time Predictions for Shoulder Fatigue: A Comparative Evaluation. Alternatively, it may utilise the datasets developed in the course of the thesis (particularly EMG data) to understand sex-based physiological or synergistic differences. Key research questions in this area may include: To what extent do sex, age, or body composition moderate the relationship between predicted ET and actual fatigue? How do muscle synergies vary with task type and what is the impact on fatigue development?

In terms of generalisability, future research may expand on the thesis work by analysing additional the joints and directions of movement, building on the task classification work to consider other tasks, or considering alternative calibration tasks for $Torque_{max}$ measurement, as well as other methods that are discussed later in the section. The suggested areas of future research discussed in this section aim to strengthen the system's real-world relevance, improve technical performance, and address remaining gaps in the current approach. Key research questions in this area may include: Can additional joints and planes of movement be incorporated without sacrificing system usability and comfort? Can the SAFE framework be deployed in sporting contexts to aid with injury prevention and performance optimisation?

In the short term, the most important avenue for future research lies in further developing the system framework and enhancing its generalisability to support deployment in longitudinal studies. This would aid with essential capabilities pertaining to real-time application and consideration of additional planes of movement and occupations. Longitudinal studies are a key element to future research for any fatigue forecasting system because large volumes of data from many individuals are required to understand this very complex phenomenon. Such studies can be conducted in collaboration with industry partners with real workers in real work environments over typical working periods, i.e. 8 hours, during cyclical and non-cyclical, non-routinised (where loads, frequency and duration vary) tasks [198]. These studies can be used to assess the impact of such systems on the worker (i.e. injury prevention, comfort, compliance, acceptance) and the organisation (i.e. productivity, mistakes, accidents, quality, process interruptions). Additionally, ET and CE metrics can also be compared with muscle models and additional ergonomic risk assessments, similar to the manner in which they were compared to RULA and NIOSH assessments in the thesis during longitudinal studies. These studies are required to effectively follow through with the proposed future research directions such as understanding system generalisability and physiological and individual factors.

6.3.1 System and Framework Development

Future work in this area may include building on the current hardware, software and modelling approaches described in the thesis. The sampling rate of the IMUs in the system should be increased to capture higher frequency movements, and the development of a mobile application could further enhance the system's deployability. Feedback via auditory or vibrotactile methods as it was found to be more effective than visual means in posture correction studies [75], [81], [104], and this would also be useful for tasks that are performed at different workstations so that users do not need to stop and look at their phone to monitor their state [75], [81]. Section 4.2 AI-based Task Classification Using Pressure Insoles for Occupational Safety called for the design of insoles that are optimised for the extraction of CoP features, such as a quadrant structure, which may aid with classification of similar tasks in future work. Efforts must be made to address the issue of magnetic disturbances in wearables, as this is particularly important in the context of industrial environments [136]. This improvement would need to be implemented before the system could be applied in real-world settings [4], [18]. Accurate external load measurement using pressure insoles would aid further reduce the need for manual input (since task-related loads are inputted manually to the app) and would aid with generalisability to other occupations where multiple loads can be associated with one task type.

The current prototype consists of different sensors that are attached using Velcro straps meaning it does not fall into the 'ready to wear' category used by Stefana *et al.* (2021) [137] when assessing ergonomic systems. Integration of sensors into smart personal protective equipment (PPE) may offer a more comfortable, discrete manner of collecting the required data [137], which may be done through smart vests which embed the sensors or through textile-based sensors. Since the success of this system's implementation largely depends on its users and the way they engage with it, which is of utmost importance in this context and compliance is key for H&S, efforts the opinion of the worker must be at the fore of the design of the system. Distraction by wearable systems was more common during cyclical work [82] and personal factors such as BMI and age affected comfort and distraction [82], thus can be considered in the design of a system that caters to a variety of needs.

Additional system development may consist of modelling improvements. Similar to the constraints that were used in Chapter 5 System for Activity-aware Fatigue Evaluation (SAFE) Framework: Predictive Fatigue Modelling for Occupational Tasks to tune the torque calculation (i.e., by setting the torque=0 Nm during rest phases), the methods used to calculate torque can be compared to simulation methods in programmes like OpenSim, which may help to fine-tune torque calculation. Inclusion of endurance and CE metrics into simulation programmes may also be useful to test out a variety of working scenarios prior to implementation in workplace settings.

Additional system improvements may also expand the framework beyond upper extremity tasks considered in the present work to other occupations. This can be done by adding to the existing datasets or placing sensors on the lower extremities and using the same methods outlined in the present work to develop the occupation-specific algorithms.

System recommendations should also be a focus of future research. For example, the CE limit that results in the system displaying a warning (for example at 70% CE), would aid in addressing the lack of defined thresholds that describe exertion states

[83]. Organisation- and work-specific recommendations can be provided to an individual based on current endurance levels, tasks they are trained in, the tasks available and the organisation's targets for the day. Alternatively, once an individual has reached their endurance limit, research into recovery times and models (such as , such as Rose *et al.* (2014) [27]) and the most suitable subsequent task that ensures diversity in biomechanical exposure is required.

There are also cross-disciplinary opportunities in future system and framework development. The integration of additional sensors and algorithms could also expand the system's functionality. For example, environmental monitoring and hazard detection could be enabled by measuring parameters such as humidity, temperature, noise levels, and air pollution [6] and EMG could help to objectively estimate current fatigue levels. Other potential capabilities include fall detection (such as [184], [274], [283]), monitoring mood, emotions, stress levels, mental alertness and psychosocial risks (such as [4], [78], [79], [194]), classifying safe and unsafe postures [336] and prompting rest breaks. While this thesis focused on monitoring the health of the worker, the proposed improvements could enable expansion to other operator types. For instance, integrating further sensors or exoskeleton technology could contribute to the development of the "super-strength" and "intelligent" worker concepts [4].

Within the framework of Industry 4.0/5.0 and the Operator 4.0 concepts, the framework presented in this thesis could contribute to WMSD prevention by integrating intelligent, real-time warnings into VR equipment (so that a mobile application is not required) or by enabling communication with other devices in the work environment. Previous research has recommended examining the influence of such collaborations on worker stress along with factors such as task smoothness and execution speed [4] and adapts cobot activities based on present fatigue levels [150]. Understanding how humans perceive and interact with machines is essential for optimising collaboration [337]. Proximity detection to tools, spaces, or other workers could also support task classification, component identification, and determination of whether a task is collaborative, either with another person or a robot. Furthermore, other studies have proposed developing dashboards for worker H&S, allowing managers to monitor absences, subjective worker well-being scores, and injury data, and to link these metrics for more proactive intervention [338].

6.3.2 Individual and Physiological Factors

Individual factors can address pertinent issues for Operator 4.0 in addition to preventing WMSDs [86], such as helping to foster a more inclusive work environment with an aging workforce [4], [185], [339]. Sections 3.2 Validation of Endurance Model for Manual Tasks and 3.3 Improving Dynamic Endurance Time Predictions for Shoulder Fatigue: A Comparative Evaluation explored the influence of individual factors on endurance. While correlation analyses were utilised in the present work to ascertain any influence in the present work, ML may be able to uncover underlying relationships between these parameters, especially since one review [195] found that integration of ML and AI into human factors and ergonomics research is still limited.

Therefore, accessible datasets for ML researchers are imperative to further advancement in the field [76], [79]. The datasets described in the thesis present great potential to contribute to the field, in particular because it was found that inclusion of females in such datasets is currently limited [118]. The EMG data in open-access endurance dataset developed in the thesis may contribute towards another limitation in the field which is a lack of understanding of male and female endurance differences from a physiological perspective [250]. Mathiassen and Ahsberg (1999) [162] note that "endurance time differs considerably between muscle synergies", raising questions about the validity of applying generalised endurance models to shoulder activity. This highlights an opportunity for future work to investigate muscle synergies more explicitly, an area that the dataset developed in this thesis could help facilitate since EMG data are included. For example, [340] applied an endurance model to static shoulder flexion tasks until exhaustion and analysed the associated muscle synergies, while [350] compared lifting and lowering tasks and found notable differences in synergy patterns. Furthermore, individuals tend to redistribute loads when they experience fatigue [127], [341], [342], for example one study found that elbow and trunk moments increased to alleviate fatigue when shoulder moments were reduced [341]. A method of detecting these fatigue-related compensation changes throughout the body and alerting the user may also aid in reducing the risk of WMSDs.

In terms of utilising the present work as a basis for cross-disciplinary research on individual factors, the endurance dataset in the present work may be used to study the link between physical and mental fatigue [79], [343], since mental fatigue data from the Karolinska Sleepiness Scale [74] are noted at the end of each task. Future datasets may also collect data for studying the influence of motivation [47], sleep and circadian rhythms [47], [109] and psychosocial risks [15] on endurance and fatigue.

6.3.3 Generalisability

The present work has demonstrated that the SAFE framework can be applied to different upper extremity tasks performed in the sagittal plane due to the torque-based nature of the model. This was demonstrated and explained in detail in 3.3 Improving Dynamic Endurance Time Predictions for Shoulder Fatigue: A Comparative Evaluation and Chapter 5 System for Activity-aware Fatigue Evaluation (SAFE) Framework: Predictive Fatigue Modelling for Occupational Tasks. Similar to the manner in which the thesis builds upon prior to work that tested the torque-based method in unloaded conditions in abduction [37] and flexion [88] directions, future research may expand the thesis work beyond tasks in the sagittal plane. Although fatigue is predicted based on the distance from the shoulder to the CoM, the muscle groups involved in movements in these planes differ, highlighting the importance of this continued investigation in future research.

To build on the novel work to determine $Torque_{max}$ in 3.3 Improving Dynamic Endurance Time Predictions for Shoulder Fatigue: A Comparative Evaluation, other calibration tasks may be more suitable to ascertain the strength of individuals during alternative tasks and should be assessed in future work. This may aid with fine tuning strength measurement or aid with application of the framework to other domains.

While the framework was tested during industry-type tasks that consisted of a variety of movements in Chapter 5 System for Activity-aware Fatigue Evaluation (SAFE) Framework: Predictive Fatigue Modelling for Occupational Tasks, additional movements may be useful for expanding the generalisability of the framework to other occupations and parts of the body. For example, an adjusted version of the NICE model [88], called NICER [321], used EMG to predict ET in overhead, unloaded movements, and this method can be investigated for use in loaded conditions. Although overhead lifting does not comply with manual handling guidelines, it is still sometimes carried out in reality. Additionally, posture and the lower extremities should be considered to deliver a whole-body fatigue forecasting system that considers full body tasks such as loaded stooping, squatting and bending. This links up with the point mentioned in 6.3.1 System and Framework Development to include lower extremity motion tracking sensors. While task-based endurance differences are considered in the thesis (Chapter 5 System for Activity-aware Fatigue Evaluation (SAFE) Framework: Predictive Fatigue Modelling for Occupational Tasks), this can be expanded on in future work to account for additional planes of movement, overhead movements, posture, lower extremities and additional work-related factors. This would aid with fine-tuning endurance predictions for additional industry-type tasks and aid with framework application to other domains, such as other occupations, sports and rehabilitation.

Application to other occupations, such as medical professionals and construction workers, would be particularly encouraged by developments to the task classification work described in Chapter 4 Load and Task Estimation. Future research in task classification can involve performing image classification as the CoP was found to be visually different for each task in section 4.2 AI-based Task Classification Using Pressure Insoles for Occupational Safety, and may provide higher accuracies. The task classification aspect to the system in the thesis also presents the potential to integrate existing empirical task-specific endurance models, such as those for pushing and pulling tasks [227], [249].

The investigation into the influence of task order on ETs in 3.2 Validation of Endurance Model for Manual Tasks found that experimental ETs were reduced in the last completed task. This type of task-related research may be expanded to assess the impact of duty cycle and cycle time of intermittent tasks [165], [344], [345], job rotations [346], work/rest scheduling [347] and task order [167] on fatigue may generate a system that accounts for all types or work and rest. However, the influence of such factors are contested as epidemiological literature reviewed in 2006 [55], showed that variations in job rotations and more breaks had limited effectiveness and that physical variations is advantageous from a physiological and psychological perspective. While the endurance modelling work in the thesis considers individuals' strength at specific load levels using the calibration task to determine $Torque_{max}$, this may be built on and combined with the aforementioned task-related influences in future work. This type of investigation may be used to inform individualised task allocation [4] which may be accounted for in an organisation's IoT system when determining an individual's targets, schedules and task allocation.

6.4 Implications of Findings

This section looks to the broader implications of the system described in the thesis and assesses the requirements for its effective implementation and integration. As discussed, there may be potential commercial impacts from the research and should the ergonomic system in the thesis, or similar, be placed on the market, the main goal is to reduce the prevalence of occupational risks related to biomechanical exposure and to improve workers' wellbeing and physical health. Yet the move towards Industry 5.0 also presents new challenges and risks for the worker, managers, management systems and work environments [3], [348], [349], therefore it is important to understand and discuss the how a worker, a manager, an organisation and organisational policies may need to adapt to these changes. In addition, there are key issues which have been raised in recent surveys [75], [152], namely privacy and security, comfort, uptake and compliance which are discussed in this section.

6.4.1 Commercial Opportunities and Reduced WMSDs

There is significant commercial opportunity for the system presented in the thesis. The cost of WMSDs is 2% of Europe's GDP both directly due to medical costs and indirectly due to absences and reduced productivity, meaning it incurs billions of euro every year [40], [44]. Thus, the research areas of ergonomics, occupational H&S and human factors exist to prevent rather than treat WMSDs, and there are additional knock-on benefits in terms of worker wellbeing and satisfaction, cost and productivity. Several market reports on the wearable technology sector present varying estimates regarding market growth and the number of devices expected. According to a report by Markets and Markets, the global wearable sensors market was estimated at 70 billion USD in 2024 with expected growth to 153 billion USD by 2029 [350], while Industry ARC forecasts a more conservative figure of 64 billion USD in 2026 [351], meanwhile Fortune Business Insights, forecasts that the market will grow to from 157 billion USD in 2024 to 1.7 trillion USD 2032 [352].[7] These figures show that the wearable sensors market is expected to significantly grow, which demonstrates scope for a potential start-up when combined with the fact that current commercial solutions

[7] Discrepancies between reports can be attributed to differences in methodology, market definitions, and projection timeframes, highlighting the challenges in predicting market dynamics in such a rapidly evolving field. As such, the actual figures may vary depending on future technological developments and market adoption.

are based on highly disputed standards whose efficacy has not been demonstrated over time [169], [170].

The path from the current system prototype to a market-ready commercial device involves following the typical product development process, Figure 53. In terms of the system so far, the *concept* has been formulated, and aspects of the *research* and *prototype* steps have been completed. From a product research point of view, thorough market research and competitor analysis would need to be completed, and a feasibility study would assess the likelihood of success. Future research work is required to improve the current prototype (discussed in section 6.3 Future Directions), when intellectual property, branding and trademarking can also be considered. The system should be further refined and developed for functionality, user experience and manufacturability with inputs from relevant stakeholders, such as policy makers, researchers, employers, employees and labour unions for the *development* phase. The *testing* stage ensures compliance with the required technical, quality and safety standards such as ISO standards for human-centred design (ISO 9241-210:2010), functional safety (ISO 26262), information security management (ISO/IEC 27001), and regulatory considerations for CE marking, such as electromagnetic compatibility directive (2014/30EU), radio equipment directive (2014/53/EU) since it uses Bluetooth, and PPE regulation (EU 2016/425). The *launch* can take place once marketing and distribution issues are addressed. Feedback from stakeholders remains a part of the products' continued development as new and improved versions of the product are released. Additional skills and/or personnel, such as those in business, computer science and engineering, may be required to add value to the product development stages in Figure 53.

Other options for commercial products include integration into other tools. For example, many simulation tools such as BoB [145] outputs risk scores from existing ergonomic risk assessments and biomechanical models and the CE model may present potential for inclusion in such systems, similar to the integration of a muscle model with simulation software in research [124]. Additionally, the model could be integrated into the XSens Ergo package [92] that integrated common ergonomic risk assessments, however inclusion of pressure insoles would be necessary. With these methods, wearables data can be used to run simulations and understand the impact of different

Figure 53: Product development process

parameters such as tools, task rotations, loads on CE as they can be virtually tested prior to implementing changes to a workstation.

In occupational settings, demands on resources such as capital and personnel to carry out risk assessments and hazard analysis are significant pose challenges and often lead to ineffective implementation of prevention measures [40], therefore the system must be designed to deal with resource-constrained environments and perhaps even aid with alleviating these pressures. According to Balkin *et al.* (2011) [105], the ideal operator monitoring system should be valid, reliable and consistent, have a high sensitivity that minimise failures to alarm and false alarms, and must find a balance between specificity and generalisability. Some systems also include productivity metrics [80] but this presents additional ethical implications that may affect compliance and user acceptance. Privacy measures should be in place and the system should provide actionable feedback in a clear and accessible manner and be adaptable to facilitate user acceptance [105]. Attributes such as resistance to magnetic interference [75], [110], high comfortability [75] are also pertinent to the system design to ensure compliance, acceptance and to increase the likelihood of successful integration into a workplace. The solution must be cost-effective and scalable and assume that it will be applied in an organisation that has limited time, personnel and financial resources [40]. There are unresolved issues in these areas with the present system and much more research and development are required, discussed in more detail later.

The diverse potential uses of the product, such as online operator monitoring, workstation assessment, training, individualised work schedules and task rotations, is attractive to a wide range of potential customers, such as employers, employees, ergonomists and H&S professionals. Since many companies do not have the capacity to perform all of these assessments in house due to expense and the requirement for expertise, many adopt cheaper and simplified approaches [41]. However, the SAFE framework presents an alternative solution while addressing many barriers to uptake. The solution presented in the thesis consists of the minimal number of sensors required for a thorough assessment, called for by many reviews [4], [75], [137], [138], and negates the need for timely, observational assessments. Once sensor placement and calibrations have been carried out under the guidance of a professional, the system enables workers to collect their own data and manage their own work schedules, freeing up resources and time for managers and ergonomists. A centralised database capable of integrating heterogenous datatypes can prove beneficial to companies handling large amounts of data, especially larger companies whose employees suffer from WMSDs to a greater extent [15].

The extension of this research work into a viable commercialisable product aligns with the shift towards Industry 5.0 in terms of creating a human-centric work environment [4], [6], [7], promoting the health of the worker [4] while integrating a key enabling technology of Industry 5.0 [10]. This system can help create human-centric workspaces by addressing WMSDs which in turn may have positive knock-on effects such as improving worker wellbeing, and productivity, reducing absences, disability and economic burdens, enabling the redesign of tasks, workstations and equipment, developing individualised work schedules and targets, and creating a more inclusive work environment after further research is pursued and once the products efficacy for WMSD prevention is demonstrated. The product aligns with the sustainability goals of Industry 5.0 because reduced fatigue can result in less mistakes [50], process interruptions [46], [51] and improve quality [45], [46], which would result in less waste. Furthermore, once the products efficacy for WMSD prevention is demonstrated, the costs associated with treating these disorders as well as absence-related costs may be reduced.

6.4.2 Implications on the Employee, Employer and Organisation

Beyond utilising wearable devices to improve safety and ergonomics, wearables can be used to assist in training, health-related decision making and they can increase empowerment and engagement for employees [10]. However, the impacts of this technology may not always be positive [353] and new industry technologies can require workers to learn new skills and perform new tasks [3] and present recurring and new risks for workers [348], [349]. For example, it can lead to increased task complexity [354], cause the work pace to speed up [355], and lead to increased cognitive demands [76], [356], stress [348], physical fatigue [357], [358] and overwork [354]. It is important that the system developed in the present work helps all stakeholders to adapt to the changing work environment and doesn’t place additional burdens on the worker.

Many surveys have found there is a reliance on observational methods to perform risk assessments, and they are not always performed when required. This highlights the need for new, easy-to-use systems (such as the device developed in this thesis) that can help drive a culture change in ergonomic practice and WMSD prevention. For example, the ESENER report [15] found that the use of interventions for WMSD prevention did not increase between the 2014 and 2019 reports, and the survey of ergonomists by Lowe *et al.* (2019) [139] found that the use of direct measurement data collection (including basic measuring tools and wearables) did not increase compared to an almost identical similar survey completed by Dempsey *et al.* (2005) [151]. While observational data collection methods did increase [139], these findings indicate that occupational H&S management systems are generally not responding to this growing issue using the most effective, objective methods. Moreover, the ESENER report [15] found that organisations are not completing risk assessments in some cases because the “risks are already known”. This indicates that, regardless of the tools or systems available, there remains a need for more intuitive, accessible technologies, like the system proposed in this thesis, that can promote more consistent and proactive ergonomic assessments. A shift in current managerial and organisational practices is needed to foster a culture of safety that prioritises regular, objective assessments for “anticipa[ting], recognis[ing], evaluat[ing] and control[ling] risks” [15] for workers.

To ensure impactful and sustainable change, preventative measures must be integrated into the broader management system as this approach has been shown to enhance overall organisation performance in addition to health and wellness [40], [359]. Successful integration may involve dashboards that monitor absenteeism, work performance, and safety incidents to trigger appropriate interventions [338]. Existing research outlines potential solutions for connecting wearable devices into a broader data management ecosystem [184], which details how wearables fit within a larger ecosystem. Without these changes, direct and objective measurement methods for WMSD prevention via wearable sensor systems, such as the one described in the thesis, cannot be easily adopted into workplace organisational structures and thus have a positive impact on reducing the prevalence of WMSDs. Integrating a wearable sensor system into a work environment presents both opportunities and challenges, particularly in larger organisations where workplace safety and productivity are key concerns, as highlighted in the ESENER report [15]. One major consideration is the practical implementation of such systems, including calibration, security, and interoperability with existing infrastructure [19]. Ensuring seamless connection and communication between devices while maintaining data privacy is critical for successful implementation.

Additionally, a holistic approach that involves collaboration among various professionals, beyond just analysing workers’ kinematics, can provide more meaningful insights into worker well-being [360]. For example, broader management changes may consist of educational and skill development programs to aid individuals to switch from older practices and to embracing newer technologies [4]. Multidisciplinary collaboration between different departments is required and a balance must be found between their goals, which can sometimes be contradictory [361]. For example, engineers may focus on improving productivity but their actions often impact the biomechanical exposure of workers, meanwhile the main goal of ergonomists lies in ensuring wellbeing and health but they also impact productivity [361]. Additionally, as previously mentioned, researchers are generally willing to deal with high costs, longer calibration and data collection time if accuracy and precision are high, whereas practitioners in the field generally do not have access to such resources and ease of use is preferred [18]. Furthermore, it is easier to convince upper management to adopt new H&S policies when it comes with productivity and quality improvements [338], which can aid with finding a compromise between production and employee well-being that new technologies and methods present [78].

Feedback from employees should be involved to ensure a human-centric approach [201], [362] which can lead to higher acceptance [201], and thus a more successful deployment of the system [4]. Company policies should be adapted to the evolving work environment while ensuring privacy and security. While researchers can design state-of-the-art tools for WMSD intervention, it is incredibly important to note that these systems alone do not prevent WMSDs; success is dependent on employee compliance and the actions of organisations and the ergonomists and occupational safety professionals therein [338]. It is their responsibility to embrace these tools, use them correctly, perform risk assessments when required and adapt existing procedures, tools and tasks accordingly.

Ultimately, integrating a wearable system into a workplace requires balancing technological feasibility, privacy, and organisational adaptability to ensure its effectiveness in improving workplace safety and efficiency.

6.4.3 Standards and Policy

Current European policies for occupational H&S, which materialise as laws in member states, are broad and do not outline specific risk assessments or instrumentation. However, the H&S organisations that enforce these laws recommend specific tools, although without strong scientific evidence in the case of the HSE UK [363], which the HSA in Ireland follows. Separately, many researchers agree that ISO standards require reassessment as they lack transparency and scientific rigour [169], [170]. ISO standards, while not mandatory, influence EN and country-specific standards that are mandatory, and wearable and simulation systems for WMSD prevention designed around such standards, both in the literature and commercially (section 1.3.2 Research Gaps Addressed and Novel Contributions). This raises concerns regarding the scientific validity of such systems, placing the H&S of workers at risk. The majority of these assessments are valid for static tasks and do not consider risk on a continuous basis, and a move towards dynamic monitoring, such as the work presented in the thesis, denotes a key advancement in the field.

Reassessing ISO standards involves gathering inputs from a multidisciplinary group of stakeholders after an unbiased presentation of scientific evidence and for the findings to be transparently presented [169]. There is much research to be done to collate a substantial body of evidence in order for this to take place, for example, longitudinal studies (repeated measurements of the same individuals over prolonged periods), and large cross-sectional studies (different individuals at a single point in time), to assess the impact of different interventions on fatigue, ergonomic risk and WMSD prevention. The research work described in the thesis presents a candidate for comparison in these studies, especially once improvements that deal with the limitations are made in future work. Addressing ISO standards has the potential to positively influence mandatory EN and member state standards as well as organisations that promote occupational H&S by prioritising scientific rigour and the inputs of all stakeholders concerned. Furthermore, national H&S organisations, such as the HSA, should recommended specific systems to employers, based on extensive research and compliance with established standards, to aid employers in adapting to newer technologies for WMSD prevention.

In addition, organisations will need to adapt organisational H&S policies and provide specific guidelines for the use of wearable ergonomic systems in work settings. A systematic review assessing the impact of digitisation and ICT on occupational H&S [84] made numerous recommendations for employers and policy makers. The human factors and AI-driven aspects of the work described in the thesis aligns with the recommendations for worker-centred design [84], while stress management programs should also feature. Ethical guidelines should be established regarding limits on employee monitoring and transparency in the decision-making process of algorithms [84], [85], which the task classification work achieves through the explainability analysis. An ethical framework should be established to describe how organisations should respond to challenges presented by such devices in a responsible manner. For example, the system in the thesis presents pertinent questions: Does the worker rest when the system alarms or is permission required? Who is permitted to dismiss safety warnings (if anyone)? Who has access to worker data? Guidance based on extensive research should be provided to policy makers and employers to aid with these ethical issues in such a way that promotes compliance, comfort and acceptance by operators.

Likewise, privacy and cybersecurity policy recommendations should also be implemented [84], [85]. It is widely acknowledged that workers should have access to their own information [4], [78], [80] which is enabled by the device described in the thesis as the data can potentially be collected on the individual's mobile phone alone. While managers and ergonomists may require access to personal information for the purposes of assessing worker health and ergonomic risk at workstations, there may be no requirement for this with the SAFE framework as employees are capable of managing their own work schedules safely and independently. Placing restrictions on the data collected and on the personnel who have access to this data should be ensured [84], [85], and compliance with GDPR policies will help to safeguard worker information in this regard [364]. While the collection of psychological and psychosocial information is recommended by many researchers [4], [78], [79], this may be viewed as too invasive [10]. Privacy policies and the data that are shared with employers can have a significant impact on employee compliance and acceptance [152], [201]. Therefore, as previously mentioned, employees should have a significant influence on the types of technology used, the types of data gathered and with whom it can be shared [78], [201].

Measures should be put in place by organisations to ascertain the views of employees and ergonomics on new technologies to ensure acceptance and efficacy. In addition to privacy and security, barriers to user acceptance include a lack of incentives, the cost-benefit ratio, and compliance issues [152], [201], which can be aided by demonstrating the immediate personal benefits to employees and ergonomists. Employers can use various technology acceptance models to assess which types of technology will be accepted by their employees [201], where factors such as perceived usefulness, ease of use, effort and comfort can be assessed, and a device that compromises between organisational and employee needs can be selected.

6.5 Conclusion

This thesis set out to answer the research question and test the hypothesis that a wearables-based system could predict physical fatigue while accounting for individual abilities while generalising across diverse manual upper extremity tasks. Through the achievement of the thesis objectives, this work demonstrated that such a system is not only feasible but offers meaningful advantages over traditional assessment methods.

The endurance modelling research established a novel torque-based approach capable of generating accurate, individualised, and task-generalisable endurance predictions across dynamic manual handling conditions. The development of a load-specific calibration method further advanced the state-of-the-art by providing a standardised and practical means of estimating individuals' strength for fatigue prediction, an existing gap in the research. Furthermore, the task classification work utilised explainable AI methods for automated load and task identification, enabling dynamic measurement and supporting real-time applicability. Both datasets generated through the thesis were disseminated openly, providing a resource for further research and contributing to increased transparency and reproducibility in the field.

The integration of endurance modelling and task classification into the SAFE framework represents a significant step forward for WMSD prevention. For the first time, a predictive, dynamic, individualised and task-aware fatigue forecasting framework was deployed on a wearable prototype capable of online operator monitoring and performing ergonomic risk assessments. This work addresses long-standing limitations of traditional ergonomic tools in research and industry, which are often reactive, labour-intensive, and limited to specific tasks or isometric conditions. By contrast, the SAFE framework demonstrates a proactive and adaptable approach, offering the potential for improved worker safety, more informed task design, and potentially reduced WMSDs in real working environments.

The findings of this thesis advance the understanding of fatigue prediction and present a unified foundation for future wearable ergonomic systems. Identified limitations highlight opportunities for refinement, optimisation, and wider deployment. Overall, this thesis contributes a substantive and innovative step toward real-time, individualised, and generalisable fatigue forecasting for occupational settings. By bridging the gap between lab-based biomechanical analysis and field-ready ergonomic tools, this work lays the groundwork for future occupational systems that not only monitor fatigue, but actively prevent injury and support sustainable, human-centric workplaces.

Appendices

Appendix 1: Linking Publications to Chapters

Chapter	Title	Publication Type	Publication Location	Publication Date
3.1	"Estimation of maximum shoulder and elbow joint torque based on demographics and anthropometrics"	Conference Article	IEEE EMBC, Glasgow, UK, July 2022	September 2022
3.2	"Validation of endurance model for manual tasks"	Conference Article	IEEE EMBC, Sydney, Australia, July 2023	December 2023
3.3, 4.1	"SWIFTIES Dataset: Subject and Wearables data for Investigation of Fatiguing Tasks In Extension/ flexion of Shoulder/ elbow"	Dataset	Zenodo	March 2024
3.3	"Improving Dynamic Endurance Time Predictions for Shoulder Fatigue: A Comparative Evaluation"	Journal Article	Applied Ergonomics, Elsevier	February 2025
4.1	"Evaluating Wearable Sensor Technologies for Predicting Shoulder Endurance"	Conference Article	IEEE EMBC, Copenhagen, Denmark 2025	December 2025
4.2	"PID4TC (Pressure insoles data for task classification)"	Dataset	Zenodo	March 2023
4.2	"AI-based task classification using pressure insoles for occupational safety"	Journal Article	IEEE Access	February 2024
5	"System for Activity-aware Fatigue Evaluation (SAFE) Framework: Predictive Fatigue Modelling for Occupational Tasks"	Journal Article	Applied Ergonomics, Elsevier	(Under review) Submitted December 2025

Appendix 2: DOIs for Thesis-Related Publications

Chapter	Publication Title	doi
3.1	"Estimation of maximum shoulder and elbow joint torque based on demographics and anthropometrics"	https://doi.org/10.1109/embc48229.2022.9870906
3.2	"Validation of endurance model for manual tasks"	https://doi.org/10.1109/embc40787.2023.10341139
3.3	"Improving Dynamic Endurance Time Predictions for Shoulder Fatigue: A Comparative Evaluation"	https://doi.org/10.1016/j.apergo.2025.104480
4.1	"Evaluating Wearable Sensor Technologies for Predicting Shoulder Endurance"	https://doi.org/10.1109/embc58623.2025.11253989
4.2	"AI-based task classification using pressure insoles for occupational safety"	https://doi.org/10.1109/access.2024.3361754
5	"System for Activity-aware Fatigue Evaluation (SAFE) Framework: Predictive Fatigue Modelling for Occupational Tasks"	Awaiting doi

Appendix 3: CRediT Author Statement for Publications

Chapter	Publication Title	CRediT Author Statement
3.1	"Estimation of maximum shoulder and elbow joint torque based on demographics and anthropometrics"	**Patricia O'Sullivan:** Conceptualisation, Methodology, Formal analysis, Investigation, Data curation, Writing – original draft, Writing – review & editing, Formal Analysis, Visualisation. **Matteo Menolotto:** Conceptualisation, Methodology, Writing – review & editing, Supervision. **Brendan O'Flynn:** Conceptualisation, Resources, Writing – review & editing, Funding acquisition. **Dimitrios-Sokratis Komaris:** Conceptualisation, Methodology, Writing – review & editing, Supervision.
3.2	"Validation of endurance model for manual tasks"	**Patricia O'Sullivan:** Conceptualisation, Methodology, Formal analysis, Investigation, Data curation, Writing – original draft, Writing – review & editing, Visualisation. **Matteo Menolotto:** Conceptualisation, Methodology, Writing – review & editing, Supervision. **Brendan O'Flynn:** Conceptualisation, Resources, Writing – review & editing, Supervision, Funding acquisition. **Dimitrios-Sokratis Komaris:** Conceptualisation, Methodology, Writing – review & editing, Supervision.
3.3	"Improving Dynamic Endurance Time Predictions for Shoulder Fatigue: A Comparative Evaluation"	**Patricia O'Sullivan:** Conceptualisation, Methodology, Formal analysis, Investigation, Data curation, Writing – original draft, Writing – review & editing, Formal Analysis, Visualisation. **Matteo Menolotto:** Conceptualisation, Methodology, Writing – review & editing, Supervision. **Brendan O'Flynn:** Conceptualisation, Resources, Writing – review & editing, Supervision, Funding acquisition. **Dimitrios-Sokratis Komaris:** Conceptualisation, Methodology, Writing – review & editing, Supervision.
4.1	"Evaluating Wearable Sensor Technologies for Predicting Shoulder Endurance"	**Patricia O'Sullivan:** Conceptualisation, Methodology, Formal analysis, Investigation, Data curation, Writing – original draft, Writing – review & editing, Visualisation. **Matteo Menolotto:** Conceptualisation, Methodology, Writing – review & editing, Supervision. **Brendan O'Flynn:** Conceptualisation, Resources, Writing – review & editing, Supervision, Funding acquisition. **Dimitrios-Sokratis Komaris:** Conceptualisation, Methodology, Writing – review & editing, Supervision.
4.2	"AI-based task classification using pressure insoles for occupational safety"	**Patricia O'Sullivan:** Conceptualisation, Methodology, Formal analysis, Investigation, Data curation, Writing – original draft, Writing – review & editing, Visualisation. **Matteo Menolotto:** Conceptualisation, Methodology, Formal analysis, Writing – review & editing, Visualisation, Supervision. **Andrea Visentin:** Formal analysis, Writing – review & editing, Visualisation. **Brendan O'Flynn:** Conceptualisation, Resources, Writing – review & editing, Supervision, Funding acquisition. **Dimitrios-Sokratis Komaris:** Conceptualisation, Methodology, Writing – review & editing, Supervision.
5	"System for Activity-aware Fatigue Evaluation (SAFE) Framework: Predictive Fatigue Modelling for Occupational Tasks"	**Patricia O'Sullivan:** Conceptualisation, Methodology, Formal analysis, Investigation, Data curation, Writing – original draft, Writing – review & editing, Formal Analysis, Validation, Visualisation. **Matteo Menolotto:** Conceptualisation, Methodology, Writing – review & editing, Supervision. **Brendan O'Flynn:** Conceptualisation, Resources, Writing – review & editing, Supervision, Funding acquisition. **Dimitrios-Sokratis Komaris:** Conceptualisation, Methodology, Writing – review & editing, Supervision.

Appendix 4: Additional Peer-Reviewed Collaborative Publications During the PhD

Title	Publication Type	Publication Location	Publication Date	Reference
"3D printed torso phantom for UHF WIMD measurements"	Conference Article	IEEE International Symposium on Antennas and Propagation and USNC-URSI Radio Science Meeting (APS/URSI)	December 2021	[365]
"Assessing Trust in Collaborative Robotics with Different Human-Robot Interfaces"	Conference Article	IEEE International Instrumentation and Measurement Technology Conference (I2MTC)	May 2024	[337]
"Fully Integrated Circulatory System in a Torso Phantom for WIMD Read Range Performance Measurements"	Conference Article	IEEE INC-USNC-URSI Radio Science Meeting (Joint with AP-S Symposium)	August 2024	[366]
"Generalizing Perceived Fatigue Estimation Across Diverse Upper Limb Tasks Using Minimal Wearable Sensors"	Journal Article	IEEE Sensor Letters	September 2025	[367]
"Hierarchical Modeling of Perceived Fatigue in Upper Limb Cross Tasks Using Wearable IMU and EMG Sensors"	Journal Article	IEEE Access	January 2026	[368]

Appendix 5: Linking Objectives with Experiments

Experiment No. (Objective No.)	Chapter No.	Description	Equipment	Measured Variables	Analysis	Output
1 (Objectives 1, 2)	3.1	Measurement of individual parameters to estimate maximum joint torque	Measuring tape, dynamometer, body composition parameter scales	Gender, age, height, body composition parameters (weight, BMI, fat %, muscle %, visceral fat), arm segment lengths, maximum force	Multiple linear regression analysis	Model to estimate maximum joint torque based on individual parameters
2 (Objectives 1, 2)	3.2	Assessed the torque-based model during loaded static and dynamic one- and two-handed tasks	Measuring tape, dynamometer, body composition parameter scales, IMU, weights	Gender, age, height, body composition parameters, maximum force, experimental endurance time, predicted endurance time, sensor data	Experimental error	Ability of endurance model to predict endurance of lifting tasks
3 (Objectives 1, 2)	3.3, 4.1	Assessed torque-based models and inputs during loaded static and dynamic one-handed lifting tasks at two standardised intensities	Measuring tape, dynamometer, body composition parameter scales, IMU, EMG, MoCap, PI, weights	Gender, age, height, body composition parameters, maximum force, experimental endurance time, predicted endurance time, sensor data	RMSE and experimental error	Ability of different endurance models and inputs to predict endurance time of lifting tasks
4 (Objective 2)	4.2	Task classification of industry-type tasks using explainable methods	Body composition parameter scales, PI, box, weights	Gender, age, height, body composition parameters, task type, sensor data	Random forest and SHAP analysis	Task prediction using PI force data

Experiment No. (Objective No.)	Chapter No.	Description	Equipment	Measured Variables	Analysis	Output
5 (Objective 3)	5	Demonstration of the system during industry-type tasks	Custom system (IMU custom application), PI, MoCap, camera, dynamometer, box, weights, body composition parameter scales	Gender, age, height, body composition parameters, task type, sensor data	Repeated measures correlation, Wilcoxon signed-rank test, Joint angle statistics	Endurance prediction and distinguishing high and low ergonomic risk conditions

Abbreviations: BMI = Body mass index; IMU = Inertial measurement unit; EMG = Electromyography; MoCap = Motion Capture; PI = Pressure insoles; RMSE = Root mean squared error; SHAP = SHapley Additive exPlanations

Appendix 6: Detailed Overview of Measurement Methods

The main methods used to assess fatigue and ergonomic risk to reduce the risks of WMSDs were summarised and compared in Table 3 and are now explored in more detail.

Subjective Questionnaires

Subjective questionnaires are commonly used with other fatigue and ergonomic risk assessment methods as the gold-standard fatigue reference measure [86] and take worker perceptions into account which is important since there is interplay between the three aspects of fatigue (central, peripheral and psychological).

Physical fatigue questionnaires include the 11-question Need for Recovery Scale [122] which assesses the need for rest. The Fatigue Assessment Scale assesses many types of fatigue, and five questions in the questionnaire relate physical fatigue level [369]. Likert scales [370] have also been used to assess fatigue and exertion. Subjective questionnaires relating to work include the Occupational Sitting and Physical Activity [371], [372] and the Multicontext Sitting Time Questionnaire [373], which focus on sitting during working and daily activities. The NASA task load index (TLX) [73] evaluates perceived workload across factors such as mental and physical demand, effort and frustration. The Job Content Questionnaire [374] assesses the psychosocial aspects of work. In many cases, a custom, one-off questionnaire developed by researchers is used [41].

Examples of subjective questionnaires that measure pain, exertion, effort and fatigue include the Borg RPE and Borg CR10 scales [72], [320] which have been strongly correlated to physiological symptoms, such as heart rate [72] and EMG [37], [344]. Points on the RPE scale (6 to 20) exhibit a linear progression of fatigue while the CR10 points (0 to 10) relate to a logarithmic scale, there is a high agreement between both scales, but the RPE tends to be more accurate since individuals can find it difficult to use logarithmic scales [318]. Borg scales are reliable at lower levels of force [156], [375] which other fatigue reference measures, such as EMG, can struggle with [23]. For these reasons, the Borg RPE scale is employed in the endurance experiments in Chapters 3 and 5 to track physical exertion and fatigue.

Subjective questionnaires are affected by individual pain perceptions, emotional and situational factors [155] which can differ on an inter-subject and intra-subject basis, presenting a challenge for fatigue detection and prediction methods that are benchmarked against this method [72], [321]. While it is important to gain insight into mental and emotional states, other factors at play such as dishonesty [99] can influence scores, and ones' ability to self-detect is potentially impeded while in a fatigued state. While they are easy to deploy and cost-effective [41], [99] and they are effective for low load levels [376], they tend to interfere with work [187], [320], [321], it is difficult to achieve precise values [320], [377] and they don't always align with physiological and performance-based measures [378]. Stirling *et al.* (2024) [41] mentioned they are too general and don't pinpoint the exact factors leading to particular health outcomes and other researchers have raised questions regarding the validity of subjective questionnaires in ergonomics in general [377], [378]. Martins *et al.* (2021) [86] discussed the classification problem where there are inconsistencies between scores that define fatigued states, for example, some studies categorised Borg RPE scores into three and four categories of exertion level with differing score ranges defining each category, while other studies used a binary classification method with a threshold acting as the indicator of fatigued states, this threshold value ranged from 13 to 18.

Most subjective questionnaires, such as those relating to work factors, do not offer insights into the development of fatigue since there are multiple questions that must be asked once tasks are complete, and Martins *et al.* (2021) [86] notes their lack of use in online operator monitoring contexts. However, Borg scales consist of one question which can be asked throughout tasks, ensuring minimal task interference while gaining insight into fatigue development and are thus employed in the present research.

Ergonomic Risk Assessments

Ergonomic risk assessments are often used to assess the risk associated with task postures and movements, they are generally based on joint angles, the distances and heights a load is lifted, and some assume repetitive work. They are useful for identifying areas where risk can be reduced and comparing the relative risk between different tasks. Some assessments provide scores based only on posture and others are based on posture and external loads. Ergonomic risk assessments have been conducted observationally in occupational settings and increasingly using direct means of measurement in research.

These tools are developed by researchers and H&S organisations such as National Institute for Occupational Safety and Health (NIOSH) and American Conference of Governmental Industrial Hygienists (ACGIH). In some cases, large companies develop their own assessment tools, for example:

- Safety & Ergonomic Risk Assessment (SERA) and Digital Workplace Stress Management (DWSM) were developed by BMW Group [379], [380], [381]
- Joshi-ten and Shisei Juryo-ten (JT-SJT) system [382] was developed by Toyota

There are multiple ergonomic risk assessments in existence, and the most common tools are included in the thesis for the purpose of brevity. Lowe *et al.* (2019) [139] surveyed over 400 ergonomics professionals in the US, Canada, UK, Australia and New Zealand on their use of ergonomic tools that address WMSD risk factors. As mentioned, ergonomic risk assessments are typically carried out using observational methods [139], meaning that several snapshots from video recordings are made of critical postures during a task for which the risk scores are analysed [80]. The most frequently used ergonomic risk assessments were:

- NIOSH Lifting Equation [65]
- Rapid Upper Limb Assessment (RULA) [63]
- Psychophysical Material Handling and Upper Extremity Data (includes Snook and Ciriello tables [168])
- Rapid Entire Body Assessment (REBA) [64]
- biomechanical or digital human modelling (using simulation tools)
- Body Discomfort Map [383]
- Strain Index [384]
- Threshold Limit Value (TLV) by the ACGIH for Lifting and Hand Activity [66]

The survey found that ergonomic risk assessments were completed by pencil and paper and through computer software equally. Meanwhile, RULA [63], REBA [64] and Ovako Working Posture Analysing System (OWAS) [174] are most commonly used in research [385].

Each of these assessments have a slightly different focus, for example, the NIOSH Lifting Index assesses the risk of injury for manual lifting tasks and suggests a recommended weight limit (RWL) by accounting for the vertical and horizontal heights a load is lifted and its distance from the worker's body [65]. RULA and REBA are more general as their scores indicate the risk of WMSDs; these tools consider the load (light, moderate or heavy) and postures of the upper extremities (RULA) or entire body (REBA) [63], [64], and assume repetitive work. Similar to RULA, the risk score that results from the Strain Index [384] indicates the risk of upper extremity WMSDs, but by assessing six key work factors: frequency, duration, intensity, posture, speed and variation. The Body Discomfort Map asks workers to indicate where discomfort is felt on the body and to provide a score for example, in a range of 1-5 or 1-10.

These assessments help ergonomists to identify problem areas and modify workstations, tools or tasks so that ergonomic risk, thus the risk of WMSDs, can be reduced. They may also highlight where individuals can benefit from training and track if ergonomic interventions are effective. Some interventions (RWL by NIOSH [65], Snook and Ciriello tables [168]) can help in the design of working tasks and schedules and contribute to the development of individualised targets.

However, ergonomic risk assessments are not without disadvantages as some authors have questioned their thoroughness [322], [323], risk classifications [322], [323], repeatability [385], and the correlation and agreement rates between different assessments [154], [322], [385]. In many cases, the neck is ignored as well as lateral bending and the degree to which twisting and lateral bends occur [136]. Anthropometry is often not considered, and an over-simplified representation of the human body is often used [150]. Risk scores are categorised into gross categories and are not on a continuous scale [18], [138] and there is lack of precision in the trunk and upper extremities, discussed by many researchers according to Lind *et al.* (2023) [18], and there are inter and intra observer differences, affecting reliability [18], [137]. Finally, intervention can only take place after the ergonomist analyses a worker's movements and postures [80]. In such cases, a worker may be exhibiting these movements for an extended period of time without correction, resulting in high risk of developing WMSDs. Therefore, ergonomic risk assessments carried out via observational methods lack proactivity from a WMSD prevention perspective.

Endurance Models

Endurance models, also called maximum endurance time (MET) models, predict ET and are used by ergonomists to design tasks at workstations and work schedules. They come in the form of power or exponential curves “with two asymptotic tendencies: a tendency towards infinity for low %MVC values, and a tendency towards zero for values bordering on 100% MVC” [70], where %MVC refers to the force of a load relative to MVC force, $\left(\frac{Force}{Force_{max}}\right)$, also referred to as standardised intensity (SI). (MVC force, or $Force_{max}$, has also been defined as joint strength [162], [208].) This means the models demonstrate reduced capacity to continue working at higher loads relative to the individual’s maximum producible force, i.e. at higher %MVC. While their validity has been questioned by some researchers, there are plenty of models, reviews and textbooks that demonstrate their validity [162].

Hundreds of MET prediction curves have been empirically developed [229], with models altered depending on the principle joint, muscle groups, and postures involved [70], [71], range of joint angles [235], individual factors [162], [239] and task type [227], [228], [249]. These MET models predict ET for isometric conditions or static muscular contractions [70] or they assume constant force [229], and in some cases static models were used to predict ET for slow isokinetic tasks [247]. They have also been used for rest allocation models to calculate recovery following static muscular work [70].

El Ahrache *et al.* (2006) [70] gave an overview of the methods used to develop MET models, and described four main reasons why there are significant differences between models present in the literature. Firstly, experimental methods and model construction issues are present as there is great variability in the subjects participating in these studies (sometimes they are students, other times skilled workers), and in some cases, models are developed using data from previously published studies. Secondly, the presence of an endurance limit, the relative force that can be produced without fatigue, in some models [123], [386] is contested. For example, in Rohmert’s MET model [123], the asymptote at 15% MVC indicates that an individual can perform tasks at 15% MVC and below for an “indefinite” [247] period of time without fatigue. Other studies contest this, and they show that 15% MVC can be maintained from 10- to 15-min [123], [235], [247] to 1 hour [162], [387]. Many researchers, as listed in [162], do not agree with the use of an asymptote, and many experimental models do not contain one. The third reason for significant differences between MET models, according to El Ahrache *et al.* (2006) [70], is muscle group and posture variability. It is questionable that some ET models use the same model for all muscle groups and postures, as it was found that there were differences in ET when these factors were varied in multiple studies. Finally, interindividual variability results in differences between these models, especially at low %MVC [70]. Other researchers mention the lack of generalisability for tasks [165] and that the influence of individual differences is unclear [162], [165].

Muscle Development Models

Muscle development models are theoretical muscle fatigue models [110], [229], although coefficients of these theoretical models are occasionally determined through experimentation. These models mainly exist within a research context, although some commercially available simulation software integrates muscle development models to simulate tasks at workstations, such as Siemens Jack [144]. They are used to assess fatigue from a muscle perspective based on the physiological mechanisms mentioned in section 2.1.1 Fatigue: Definitions, Classifications, and Contributing Factors and are usually expressed using differential equations. These models estimate fatigue or muscle recovery from the point of view of the cross-bridge [30], other times by considering the force-pH relationship and the accumulation of muscle by-products during fatigue [69], [110], or motor unit principles in combination with $Force_{max}$ or torque and exertion history [68], [108], [119], [124], [125], [149], [166]. Some of these models consider differences between muscle groups [119], [124], [149] using studies that examined muscle-specific fatigue rates [67], arm postures [68], individual variations [68], [119], [124], recovery [119], [208], or the production and diffusion rate of muscle by-products during fatigue [110]. Some models have been experimentally validated under static [124], [125] and dynamic [68], [110], [124] conditions, some of which struggle accounting for submaximal contractions [125].

These models typically estimate current fatigue level or maximum exertable force (MEF) rather than predicted ET and often have complex equations with multiple parameters that make real-time integration difficult [99]. MEF is also called force or torque capacity, expressed in %MVC after a particular period depending on current and past loading conditions and the person's maximum strength which can be expressed as $Force_{max}$ or $Torque_{max}$ [110], [124], [149], [165]. These models can indirectly provide ET, determined as the time at which the MEF is equal to or below the current %MVC [110], [165], although they do not predict ET. For example, an individual with 50 N MVC force holds a 1.5 kg object, and after 83 s the model estimates current MEF as 30% MVC, this means the current MEF is approximately $\frac{50}{9.81} \times \frac{30}{100} \approx 1.5$ kg, therefore MEF is equal to the %MVC of the current load, therefore the time taken to reach this MEF, i.e., 83 s is the ET. In order for these models to provide pre-emptive outputs that allow for timely intervention prior to fatigue onset, the individual would need to cease the tasks before MEF=30%, and one would need to determine the %MVC thresholds required for fatigue mitigation. For example, the task should be ceased at 80% of the fatiguing MEF, i.e., MEF is equal to $100 - \left[(100 - 30) \times \frac{80}{100}\right] = 44\%$ MVC (i.e., after $\approx 83 \times .8 = 66$ s). Nevertheless, these models tend to focus on force capacity rather than ET and are developed with the aim of integration to simulation software [99], [208].

Other models output an expected subjective fatigue level [68], [196], making it difficult to compare muscle models in the field [3]. Many muscle models are not suitable for real-time use in industrial applications due to high model complexity, for example some models [30], [166] have many parameters which "weaken the model quality in information theory" [165] and are not suitable for applications where there is a requirement for computational efficiency [108], for example, real-time fatigue estimation. Oftentimes, these models consider the cumulative effects of fatigue and the transition between rest, active and fatigued states which is practical in terms of assessment throughout a prolonged period, i.e. an entire work shift. Theoretical models have been validated against endurance models [108], [124], some are valid for static maximal tasks [125], while others have been applied to dynamic tasks [108], [124] but estimations are not adjusted based on joint configurations.

Physiological Indicators

Physiological indicators are considered an objective method of assessing physical fatigue [99] and measured signals include heart rate, skin temperature, skin conductivity, and breathing rate. When the body experiences physical exertion, heart rate increases to increase blood supply to working muscles and to remove accumulated metabolites such as phosphates [388]. Wearable sensors can measure physiological changes in the individual due that occur due to this physiological response. Sensors are worn throughout a work period to ascertain the state of the worker and to provide rest/work recommendations. Out of the measurement methods mentioned in this section, physiological indicators are currently utilised by ergonomists the least [139] and feature in current research to a greater extent.

Appendix 7: Detailed Overview of Current Interventions

Current methods used to assess fatigue and ergonomic risk to reduce the risks of WMSDs in occupational settings today were summarised and compared in Table 4 and are now discussed in more detail.

Occupational Health and Safety Policies

In Europe, the prevention of WMSDs is a major focus of occupational H&S policies. The EU develops *directives* which are then transferred into national laws and regulations by member states. Directives are proposed by the European Commission who consult with stakeholders and researchers, they are then examined, debated and revisions are requested by the European Parliament and the Council of the EU [389]. The *framework directive* relating to occupational H&S (89/391/EEC) outlines how employers are required to address risks in general and integrate ergonomics and human factors into workplace design, and the framework directive contains *specific directives* which provide more targeted requirements and guidelines [33], [34]. As mentioned throughout the introduction, risks for WMSDs include carrying heavy loads, repeated loading and unloading, awkward postures, and mid-air repetitive tasks. These risks are associated with the following specific directives that are currently in force: 90/269/EEC for minimum safety and health requirements for the manual handling of loads where there is a risk of back injury to workers [33]; 90/270/EEC for minimum safety and health requirements for work with display screen equipment [34].

90/269/EEC requires employers to carry out risk assessments for manual handling tasks, whereby the weight, frequency and posture of the tasks are evaluated, and risks are identified. manual handling is to be avoided where possible and measures must be taken to reduce the risk where manual handling is necessary, such as reducing the need for awkward postures and redesigning a task to fit a worker's capabilities. Minimising manual handling can also be done through the design of the workplace and the equipment provided to employees. In addition, training for safe manual handling must be provided to employees. 90/270/EEC mainly concerns display screen equipment, and while this is potentially more relevant to workers sitting at a desk in front of a computer, factory workers may be required to use displays, especially where cobots are present in a smart factory setting. The main guidelines concern workstations being designed to accommodate the needs of users and a comfortable posture (i.e. using adjustable equipment), furthermore, regular breaks, changes in activity and training in relation to displays are required. Specific ergonomic risk assessments are not specifically recommended by 90/269/EEC or 90/270/EEC but tend to be used to meet the directive's requirements.

Other specific directives related to WMSD prevention include 2009/104/EC for minimum safety and health requirements for the use of work equipment by workers at work (i.e. the equipment should not pose a risk to workers), 2002/44/EC for assessing and controlling risk of vibration exposure, and 2003/88/EC indirectly addresses WMSDs as it refers to work/rest schedules.

As mentioned, the directives are transposed into national laws and regulations by member states, and in Ireland this is called the Safety, Health and Welfare at Work Regulations 2007 and the implementation of these laws are overseen by the Health and Safety Authority (HSA) who perform inspections and provide valuable information to employers for compliance with those laws. Examples of national H&S organisations in other member states include the National Institute for Research and Safety in France, the Work Environment Authority in Sweden, and the National Institute for Occupational Safety and Prevention in Italy. The EU-OSHA website also provides valuable information for employers for the practical implementation of policies for WMSD prevention.

These organisations aid employers regarding their responsibilities around occupational H&S, they provide manual handling training, templates for ergonomic risk assessments, and guidelines for internal audits to assess the effectiveness of WMSD intervention measures in the organisation. For ergonomic risk assessments, the HSA recommends a 5 step process: (1) Task description, where key stages of the task are identified and may involve recording a video of the task being performed, (2) Collect technical information, such as the heights and distances loads are carried during a task, (3) Identify risk factors using a risk assessment tool, (4) Identify improvements to be put in place, and (5) Review the effectiveness of the changes. For step 3, the HSA recommends acquiring training or requesting expertise to carry out ergonomic risk assessments and endorses the three risk assessment tools used by the HSE UK: the manual handling assessment chart (MAC tool) [171], risk assessment of pushing and pulling (RAPP tool) [173], and assessment of repetitive tasks of the upper limbs (ART tool) [172]. These tools assign a risk score for lifting, pushing and pulling and repetitive tasks with upper limbs based on load, frequency, carrying distance, and posture, among other parameters. The scores associated with these parameters can help identify where the highest risks reside so that they can be reduced by the employer. However, these tools do not appear in the results from Lowe *et al.* (2019) [139], whose survey included the UK.

ISO and EN Standards

The ISO is an independent international body that develops voluntary standards aimed at supporting innovation and addressing global challenges [169], [390]. Experts use a consensus-based approach to develop standards which provide "requirements, specifications, guidelines or characteristics…[to ensure] materials, products, processes and services are fit for their purposes", and they are not necessarily based on scientific process [169]. ISO standards relevant to ergonomic issues were developed by the Anthropometry and Biomechanics Subcommittee (ISO159/SC3), and include ISO 11226 (static working postures), 11228-1 (manual handling - lifting and carrying), 11228-2 (manual handling - pushing and pulling), and 11228-3 (manual handling - carrying low loads at high frequency) [391], [392], [393], [394]. Other related documents include technical reports TR 12295, concerning the application of manual handling standards, and TS 20646, dealing with optimising musculoskeletal workload for ergonomics.

ISO 11226 recommends the OWAS [174], RULA [63], REBA [64]; ISO 11228-1 recommends NIOSH Lifting Equation [65]; ISO 1228-2 recommends the Snook and Ciriello tables [168]; and ISO 11228-3 detailed three risk assessments but chose to recommend the concise index for the assessment of exposure to repetitive hand movements of the upper limbs (OCRA) [175] over ACGIH hand activity level (HAL) [66] and the Strain Index [384].

Fallentin (2001) [170] reviewed standards relating to physical workload, and found they presented very specific and unsupported limits, and the scientific validity was unclear. Armstrong *et al.* (2018) [169] also noted the need for transparency in the process of developing standards, and assessed the scientific basis of ISO standards using a checklist to evaluate quality and bias commonly used in medical practice guidelines: Appraisal of Guidelines, Research and Evaluation (AGREE II) [395]. Armstrong *et al.* (2018) [169] found that the ISO standards did not fulfil most of the

AGREE II criteria, for instance, authors and their scientific profile, affiliations and conflicts of interest was not disclosed, involvement of key stakeholders was not clear, the standards did not undergo external review, and there was no mention of the expected impact on WMSD risk. Perhaps most critically, it was found that the recommendations are not evidence-based, that is, it is not clear why one risk assessment methodology is chosen over the other (for example, recommending OCRA [175] over ACGIH HAL [66] and the Strain Index [384] in ISO 11228-3) as there was no systematic literature review and no scientific basis or comparisons were provided, although Armstrong *et al.* (2018) [169] notes these are available in the literature in some cases. Where statements were supported by referencing, these were sometimes poorly designed studies. The authors also noted the lack of attention given by the scientific community to the ISO standards as there are no validation studies that support them and they are rarely discussed in the light of new evidence, therefore it was not clear to the authors if the standards are generally accepted.

Ultimately, ISO standards are voluntary, and policies put in place by governments and companies currently have the most impact due to the fact they are mandatory. Nevertheless, there is significant alignment between the ISO standards and European standards, referred to as European norm (EN), and since these standards are mentioned in EU legislation, they are essentially mandatory to ensure legal compliance. EN 1005-4 has the same recommendations as ISO 11226, EN 1005-2 has the same recommendations as ISO 11228-1, EN 1005-3 aligns with ISO 11228-2 and EN 1005-5 aligns with ISO 11228-3.

Current Ergonomic Assessment Tools

A summary of current ergonomic tools, shown in Figure 10, is provided in Table 5. Lowe *et al.* (2019) [139] found that pen and paper, software and simulation tools (for example, Siemens Jack [144], Figure 10a) were most commonly used methods of carrying out risk assessments, and mobile applications, for example Ergodroid ([180], Figure 10b) are in the early adoption phase with 24-28% of survey respondents using them. Relevant applications include those for MH, ergonomic risk/biomechanics assessment, posture/motion assessment and fitness-related (which accounted for 75/129 apps identified by the respondents), others were for environmental or other uses. Use of MoCap and wearables is relatively low compared to ergonomic risk assessments and simulation tools, with EMG, optical MoCap and non-optical MoCap accounting for approximately 22%, 24% and 15% respectively [139].

Patel *et al.* (2021) [184] reviewed worker solutions currently on the market that promote *total worker health* from the centre for disease control and prevention (CDC) and NIOSH, which is defined as "policies, programs and practices that integrate protection from work-related safety and health hazards with promotion of injury and illness prevention efforts to advance worker wellbeing" [396]. The reviewed systems comprise smart hardware and software tools to reduce the risks that workplace hazards present, including ergonomic risk, fatigue and WMSDs. While some of the systems automate the ergonomic risk assessment process, they often directly deal with the aspects that cause WMSDs (i.e. repetitive movements, heavy loads, awkward postures, etc.) by offering assist with lifts, posture correction and visual feedback.

Exoskeletons generally transfer the load from the upper body to the legs, in some cases using a purely mechanical system that operates by means of springs, pulleys and cables. There are a number of these systems on the market, such as the Skelex 360 from Skelex [176], Figure 10c, mainly deals with reducing strain in over-shoulder activities; the Technologies AirFrame [177], Figure 10d, exoskeleton is designed specifically for repetitive tasks. The SuitX by Ottobock [178], Figure 10e, is a full-body exoskeleton that reduces fatigue and increases endurance in the back, shoulder and legs with separate modules that can also act independently. Instead of transferring load from the upper body to the legs, the Noonee Chairless Chair [179], Figure 10f, is worn only on the legs and helps assembly line workers to switch between sitting, standing, walking and industrial operations on the line so that strain on the lower extremities can be reduced. These systems are currently being used in industry, for example, the AirFrame is mandatory for workers in welding some Toyota plants [184].

The Kinetic Reflex [89], Figure 10g, is worn on the worker's belt and detects high risk bending, reaching and twisting using IMUs and biomechanical analysis, and encourages the worker to correct their posture via vibrotactile feedback. The SafeWork Sensor by StrongArm [90], Figure 10h, is a safety vest with an IMU placed at the torso, and similar to the Kinetic Reflex, it monitors awkward postures and offers vibrotactile feedback for correction, in addition to an extensive platform for workers, managers and safety leaders to review safety analytics. The Honeywell Bioharness

[91], Figure 10i, is a chest-worn device used to monitor workers by extracting physiological indicators related to heart and breath rate, temperature, activity and posture in real-time, it also includes a GPS sensor for location tracking. Patel *et al.* (2021) [184] also identified wearable devices on the market that can be used in the research for the monitoring of health and physical activity of workers, these include the Omron HeartGuide and VitalConnect VitalPatch for monitoring physiological indicators relating to heart rate and blood pressure, and smart watches in general which normally include accelerometer, gyroscope, pedometer, and heart rate sensors, among others. Other wearable devices for fall detection, stress detection, productivity monitoring and exposure to vibration, noise and gas were also identified in the review by Patel *et al.* (2021) [184] but fall outside the scope of this research.

Wearable devices on the market that were not included by Patel *et al.* (2021) [184] include those for ergonomic risk assessment, such as software products by Movella Xsens (Xsens Technologies B.V., Enschede, The Netherlands) [92], Ergo, Ergo Live and Ergo Expert, that link up with their hardware systems Xsens Awinda IMUs, Figure 10j. Ergo produces standardised ergonomic reporting of RULA [63], REBA [64] and Adjustable Ergonomics, the latter of which is based on ergonomic and range of motion thresholds based on European Standards (in this case UNE 1005-4 which is the Spanish standard corresponding to EN 1005-4). Ergo Live features real-time ergonomic reporting with Scale Fit [397] developed by a team of biomechanical and software engineers and checks twenty-one load parameters to provide reports based on DIN (German), EN (European) and NIOSH standards, and biofeedback via visual cues can help with real-time correction of postures, Figure 10k. Ergo Expert offers additional features in terms of full data access, streaming and exporting, and integration with third-party software (for example, AnyBody [134], BoB Biomechanics [145], OpenSim [133]) and custom ergonomic models using MVN Analyse software. Examples of custom ergonomic tools include the case where MVN Analyze is utilised by BMW Group with their own ergonomic tools [398], SERA [379], [381] and DWSM [380], and by Toyota with the JT-SJT system [382].

Additional commercial devices that are used in fatigue and WMSD prevention research includes activePAL (PAL technologies, Glasgow, UK), Acti4 and ActiLife 6 (ActiGraph, Florida) [75] and the following devices which are primarily used in sporting and animation applications pose potential for use in ergonomics [18]:

Wearnotch (Notch Interfaces Inc, New York, NY, USA), Axtivity (Axivity Ltd., Newcastle, UK), Rokoko (Rokoko Electronics ApS, Copenhagen, Denmark, LPMS-B2 and LPMOCAP (P-RESEARCH Inc., Tokyo, Japan).

Appendix 8: Poster Presented at the EMBC Conference in Glasgow, July 2021

EMBC 2022 Glasgow

Estimation of maximum elbow and shoulder joint torques based on demographics and anthropometrics

P. O'SULLIVAN, M. MENOLOTTO, B. O'FLYNN and D.S. KOMARIS

Tyndall National Institute Institiúid Náisiúnta

Confirm Smart Manufacturing

INTRODUCTION

Repetitive movements involving a significant shift of the body's center of mass can lead to **shoulder and elbow fatigue**, which are linked to **musculoskeletal disorders** if not addressed in time. Joint torque is relevant to a wide variety of contexts, such as **sports performance** [1], **ergonomics** [2] **and robotics** [3].
Current state-of-the-art consists of studying the influence of a specific parameter on the joint torque generated (often using specialized equipment) and torque tables.

AIM

To develop models for the prediction of maximum joint torque which can be used in sectors that utilize joint torque data to **reduce the frequency of injuries** in clinical and industrial settings.
Demographic and anthropometric variables are chosen as inputs for the estimation models, with a preference for easily and quickly measured parameters (Table 1). Such models can **significantly simplify and accelerate measurement processes** and **negate the need for specialized equipment**.

METHOD

- **Body composition parameters** (BMI, muscle %, fat %) were measured using OMRON BF511. **Girth of the forearm** was measured at three points, 7cm a part.
- Subjects performed a **maximal voluntary contraction** pushing their mid-palm against the Walfront NK-500 push/pull dynamometer. Three **peak force measurements** were recorded with a one minute rest between measurements; the average force value was used in the analysis. Testing positions in Figure 1 and Figure 2 were used.
- The *partial frustum sign model* (Figure 3 [4]), which has a high correlation to the gold standard 'water tank method', was employed to calculate **upper forearm volume** (formula below).
- *V* is the volume of the section (cm^3), *C* and *c* are the circumference measurements at either end of the section (*cm*), and *h* is the distance between *C* and *c* (*cm*).

$$V = h \times \frac{(C^2 + C \cdot c + c^2)}{12\pi}$$

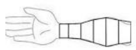

Figure 3. Partial frustum sign model.

- **Maximum joint torque** produced by each participant was calculated from the force data collected, using the distance from acromion to mid-palm and the distance from elbow to mid-palm, using anthropometric data tables from Winters (2009) [5].

Figure 1. Shoulder testing position: Hand is supinated, wrist and elbow joints aligned

Figure 2. Elbow testing position: Hand is supinated, elbow joint flexed 90°

RESULTS

Table 1. Anthropometric and demographic data.

Subject Data	
Participants (No)	19
Age (years)	37 ± 10
Sex (males/females)	10 Males, 9 Females
Dominant Hand (right/left)	16 Right-Handed, 3 Left-Handed
Height (m)	1.73 ± 0.08
BMI (kg/m²)	25.2 ± 3.8
Muscle %	31.9 ± 6.4
Fat %	29.1 ± 10.5
Forearm girth 1, 2, 3 (cm)	26.4 ± 2.4; 25.8 ± 3.0; 20.8 ± 3.4

Regression analysis was performed on each factor against maximum shoulder and elbow joint torques. ***Height*** and ***upper forearm volume*** produced the highest coefficient of determination values for both shoulder and elbow joint models, with *P<0.001* and *P<0.005* respectively. Using SPSS, **linear regression analysis** related the relevant factors to maximum joint torque. Table 2 shows the results of the analysis, accompanied by predicted value formulae, $T_{S_{MAX}}$ and $T_{E_{MAX}}$. Residual analysis with a random distribution of residuals is included.

Table 2. Regression and residual analysis results for maximum shoulder and elbow joint torque models.

Maximum Shoulder Joint Torque

$$x_s = 3289.70 + 1153.97(H^2) - 3904.52(H) + 0.07(UFV)$$

$$T_{S_{MAX}} = 2.76 \times 10^{-12} + x_s \qquad (R^2 = 0.70)$$

$$\bar{x} = 47.69Nm \quad \sigma = 13.05Nm$$

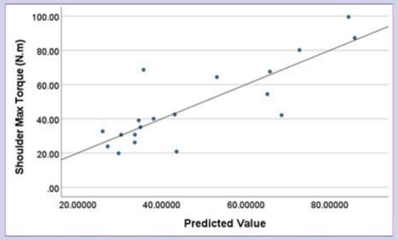

Figure 4. Linear model to estimate maximum shoulder joint torque.

Maximum Elbow Joint Torque

$$x_E = 2962.00 + 1006.85(H^2) - 3469.21(H) + 0.09(UFV)$$

$$T_{E_{MAX}} = 7.74 \times 10^{-13} + x_E \qquad (R^2 = 0.63)$$

$$\bar{x} = 44.81Nm \quad \sigma = 14.22Nm$$

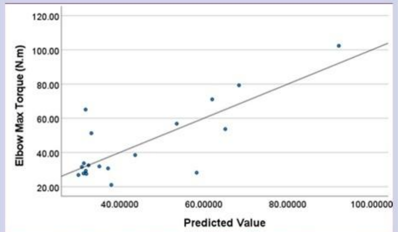

Figure 5. Linear model to estimate maximum elbow joint torque.

CONCLUSIONS

Demographic and anthropometric factors that influence maximum shoulder and elbow joint torque were identified and, through linear regression analysis, models for the estimation of maximum joint torque were developed. **Coefficient of determination values of 0.70 and 0.63 to a significance of *P<0.001* and *P<0.005* were found for shoulder and elbow models respectively.** The models are impactful in **biomechanics and biorobotics applications** that require joint torque estimations.

In terms of limitations, only flexion of the joints and maximal contractions are studied, whereas other planes of movement and level of contractions may be more significant in certain domains. The number of participants and age of the cohort is an additional limitation.

REFERENCES

1. Aguinaldo AL, Buttermore J, Chambers H. Effects of upper trunk rotation on shoulder joint torque among baseball pitchers of various levels. Journal of Applied Biomechanics. 2007;23(1):42-51.
2. Hincapié-Ramos JD, Guo X, Moghadasian P, Irani P, editors. Consumed endurance: a metric to quantify arm fatigue of mid-air interactions. Proceedings of the SIGCHI Conference on Human Factors in Computing Systems; 2014.
3. Kim W, Peternel L, Lorenzini M, Babič J, Ajoudani A. A human-robot collaboration framework for improving ergonomics during dexterous operation of power tools. Robotics and Computer-Integrated Manufacturing. 2021;68:102084.
4. Casley-Smith J. Measuring and representing peripheral oedema and its alterations. Lymphology. 1994;27(2):56-70.
5. Winter DA. Biomechanics and motor control of human movement: John Wiley & Sons; 2009.

ACKNOWLEDGEMENTS

Research supported by Science Foundation Ireland (SFI) under grant number 16/RC/3918 (CONFIRM), aspects of this research have been supported by12/RC/2289-P2 (INSIGHT).

CONTACT INFORMATION

P. O'Sullivan is with Tyndall National Institute, University College Cork, T12 R5CP, Ireland (corresponding author e-mail: patricia.osallivan@tyndall.ie).

Appendix 9: Linearity Tests for All Independent Variables Against the Dependent Variable: Shoulder Maximum Torque

(a) Age

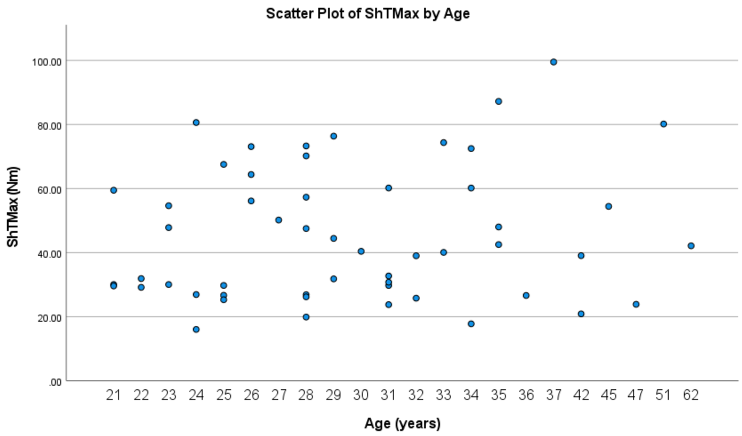

(b) Height

(c) Weight

(d) BMI

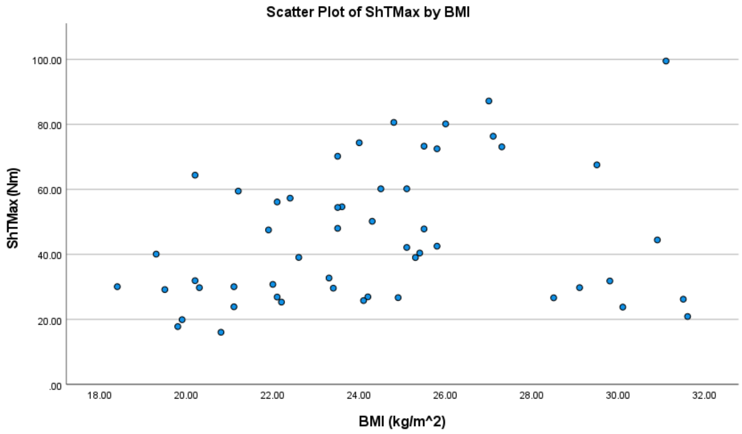

(e) Fat%

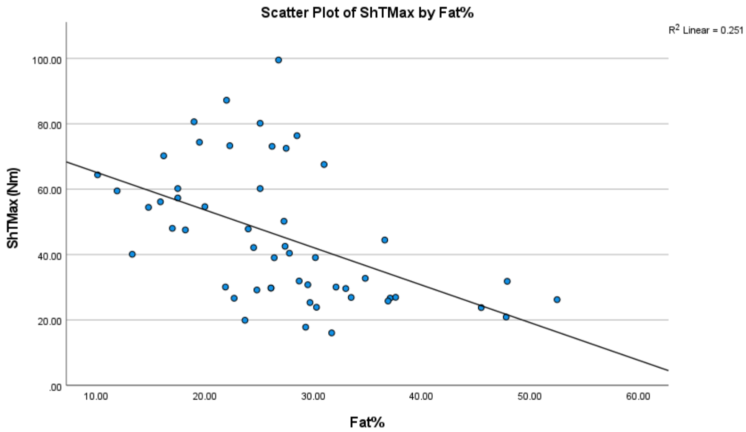

(f) Muscle%

(g) Visceral Fat

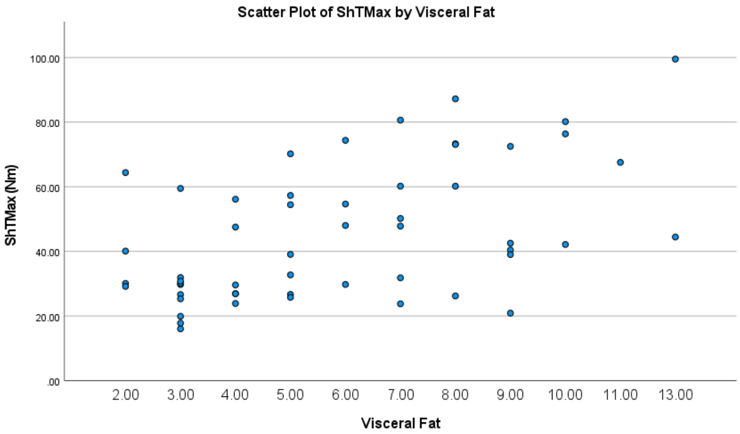

(h) Forearm Circumference

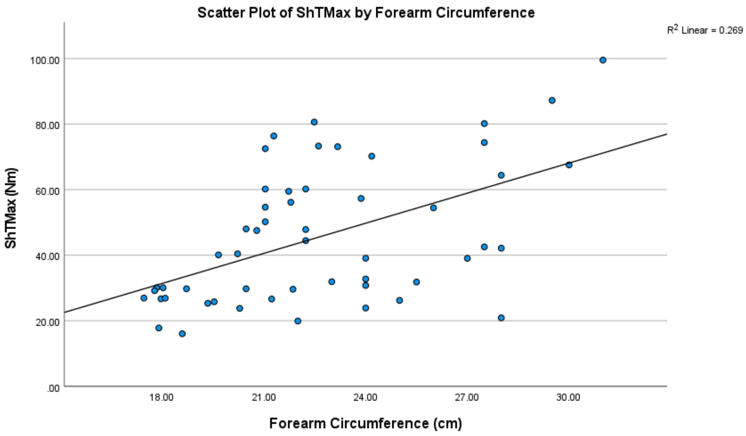

Appendix 10: Linearity Tests for All Independent Variables Against the Dependent Variable: Elbow Maximum Torque

(a) Age

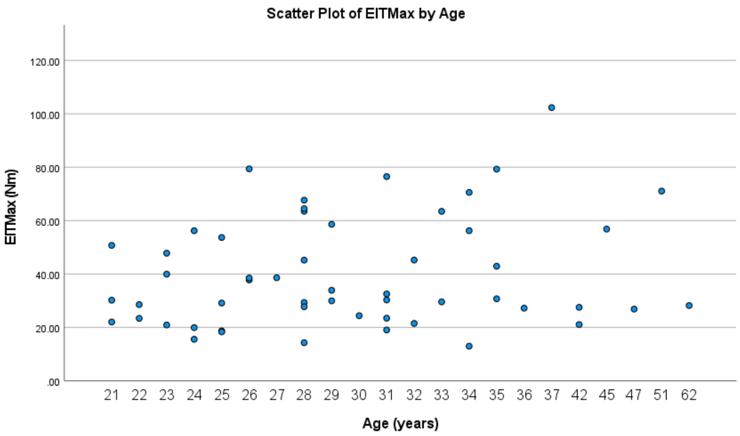

(b) Height

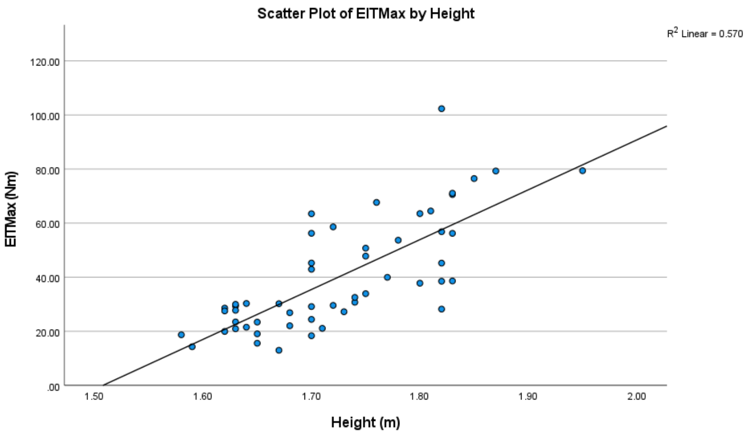

(c) Weight

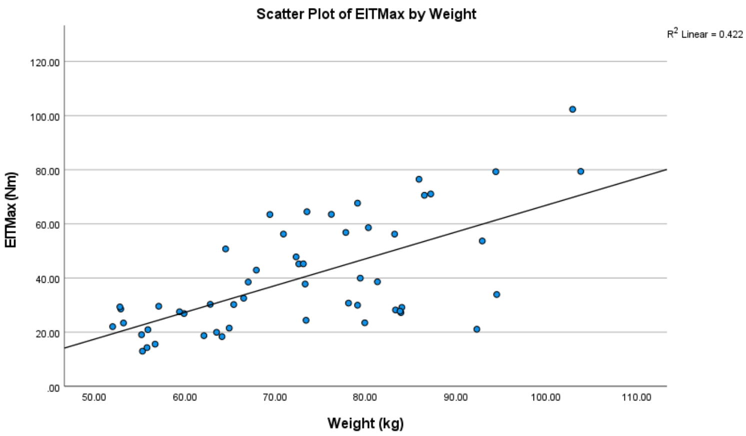

(d) BMI

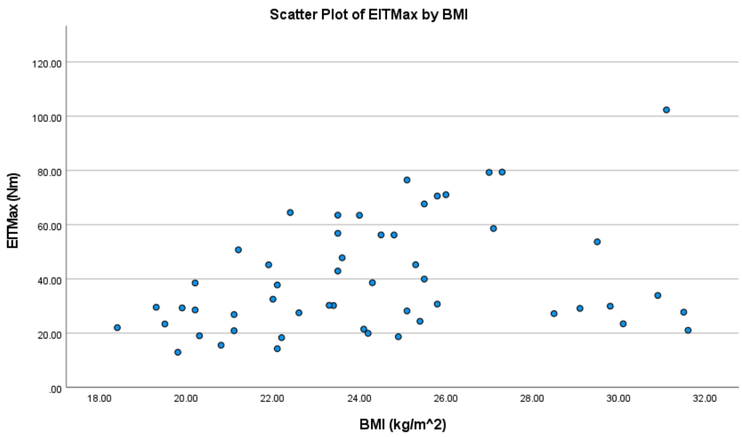

(e) Fat%

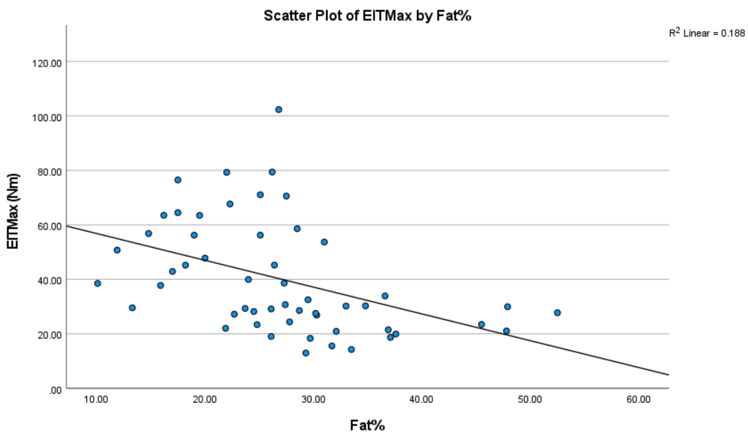

(f) Muscle%

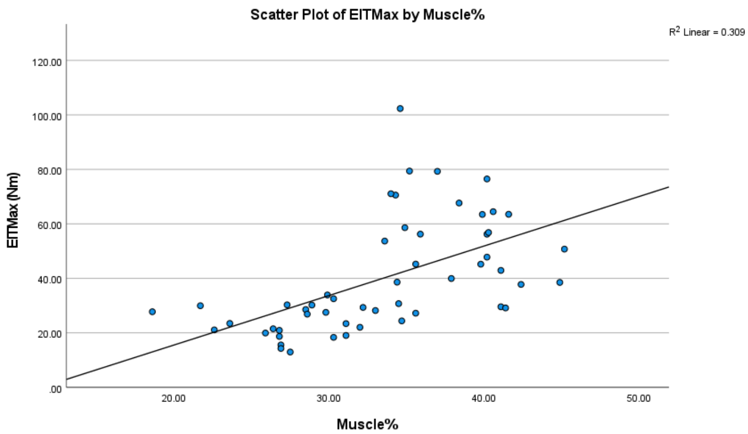

(g) Visceral Fat

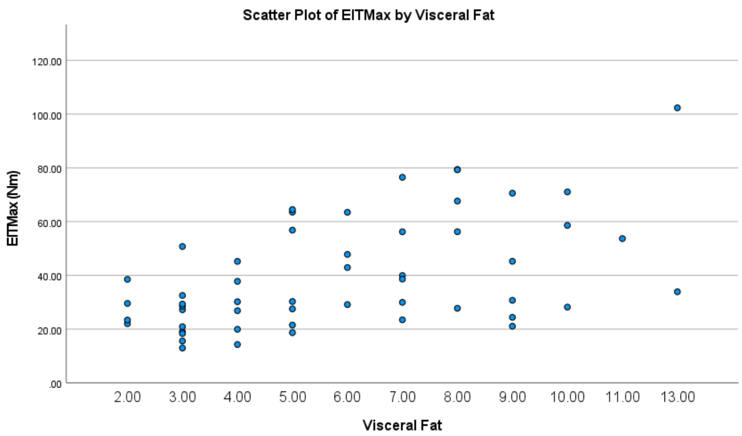

(h) Forearm Circumference

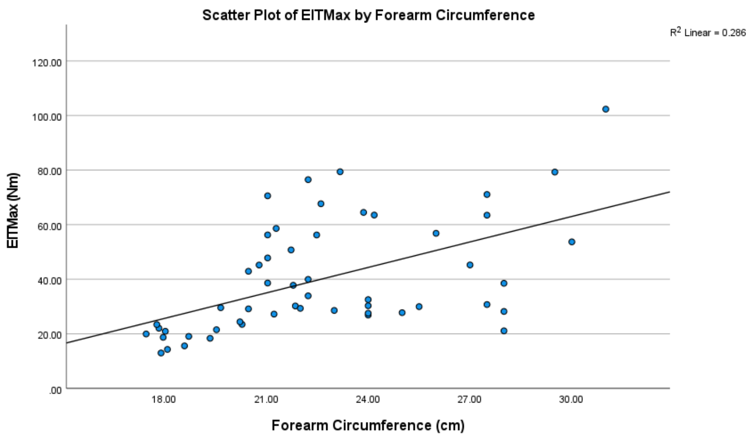

Appendix 11: Regression Analysis Results - Shoulder Maximum Torque

Model Summary[d]

Model	R	R Square	Adjusted R Square	Std. Error of the Estimate	Change Statistics: R Square Change	F Change	df1	df2	Sig. F Change
1	.756[a]	.571	.562	13.75418	.571	67.834	1	51	<.001
2	.779[b]	.606	.590	13.30578	.035	4.495	1	50	.039
3	.809[c]	.655	.634	12.58097	.049	6.927	1	49	.011

a. Predictors: (Constant), Height

b. Predictors: (Constant), Height, All_Circ

c. Predictors: (Constant), Height, All_Circ, MusclePerc

d. Dependent Variable: ShTMax

ANOVA[a]

Model		Sum of Squares	df	Mean Square	F	Sig.
1	Regression	12832.629	1	12832.629	67.834	<.001[b]
	Residual	9648.047	51	189.177		
	Total	22480.676	52			
2	Regression	13628.488	2	6814.244	38.489	<.001[c]
	Residual	8852.188	50	177.044		
	Total	22480.676	52			
3	Regression	14724.916	3	4908.305	31.010	<.001[d]
	Residual	7755.760	49	158.281		
	Total	22480.676	52			

a. Dependent Variable: ShTMax

b. Predictors: (Constant), Height

c. Predictors: (Constant), Height, All_Circ

d. Predictors: (Constant), Height, All_Circ, MusclePerc

Coefficients[a]

Model		Unstandardized Coefficients B	Std. Error	Standardized Coefficients Beta	t	Sig.	95.0% Confidence Interval for B Lower Bound	Upper Bound	Collinearity Statistics Tolerance	VIF
1	(Constant)	-276.942	39.205		-7.064	<.001	-355.650	-198.234		
	Height	186.961	22.700	.756	8.236	<.001	141.389	232.533	1.000	1.000
2	(Constant)	-262.969	38.496		-6.831	<.001	-340.290	-185.648		
	Height	162.404	24.827	.656	6.541	<.001	112.537	212.271	.782	1.278
	All_Circ	1.254	.592	.213	2.120	.039	.066	2.442	.782	1.278
3	(Constant)	-210.252	41.546		-5.061	<.001	-293.742	-126.763		
	Height	108.764	31.087	.440	3.499	.001	46.292	171.237	.446	2.242
	All_Circ	1.560	.571	.265	2.731	.009	.412	2.708	.750	1.333
	MusclePerc	.982	.373	.297	2.632	.011	.232	1.731	.554	1.803

a. Dependent Variable: ShTMax

Appendix 12: Regression Analysis Results - Elbow Maximum Torque

Model Summary[c]

Model	R	R Square	Adjusted R Square	Std. Error of the Estimate	Change Statistics				
					R Square Change	F Change	df1	df2	Sig. F Change
1	.755[a]	.570	.561	13.60385	.570	67.477	1	51	<.001
2	.782[b]	.612	.597	13.04115	.043	5.496	1	50	.023

a. Predictors: (Constant), Height

b. Predictors: (Constant), Height, All_Circ

c. Dependent Variable: ElTMax

ANOVA[a]

Model		Sum of Squares	df	Mean Square	F	Sig.
1	Regression	12487.527	1	12487.527	67.477	<.001[b]
	Residual	9438.304	51	185.065		
	Total	21925.831	52			
2	Regression	13422.252	2	6711.126	39.461	<.001[c]
	Residual	8503.579	50	170.072		
	Total	21925.831	52			

a. Dependent Variable: ElTMax

b. Predictors: (Constant), Height

c. Predictors: (Constant), Height, All_Circ

Coefficients[a]

Model		Unstandardized Coefficients		Standardized Coefficients	t	Sig.	95.0% Confidence Interval for B		Collinearity Statistics	
		B	Std. Error	Beta			Lower Bound	Upper Bound	Tolerance	VIF
1	(Constant)	-278.073	38.777		-7.171	<.001	-355.921	-200.225		
	Height	184.430	22.452	.755	8.214	<.001	139.356	229.504	1.000	1.000
2	(Constant)	-262.929	37.730		-6.969	<.001	-338.712	-187.146		
	Height	157.816	24.334	.646	6.486	<.001	108.941	206.692	.782	1.278
	All_Circ	1.359	.580	.233	2.344	.023	.195	2.524	.782	1.278

a. Dependent Variable: ElTMax

Appendix 13: Borg Rate of Perceived Exertion Scale

Borg's Rating of Perceived Exertion (RPE) Scale	
Perceived Exertion Rating	**Description of Exertion**
6	No exertion; sitting and resting
7	Extremely light
8	
9	Very light
10	
11	Light
12	
13	Somewhat hard
14	
15	Hard
16	
17	Very hard
18	
19	Extremely hard
20	Maximal exertion

Appendix 14: Karolinska Sleepiness Scale

Rate	Verbal descriptions
1	extremely alert
2	very alert
3	Alert
4	fairly alert
5	neither alert nor sleepy
6	some signs of sleepiness
7	sleepy, but no effort to keep awake
8	sleepy, some effort to keep awake
9	very sleepy, great effort to keep awake, fighting sleep

Appendix 15: Breakdown of Predicted ET RMSEs Based on Gender and Movement. RMSEs for Each Model and TT Combination for Female Subjects During (a) Static Tasks and (b) Dynamic Tasks, and for Males During (c) Static Tasks and (d) Dynamic Tasks.

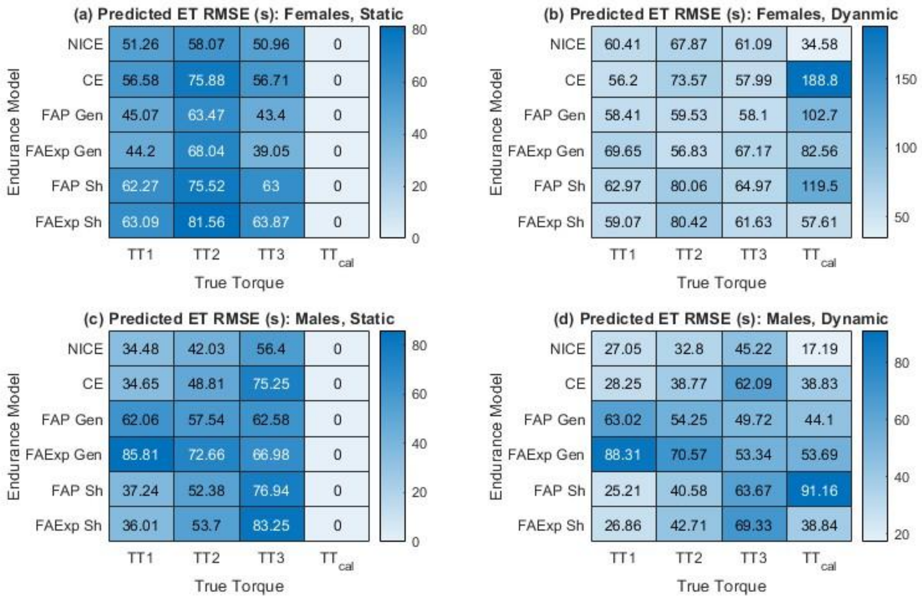

Appendix 16: Breakdown of Predicted ET RMSEs Based on Gender and Load. RMSEs for Each Model and TT Combination for Female Subjects During (a) 25% SI tasks and (b) 45% SI tasks, and for Males During (c) 25% SI tasks and (d) 45% SI tasks.

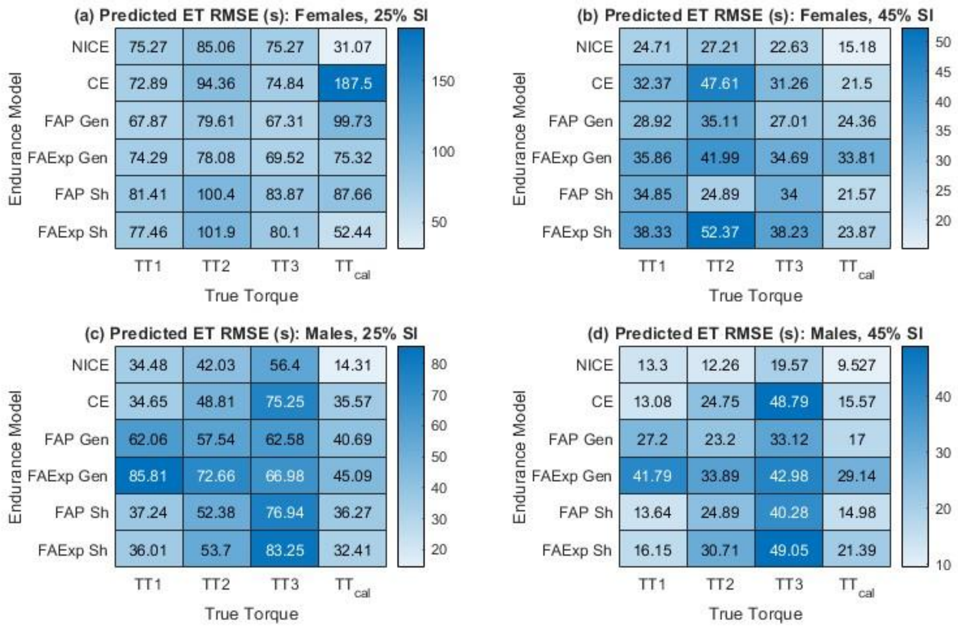

Abbreviations: NICE = New improved consumed endurance model, CE = Consumed endurance model, FAP Gen = Frey Law and Avin general power model, FAExp Gen = Frey Law and Avin general exponential model, FAP Sh = Frey Law and Avin shoulder power model, FAExp Sh = Frey Law and Avin shoulder exponential model. TT1= TT calculated using measured shoulder MVC for $Torque_{max}$, TT2= TT calculated using measured elbow MVC for $Torque_{max}$, TT3 = TT calculated using gender-based MVC for $Torque_{max}$, TT_{cal} = TT calculated using the calibration task.

Appendix 17: Predicted ET RMSEs Including Maximum Torque Regression Models. RMSEs for Each Model and TT Combination for (a) All Subjects and All Tasks, (b) Male Subjects and All Tasks (c) Female Subjects and All Tasks.

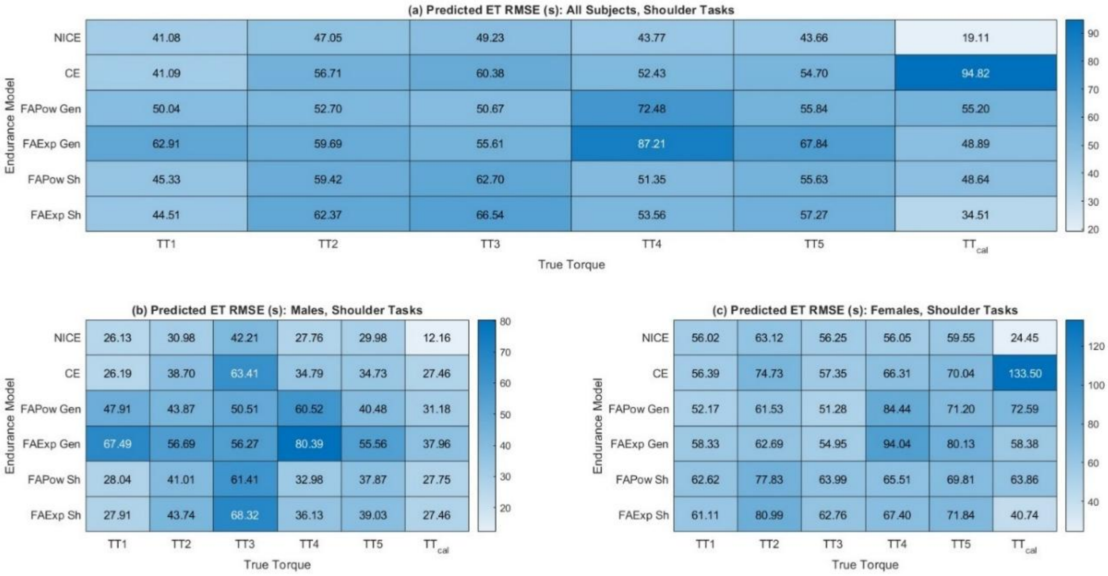

Appendix 18: Predicted ET RMSEs including maximum torque regression models, based on gender and movement. RMSEs for each model and TT combination for male subjects during (a) static tasks and (b) dynamic tasks and for females during (c) static tasks and (d) dynamic tasks.

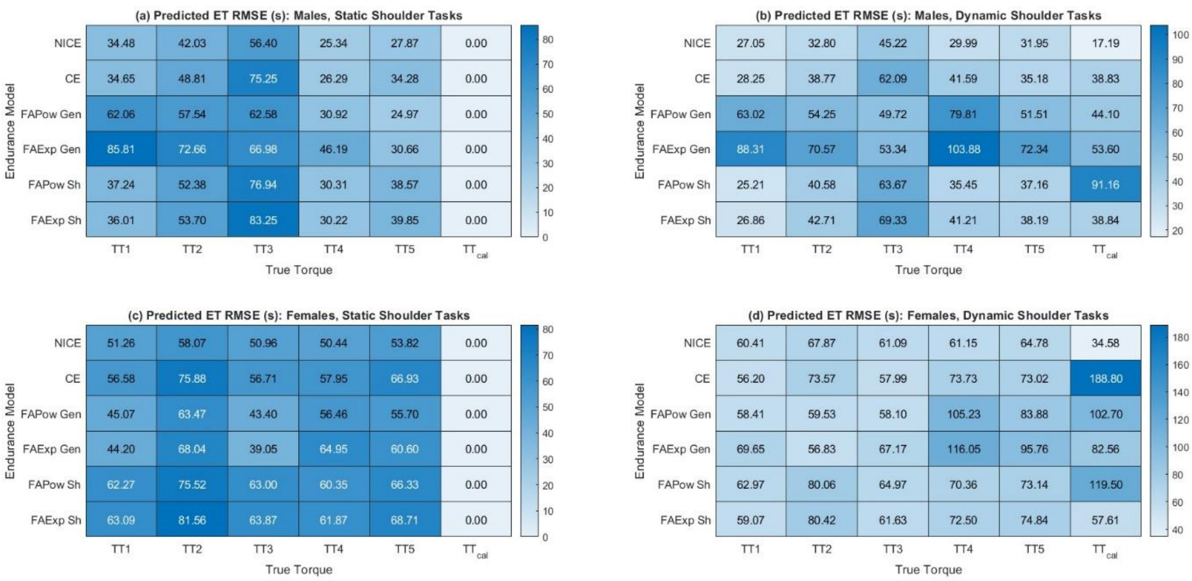

Abbreviations: NICE = New improved consumed endurance model, CE = Consumed endurance model, FAP Gen = Frey Law and Avin general power model, FAExp Gen = Frey Law and Avin general exponential model, FAP Sh = Frey Law and Avin shoulder power model, FAExp Sh = Frey Law and Avin shoulder exponential model. TT1= TT calculated using measured shoulder MVC for $Torque_{max}$, TT2= TT calculated using measured elbow MVC for $Torque_{max}$, TT3 = TT calculated using gender-based MVC for $Torque_{max}$, TT_{cal} = TT calculated using the calibration task.

Appendix 19: Predicted ET RMSEs including maximum torque regression models based on gender and load. RMSEs for each model and TT combination for male subjects during (a) 25% SI tasks and (b) 45% SI tasks and for females during (c) 25% SI tasks and (d) 45% SI tasks.

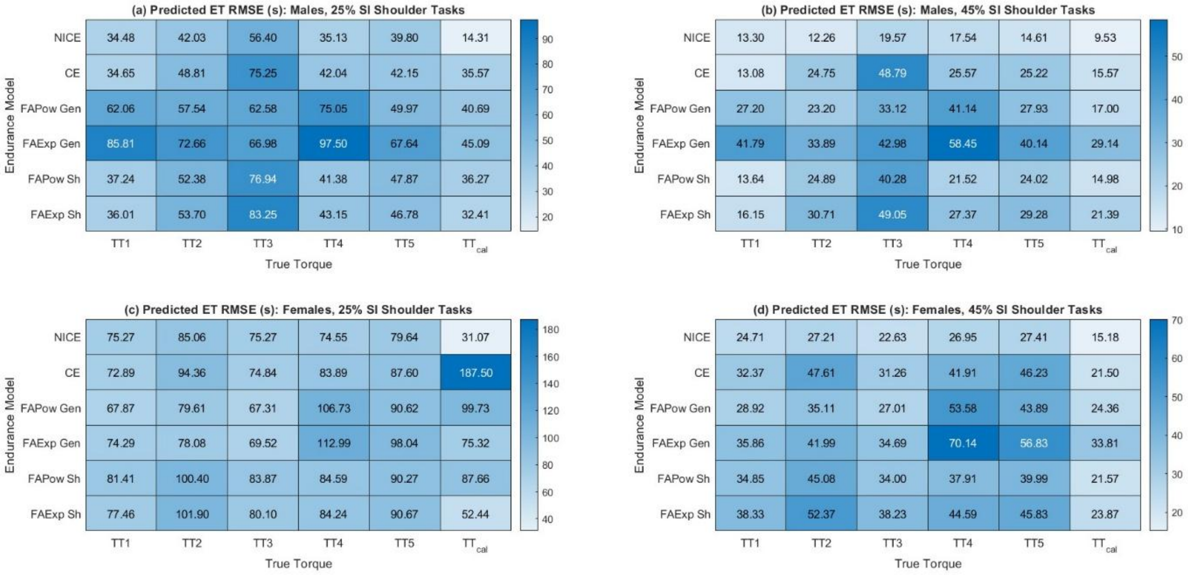

Abbreviations: NICE = New improved consumed endurance model, CE = Consumed endurance model, FAP Gen = Frey Law and Avin general power model, FAExp Gen = Frey Law and Avin general exponential model, FAP Sh = Frey Law and Avin shoulder power model, FAExp Sh = Frey Law and Avin shoulder exponential model. TT1= TT calculated using measured shoulder MVC for $Torque_{max}$, TT2= TT calculated using measured elbow MVC for $Torque_{max}$, TT3 = TT calculated using gender-based MVC for $Torque_{max}$, TT_{cal} = TT calculated using the calibration task.

Appendix 20: Supplementary Material for Section 4.2

IEEE Access
Multidisciplinary | Rapid Review | Open Access Journal

Date of publication xxxx 00, 0000, date of current version xxxx 00, 0000.

Digital Object Identifier 10.1109/ACCESS.2022.Doi Number

AI-based Task Classification with Pressure Insoles for Occupational Safety - Supplementary Material

Patricia O'Sullivan[1], Student Member, IEEE, Matteo Menolotto[1], Member, IEEE, Andrea Visentin[2], Brendan O'Flynn[1], Senior Member, IEEE, Dimitrios-Sokratis Komaris[3]

[1]Wireless Sensor Networks, Tyndall National Institute, University College Cork, T12 R5CP Cork, Ireland
[2]School of Computer Science & IT, University College Cork, T12 XF62 Cork, Ireland.
[3]Mechanical Engineering Department, Aston University, B4 7ET Birmingham, United Kingdom

Corresponding author: Patricia O'Sullivan (e-mail: patricia.osullivan@tyndall.ie).

This research has been supported by Science Foundation Ireland (SFI) under grant number 16/RC/3918 (CONFIRM). Aspects of this publication have emanated from research conducted with the financial support of Science Foundation Ireland under Grant number 12/RC/2289-P2-INSIGHT, and 13/RC/2077-CONNECT, which are co-funded under the European Regional Development Fund

INTRODUCTION

The search was conducted on the 18th of May 2023 with the search terms TITLE-ABS-KEY (pressure AND insoles AND machine AND learning). Inclusion criteria, and subsequently the elements presented in the supplementary tables, are activity classified, number of subjects, segmentation approach, features extracted, classifier used, model validation methods and assessment, results, and sensors used. In some activity classification cases (for example, [1]-[3]), a range of windows of time or segmentation overlaps were tested, and the window size that achieved the highest accuracy is noted in the table. Exclusion criteria for the table were research studies that did not include machine learning, those with fewer than 3 subjects, more than one inclusion criteria element was not specified, or features were not specified, and cases where the type of insoles was not specified. Only papers in English were assessed and papers from all years were considered. It was observed that many research groups have used their own custom designed insoles [4],[5], where ML-based classification is often used for validation purposes. In most cases, the pressure insoles incorporate their own accelerometer and/or gyroscope; however, where inertial measurement unit (IMU) is mentioned in the table, an additional IMU is used on a different part of the body such as shin or torso.

The results of the review are divided into 3 tables, according to the categories De Pinho (2017) [6] described for classification using pressure insoles; Tables 1, 2 and 3 present papers associated with gait phases and patterns, common movement activities and specific activities, respectively. Research involving fall and frailty detection in those with medical conditions is included in Table 1, while slips, trips and falls in occupational settings are in Table 3 since they are occupation specific. The tables show there is little consistency in the classification techniques employed, often a variety of techniques [7]-[9], as well as the validation and assessment methods, where area under curve [10], accuracy [11], [12], [1], F-score [4], root mean square error [13] and correlation coefficient [14],[15] have all been used as the primary measure of prediction. Statistical features appear most frequently, although frequency domain features are present [16], [17]. In other cases, important details are not mentioned in the study, denoted with a '-', most commonly the segmentation approach, a category in which a high degree of variability was apparent [1],[18]-[20].

TABLE 1: GAIT PHASES AND PATTERNS

Author	Classification	Sub	Time Window or Segmentation	Features	Classifier	Assessment	Results	Insoles Type / Other Sensors
Agrawal et al. [10]	Fall detection	1101	Gait cycle	cad, stt, st, gct, CoP	SVM, RF, LR, NB, DT, KNN	AUC	0.82	Surasole (Suratech, Thailand)
Arumuga raja et al. [21]	Knee pain detection	36	4 gait events	p (energy, entropy, homogeneity, max. probability, sum of var, contrast, cor, acor)	DT, KNN, LR, NB, SVM	5-fold CV, Acc, Pre, Sen, F, Spec, error rate	99.4% (KNN)	Custom
Brome et al. [22]	Fall detection	411	-	Pressure data converted to 2D heat map (input)	CNN	10-fold CV, Acc, Spec, Sen, Pre	81.2%	Custom
Chatzaki et al. [23]	Detecting severity level of Parkinson's disease patients	44	Gait events	Step, stride, SS, DS, st, and swt, SS %	DT, RF	5-fold CV, Acc	>78%	Moticon
Chen et al. [24]	Gait phase detection	24	5 gait phases	vel, dis, p (m), pp	SVM	Success rate, early/ late/ failed detection	94.08%	Custom insole
Choi et al. [25]	Prediction of COP trajectories	20	Heel contact of one foot to toe off of the other foot	CoP, vertical GRF	ANN, LSTM	10-fold CV, 18 subjects: 2 subjects (Train:Test), cor, RMSE, rRMSE, t test, U tests	>0.96 (cor)	Pedar-X / MC, FP
Crea et al. [20]	Gait phase detection	5	6 gait phases	Raw signals, calibrated signals, biomechanical variables (p, CoP)	HMM	LOOCV, Acc	96%	Custom insoles
D'Arco et al. [17]	Classification of Parkinson's Disease by gait	29	5 seconds	p (m, var, skewness, kurtosis, energy, entropy)	RF, KNN, SVM, LDA	10-fold CV, Acc, Pre, Sen, F, AUC	98.89% (KNN)	Moticon
Howcroft et al. [26]	Fall risk prediction	75	Stride	m and std of: cad, stride time, stt, swt, %DS, CoP (posterior, m-l, a-p features), impulse (AUC, normalized body mass), cov of: stride time, stt, swt	NN, NB, SVM	CV, 75:25 (Train:Test), Acc, F, MCC, CI	57% (NN)	F-Scan/ Accelerometers
Howcroft et al. [27]	Fall prediction	75	Stride	m and std of: cad, stride time, stt, swt, %DS, CoP (posterior, m-l, a-p features), impulse (AUC, normalized body mass), cov of: stride time, stt, swt	NN, NB, SVM	CV, 75:25 (Train:Test), Acc, Spec, PPV, NPV, F, MCC	94% (SVM)	F-Scan/ Accelerometers
Jacobs and Ferris [18]	Predicting ground contact kinetics	10	Gait cycle phase	p (a-p, m-l, vertical), CoP (a-p, m-l), vertical torque	NN regression model	RMSE, nRMSE	3.1-12.9% (walk), 3.3-21.3% (tasks)	Custom insoles / MC, IT, FP
Laufer et al. [28]	Gait phase detection	12	HS-TO	Sagittal ω, accel	SVM	LOOCV, Pre, Re, Recall-10	0.455 - 0.984 (Pre)	Smart Foot Sensor, Lux.) / IMU
Luna-Perejon et al. [19]	Gait phase detection	6	Step	p	ANN	85:15 (Test:Train), Acc, Spec, Pre, Re, F	99%	Custom insoles

[a]p = Pressure, pp = Peak pressure , GRF = Ground reaction force, CoP = Centre of pressure, HS-TO = Heel strike – Toe off,, a-p = Anterior – posterior, m-l = Medial – lateral, ω = Angular velocity, accel = Acceleration, vel = Velocity, dis = Displacement, cad = Cadence, m = Mean, std = Standard deviation, var = Variance, cov = Coefficient of variance, cor = Correlation, acor = Autocorrelation, SS = Single support, DS = Double support time, st = Stance, stt = Stance time, swt = Swing time, gct = Gait cycle time, DT = Decision tree, RF = Random forest, SVM = Support vector machine, NN = Neural network, KNN = k-Nearest Neighbour, LR = Logistic regression, NB = Naïve Bayes, ANN = Artificial neural network, CNN = Convolutional neural network, LSTM = Long short-term memory, LDA = Linear discriminant analysis, HMM = Hidden Markov Model, MCC = Matthew's correlation coefficient, CV = cross-validation, LOOCV = Leave one out cross validation, Acc = Accuracy, Pre = Precision, Sen = Sensitivity, Spec = Specificity, F = F-Score, RMSE = Root mean square error, rRMSE= Relative root mean square error, nRMSE = Normalised root mean square error, AUC = Area under curve, PPV = Positive predictive value, NPV = Negative predictive value, CI = Confidence intervals, MC = Motion capture, FP = Force plates, IMU = Inertial measurement units, IT = Instrumented Treadmill.

TABLE 1: GAIT PHASES AND PATTERNS (CONTINUED)

Author	Classification	Sub	Time Window or Segmentation	Features	Classifier	Assessment	Results	Insoles Type / Other Sensors
Moon et al. [29]	(a)Gait phase detection and (b)CoG prediction	30	(a)5 frames, (b)Gait phase from (a)	p (m , r, max., min., m absolute deviation, skewness, kurtosis, raw data)	(a)SVM, (b)Bi-LSTM	5-fold CV, (a)Pre, Re, F, (b)cor, RMSE, rRMSE	(a)0.91-0.95, (b)2.12%-12.97%	Custom insoles / MC
Moore et al. [30]	Foot strike pattern	30	Step	Impulse ratio, pp ratio, p RFD ratio, Ln p RFD	MR, RF, CIT	70:30 (Train:Test), Acc, Re, Pre	> 90% for all models	Loadsol / MC, FP
Munoz-Organero et al. [31]	Estimation of mobile index	14	Step	p (max., time p>80%, p_forefoot:p_heel, p_anterior:p_posterior, p length)	DT	10-fold CV, RMI, a-p NPA, ABC	Pos cor (RMI, a-p NPA), Neg cor (RMI, ABC)	Walk in-sense (Kinematix, Portugal)
Novak et al. [32]	Detection of gait initiation and termination	10	Step	Joint angles, sagittal ω for ankles, knees and hips, CoP, p	DT	WS, SI (10-fold CV), CA, abs error (m, med), % undetected	>80%	Custom insoles / IMU
Oubre et al. [5]	Estimating GRF and CoP	17	Stance phase	Knee angle, p, derivatives of inputs	RF	LOOCV, RMSE, nRMSE	Between 5-8.1%	Custom insoles / Pot, FP, MC
Potluri et al. [33]	Gait phase detection	10	Gait cycle (phases and sub-phases)	p, shank-thigh angle	(a)KNN, (b)SVM, (c)ANN	(a)8:2 subjects (Train:Test), (b, c)70:30 (Train: Val)	94.07% (SVM)	Custom insoles / IMU
Rathore et al. [34]	Abnormal or normal gait	58	Gait phases	AS, knee angle, SI, vel, pp, l	ELM	Acc, Sen, F, Spec	92.3%	Flexiforce / Pot
Song et al. [7]	Assessment of weak foot	48	Gait cycle	CoP, GL (m, std for a-p, m-l), RD (m, std), totex, CCA, JSD, GA, SIM, GIC	LR, KNN, SVM, DT, RF, GBDT	LOOCV, Acc, Sen, Spec, PPV, NPV	87.5%	Custom insoles
Tsakanikas et al [15]	Gait impairment in Parkinson's Disease	19	Gait cycle	p, accel, ω, CoP	SVM, RF, GBDT, AdaBoost	cor, ICC, AUC, Acc, F, Pre, Re	93%	Moticon / IMU
Turner et al. [35]	Diagnosis of gait abnormalities	8	5 seconds	p, CoP	LSTM	6:2 (Train:Test), Acc	97%	Moticon

[a]p = Pressure, pp = Peak pressure, CoP = Centre of pressure, a-p = Anterior – posterior, m-l = Medial – lateral, l = Step length, vel = Velocity, ω = Angular velocity, accel = Acceleration, m = Mean, abs = Absolute, r = range, GL = Gait line, totex = Total excursions, CoG = Centre of gravity, CCA = Confidence circle area, RD = Resultant distance, RFD = Rate of force development, JSD = JS – divergence, GA = Gait symmetry, AS = Asymmetry, SIM = Similarity, GIC = Gait inconsistency, DT = Decision tree, CIT = Conditional inference tree, GBDT = Gradient boosting decision tree, ELM = Extreme learning machine, RF = Random forest, SVM = Support vector machine, KNN = k-Nearest Neighbour, LSTM = Long short-term memory, MR = Multiple linear regression, LR = Logistic regression, CV = Cross valildation, LOOCV = Leave one out cross validation, RMI = Rivermead Mobility Index, WS = Within subject, SI = Subject independent, Val = Validation, CA = Classification accuracy, Acc = Accuracy, Pre = Precision, Sen = Sensitivity, Spec = Specificity, ABC = Area between curves, Re = Recall, F = F-Score, PPV = Positive predictive value, NPV = Negative predictive value, Pos = Positive, Neg = Negative, NPA = Normalized pressure amplitude, AUC = Area under curve, IMU = Inertial measurement unit, Pot = Potentiometer.

TABLE 2: COMMON MOVEMENT ACTIVIITIES (CONTINUED)

Author	Classification	Sub	Segmentation	Features	Classifier	Assessment	Results	Insoles Type / Other Sensors
Chen et al. [11]	HAR	10	Stride	stt, swt, gct, st, SST, DST, cad, CoP, p, pp location, PO, MSF, GA, GIC, turning (time, steps, angle)	SVM	5-fold CV, Acc	99.8%	Custom
Chen et al. [36]	Brunnstrom recovery stage recognition	30	Gait cycle	GL, gait phase, p, l, accel, joint angle	RF, NB, SVM, KNN	LOOCV, Acc, Pre, F	94.2%	Custom / IMUs
D'Arco et al. [37]	HAR	5	10s (50% overlap)	p (m, std, r, skewness, kurtosis, entropy, energy, dominant frequency ratio)	SVM	5-fold CV, Acc, Pre, Sen, F, TPR, FPR, AUC	94.66%	Custom

[a]HAR = Human activity recognition (for example, walk, stand, stairs, slopes, jog, run, skip, jump), p = Pressure, pp = Peak pressure, CoP = Centre of pressure, accel = Acceleration, cad = Cadence, mean = Mean, std = Standard deviation, r =Range, stt = Stance time, swt = Swing time, gct = Gait cycle time, st = Step time, SST = Single support time, DST = Double support time, PO = Push-off force and rate, MSF = Mid-stance force, GA = Gait symmetry, GIC = Gait inconsistency, GL = Gait line, l = Length of stride, RF = Random forest, SVM = Support vector machine, KNN = k-Nearest Neighbour, NB = Naïve Bayes, CV = cross-validation, LOOCV = Leave one out cross validation, TPR = True positive, rate, FPR = False positive rate, AUC = Area under curve, Acc = Accuracy, Pre = Precision, Sen = Sensitivity, F = F-Score, IMU = Inertial measurement unit

TABLE 2: COMMON MOVEMENT ACTIVIITIES (CONTINUED)

Author	Classification	Sub	Segmentation	Features	Classifier	Assessment	Results	Insoles Type / Other Sensors
D'Arco et al [38]	HAR	5	2s (50% overlap)	Raw data	FFNN	10-fold CV, Acc, F, Pre, Sen, AUC	98.6%	ActiSense (IEE Luxembourg S.A.)
De Pinho Andre et al. [6]	HAR	11	0.3s	All sensor signals (m, std, var, min., max.), CD, EA.	RF	LOOCV, Acc	93.34%	Custom / IMU, Temp, Alt, RF
Elvitigala et al. [39]	To discriminate acute stress and relaxation	34	10s	p, sop, CoP, dominant and median frequency, accel	RF, KNN, SVM, DT, LDA	LOOCV, Acc	0.87	Custom / Empatica E4 Wristband
Guo et al. [40]	HAR	13	2s	p (m, std)	SVM, RF, ANN	80:20 (Train: Test), Acc	97.9%	Custom / FP, PSAM
Hayakawa et al. [4]	HAR	6	250ms	p (m, min. max., med), sop, accel, ω	RF, KNN, ANN	LOOCV, F	78.6%	Custom
Ivanov et al. [3]	HAR	59	5s (70% overlap)	Raw data	CNN	67:33 (Train and Validate : Test), Statistical tests, Acc	93.3%	Custom
Lara-Barrios et al. [41]	HAR	6	150ms	p (m, std, RMSE, 3OAM, 6OAM)	LDA	5-fold CV, Pre, Re, F, mean classification error	7.85±4.76%	F-Scan
Martindale et al. [42]	HAR	80	5ms	p (raw data, var, coefficients of 2nd order polynomial fit)	HMM	20sub:10sub (Train:Test),+10sub/ test , F, mr, fdr, e	89.5%	Moticon / IMU
Martinez et al. [43]	Gait patterns - Parkinson's disease	39	Stride	gct, stt, swt, %st, %swt, DST, cov (gct, stt, swt, DST), GA, BC	LDA	39-fold CV, Acc, Sen, Spec	64.1%	F-Scan
Munoz-Organero et al. [44]	Walking with early stage osteoarthritis	28	Stance phase	Time differences between maximum values of sensors (m, std), p, pp	SVM, LR, MLP	Correct classifications	>12/14	Kinematix (Portugal)
Park et al. [45]	Detect gait changes due to alcohol intoxication	20	HS-TO	sp, cad, l, stt (m, std, var), s, SI, gct (m, std, var), pp (m, std, var), sop	RF	LOOCV, Acc, Pre, Re, F, MCC, AUC, PRC	86.2%	Custom
Ren et al. [2]	HAR	17	20s	p (m, max.,med), pp (m, std), peak width (m, std), PD, m frequency, diff. b/w.forces, DFD	RF	6:11 (Train:Test), Acc, Sen	0.89	Custom
Shalin et al. [46]	Detecting freeing of gait for Parkinson's disease patients	11	Timestamps of freeze events	CoP (coordinates, vel, accel), p (sum), fraction of total GRP	LSTM	LOOCV, Sen, Spec, Pre, F	95%	F-Scan
Wei et al. [14]	Estimating human walking speed	4	Stride	Gait frequency, horizontal and vertical accel (max., min., var), CoP (max., min., std, diff between max. and min.)	ANNs	83.7 : 16.3 (Test : Train), cor, error	0.003 ± 0.043 m/s	OpenGo
Yuan et al. [47]	HAR	3	Foot strike	Hip joint angle, CoP	Fuzz-logic	2 Trials:8 Trials (Train:Evaluation), Acc	>99.94%	Custom / Angle sensor

[a]HAR = Human activity recognition (for example, walk, stand, stairs, slopes, jog, run, skip, jump), p = Pressure, pp = Peak pressure, sop =sum of pressure, CoP = Centre of pressure, accel = Acceleration, m = Mean, std = Standard deviation, var = Variance, cov = Coefficient of variance, stt = Stance time, swt = Swing time, gct = Gait cycle time, st = Step time, DST = Double support time, DFD = Double float duration, cad = Cadence, GA = Gait symmetry, SI = Symmetry Index, BC = Bilateral coordination, l = Length of stride, 3OAM = 3rd order autoregressive model, 6OAM = 6th order autoregressive model, PD = Power density, sub = Subjects, CD = Cumulative difference between samples for each feature, EA = Euler angles, RF = Random forest, DT = Decision tree, LSTM = Long short-term memory, FFNN = Feed-forward neural network, SVM = Support vector machine, CNN = Convolutional neural network, KNN = k-Nearest Neighbour, ANN = Artificial neural network, LDA = Linear discriminant analysis, CV = cross-validation, LOOCV = Leave one out cross validation, cor = Correlation, Acc = Accuracy, Pre = Precision, Sen = Sensitivity, F = F-Score, mr = Miss rate, fdr = False discovery rate, e = Effort, MCC = Matthew's correlation coefficient, AUC = Area under curve, RMSE = Root mean square error, IMU = Inertial measurement unit, Temp = Temperature sensor, Alt = Altitude sensor, RF = Range finder, FP = Force plates, PSAM = Proprioceptive-stabilometric assessment machine.

TABLE 3: SPECIFIC ACTIVITIES

Author	Classification	Sub	Segmentation	Features	Classifier	Assessment	Results	Insoles Type / Other Sensors
Anderson et al. [12]	WAD	34	Heel-off	p (m, std), PTI	SVM, NN, KNN	4 fold CV, Acc	86%	Custom
Antwi-Afari et al. [16]	Detection and classification of slip, trips, loss of balance events	3	0.64s (50% overlap)	p (m, var, max., min., r, std, k, spectral energy, entropy), PTI	ANN, DT, KNN, SVM	10-fold CV, Acc, Sen	85%	OpenGo
Antwi-Afari et al. [48]	Detection of awkward working postures	10	032s (50% overlap)	p (m, var, max., min., r, std, k, spectral energy, entropy), PTI	ANN, DT, KNN, SVM	10-fold CV, Acc, Sen	98.6%	OpenGo
Antwi-Afari et al. [1]	Detection and classification of loss of balance events	10	0.32s	p (m, var, max., min., r, std, k, spectral energy, entropy), PTI	ANN, RF, KNN, SVM	10-fold CV, Acc, Sen	91.7%	OpenGo
Antwi_afari et al. [49]	Detection of awkward working postures	10	5.12s (sliding)	Raw Data	LSTM, Bi_LSTM, GRU	10-fold CV,72:18:10 (Train:Val:Test), Acc, Pre, Re, Spec, F	99.01%	OpenGo
Antwi-Afari et al. [9]	Identification and classification of fatigue levels	10	2.56s (sliding)	p (m, var, max., min., std, rms, iqr, k, sk, signal magnitude area, spectral energy, entropy), CoP	ANN, DT, RF, KNN, SVM	10-fold CV, Acc, Pre, Re, Spec,	86%	OpenGo
Kitagawa et al. [50]	Postural recognition method for caregivers	4	1s (50% overlap)	For p, accel and ω: m, max., min., std, rms, k, sk	ANN, DT, SVM	10-fold CV, Acc, Pre, Re, F	0.75 (arm), 0.97 (foot)	FlexiForce sensors / IMU
Kitagawa et al. [8]	Recognition method for patient handling	5	-	Trunk angle (rms, m), p (rms, m)	ANN, DT, KNN, RF, NB, SVM	10-fold CV, Acc, Pre, Re, F	0.97	FlexiForce sensors / IMU
Krumm et al. [13]	Determining push-off forces during speed skating imitation drills	7	Each time point	Bar contact and push-off timing and force related features	NN, LMVR	3 trials:14 trials (Train:Test), RMSE	<5%	Smart footwear sensors, Echternach, LUX / ISB
Lin et al. [51]	Recognition of patient handling activities	8	-	Differential raw pressure	KNN	LOOCV, Acc	86.6%	Custom
Matijevich et al. [52]	Monitoring lower back loading during manual handling tasks	10	-	p, CoP	DT	10-fold CV, codet, MAPE, RMSE	92%	Pedar-X / IMU, MC, FP

[a]WAD = Work activity detection, p = Pressure, accel = Acceleration, ω = Angular velocity, PTI = Pressure time integral, m = Mean, std = Standard deviation, var = Variance, r = Range, CoP = Center of pressure, rms = Root mean square, iqr = Interquartile range, k = Kurtosis, sk = Skewness, ANN = Artificial neural network, DT = Decision tree, KNN = k-Nearest neighbours, NN = Neural network, LMVR = Linear multiple variable regression model, SVM = Support vector machine, GRU = Gated recurrent units, LSTM = Long short-term memory, Bi = Bidirectional, RF = Random forest, NB = Naïve Bayes, CV = Cross-validation, Val = Validation, Acc = Accuracy, Sen = Sensitivity, F = F-Score, Pre = Precision, Re = Recall, Spec = Specificity, codet = Coefficient of determination, MAPE = Mean absolute error percentage, RMSE = Root mean square error, IMU = Inertial measurement unit, ISB = Instrumented slide board, MC = Motion capture, FP = Force plates.

REFERENCES

[1] M. F. Antwi-Afari, H. Li, J. Seo, and A. Y. L. Wong, 'Automated detection and classification of construction workers' loss of balance events using wearable insole pressure sensors', *Automation in Construction*, vol. 96, pp. 189–199, Dec. 2018, doi: 10.1016/j.autcon.2018.09.010.

[2] D. Ren, N. Aubert-Kato, E. Anzai, Y. Ohta, and J. Tripette, 'Random forest algorithms for recognizing daily life activities using plantar pressure information: a smart-shoe study', PeerJ, vol. 8, p. e10170, Oct. 2020, doi: 10.7717/peerj.10170.

[3] K. Ivanov et al., 'Identity Recognition by Walking Outdoors Using Multimodal Sensor Insoles', IEEE Access, vol. 8, pp. 150797–150807, 2020, doi: 10.1109/ACCESS.2020.3016970.

[4] Y. Hayakawa, Y. Kimata, K. Kida, Department of Control Engineering, National Institute of Technology, Nara College 22 Yata-cho, Yamatokoriyama, Nara 639-1058, Japan, and Advanced Mechanical Engineering Course, National Institute of Technology, Nara College 22 Yata-cho, Yamatokoriyama, Nara 639-1058, Japan, 'Study on Human Behavior Classification by Using High-Performance Shoes Equipped with Pneumatic Actuators', JRM, vol. 32, no. 5, pp. 947–957, Oct. 2020, doi: 10.20965/jrm.2020.p0947.

[5] B. Oubre, S. Lane, S. Holmes, K. Boyer, and S. I. Lee, 'Estimating Ground Reaction Force and Center of Pressure Using Low-Cost Wearable Devices', IEEE Trans. Biomed. Eng., vol. 69, no. 4, pp. 1461–1468, Apr. 2022, doi: 10.1109/TBME.2021.3120346.

[6] R. De Pinho André, P. H. F. S. Diniz, and H. Fuks, 'Bottom-up Investigation: Human Activity Recognition Based on Feet Movement and Posture Information', in Proceedings of the 4th International Workshop on Sensor-based Activity Recognition and Interaction, Rostock Germany: ACM, Sep. 2017, pp. 1–6. doi: 10.1145/3134230.3134240.

[7] Z. Song et al., 'Fall Risk Assessment for the Elderly Based on Weak Foot Features of Wearable Plantar Pressure', IEEE Trans. Neural Syst. Rehabil. Eng., vol. 30, pp. 1060–1070, 2022, doi: 10.1109/TNSRE.2022.3167473.

[8] K. Kitagawa, T. Nagasaki, S. Nakano, M. Hida, S. Okamatsu, and C. Wada, 'Comparison of Machine Learning Algorithms for Patient Handling Recognition based on Body Mechanics', in *2021 IEEE 3rd Global Conference on Life Sciences and Technologies (LifeTech)*, Nara, Japan: IEEE, Mar. 2021, pp. 77–79. doi: 10.1109/LifeTech52111.2021.9391968.

[9] M. F. Antwi-Afari *et al.*, 'Machine learning-based identification and classification of physical fatigue levels: A novel method based on a wearable insole device', *International Journal of Industrial Ergonomics*, vol. 93, p. 103404, Jan. 2023, doi: 10.1016/j.ergon.2022.103404.

[10] D. K. Agrawal, W. Usaha, S. Pojprapai, and P. Wattanapan, 'Fall Risk Prediction Using Wireless Sensor Insoles With Machine Learning', IEEE Access, vol. 11, pp. 23119–23126, 2023, doi: 10.1109/ACCESS.2023.3252886.

[11] D. Chen et al., 'Bring Gait Lab to Everyday Life: Gait Analysis in Terms of Activities of Daily Living', IEEE Internet Things J., vol. 7, no. 2, pp. 1298–1312, Feb. 2020, doi: 10.1109/JIOT.2019.2954387.

[12] W. Anderson, Z. Choffin, N. Jeong, M. Callihan, S. Jeong, and E. Sazonov, 'Empirical Study on Human Movement Classification Using Insole Footwear Sensor System and Machine Learning', *Sensors*, vol. 22, no. 7, p. 2743, Apr. 2022, doi: 10.3390/s22072743.

[13] D. Krumm, N. Kuske, M. Neubert, J. Buder, F. Hamker, and S. Odenwald, 'Determining push-off forces in speed skating imitation drills', *Sports Engineering*, vol. 24, no. 1, 2021, doi: 10.1007/s12283-021-00362-1.

[14] W. Wei, Y. Kaiming, Z. Yu, Q. Yuyang, W. Chenhui, and L. Min, 'Walking Speed Estimation From a Wearable Insole Pressure System Using a Bayesian Regularized Back Propagation Neural Network', in Volume 5: Biomedical and Biotechnology, Virtual, Online: American Society of Mechanical Engineers, Nov. 2020, p. V005T05A001. doi: 10.1115/IMECE2020-23363.

[15] V. Tsakanikas et al., 'Evaluating Gait Impairment in Parkinson's Disease from Instrumented Insole and IMU Sensor Data', Sensors, vol. 23, no. 8, p. 3902, Apr. 2023, doi: 10.3390/s23083902.

[16] M. F. Antwi-Afari, H. Li, J. Seo, S. Lee, D. J. Edwards, and A. Y. Lok Wong, 'Wearable Insole Pressure Sensors for Automated Detection and Classification of Slip-Trip-Loss of Balance Events in Construction Workers', in *Construction Research Congress 2018*, New Orleans, Louisiana: American Society of Civil Engineers, Mar. 2018, pp. 73–83. doi: 10.1061/9780784481288.008.

[17] L. D'Arco, H. Wang, and H. Zheng, 'A Rapid Detection of Parkinson's Disease using Smart Insoles: A Statistical and Machine Learning Approach', in 2022 IEEE International Conference on Bioinformatics and Biomedicine (BIBM), Las Vegas, NV, USA: IEEE, Dec. 2022, pp. 2985–2992. doi: 10.1109/BIBM55620.2022.9995237.

[18] D. A. Jacobs and D. P. Ferris, 'Evaluation of a Low-Cost Pneumatic Plantar Pressure Insole for Predicting Ground Contact Kinetics', Journal of Applied Biomechanics, vol. 32, no. 2, pp. 215–220, Apr. 2016, doi: 10.1123/jab.2015-0142.

[19] F. Luna-Perejón, M. Domínguez-Morales, D. Gutiérrez-Galán, and A. Civit-Balcells, 'Low-Power Embedded System for Gait Classification Using Neural Networks', JLPEA, vol. 10, no. 2, p. 14, May 2020, doi: 10.3390/jlpea10020014.

[20] S. Crea et al., 'Development of gait segmentation methods for wearable foot pressure sensors', in 2012 Annual International Conference of the IEEE Engineering in Medicine and Biology Society, San Diego, CA: IEEE, Aug. 2012, pp. 5018–5021. doi: 10.1109/EMBC.2012.6347120.

[21] M. Arumugaraja, B. Padmapriya, and S. Poornachandra, 'Design and development of foot worn piezoresistive sensor for knee pain analysis with supervised machine learning algorithms based on gait pattern', Measurement, vol. 200, p. 111603, Aug. 2022, doi: 10.1016/j.measurement.2022.111603.

[22] R. Brome, J. Nasreddine, F. Bonnardot, M. E. Badaoui, and M. O. Diab, 'Fall Risk Assessment Using Pressure Insole Sensors and Convolutional Neural Networks', in 2022 IEEE-EMBS Conference on Biomedical Engineering and Sciences (IECBES), Kuala Lumpur, Malaysia: IEEE, Dec. 2022, pp. 177–182. doi: 10.1109/IECBES54088.2022.10079580.

[23] C. Chatzaki et al., 'Can Gait Features Help in Differentiating Parkinson's Disease Medication States and Severity Levels? A Machine Learning Approach', Sensors, vol. 22, no. 24, p. 9937, Dec. 2022, doi: 10.3390/s22249937.

[24] W. Chen, Y. Xu, J. Wang, and J. Zhang, 'Kinematic Analysis of Human Gait Based on Wearable Sensor System for Gait Rehabilitation', J. Med. Biol. Eng., vol. 36, no. 6, pp. 843–856, Dec. 2016, doi: 10.1007/s40846-016-0179-z.

[25] A. Choi, H. Jung, K. Y. Lee, S. Lee, and J. H. Mun, 'Machine learning approach to predict center of pressure trajectories in a complete gait cycle: a feedforward neural network vs. LSTM network', Med Biol Eng Comput, vol. 57, no. 12, pp. 2693–2703, Dec. 2019, doi: 10.1007/s11517-019-02056-0.

[26] J. Howcroft, J. Kofman, and E. D. Lemaire, 'Prospective Fall-Risk Prediction Models for Older Adults Based on Wearable Sensors', IEEE Trans. Neural Syst. Rehabil. Eng., vol. 25, no. 10, pp. 1812–1820, Oct. 2017, doi: 10.1109/TNSRE.2017.2687100.

[27] J. Howcroft, E. D. Lemaire, and J. Kofman, 'Prospective elderly fall prediction by older-adult fall-risk modeling with feature selection', Biomedical Signal Processing and Control, vol. 43, pp. 320–328, May 2018, doi: 10.1016/j.bspc.2018.03.005.

[28] F. Laufer, M. Lorenz, B. Taetz, and G. Bleser, 'On Expressive Features for Gait Analysis using Lower Limb Inertial Sensor Data', IFAC-PapersOnLine, vol. 53, no. 2, pp. 15990–15997, 2020, doi: 10.1016/j.ifacol.2020.12.396.

[29] J. Moon, D. Lee, H. Jung, A. Choi, and J. H. Mun, 'Machine Learning Strategies for Low-Cost Insole-Based Prediction of Center of Gravity during Gait in Healthy Males', Sensors, vol. 22, no. 9, p. 3499, May 2022, doi: 10.3390/s22093499.

[30] S. R. Moore, C. Kranzinger, J. Fritz, T. Stöggl, J. Kröll, and H. Schwameder, 'Foot Strike Angle Prediction and Pattern Classification Using LoadsolTM Wearable Sensors: A Comparison of Machine Learning Techniques', Sensors, vol. 20, no. 23, p. 6737, Nov. 2020, doi: 10.3390/s20236737.

[31] M. Munoz-Organero, J. Parker, L. Powell, and S. Mawson, 'Assessing Walking Strategies Using Insole Pressure Sensors for Stroke Survivors', Sensors, vol. 16, no. 10, p. 1631, Oct. 2016, doi: 10.3390/s16101631.

[32] D. Novak et al., 'Automated detection of gait initiation and termination using wearable sensors', Medical Engineering & Physics, vol. 35, no. 12, pp. 1713–1720, Dec. 2013, doi: 10.1016/j.medengphy.2013.07.003.

[33] S. Potluri, A. B. Chandran, C. Diedrich, and L. Schega, 'Machine Learning based Human Gait Segmentation with Wearable Sensor Platform',

in 2019 41st Annual International Conference of the IEEE Engineering in Medicine and Biology Society (EMBC), Berlin, Germany: IEEE, Jul. 2019, pp. 588–594. doi: 10.1109/EMBC.2019.8857509.

[34] R. Rathore, A. K. Singh, H. Chaudhary, and K. Kandan, 'Gait Abnormality Detection in Unilateral Trans-tibial Amputee in Real Time Gait using Wearable Setup', IEEE Sensors J., pp. 1–1, 2023, doi: 10.1109/JSEN.2023.3263399.

[35] A. Turner, D. Scott, and S. Hayes, 'The Classification of Multiple Interacting Gait Abnormalities Using Insole Sensors and Machine Learning', in 2022 IEEE International Conference on Digital Health (ICDH), Barcelona, Spain: IEEE, Jul. 2022, pp. 69–76. doi: 10.1109/ICDH55609.2022.00020.

[36] X. Chen et al., 'Interpretable evaluation for the Brunnstrom recovery stage of the lower limb based on wearable sensors', Front. Neuroinform., vol. 16, p. 1006494, Sep. 2022, doi: 10.3389/fninf.2022.1006494.

[37] L. D'Arco, H. Wang, and H. Zheng, 'Assessing Impact of Sensors and Feature Selection in Smart-Insole-Based Human Activity Recognition', MPs, vol. 5, no. 3, p. 45, May 2022, doi: 10.3390/mps5030045.

[38] L. D'Arco, H. Wang, and H. Zheng, 'DeepHAR: a deep feed-forward neural network algorithm for smart insole-based human activity recognition', Neural Comput & Applic, Mar. 2023, doi: 10.1007/s00521-023-08363-w.

[39] D. S. Elvitigala, D. J. C. Matthies, and S. Nanayakkara, 'StressFoot: Uncovering the Potential of the Foot for Acute Stress Sensing in Sitting Posture', Sensors, vol. 20, no. 10, p. 2882, May 2020, doi: 10.3390/s20102882.

[40] R. Guo et al., 'A Shoe-Integrated Sensor System for Long- Term Center of Pressure Evaluation', IEEE Sensors J., vol. 21, no. 23, pp. 27037–27044, Dec. 2021, doi: 10.1109/JSEN.2021.3116249.

[41] C. M. Lara-Barrios, P. C. Formento, E. M. Larrosa, and A. Blanco-Ortega, 'Evaluation of the offline classification error of human locomotion modes using virtual force-sensing resistor data', in 2020 International Conference on Mechatronics, Electronics and Automotive Engineering (ICMEAE), Cuernavaca, Mexico: IEEE, Nov. 2020, pp. 161–168. doi: 10.1109/ICMEAE51770.2020.00035.

[42] C. F. Martindale, S. Sprager, and B. M. Eskofier, 'Hidden Markov Model-Based Smart Annotation for Benchmark Cyclic Activity Recognition Database Using Wearables', Sensors, vol. 19, no. 8, p. 1820, Apr. 2019, doi: 10.3390/s19081820.

[43] M. Martínez, F. Villagra, J. Castellote, and M. Pastor, 'Kinematic and Kinetic Patterns Related to Free-Walking in Parkinson's Disease', Sensors, vol. 18, no. 12, p. 4224, Dec. 2018, doi: 10.3390/s18124224.

[44] M. Munoz-Organero, C. Littlewood, J. Parker, L. Powell, C. Grindell, and S. Mawson, 'Identification of Walking Strategies of People With Osteoarthritis of the Knee Using Insole Pressure Sensors', IEEE Sensors J., vol. 17, no. 12, pp. 3909–3920, Jun. 2017, doi: 10.1109/JSEN.2017.2696303.

[45] E. Park et al., 'Unobtrusive and Continuous Monitoring of Alcohol-impaired Gait Using Smart Shoes', Methods Inf Med, vol. 56, no. 01, pp. 74–82, 2017, doi: 10.3414/ME15-02-0008.

[46] G. Shalin, S. Pardoel, E. D. Lemaire, J. Nantel, and J. Kofman, 'Prediction and detection of freezing of gait in Parkinson's disease from plantar pressure data using long short-term memory neural-networks', J NeuroEngineering Rehabil, vol. 18, no. 1, p. 167, Dec. 2021, doi: 10.1186/s12984-021-00958-5.

[47] K. Yuan et al., 'Fuzzy-logic-based hybrid locomotion mode classification for an active pelvis orthosis: Preliminary results', presented at the 2015 37th Annual International Conference of the IEEE Engineering in Medicine and Biology Society (EMBC), IEEE, 2015, pp. 3893–3896.

[48] M. F. Antwi-Afari, H. Li, Y. Yu, and L. Kong, 'Wearable insole pressure system for automated detection and classification of awkward working postures in construction workers', *Automation in Construction*, vol. 96, pp. 433–441, Dec. 2018, doi: 10.1016/j.autcon.2018.10.004.

[49] M. F. Antwi-Afari *et al.*, 'Deep learning-based networks for automated recognition and classification of awkward working postures in construction using wearable insole sensor data', *Automation in Construction*, vol. 136, p. 104181, Apr. 2022, doi: 10.1016/j.autcon.2022.104181.

[50] K. Kitagawa *et al.*, 'Posture Recognition Method for Caregivers during Postural Change of a Patient on a Bed using Wearable Sensors', *Adv. sci. technol. eng. syst. j.*, vol. 5, no. 5, pp. 1093–1098, Oct. 2020, doi: 10.25046/aj0505133.

[51] F. Lin, C. Song, X. Xu, L. Cavuoto, and W. Xu, 'Patient handling activity recognition through pressure-map manifold learning using a footwear sensor', *Smart Health*, vol. 1–2, pp. 77–92, Jun. 2017, doi: 10.1016/j.smhl.2017.04.005.

[52] E. S. Matijevich, P. Volgyesi, and K. E. Zelik, 'A Promising Wearable Solution for the Practical and Accurate Monitoring of Low Back Loading in Manual Material Handling', *Sensors*, vol. 21, no. 2, p. 340, Jan. 2021, doi: 10.3390/s21020340.

Appendix 21: Poster Presented at INSIGHT Plenary in Galway, October 2023.

AI-based Task Classification with Pressure Insoles for Occupational Safety

Insight
SFI RESEARCH CENTRE FOR DATA ANALYTICS

Patricia O'Sullivan[a], Matteo Menolotto[a], Andrea Visentin[b], Brendan O'Flynn[a], Dimitrios-Sokratis Komaris[a,c]

a Tyndall National Institute, University College Cork, T12 R5CP Cork, Ireland
b University College Cork, Cork, Ireland
c Aston University, B4 7ET Birmingham, United Kingdom

A World Leading SFI Research Centre

Introduction

Pressure insoles (PI) measure the plantar pressure between the foot and the shoe, and they allow for the collection of real time pressure data inside and outside a laboratory setting, as such devices are non-intrusive and can be simply integrated into everyday life. PI are being used in a range of sectors, from sports performance [1] to occupational health and safety for the monitoring of slips [2] and lower back loading [3]. Activity recognition through machine learning algorithms has been implemented using pressure insoles in a wide variety of domains [4, 5].

Objective

The aim of the research was to **identify significant force, peak morphology and centre of pressure (CoP) features for task classification in the Industry 4.0 domain** using a random forest classifier.

Methodology

Data Collection → Feature Extraction → Supervised Machine Learning Classifier

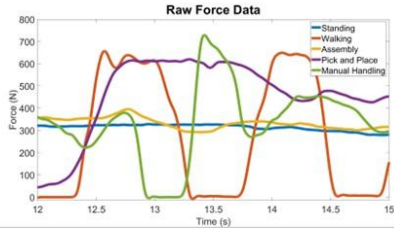

Fig. 1: Raw total force data for all tasks.

Results and Discussion

→**Accuracy levels of 82%** when evaluated over a window of 5 seconds.

→From the confusion matrix (Fig. 3), we see that the **accuracy decreases where the CoP is more confined**, see Fig. 2

→**SHAP analysis** shows feature importance, re-analysis of top 5 features was done (Fig. 4).

→These methods denote a move away from the 'black box' approach of certain ML classifiers that may lead to a lack of trust. **Random forest provide a good balance between accuracy and interpretability.**

→Raw dataset [7], feature database, and analysis are all publicly available.

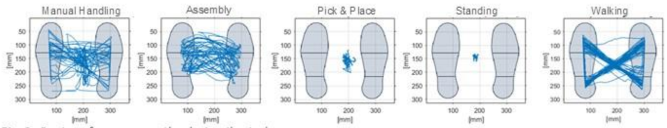

Fig. 2: Centre of pressure paths during the tasks.

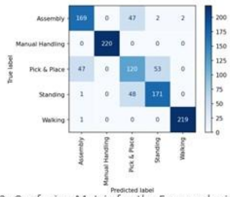

Fig. 3: Confusion Matrix for the 5 second window.

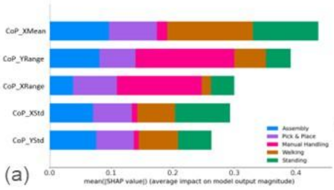

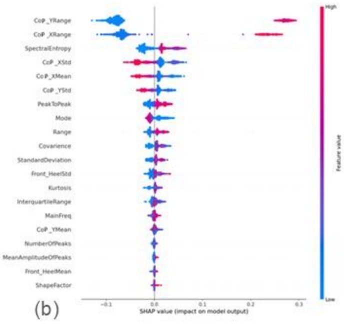

Fig. 4: SHAP analysis of feature importance for the top 5 significant features (a) and for manual handling (b).

Conclusions

Our results show that pressure insoles can be used for **real-time task detection** in industry settings. The results can be used to **reduce misclassifications** and may **inform pressure insoles design** optimized for the extraction of CoP to reduce misclassifications, to optimize data throughput and consumption, making them suitable for IoT smart manufacturing environments.

Acknowledgements

Research supported by Science Foundation Ireland (SFI) under grant no. 12/RC/2289-P2 (INSIGHT) and 16/RC/3918 (CONFIRM).

References

[1]V. Cigrovski, M. Očić, I. Bon, B. Matković, and P. Šagát, 'Inline Skating as an Additional Activity for Alpine Skiing: The Role of the Outside Leg in Short Turn Performance', International Journal of Environmental Research and Public Health, vol. 19, no. 3, 2022.
[2]M. F. Antwi-Afari, H. Li, J. Seo, and A. Y. L. Wong, 'Automated detection and classification of construction workers' loss of balance events using wearable insole pressure sensors', Automation in Construction, vol. 96, pp. 189–199, Dec. 2018.
[3]E. S. Matijevich, P. Volgyesi, and K. E. Zelik, 'A Promising Wearable Solution for the Practical and Accurate Monitoring of Low Back Loading in Manual Material Handling', Sensors, vol. 21, no. 2, p. 340, Jan. 2021, doi: 10.3390/s21020340.
[4]M. F. Antwi-Afari, H. Li, W. Umer, Y. Yu, and X. Xing, 'Construction Activity Recognition and Ergonomic Risk Assessment Using a Wearable Insole Pressure System', J. Constr. Eng. Manage., vol. 146, no. 7, p. 04020077, Jul. 2020.
[5]H. Leutheuser, D. Schuldhaus, and B. M. Eskofier, 'Hierarchical, Multi-Sensor Based Classification of Daily Life Activities: Comparison with State-of-the-Art Algorithms Using a Benchmark Dataset', PLoS ONE, vol. 8, no. 10, p. e75196, Oct. 2013.
[6]S. M. Lundberg and S.-I. Lee, 'A unified approach to interpreting model predictions', Advances in neural information processing systems, vol. 30, 2017.
[7]P. O'Sullivan and M. Menolotto, 'PID4TC (Pressure Insoles Data for Task Classification)'. Zenodo, Mar. 21, 2023. doi: 10.5281/ZENODO.7755802.

Appendix 22: Supplementary Material for Chapter 5

(a) Subject Information Panel

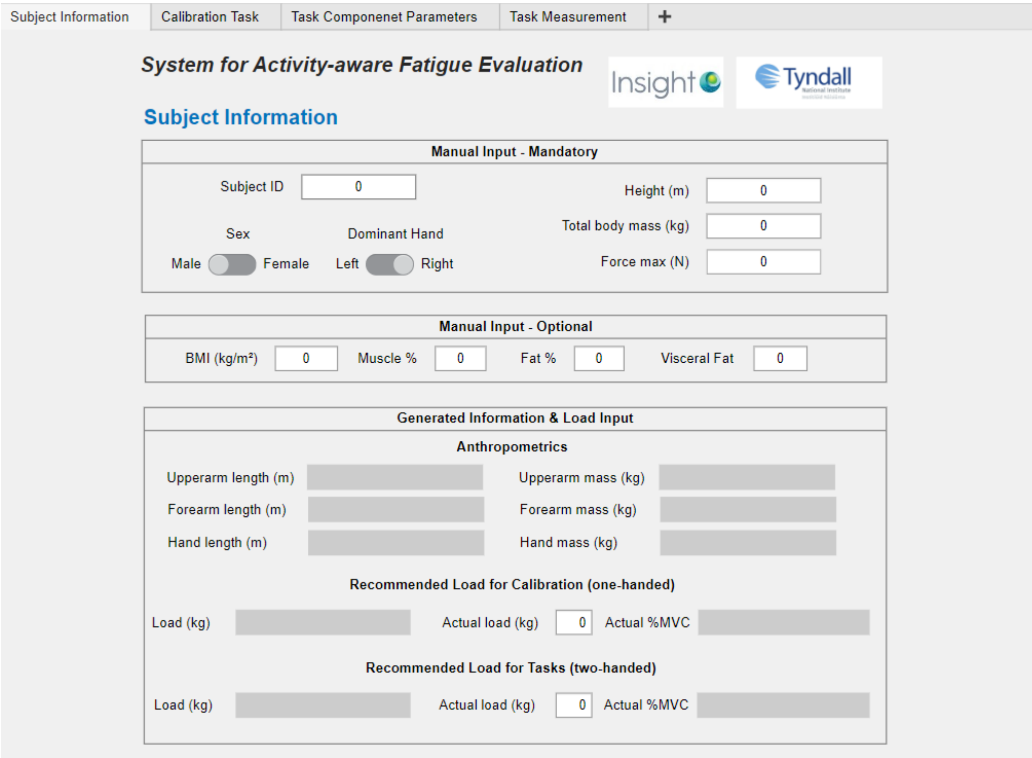

(b) Calibration Task Panel

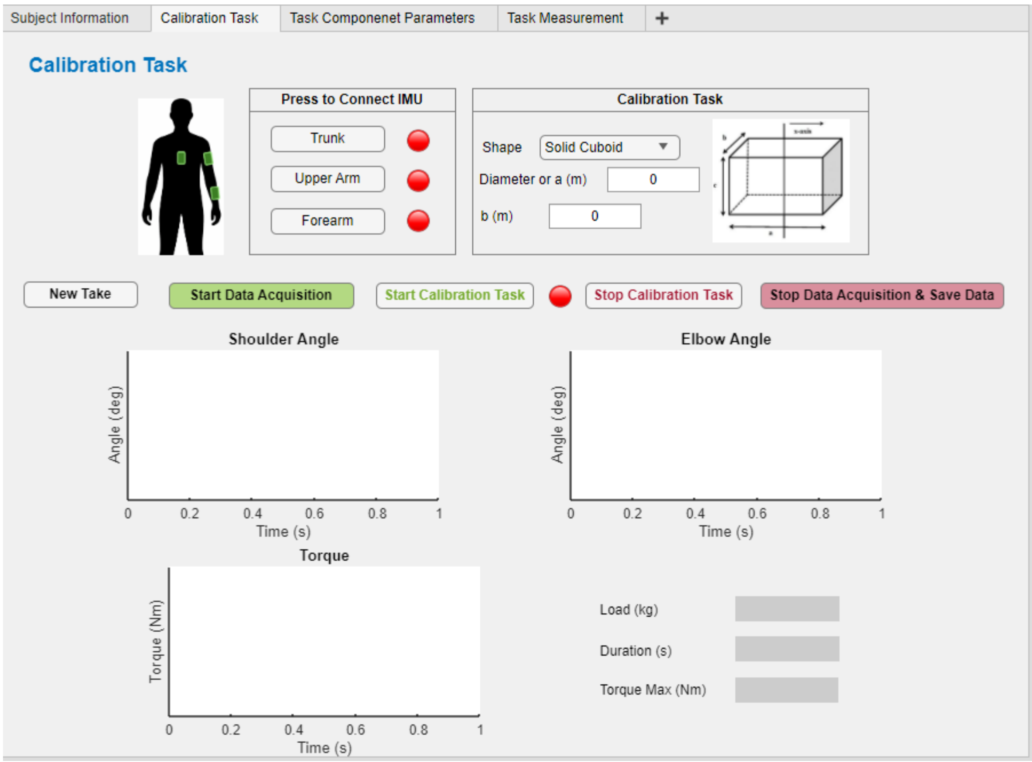

(c) Task Component Parameters Panel

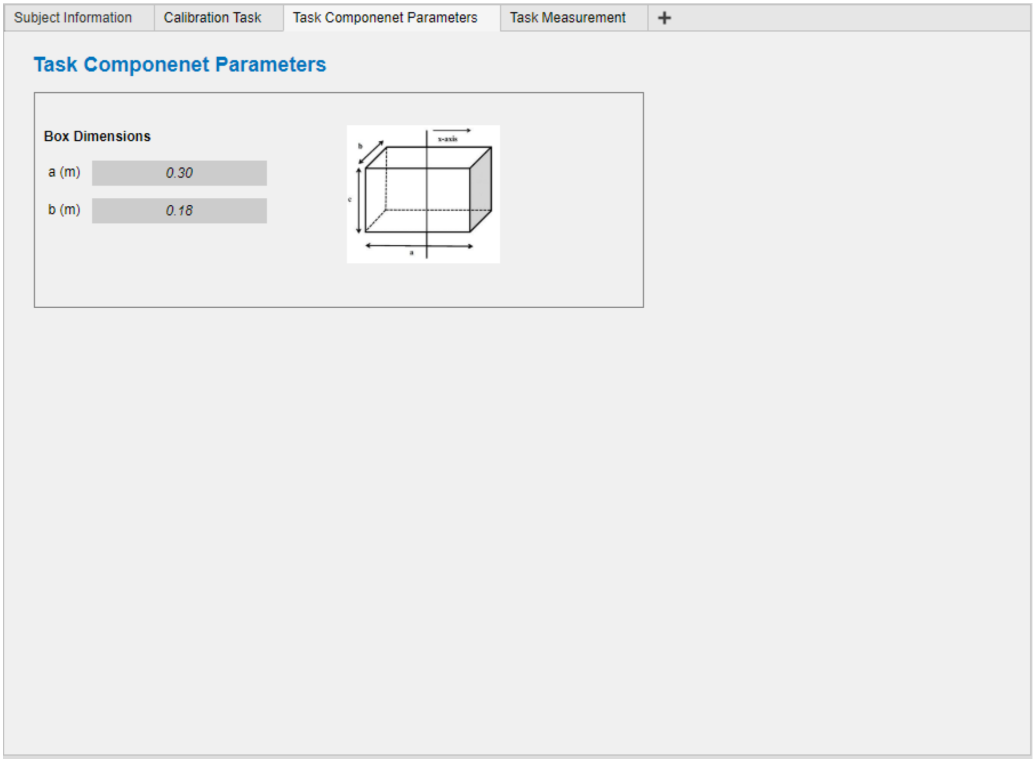

(d) Task Measurement Panel

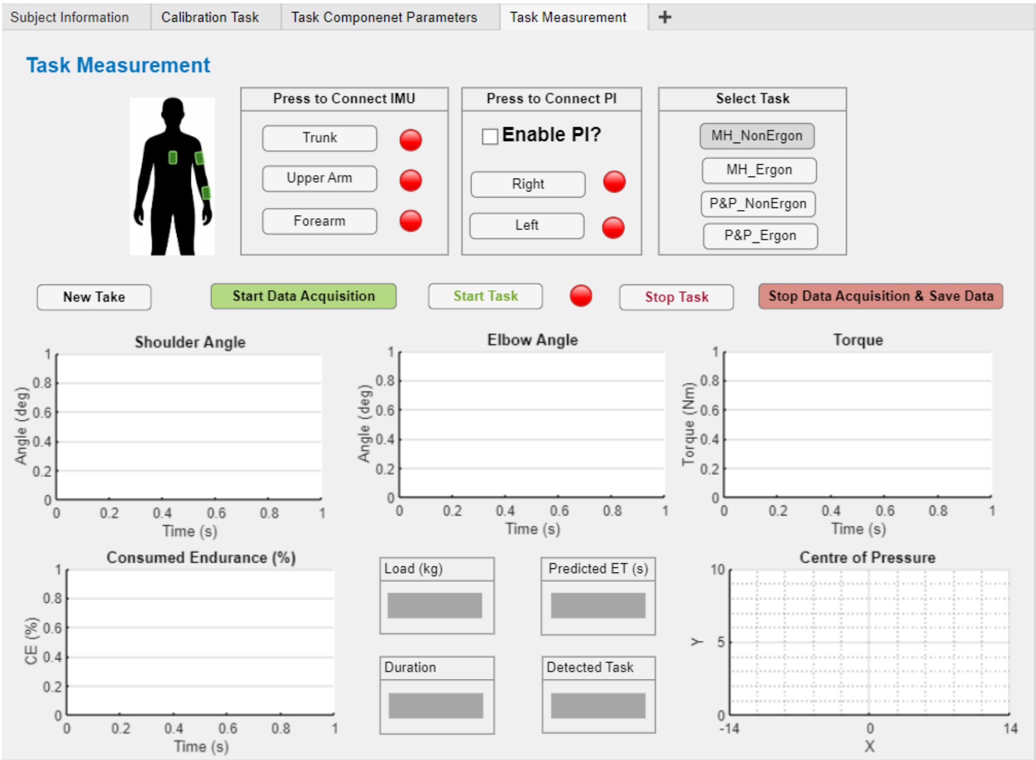

References

[1] S. Nahavandi, ‘Industry 5.0—A Human-Centric Solution’, *Sustainability*, vol. 11, no. 16, p. 4371, Aug. 2019, doi: 10.3390/su11164371.
[2] C. Bai, P. Dallasega, G. Orzes, and J. Sarkis, ‘Industry 4.0 technologies assessment: A sustainability perspective’, *Int. J. Prod. Econ.*, vol. 229, p. 107776, Nov. 2020, doi: https://doi.org/10.1016/j.ijpe.2020.107776.
[3] S. K. Kheiri, Z. Vahedi, H. Sun, F. M. Megahed, and L. A. Cavuoto, ‘Human reliability modeling in occupational environments toward a safe and productive operator 4.0’, *Int. J. Ind. Ergon.*, vol. 97, p. 103479, Sep. 2023, doi: 10.1016/j.ergon.2023.103479.
[4] M. Ciccarelli, A. Papetti, and M. Germani, ‘Exploring how new industrial paradigms affect the workforce: A literature review of Operator 4.0.’, *J. Manuf. Syst.*, vol. 70, pp. 464–483, Oct. 2023, doi: 10.1016/j.jmsy.2023.08.016.
[5] A. Alhakamy, ‘Extended Reality (XR) Toward Building Immersive Solutions: The Key to Unlocking Industry 4.0’, *ACM Comput. Surv.*, vol. 56, no. 9, pp. 1–38, Oct. 2024, doi: 10.1145/3652595.
[6] A. Simeone, R. Grant, W. Ye, and A. Caggiano, ‘A human-cyber-physical system for Operator 5.0 smart risk assessment’, *Int. J. Adv. Manuf. Technol.*, vol. 129, no. 5–6, pp. 2763–2782, Nov. 2023, doi: 10.1007/s00170-023-12481-z.
[7] D. Romero, P. Bernus, O. Noran, J. Stahre, and Å. Fast-Berglund, ‘The Operator 4.0: Human Cyber-Physical Systems & Adaptive Automation Towards Human-Automation Symbiosis Work Systems’, in *Advances in Production Management Systems. Initiatives for a Sustainable World*, vol. 488, I. Nääs, O. Vendrametto, J. Mendes Reis, R. F. Gonçalves, M. T. Silva, G. Von Cieminski, and D. Kiritsis, Eds., in IFIP Advances in Information and Communication Technology, vol. 488. , Cham: Springer International Publishing, 2016, pp. 677–686. doi: 10.1007/978-3-319-51133-7_80.
[8] A. Bhatia, ‘The Role of Cutting-Edge Technologies in Revolutionary Industry 5.0’, *Artif. Intell. Commun. Tech. Ind. 50*, p. 128, 2024.
[9] D. Romero and J. Stahre, ‘Towards The Resilient Operator 5.0: The Future of Work in Smart Resilient Manufacturing Systems’, *Procedia CIRP*, vol. 104, pp. 1089–1094, 2021, doi: 10.1016/j.procir.2021.11.183.
[10] J. D. A. Dornelles, N. F. Ayala, and A. G. Frank, ‘Smart Working in Industry 4.0: How digital technologies enhance manufacturing workers’ activities’, *Comput. Ind. Eng.*, vol. 163, p. 107804, Jan. 2022, doi: 10.1016/j.cie.2021.107804.
[11] ‘Recommended Practices for Safety and Health Programs’, Occupational Health and Safety Administration. Accessed: Feb. 25, 2026. [Online]. Available: https://www.osha.gov/safety-management/hazard-identification#ai1
[12] ‘OSHwiki Topics - themes’, European Occupational Health and Safety Administration. Accessed: Feb. 25, 2026. [Online]. Available: https://osha.europa.eu/en/tools-and-resources/oshwiki
[13] T. Cox and A. Griffiths, ‘The nature and measurement of work-related stress: theory and practice’, in *Evaluation of Human Work*, 3rd Edition., Abingdon, UK: Routledge, 2005.
[14] D. Scheer *et al.*, ‘The Distinction Between Risk and Hazard: Understanding and Use in Stakeholder Communication’, *Risk Anal.*, vol. 34, no. 7, pp. 1270–1285, Jul. 2014, doi: 10.1111/risa.12169.
[15] European Agency for Safety and Health at Work., *Third European survey of enterprises on new and emerging risks (ESENER 2019): how European workplaces manage safety and health : overview report.* LU: Publications Office, 2022. Accessed: Aug. 09, 2024. [Online]. Available: https://data.europa.eu/doi/10.2802/881291
[16] European Foundation for the Improvement of Living and Working Conditions., *6th European working conditions survey: 2017 update.* LU: Publications Office, 2017. Accessed: Oct. 01, 2024. [Online]. Available: https://data.europa.eu/doi/10.2806/422172
[17] R. Govaerts *et al.*, ‘Prevalence and incidence of work-related musculoskeletal disorders in secondary industries of 21st century Europe: a systematic review and meta-analysis’, *BMC Musculoskelet. Disord.*, vol. 22, no. 1, p. 751, Dec. 2021, doi: 10.1186/s12891-021-04615-9.
[18] C. M. Lind, F. Abtahi, and M. Forsman, ‘Wearable Motion Capture Devices for the Prevention of Work-Related Musculoskeletal Disorders in Ergonomics—An Overview of Current Applications, Challenges, and Future Opportunities’, *Sensors*, vol. 23, no. 9, p. 4259, Apr. 2023, doi: 10.3390/s23094259.
[19] V. Putz-Anderson, *Cumulative Trauma Disorders*, 1st ed. CRC Press, 1988. doi: 10.1201/9781315140704.

[20] S. Kumar, ‘Theories of musculoskeletal injury causation’, *Ergonomics*, vol. 44, no. 1, pp. 17–47, Jan. 2001, doi: 10.1080/00140130120716.
[21] S. Gallagher, M. C. Schall, R. F. Sesek, and R. Huangfu, ‘An Upper Extremity Risk Assessment Tool Based on Material Fatigue Failure Theory: The Distal Upper Extremity Tool (DUET)’, *Hum. Factors J. Hum. Factors Ergon. Soc.*, vol. 60, no. 8, pp. 1146–1162, Dec. 2018, doi: 10.1177/0018720818789319.
[22] R. G. Radwin, W. S. Marras, and S. A. Lavender, ‘Biomechanical aspects of work-related musculoskeletal disorders’, *Theor. Issues Ergon. Sci.*, vol. 2, no. 2, pp. 153–217, Jan. 2001, doi: 10.1080/14639220110102044.
[23] J. Santos, J. S. Baptista, P. R. R. Monteiro, A. S. Miguel, R. Santos, and M. A. P. Vaz, ‘The influence of task design on upper limb muscles fatigue during low-load repetitive work: A systematic review’, *Int. J. Ind. Ergon.*, vol. 52, pp. 78–91, Mar. 2016, doi: 10.1016/j.ergon.2015.09.010.
[24] W. A. Latko, T. J. Armstrong, A. Franzblau, S. S. Ulin, R. A. Werner, and J. W. Albers, ‘Cross-sectional study of the relationship between repetitive work and the prevalence of upper limb musculoskeletal disorders’, *Am. J. Ind. Med.*, vol. 36, no. 2, pp. 248–259, Aug. 1999, doi: 10.1002/(SICI)1097-0274(199908)36:2<248::AID-AJIM4>3.0.CO;2-Q.
[25] B. A. Silverstein, L. J. Fine, and T. J. Armstrong, ‘Occupational factors and carpal tunnel syndrome’, *Am. J. Ind. Med.*, vol. 11, no. 3, pp. 343–358, Jan. 1987, doi: 10.1002/ajim.4700110310.
[26] M. D. Looze, T. Bosch, and J. V. Dieën, ‘Manifestations of shoulder fatigue in prolonged activities involving low-force contractions’, *Ergonomics*, vol. 52, no. 4, pp. 428–437, Apr. 2009, doi: 10.1080/00140130802707709.
[27] L. M. Rose, W. P. Neumann, G. M. Hägg, and G. Kenttä, ‘Fatigue and recovery during and after static loading’, *Ergonomics*, vol. 57, no. 11, pp. 1696–1710, Nov. 2014, doi: 10.1080/00140139.2014.952347.
[28] B. Visser and J. H. Van Dieën, ‘Pathophysiology of upper extremity muscle disorders’, *J. Electromyogr. Kinesiol.*, vol. 16, no. 1, pp. 1–16, Feb. 2006, doi: 10.1016/j.jelekin.2005.06.005.
[29] W. M. Keyserling, M. Brouwer, and B. A. Silverstein, ‘A checklist for evaluating ergonomic risk factors resulting from awkward postures of the legs, trunk and neck’, *Int. J. Ind. Ergon.*, vol. 9, no. 4, pp. 283–301, Jun. 1992, doi: 10.1016/0169-8141(92)90062-5.
[30] J. Ding, A. S. Wexler, and S. A. Binder-Macleod, ‘A predictive model of fatigue in human skeletal muscles’, *J. Appl. Physiol.*, vol. 89, no. 4, pp. 1322–1332, Oct. 2000, doi: 10.1152/jappl.2000.89.4.1322.
[31] M. A. Nussbaum, L. L. Clark, M. A. Lanza, and K. M. Rice, ‘Fatigue and Endurance Limits During Intermittent Overhead Work’, *AIHAJ - Am. Ind. Hyg. Assoc.*, vol. 62, no. 4, pp. 446–456, Jul. 2001, doi: 10.1080/15298660108984646.
[32] K. V. Lomond and J. N. Côté, ‘Shoulder functional assessments in persons with chronic neck/shoulder pain and healthy subjects: Reliability and effects of movement repetition’, *Work*, vol. 38, no. 2, pp. 169–180, 2011, doi: 10.3233/WOR-2011-1119.
[33] European Parliament and Council, ‘Consolidated text: Council Directive of 29 May 1990 on the minimum health and safety requirements for the manual handling of loads where there is a risk particularly of back injury to workers (fourth individual Directive within the meaning of Article 16 (1) of Directive 89/391/EEC) (90/269/EEC)’, 90/269/EEC, Jul. 2019. Accessed: Aug. 13, 2024. [Online]. Available: http://data.europa.eu/eli/dir/1990/269/2019-07-26
[34] European Parliament and Council, ‘Consolidated text: Council Directive of 29 May 1990 on the minimum safety and health requirements for work with display screen equipment (fifth individual Directive within the meaning of Article 16 (1) of Directive 89/391/EEC) (90/270/EEC)’, 90/270/EEC, Jul. 2019. Accessed: Aug. 13, 2024. [Online]. Available: http://data.europa.eu/eli/dir/1990/269/2019-07-26
[35] B. R. Da Costa and E. R. Vieira, ‘Risk factors for work-related musculoskeletal disorders: a systematic review of recent longitudinal studies’, *Am. J. Ind. Med.*, vol. 53, no. 3, pp. 285–323, Mar. 2010, doi: 10.1002/ajim.20750.
[36] ‘Upper limb disorders’, HSE UK. Accessed: Aug. 13, 2024. [Online]. Available: https://www.hse.gov.uk/msd/uld/index.htm
[37] J. D. Hincapié-Ramos, X. Guo, P. Moghadasian, and P. Irani, ‘Consumed endurance: a metric to quantify arm fatigue of mid-air interactions’, in *Proceedings of the SIGCHI Conference on Human Factors in Computing Systems*, in CHI ’14. New York, NY, USA: Association for Computing Machinery, Apr. 2014, pp. 1063–1072. doi: 10.1145/2556288.2557130.
[38] S. N. Singh, K. R. Rajesh, and S. Sunil, ‘Ergonomics control – Assembly station’, *Mater. Today Proc.*, vol. 54, pp. 513–518, 2022, doi: 10.1016/j.matpr.2021.11.505.

[39] S. Safiri *et al.*, 'Prevalence, deaths, and disability-adjusted life years due to musculoskeletal disorders for 195 countries and territories 1990–2017', *Arthritis Rheumatol.*, vol. 73, no. 4, pp. 702–714, 2021.
[40] J. O. Crawford *et al.*, 'Musculoskeletal health in the workplace', *Best Pract. Res. Clin. Rheumatol.*, vol. 34, no. 5, p. 101558, Oct. 2020, doi: 10.1016/j.berh.2020.101558.
[41] L. Stirling, Y. Acosta-Sojo, and J. T. Dennerlein, 'Defining a systems framework for characterizing physical work demands with wearable sensors', *Ann. Work Expo. Health*, vol. 68, no. 5, pp. 443–465, Jun. 2024, doi: 10.1093/annweh/wxae024.
[42] S. L. James *et al.*, 'Global, regional, and national incidence, prevalence, and years lived with disability for 354 diseases and injuries for 195 countries and territories, 1990–2017: a systematic analysis for the Global Burden of Disease Study 2017', *The Lancet*, vol. 392, no. 10159, pp. 1789–1858, Nov. 2018, doi: 10.1016/S0140-6736(18)32279-7.
[43] A. Cieza, K. Causey, K. Kamenov, S. W. Hanson, S. Chatterji, and T. Vos, 'Global estimates of the need for rehabilitation based on the Global Burden of Disease study 2019: a systematic analysis for the Global Burden of Disease Study 2019', *The Lancet*, vol. 396, no. 10267, pp. 2006–2017, Dec. 2020, doi: 10.1016/S0140-6736(20)32340-0.
[44] S. Bevan, 'Economic impact of musculoskeletal disorders (MSDs) on work in Europe', *Best Pract. Res. Clin. Rheumatol.*, vol. 29, no. 3, pp. 356–373, Jun. 2015, doi: 10.1016/j.berh.2015.08.002.
[45] M. Yung, A. Kolus, R. Wells, and W. P. Neumann, 'Examining the fatigue-quality relationship in manufacturing', *Appl. Ergon.*, vol. 82, p. 102919, Jan. 2020, doi: 10.1016/j.apergo.2019.102919.
[46] A. Kolus, R. Wells, and P. Neumann, 'Production quality and human factors engineering: A systematic review and theoretical framework', *Appl. Ergon.*, vol. 73, pp. 55–89, Nov. 2018, doi: 10.1016/j.apergo.2018.05.010.
[47] A. Williamson, D. A. Lombardi, S. Folkard, J. Stutts, T. K. Courtney, and J. L. Connor, 'The link between fatigue and safety', *Accid. Anal. Prev.*, vol. 43, no. 2, pp. 498–515, Mar. 2011, doi: 10.1016/j.aap.2009.11.011.
[48] R. Nangoy, T. N. Mursitama, N. J. Setiadi, and Y. D. Pradipto, 'Creating sustainable performance in the fourth industrial revolution era: The effect of employee's work well-being on job performance', *Manag. Sci. Lett.*, pp. 1037–1042, 2020, doi: 10.5267/j.msl.2019.11.006.
[49] D. Battini, M. Faccio, A. Persona, and F. Sgarbossa, 'New methodological framework to improve productivity and ergonomics in assembly system design', *Int. J. Ind. Ergon.*, vol. 41, no. 1, pp. 30–42, Jan. 2011, doi: 10.1016/j.ergon.2010.12.001.
[50] J. A. Ricci, E. Chee, A. L. Lorandeau, and J. Berger, 'Fatigue in the US workforce: prevalence and implications for lost productive work time', *J. Occup. Environ. Med.*, vol. 49, no. 1, pp. 1–10, 2007.
[51] A. Setayesh, E. H. Grosse, C. H. Glock, and W. P. Neumann, 'Determining the source of human-system errors in manual order picking with respect to human factors', *Int. J. Prod. Res.*, vol. 60, no. 20, pp. 6350–6372, Oct. 2022, doi: 10.1080/00207543.2021.1991022.
[52] M. Yung, P. L. Bigelow, D. M. Hastings, and R. P. Wells, 'Detecting within-and between-day manifestations of neuromuscular fatigue at work: an exploratory study', *Ergonomics*, vol. 57, no. 10, pp. 1562–1573, 2014.
[53] L. G. Lulli *et al.*, 'Identifying psychosocial risks and protective measures for workers' mental wellbeing at the time of COVID-19: a narrative review', *Sustainability*, vol. 13, no. 24, p. 13869, 2021.
[54] C. M. Lind, J. A. Diaz-Olivares, K. Lindecrantz, and J. Eklund, 'A Wearable Sensor System for Physical Ergonomics Interventions Using Haptic Feedback', *Sensors*, vol. 20, no. 21, p. 6010, Oct. 2020, doi: 10.3390/s20216010.
[55] S. E. Mathiassen, 'Diversity and variation in biomechanical exposure: What is it, and why would we like to know?', *Appl. Ergon.*, vol. 37, no. 4, pp. 419–427, Jul. 2006, doi: 10.1016/j.apergo.2006.04.006.
[56] W. P. Neumann, S. Kihlberg, P. Medbo, S. E. Mathiassen, and J. Winkel, 'A case study evaluating the ergonomic and productivity impacts of partial automation strategies in the electronics industry', *Int. J. Prod. Res.*, vol. 40, no. 16, pp. 4059–4075, 2002.
[57] 'Smart glasses for multifacEted visual loss mitigation and chronic disEase prevention indicator for healthier, saFer, and more productive workplAce foR ageing population', UNIVERSIDAD DE SEVILLA, Spain, May 2022. Accessed: Apr. 09, 2025. [Online]. Available: https://cordis.europa.eu/project/id/826429
[58] 'FlExible assembLy manufacturIng with human-robot Collaboration and digital twin modEls', EREVNITIKO PANEPISTIMIAKO INSTITOUTO SYSTIMATON EPIKOINONION KAI

YPOLOGISTON, Greece, Grant agreement ID: 101017151, Dec. 2024. Accessed: Apr. 09, 2025. [Online]. Available: https://cordis.europa.eu/project/id/101017151
[59] 'Smart environments for person-centered sustainable work and well-being', IDRYMA TECHNOLOGIAS KAI EREVNAS, Greece, Grant agreement ID: 826506, Jun. 2022. Accessed: Apr. 09, 2025. [Online]. Available: https://cordis.europa.eu/project/id/826506
[60] 'Smart Working environments for all Ages', Fundacion Instituto Technologico de Castilla y Leon, Spain, Grant agreement ID: 826232, Jul. 2022. Accessed: May 09, 2025. [Online]. Available: https://cordis.europa.eu/project/id/826232
[61] 'Personalised Body Sensor Networks with Built-In Intelligence for Real-Time Risk Assessment and Coaching of Ageing workers, in all types of working and living environments', Deutsches Forschungszentrum für Künstliche Intelligenz GmbH, Germany, Grant agreement ID: 826304, Mar. 2022. Accessed: Apr. 09, 2025. [Online]. Available: https://cordis.europa.eu/project/id/826304
[62] 'Smart, Personalized and Adaptive ICT Solutions for Active, Healthy and Productive Ageing with enhanced Workability', Ethniko Kentro Erevnas kai Technologikis Anaptyxis, Greece, Grant agreement ID: 826299, Jun. 2022. Accessed: May 09, 2025. [Online]. Available: https://cordis.europa.eu/project/id/826299/reporting
[63] L. McAtamney and N. Corlett, 'Rapid upper limb assessment (RULA)', in *Handbook of human factors and ergonomics methods*, CRC Press, 2004, pp. 86–96.
[64] L. McAtamney and S. Hignett, 'Rapid entire body assessment', in *Handbook of human factors and ergonomics methods*, CRC Press, 2004, pp. 97–108.
[65] T. R. Waters, V. Putz-Anderson, A. Garg, and L. J. Fine, 'Revised NIOSH equation for the design and evaluation of manual lifting tasks', *Ergonomics*, vol. 36, no. 7, pp. 749–776, 1993.
[66] American Conference of Governmental Industrial Hygienists :: ACGIH, *2017 TLVs and BEIs: Based on the documentation of the threshold limit values for chemical substances and physical agents & biological exposure indices*. Cincinnati, OH: ACGIH, 2017.
[67] L. Ma, W. Zhang, B. Hu, D. Chablat, F. Bennis, and F. Guillaume, 'Determination of subject-specific muscle fatigue rates under static fatiguing operations', *Ergonomics*, vol. 56, no. 12, pp. 1889–1900, Dec. 2013, doi: 10.1080/00140139.2013.851283.
[68] A. Villanueva, S. Jang, W. Stuerzlinger, S. Ambike, and K. Ramani, 'Advanced modeling method for quantifying cumulative subjective fatigue in mid-air interaction', *Int. J. Hum.-Comput. Stud.*, vol. 169, p. 102931, Jan. 2023, doi: 10.1016/j.ijhcs.2022.102931.
[69] Y. Giat, J. Mizrahi, and M. Levy, 'A musculotendon model of the fatigue profiles of paralyzed quadriceps muscle under FES', *IEEE Trans. Biomed. Eng.*, vol. 40, no. 7, pp. 664–674, Jul. 1993, doi: 10.1109/10.237696.
[70] K. El Ahrache, D. Imbeau, and B. Farbos, 'Percentile values for determining maximum endurance times for static muscular work', *Int. J. Ind. Ergon.*, vol. 36, no. 2, pp. 99–108, Feb. 2006, doi: 10.1016/j.ergon.2005.08.003.
[71] L. A. Frey Law and K. G. Avin, 'Endurance time is joint-specific: A modelling and meta-analysis investigation', *Ergonomics*, vol. 53, no. 1, pp. 109–129, Jan. 2010, doi: 10.1080/00140130903389068.
[72] G. Borg, *Borg's perceived exertion and pain scales.* Champaign, IL, US: Human Kinetics, 1998, pp. viii, 104.
[73] S. Hart, 'Development of NASA-TLX (Task Load Index): Results of empirical and theoretical research', *Hum. Ment. Workload.*, 1988.
[74] T. Åkerstedt and M. Gillberg, 'Subjective and objective sleepiness in the active individual', *Int. J. Neurosci.*, vol. 52, no. 1–2, pp. 29–37, 1990.
[75] S. Lim and C. D'Souza, 'A narrative review on contemporary and emerging uses of inertial sensing in occupational ergonomics', *Int. J. Ind. Ergon.*, vol. 76, p. 102937, Mar. 2020, doi: 10.1016/j.ergon.2020.102937.
[76] V. C. H. Chan, G. B. Ross, A. L. Clouthier, S. L. Fischer, and R. B. Graham, 'The role of machine learning in the primary prevention of work-related musculoskeletal disorders: A scoping review', *Appl. Ergon.*, vol. 98, p. 103574, Jan. 2022, doi: 10.1016/j.apergo.2021.103574.
[77] S. Hajifar, H. Sun, F. M. Megahed, L. A. Jones-Farmer, E. Rashedi, and L. A. Cavuoto, 'A forecasting framework for predicting perceived fatigue: Using time series methods to forecast ratings of perceived exertion with features from wearable sensors', *Appl. Ergon.*, vol. 90, p. 103262, Jan. 2021, doi: 10.1016/j.apergo.2020.103262.
[78] R. Zorzenon, F. L. Lizarelli, and D. B. A. De A. Moura, 'What is the potential impact of industry 4.0 on health and safety at work?', *Saf. Sci.*, vol. 153, p. 105802, Sep. 2022, doi: 10.1016/j.ssci.2022.105802.

[79] S. Lee, L. Liu, R. Radwin, and J. Li, ‘Machine Learning in Manufacturing Ergonomics: Recent Advances, Challenges, and Opportunities’, *IEEE Robot. Autom. Lett.*, vol. 6, no. 3, pp. 5745–5752, Jul. 2021, doi: 10.1109/LRA.2021.3084881.
[80] D. Battini, N. Berti, S. Finco, M. Guidolin, M. Reggiani, and L. Tagliapietra, ‘WEM-Platform: A real-time platform for full-body ergonomic assessment and feedback in manufacturing and logistics systems’, *Comput. Ind. Eng.*, vol. 164, p. 107881, Feb. 2022, doi: 10.1016/j.cie.2021.107881.
[81] E. Valero, A. Sivanathan, F. Bosché, and M. Abdel-Wahab, ‘Musculoskeletal disorders in construction: A review and a novel system for activity tracking with body area network’, *Appl. Ergon.*, vol. 54, pp. 120–130, May 2016, doi: 10.1016/j.apergo.2015.11.020.
[82] X. Zhang, M. C. Schall, H. Chen, S. Gallagher, G. A. Davis, and R. Sesek, ‘Manufacturing worker perceptions of using wearable inertial sensors for multiple work shifts’, *Appl. Ergon.*, vol. 98, p. 103579, Jan. 2022, doi: 10.1016/j.apergo.2021.103579.
[83] M. Moshawrab, M. Adda, A. Bouzouane, H. Ibrahim, and A. Raad, ‘Smart Wearables for the Detection of Occupational Physical Fatigue: A Literature Review’, *Sensors*, vol. 22, no. 19, p. 7472, Oct. 2022, doi: 10.3390/s22197472.
[84] I. C. Obasi and C. Benson, ‘The Impact of Digitalization and Information and Communication Technology on the Nature and Organization of Work and the Emerging Challenges for Occupational Safety and Health’, *Int. J. Environ. Res. Public. Health*, vol. 22, no. 3, p. 362, Feb. 2025, doi: 10.3390/ijerph22030362.
[85] M. S. Lodovici, E. Ferrari, E. Paladino, F. Pesce, P. Frecassetti, and E. Aram, ‘The impact of teleworking and digital work on workers and society’, *Study Requested EMPL Comm.*, 2021.
[86] N. R. A. Martins, S. Annaheim, C. M. Spengler, and R. M. Rossi, ‘Fatigue Monitoring Through Wearables: A State-of-the-Art Review’, *Front. Physiol.*, vol. 12, p. 790292, Dec. 2021, doi: 10.3389/fphys.2021.790292.
[87] R. Patial, H. Gusain, B. P. Yadav, and N. Siddiqui, ‘A review of ergonomic risk assessment techniques employed in construction industry’, *Adv. Constr. Saf. Proc. HSFEA 2020*, pp. 117–131, 2022.
[88] Y. Li *et al.*, ‘Revisiting Consumed Endurance: A NICE Way to Quantify Shoulder Fatigue in Virtual Reality’, in *29th ACM Symposium on Virtual Reality Software and Technology*, Christchurch New Zealand: ACM, Oct. 2023, pp. 1–10. doi: 10.1145/3611659.3615702.
[89] ‘Kinetic Technologies’. Accessed: Aug. 14, 2024. [Online]. Available: https://kineticcomp.com/
[90] ‘StrongArm Technologies’. Accessed: Aug. 14, 2024. [Online]. Available: https://www.strongarmtech.com/
[91] ‘Honeywell’. Accessed: Aug. 14, 2024. [Online]. Available: https://www.honeywell.com/us/en/industries/products
[92] ‘Movella Xsens’. Accessed: Aug. 14, 2024. [Online]. Available: https://www.movella.com/products/xsens
[93] N. Vignais, M. Miezal, G. Bleser, K. Mura, D. Gorecky, and F. Marin, ‘Innovative system for real-time ergonomic feedback in industrial manufacturing’, *Appl. Ergon.*, vol. 44, no. 4, pp. 566–574, Jul. 2013, doi: 10.1016/j.apergo.2012.11.008.
[94] L. Peppoloni, A. Filippeschi, E. Ruffaldi, and C. A. Avizzano, ‘A novel wearable system for the online assessment of risk for biomechanical load in repetitive efforts’, *Int. J. Ind. Ergon.*, vol. 52, pp. 1–11, Mar. 2016, doi: 10.1016/j.ergon.2015.07.002.
[95] S. Arroyave-Tobón and G. Osorio-Gómez, ‘Ergonomic analysis in conceptual design stage using a gesture-based modelling tool’, *Int. J. Interact. Des. Manuf. IJIDeM*, vol. 11, no. 3, pp. 481–488, Aug. 2017, doi: 10.1007/s12008-015-0289-9.
[96] M. Mengoni, S. Ceccacci, A. Generosi, and A. Leopardi, ‘Spatial Augmented Reality: an application for human work in smart manufacturing environment’, *Procedia Manuf.*, vol. 17, pp. 476–483, 2018, doi: 10.1016/j.promfg.2018.10.072.
[97] C. Lins, S. J. Fudickar, A. Gerka, and A. Hein, ‘A Wearable Vibrotactile Interface for Unfavorable Posture Awareness Warning.’, presented at the ICT4AWE, 2018, pp. 178–183.
[98] W. Kim, M. Lorenzini, K. Kapicioglu, and A. Ajoudani, ‘ErgoTac: A Tactile Feedback Interface for Improving Human Ergonomics in Workplaces’, *IEEE Robot. Autom. Lett.*, vol. 3, no. 4, pp. 4179–4186, Oct. 2018, doi: 10.1109/lra.2018.2864356.
[99] Y. Yu, H. Li, X. Yang, L. Kong, X. Luo, and A. Y. L. Wong, ‘An automatic and non-invasive physical fatigue assessment method for construction workers’, *Autom. Constr.*, vol. 103, pp. 1–12, 2019, doi: 10.1016/j.autcon.2019.02.020.

[100] V. M. Manghisi, A. E. Uva, M. Fiorentino, M. Gattullo, A. Boccaccio, and A. Evangelista, ‘Automatic Ergonomic Postural Risk Monitoring on the Factory Shopfloor – The Ergosentinel Tool’, *Procedia Manuf.*, vol. 42, pp. 97–103, 2020, doi: 10.1016/j.promfg.2020.02.091.
[101] S. M. Cerqueira, A. F. D. Silva, and C. P. Santos, ‘Smart Vest for Real-Time Postural Biofeedback and Ergonomic Risk Assessment’, *IEEE Access*, vol. 8, pp. 107583–107592, 2020, doi: 10.1109/access.2020.3000673.
[102] P. Giannini, G. Bassani, C. A. Avizzano, and A. Filippeschi, ‘Wearable Sensor Network for Biomechanical Overload Assessment in Manual Material Handling’, *Sensors*, vol. 20, no. 14, p. 3877, Jul. 2020, doi: 10.3390/s20143877.
[103] M. Trkov, D. T. Stevenson, and A. S. Merryweather, ‘Classifying hazardous movements and loads during manual materials handling using accelerometers and instrumented insoles’, *Appl. Ergon.*, vol. 101, p. 103693, May 2022, doi: 10.1016/j.apergo.2022.103693.
[104] C. M. Lind *et al.*, ‘Effectiveness and usability of real-time vibrotactile feedback training to reduce postural exposure in real manual sorting work’, *Ergonomics*, vol. 66, no. 2, pp. 198–216, Feb. 2023, doi: 10.1080/00140139.2022.2069869.
[105] T. J. Balkin, W. J. Horrey, R. C. Graeber, C. A. Czeisler, and D. F. Dinges, ‘The challenges and opportunities of technological approaches to fatigue management’, *Accid. Anal. Prev.*, vol. 43, no. 2, pp. 565–572, Mar. 2011, doi: 10.1016/j.aap.2009.12.006.
[106] P. O’Sullivan, ‘SWIFTIES (Subject and Wearables data for Investigation of Fatiguing Tasks In Extension/flexion of Shoulder/elbow)’. Zenodo, Sep. 17, 2024. doi: 10.5281/zenodo.15172815.
[107] P. O’Sullivan and M. Menolotto, ‘PID4TC (Pressure Insoles Data for Task Classification)’. Zenodo, Mar. 21, 2023. doi: 10.5281/ZENODO.7755802.
[108] T. Xia and L. A. Frey Law, ‘A theoretical approach for modeling peripheral muscle fatigue and recovery’, *J. Biomech.*, vol. 41, no. 14, pp. 3046–3052, Oct. 2008, doi: 10.1016/j.jbiomech.2008.07.013.
[109] D. Dawson, Y. Ian Noy, M. Härmä, T. Åkerstedt, and G. Belenky, ‘Modelling fatigue and the use of fatigue models in work settings’, *Accid. Anal. Prev.*, vol. 43, no. 2, pp. 549–564, Mar. 2011, doi: 10.1016/j.aap.2009.12.030.
[110] H. Jebelli, J. Seo, S. Hwang, and S. Lee, ‘Physiology-based dynamic muscle fatigue model for upper limbs during construction tasks’, *Int. J. Ind. Ergon.*, vol. 78, p. 102984, Jul. 2020, doi: 10.1016/j.ergon.2020.102984.
[111] J. Wan, Z. Qin, P. Wang, Y. Sun, and X. Liu, ‘Muscle fatigue: general understanding and treatment’, *Exp. Mol. Med.*, vol. 49, no. 10, pp. e384–e384, Oct. 2017, doi: 10.1038/emm.2017.194.
[112] T. Chalder *et al.*, ‘Development of a fatigue scale’, *J. Psychosom. Res.*, vol. 37, no. 2, pp. 147–153, Feb. 1993, doi: 10.1016/0022-3999(93)90081-P.
[113] X. Hu and G. Lodewijks, ‘Detecting fatigue in car drivers and aircraft pilots by using non-invasive measures: The value of differentiation of sleepiness and mental fatigue’, *J. Safety Res.*, vol. 72, pp. 173–187, Feb. 2020, doi: 10.1016/j.jsr.2019.12.015.
[114] L. Zhang, M. M. Diraneyya, J. Ryu, C. T. Haas, and E. M. Abdel-Rahman, ‘Jerk as an indicator of physical exertion and fatigue’, *Autom. Constr.*, vol. 104, pp. 120–128, Aug. 2019, doi: 10.1016/j.autcon.2019.04.016.
[115] R. H. T. Edwards, ‘Human Muscle Function and Fatigue’, in *Novartis Foundation Symposia*, 1st ed., R. Porter and J. Whelan, Eds., Wiley, 1981, pp. 1–18. doi: 10.1002/9780470715420.ch1.
[116] R. B. Layzer, ‘3 Muscle metabolism during fatigue and work’, *Baillières Clin. Endocrinol. Metab.*, vol. 4, no. 3, pp. 441–459, Sep. 1990, doi: 10.1016/S0950-351X(05)80064-3.
[117] S. P. Cairns, ‘Lactic acid and exercise performance: culprit or friend?’, *Sports Med.*, vol. 36, pp. 279–291, 2006.
[118] S. K. Hunter, ‘The relevance of sex differences in performance fatigability’, *Med. Sci. Sports Exerc.*, vol. 48, no. 11, p. 2247, 2016.
[119] L. Ma, W. Zhang, S. Wu, and Z. Zhang, ‘A new simple local muscle recovery model and its theoretical and experimental validation’, *Int. J. Occup. Saf. Ergon.*, vol. 21, no. 1, pp. 86–93, Jan. 2015, doi: 10.1080/10803548.2015.1017961.
[120] M. Cifrek, V. Medved, S. Tonković, and S. Ostojić, ‘Surface EMG based muscle fatigue evaluation in biomechanics’, *Clin. Biomech.*, vol. 24, no. 4, pp. 327–340, May 2009, doi: 10.1016/j.clinbiomech.2009.01.010.
[121] P. W. Humphreys and A. R. Lind, ‘The blood flow through active and inactive muscles of the forearm during sustained hand-grip contractions’, *J. Physiol.*, vol. 166, no. 1, pp. 120–135, Apr. 1963, doi: 10.1113/jphysiol.1963.sp007094.

[122] M. Van Veldhoven and S. Broersen, ‘Measurement quality and validity of the “need for recovery scale”’, *Occup. Environ. Med.*, vol. 60, no. suppl 1, pp. i3–i9, Jun. 2003, doi: 10.1136/oem.60.suppl_1.i3.

[123] W. Rohmert, ‘Ermittlung von Erholungspausen für statische Arbeit des Menschen’, *Int. Z. Für Angew. Physiol. Einschließlich Arbeitsphysiologie*, vol. 18, pp. 123–164, 1960.

[124] L. Ma, D. Chablat, F. Bennis, and W. Zhang, ‘A new simple dynamic muscle fatigue model and its validation’, *Int. J. Ind. Ergon.*, vol. 39, no. 1, pp. 211–220, Jan. 2009, doi: 10.1016/j.ergon.2008.04.004.

[125] J. Z. Liu, R. W. Brown, and G. H. Yue, ‘A Dynamical Model of Muscle Activation, Fatigue, and Recovery’, *Biophys. J.*, vol. 82, no. 5, Art. no. 5, May 2002, doi: 10.1016/S0006-3495(02)75580-X.

[126] M. Rosselli *et al.*, ‘Workers Fatigue Monitoring for Well-being Improvement in Manufacturing’, presented at the 18th IFAC Symposium on Information Control Problems in Manufacturing, Elsevier, 2024.

[127] S. Otálora, M. E. V. Segatto, M. E. Monteiro, M. Múnera, C. A. R. Díaz, and C. A. Cifuentes, ‘Data-Driven Approach for Upper Limb Fatigue Estimation Based on Wearable Sensors’, *Sensors*, vol. 23, no. 22, p. 9291, Nov. 2023, doi: 10.3390/s23229291.

[128] W. Li, X. Hu, R. Gravina, and G. Fortino, ‘A Neuro-Fuzzy Fatigue-Tracking and Classification System for Wheelchair Users’, *IEEE Access*, vol. 5, pp. 19420–19431, 2017, doi: 10.1109/ACCESS.2017.2730920.

[129] S. Anwer *et al.*, ‘Identification and Classification of Physical Fatigue in Construction Workers Using Linear and Nonlinear Heart Rate Variability Measurements’, *J. Constr. Eng. Manag.*, vol. 149, no. 7, p. 04023057, Jul. 2023, doi: 10.1061/JCEMD4.COENG-13100.

[130] M. J. Pinto-Bernal, C. A. Cifuentes, O. Perdomo, M. Rincón-Roncancio, and M. Múnera, ‘A Data-Driven Approach to Physical Fatigue Management Using Wearable Sensors to Classify Four Diagnostic Fatigue States’, *Sensors*, vol. 21, no. 19, p. 6401, Sep. 2021, doi: 10.3390/s21196401.

[131] C. Albarrán Morillo, M. Demichela, D. Jawla, and J. Kelleher, ‘Wearable Technology and Machine Learning for Assessing Physical Fatigue in Industry 4.0’, presented at the 15th International Conference on Applied Human Factors and Ergonomics (AHFE 2024), 2024. doi: 10.54941/ahfe1005052.

[132] ‘3D Static Strength Prediction Programme’. Accessed: Oct. 01, 2024. [Online]. Available: https://c4e.engin.umich.edu/tools-services/3dsspp-software/

[133] S. L. Delp *et al.*, ‘OpenSim: Open-Source Software to Create and Analyze Dynamic Simulations of Movement’, *IEEE Trans. Biomed. Eng.*, vol. 54, no. 11, pp. 1940–1950, Nov. 2007, doi: 10.1109/TBME.2007.901024.

[134] ‘AnyBody Modelling System’. Accessed: Oct. 01, 2024. [Online]. Available: https://www.anybodytech.com/software/anybodymodelingsystem/

[135] G. C. David, ‘Ergonomic methods for assessing exposure to risk factors for work-related musculoskeletal disorders’, *Occup. Med.*, vol. 55, no. 3, pp. 190–199, May 2005, doi: 10.1093/occmed/kqi082.

[136] D. Battini, A. Persona, and F. Sgarbossa, ‘Innovative real-time system to integrate ergonomic evaluations into warehouse design and management’, *Comput. Ind. Eng.*, vol. 77, pp. 1–10, Nov. 2014, doi: 10.1016/j.cie.2014.08.018.

[137] E. Stefana, F. Marciano, D. Rossi, P. Cocca, and G. Tomasoni, ‘Wearable Devices for Ergonomics: A Systematic Literature Review’, *Sensors*, vol. 21, no. 3, p. 777, Jan. 2021, doi: 10.3390/s21030777.

[138] A. Ranavolo, F. Draicchio, T. Varrecchia, A. Silvetti, and S. Iavicoli, ‘Wearable Monitoring Devices for Biomechanical Risk Assessment at Work: Current Status and Future Challenges—A Systematic Review’, *Int. J. Environ. Res. Public. Health*, vol. 15, p. 2001, Sep. 2018, doi: 10.3390/ijerph15092001.

[139] B. D. Lowe, P. G. Dempsey, and E. M. Jones, ‘Ergonomics assessment methods used by ergonomics professionals’, *Appl. Ergon.*, vol. 81, p. 102882, Nov. 2019, doi: 10.1016/j.apergo.2019.102882.

[140] J. Winkel and S. E. Mathiassen, ‘Assessment of physical work load in epidemiologic studies: concepts, issues and operational considerations’, *Ergonomics*, vol. 37, no. 6, pp. 979–988, Jun. 1994, doi: 10.1080/00140139408963711.

[141] A. Burdorf and A. Van Der Beek, ‘Exposure assessment strategies for work-related risk factors for musculoskeletal disorders’, *Scand. J. Work. Environ. Health*, pp. 25–30, 1999.

[142] K. Sadeghniiat-Haghighi and Z. Yazdi, ‘Fatigue management in the workplace’, *Ind. Psychiatry J.*, vol. 24, no. 1, pp. 12–17, 2015.

[143] S. C. Segerstrom and L. S. Nes, ‘Heart Rate Variability Reflects Self-Regulatory Strength, Effort, and Fatigue’, *Psychol. Sci.*, vol. 18, no. 3, pp. 275–281, Mar. 2007, doi: 10.1111/j.1467-9280.2007.01888.x.
[144] ‘Siemens Jack’. Accessed: Oct. 02, 2024. [Online]. Available: https://pmcorp.com/simulation/jack/
[145] ‘Biomechanics of Bodies’. Accessed: Oct. 02, 2024. [Online]. Available: https://www.bob-biomechanics.com/
[146] ‘RAMSIS’. Accessed: Oct. 02, 2024. [Online]. Available: https://www.human-solutions.com/en/products/ramsis-general/index.html
[147] A. Tahir, S. Bai, and M. Shen, ‘A Wearable Multi-Modal Digital Upper Limb Assessment System for Automatic Musculoskeletal Risk Evaluation’, *Sensors*, vol. 23, no. 10, p. 4863, May 2023, doi: 10.3390/s23104863.
[148] I. Sabino *et al.*, ‘Application of wearable technology for the ergonomic risk assessment of healthcare professionals: A systematic literature review’, *Int. J. Ind. Ergon.*, vol. 100, p. 103570, Mar. 2024, doi: 10.1016/j.ergon.2024.103570.
[149] L. Peternel, N. Tsagarakis, D. Caldwell, and A. Ajoudani, ‘Robot adaptation to human physical fatigue in human–robot co-manipulation’, *Auton. Robots*, vol. 42, no. 5, pp. 1011–1021, Jun. 2018, doi: 10.1007/s10514-017-9678-1.
[150] Y. You, B. Cai, D. T. Pham, Y. Liu, and Z. Ji, ‘A human digital twin approach for fatigue-aware task planning in human-robot collaborative assembly’, *Comput. Ind. Eng.*, vol. 200, p. 110774, Feb. 2025, doi: 10.1016/j.cie.2024.110774.
[151] P. G. Dempsey, R. W. McGorry, and W. S. Maynard, ‘A survey of tools and methods used by certified professional ergonomists’, *Appl. Ergon.*, vol. 36, no. 4, pp. 489–503, 2005.
[152] M. C. Schall, R. F. Sesek, and L. A. Cavuoto, ‘Barriers to the Adoption of Wearable Sensors in the Workplace: A Survey of Occupational Safety and Health Professionals’, *Hum. Factors J. Hum. Factors Ergon. Soc.*, vol. 60, no. 3, pp. 351–362, May 2018, doi: 10.1177/0018720817753907.
[153] M. Menolotto, D.-S. Komaris, S. Tedesco, B. O’Flynn, and M. Walsh, ‘Motion Capture Technology in Industrial Applications: A Systematic Review’, *Sensors*, vol. 20, no. 19, Art. no. 19, Jan. 2020, doi: 10.3390/s20195687.
[154] T. Jones and S. Kumar, ‘Comparison of Ergonomic Risk Assessment Output in Four Sawmill Jobs’, *Int. J. Occup. Saf. Ergon.*, vol. 16, no. 1, pp. 105–111, Jan. 2010, doi: 10.1080/10803548.2010.11076834.
[155] L. Zhang, Y. He, and H. Zhu, ‘Can Electromyography and Subjective Metrics Work Better Together? Exploring Dynamic Muscle Fatigue to Promote the Design of Health and Fitness Technology’, in *Design, User Experience, and Usability: Design for Emotion, Well-being and Health, Learning, and Culture*, vol. 13322, M. M. Soares, E. Rosenzweig, and A. Marcus, Eds., in Lecture Notes in Computer Science, vol. 13322. , Cham: Springer International Publishing, 2022, pp. 223–237. doi: 10.1007/978-3-031-05900-1_15.
[156] T. Öberg, L. SANDSJö, and R. Kadefors, ‘Subjective and objective evaluation of shoulder muscle fatigue’, *Ergonomics*, vol. 37, no. 8, pp. 1323–1333, Aug. 1994, doi: 10.1080/00140139408964911.
[157] N. A. Kamaruddin, P. I. Khalid, and A. Z. Shaameri, ‘The Use of Surface Electromyography in Muscle Fatigue Assessmentsâ€“A Review’, *J. Teknol.*, vol. 74, no. 6, 2015.
[158] M. González-Izal, A. Malanda, E. Gorostiaga, and M. Izquierdo, ‘Electromyographic models to assess muscle fatigue’, *J. Electromyogr. Kinesiol.*, vol. 22, no. 4, pp. 501–512, Aug. 2012, doi: 10.1016/j.jelekin.2012.02.019.
[159] N. Hegde, M. Bries, and E. Sazonov, ‘A Comparative Review of Footwear-Based Wearable Systems’, *Electronics*, vol. 5, no. 3, p. 48, Aug. 2016, doi: 10.3390/electronics5030048.
[160] H. Z. Tan, M. A. Srinivasan, B. Eberman, and B. Cheng, ‘Human factors for the design of force-reflecting haptic interfaces’, *Dyn. Syst. Control*, vol. 55, no. 1, pp. 353–359, 1994.
[161] D. B. Chaffin, G. B. Andersson, and B. J. Martin, *Occupational biomechanics*, 3rd Edition. John Wiley & Sons, 1999.
[162] S. E. Mathiassen and E. Åhsberg, ‘Prediction of shoulder flexion endurance from personal factors’, *Int. J. Ind. Ergon.*, vol. 24, no. 3, pp. 315–329, Jun. 1999, doi: 10.1016/S0169-8141(98)00039-0.
[163] D. B. Chaffin, ‘Ergonomics Guide for The Assessment of Human Static Strength’, *Am. Ind. Hyg. Assoc. J.*, vol. 36, no. 7, pp. 505–511, Jul. 1975, doi: 10.1080/0002889758507283.

[164] M. Amann, L. M. Romer, D. F. Pegelow, A. J. Jacques, C. J. Hess, and J. A. Dempsey, ‘Effects of arterial oxygen content on peripheral locomotor muscle fatigue’, *J. Appl. Physiol.*, vol. 101, no. 1, pp. 119–127, Jul. 2006, doi: 10.1152/japplphysiol.01596.2005.

[165] J. Fu, Q. Zhang, and L. Ma, ‘Novel approach to estimate endurance limits in intermittent tasks’, *Hum. Factors Ergon. Manuf. Serv. Ind.*, vol. 32, no. 4, pp. 321–334, Jul. 2022, doi: 10.1002/hfm.20945.

[166] J. M. Looft and L. A. Frey-Law, ‘Adapting a fatigue model for shoulder flexion fatigue: Enhancing recovery rate during intermittent rest intervals’, *J. Biomech.*, vol. 106, p. 109762, Jun. 2020, doi: 10.1016/j.jbiomech.2020.109762.

[167] M. W. Sonne, J. N. Hodder, R. Wells, and J. R. Potvin, ‘Force time-history affects fatigue accumulation during repetitive handgrip tasks’, *J. Electromyogr. Kinesiol.*, vol. 25, no. 1, pp. 130–135, Feb. 2015, doi: 10.1016/j.jelekin.2014.10.017.

[168] S. H. Snook and V. M. Ciriello, ‘The design of manual handling tasks: revised tables of maximum acceptable weights and forces’, *Ergonomics*, vol. 34, no. 9, pp. 1197–1213, Sep. 1991, doi: 10.1080/00140139108964855.

[169] T. J. Armstrong *et al.*, ‘Scientific basis of ISO standards on biomechanical risk factors’, *Scand. J. Work. Environ. Health*, vol. 44, no. 3, pp. 323–329, May 2018, doi: 10.5271/sjweh.3718.

[170] N. Fallentin, ‘Regulatory actions to prevent work-related musculoskeletal disorders—the use of research-based exposure limits’, *Scand. J. Work. Environ. Health*, vol. 29, no. 4, pp. 247–250, 2003.

[171] UK Health and Safety Executive, ‘Manual handling assessment charts (the MAC tool)’, HSE, 2019, p. 20. [Online]. Available: https://www.hse.gov.uk/pubns/indg383.pdf

[172] UK Health and Safety Executive, ‘Assessment of repetitive tasks of the upper limbs (the ART tool)’, HSE, 2010, p. 15. [Online]. Available: https://www.hse.gov.uk/pubns/indg438.pdf

[173] UK Health and Safety Executive, ‘Risk assessment of pushing and pulling (RAPP) tool’, HSE, 2016, p. 15. [Online]. Available: https://www.hse.gov.uk/pubns/indg478.pdf

[174] O. Karhu, P. Kansi, and I. Kuorinka, ‘Correcting working postures in industry: A practical method for analysis’, *Appl. Ergon.*, vol. 8, no. 4, pp. 199–201, 1977.

[175] E. Occhipinto and D. Colombini, ‘Proposta di un indice sintetico per la valutazione dell’esposizione a movimenti ripetitivi degli arti superiori (OCRA index) [Proposal of a concise index for the evaluation of the exposure to repetitive movements of the upper extremity (OCRA index)].’, *Med Lav*, vol. 87, no. 6, pp. 526–48, Dec. 1996.

[176] ‘Skelex’. Accessed: Aug. 14, 2024. [Online]. Available: https://www.skelex.com/

[177] ‘Levitate Technologies’. Accessed: Aug. 14, 2024. [Online]. Available: https://www.levitatetech.com/

[178] ‘SuitX by Ottobock’. Accessed: Aug. 14, 2024. [Online]. Available: https://www.suitx.com/en/home

[179] ‘Noonee’. Accessed: Aug. 14, 2024. [Online]. Available: https://www.noonee.com/

[180] ‘Ergodroid’, Google Play. Accessed: Apr. 30, 2025. [Online]. Available: https://play.google.com/store/apps/details?id=com.ergodroid.ergodroid&hl=en_IE

[181] ‘APECS’, Google Play. Accessed: Apr. 30, 2025. [Online]. Available: https://play.google.com/store/apps/details?id=corpusnovus.silverblood.apecs&hl=en_IE

[182] G. Li and P. Buckle, ‘A practical method for the assessment of work-related musculoskeletal risks-Quick Exposure Check (QEC)’, presented at the Proceedings of the human factors and ergonomics society annual meeting, SAGE Publications Sage CA: Los Angeles, CA, 1998, pp. 1351–1355.

[183] B. Buchholz, V. Paquet, L. Punnett, D. Lee, and S. Moir, ‘PATH: A work sampling-based approach to ergonomic job analysis for construction and other non-repetitive work’, *Appl. Ergon.*, vol. 27, no. 3, pp. 177–187, 1996.

[184] V. Patel, A. Chesmore, C. M. Legner, and S. Pandey, ‘Trends in Workplace Wearable Technologies and Connected-Worker Solutions for Next-Generation Occupational Safety, Health, and Productivity’, *Adv. Intell. Syst.*, vol. 4, no. 1, p. 2100099, Jan. 2022, doi: 10.1002/aisy.202100099.

[185] F. Sgarbossa, E. H. Grosse, W. P. Neumann, D. Battini, and C. H. Glock, ‘Human factors in production and logistics systems of the future’, *Annu. Rev. Control*, vol. 49, pp. 295–305, 2020, doi: 10.1016/j.arcontrol.2020.04.007.

[186] R. Bavaresco, H. Arruda, E. Rocha, J. Barbosa, and G.-P. Li, ‘Internet of Things and occupational well-being in industry 4.0: A systematic mapping study and taxonomy’, *Comput. Ind. Eng.*, vol. 161, p. 107670, Nov. 2021, doi: 10.1016/j.cie.2021.107670.

[187] Z. Sedighi Maman, Y.-J. Chen, A. Baghdadi, S. Lombardo, L. A. Cavuoto, and F. M. Megahed, 'A data analytic framework for physical fatigue management using wearable sensors', *Expert Syst. Appl.*, vol. 155, p. 113405, Oct. 2020, doi: 10.1016/j.eswa.2020.113405.

[188] A. Greco, M. Muoio, M. Lamberti, S. Gerbino, F. Caputo, and N. Miraglia, 'Integrated wearable devices for evaluating the biomechanical overload in manufacturing', in *2019 II Workshop on Metrology for Industry 4.0 and IoT (MetroInd4.0&IoT)*, Naples, Italy: IEEE, Jun. 2019, pp. 93–97. doi: 10.1109/METROI4.2019.8792868.

[189] G. Bernal, S. Colombo, M. Al Ai Baky, and F. Casalegno, 'Safety++: Designing IoT and Wearable Systems for Industrial Safety through a User Centered Design Approach', in *Proceedings of the 10th International Conference on PErvasive Technologies Related to Assistive Environments*, Island of Rhodes Greece: ACM, Jun. 2017, pp. 163–170. doi: 10.1145/3056540.3056557.

[190] L. Tamazirt, F. Alilat, and N. Agoulmine, 'NFC-based ubiquitous monitoring system for e-industry', in *2017 Third International Conference on Mobile and Secure Services (MobiSecServ)*, Miami Beach, FL, USA: IEEE, Feb. 2017, pp. 1–4. doi: 10.1109/MOBISECSERV.2017.7886568.

[191] R. K. Kodali, S. Yerroju, and B. Y. Krishna Yogi, 'IoT Based Wearable Device for Workers in Industrial Scenarios', in *TENCON 2018 - 2018 IEEE Region 10 Conference*, Jeju, Korea (South): IEEE, Oct. 2018, pp. 1893–1898. doi: 10.1109/TENCON.2018.8650187.

[192] B. Weber *et al.*, 'Assessing arm elevation at work with technical systems', 2018.

[193] S. M. Mirvakili and I. W. Hunter, 'Artificial muscles: Mechanisms, applications, and challenges', *Adv. Mater.*, vol. 30, no. 6, p. 1704407, 2018.

[194] M. A. A. Imran, F. Nasirzadeh, and C. Karmakar, 'Designing a practical fatigue detection system: A review on recent developments and challenges', *J. Safety Res.*, vol. 90, pp. 100–114, Sep. 2024, doi: 10.1016/j.jsr.2024.05.015.

[195] M. I. Adelino, H. R. Zadry, and L. Susanti, 'Contemporary Trends in Human Factors and Ergonomics Within Engineering Research', *J. Tek. Ind.*, vol. 26, no. 1, pp. 61–76, May 2024, doi: 10.9744/jti.26.1.61-76.

[196] S. Jang, W. Stuerzlinger, S. Ambike, and K. Ramani, 'Modeling Cumulative Arm Fatigue in Mid-Air Interaction based on Perceived Exertion and Kinetics of Arm Motion', in *Proceedings of the 2017 CHI Conference on Human Factors in Computing Systems*, Denver Colorado USA: ACM, May 2017, pp. 3328–3339. doi: 10.1145/3025453.3025523.

[197] M. A. García-Luna, D. Ruiz-Fernández, J. Tortosa-Martínez, C. Manchado, M. García-Jaén, and J. M. Cortell-Tormo, 'Transparency as a Means to Analyse the Impact of Inertial Sensors on Users during the Occupational Ergonomic Assessment: A Systematic Review', *Sensors*, vol. 24, no. 1, p. 298, Jan. 2024, doi: 10.3390/s24010298.

[198] V. Paquet, L. Punnett, S. Woskie, and B. Buchholz, 'Reliable exposure assessment strategies for physical ergonomics stressors in construction and other non-routinized work', *Ergonomics*, vol. 48, no. 9, pp. 1200–1219, Jul. 2005, doi: 10.1080/00140130500197302.

[199] K. El Ahrache and D. Imbeau, 'Comparison of rest allowance models for static muscular work', *Int. J. Ind. Ergon.*, vol. 39, no. 1, pp. 73–80, Jan. 2009, doi: 10.1016/j.ergon.2008.10.012.

[200] L. Vervier, P. Brauner, and M. Ziefle, 'Perception of Privacy and Willingness to Share Personal Data in the Smart Factory', in *HCI for Cybersecurity, Privacy and Trust*, vol. 14045, A. Moallem, Ed., in Lecture Notes in Computer Science, vol. 14045. , Cham: Springer Nature Switzerland, 2023, pp. 213–231. doi: 10.1007/978-3-031-35822-7_15.

[201] L. Strawderman *et al.*, 'The applicability of existing acceptance models for enterprise organizational technology acceptance of wearables', *Int. J. Ind. Ergon.*, vol. 92, p. 103381, Nov. 2022, doi: 10.1016/j.ergon.2022.103381.

[202] P. O'Sullivan, M. Menolotto, B. O'Flynn, and D. S. Komaris, 'Estimation of Maximum Shoulder and Elbow Joint Torques Based on Demographics and Anthropometrics', in *2022 44th Annual International Conference of the IEEE Engineering in Medicine & Biology Society (EMBC)*, Glasgow, Scotland, United Kingdom: IEEE, Jul. 2022, pp. 4346–4349. doi: 10.1109/EMBC48229.2022.9870906.

[203] P. O'Sullivan, M. Menolotto, B. O'Flynn, and D.-S. Komaris, 'Validation of Endurance Model for Manual Tasks', in *2023 45th Annual International Conference of the IEEE Engineering in Medicine & Biology Society (EMBC)*, Sydney, Australia: IEEE, Jul. 2023, pp. 1–5. doi: 10.1109/EMBC40787.2023.10341139.

[204] P. O'Sullivan, M. Menolotto, B. O'Flynn, and D.-S. Komaris, 'Improving dynamic endurance time predictions for shoulder fatigue: A comparative evaluation', *Appl. Ergon.*, vol. 125, p. 104480, May 2025, doi: 10.1016/j.apergo.2025.104480.

[205] Y. Jiang, T. Van Wouwe, F. De Groote, and C. K. Liu, 'Synthesis of biologically realistic human motion using joint torque actuation', *ACM Trans. Graph.*, vol. 38, no. 4, Art. no. 4, Jul. 2019, doi: 10.1145/3306346.3322966.

[206] W. Kim, L. Peternel, M. Lorenzini, J. Babič, and A. Ajoudani, 'A Human-Robot Collaboration Framework for Improving Ergonomics During Dexterous Operation of Power Tools', *Robot. Comput.-Integr. Manuf.*, vol. 68, p. 102084, Apr. 2021, doi: 10.1016/j.rcim.2020.102084.

[207] A. Aguinaldo, J. Buttermore, and H. Chambers, 'Effects of Upper Trunk Rotation on Shoulder Joint Torque among Baseball Pitchers of Various Levels', *J. Appl. Biomech.*, vol. 23, pp. 42–51, Mar. 2007, doi: 10.1123/jab.23.1.42.

[208] L. Ma, D. Chablat, F. Bennis, W. Zhang, and F. Guillaume, 'A new muscle fatigue and recovery model and its ergonomics application in human simulation', *Virtual Phys. Prototyp.*, vol. 5, no. 3, pp. 123–137, Sep. 2010, doi: 10.1080/17452759.2010.504056.

[209] J. C. Otis, R. F. Warren, S. I. Backus, T. J. Santner, and J. D. Mabrey, 'Torque production in the shoulder of the normal young adult male: The interaction of function, dominance, joint angle, and angular velocity', *Am. J. Sports Med.*, vol. 18, no. 2, Art. no. 2, Mar. 1990, doi: 10.1177/036354659001800201.

[210] F. Guenzkofer, F. Engstler, H. Bubb, and K. Bengler, 'Isometric elbow flexion and extension joint torque measurements considering biomechanical aspects', Jan. 2011.

[211] N. J. La Delfa, Z. C. T. Evans, and J. R. Potvin, 'The influence of hand location and handle orientation on female manual arm strength', *Appl. Ergon.*, vol. 81, p. 102896, Nov. 2019, doi: 10.1016/j.apergo.2019.102896.

[212] H. Coury, S. Kumar, S. Rodgher, and Y. Narayan, 'Measurements of shoulder adduction strength in different postures', *Int. J. Ind. Ergon.*, vol. 22, no. 3, pp. 195–206, Sep. 1998, doi: 10.1016/S0169-8141(97)00015-2.

[213] S. Shaunak, L. Ang, K. Colston, S. Patel, M. Bland, and J. Maxwell, 'Muscle strength in healthy white and Asian subjects: the relationship of quadriceps maximum voluntary contraction to age, sex, body build and vitamin D.', *Clin. Sci. Lond. Engl. 1979*, vol. 73, no. 5, pp. 541–546, 1987.

[214] D. Meldrum, E. Cahalane, R. Conroy, D. Fitzgerald, and O. Hardiman, 'Maximum voluntary isometric contraction: reference values and clinical application', *Amyotroph. Lateral Scler.*, vol. 8, no. 1, pp. 47–55, 2007.

[215] K. A. Provins and N. Salter, 'Maximum torque exerted about the elbow joint', *J. Appl. Physiol.*, vol. 7, no. 4, Art. no. 4, Jan. 1955, doi: 10.1152/jappl.1955.7.4.393.

[216] T. Fukunaga, M. Miyatani, M. Tachi, M. Kouzaki, Y. Kawakami, and H. Kanehisa, 'Muscle volume is a major determinant of joint torque in humans', *Acta Physiol. Scand.*, vol. 172, no. 4, Art. no. 4, 2001, doi: 10.1046/j.1365-201x.2001.00867.x.

[217] G. Hajian, E. Morin, and A. Etemad, 'Convolutional Neural Network Approach for Elbow Torque Estimation during Quasi-dynamic and Dynamic Contractions', in *2021 43rd Annual International Conference of the IEEE Engineering in Medicine Biology Society (EMBC)*, Nov. 2021, pp. 665–668. doi: 10.1109/EMBC46164.2021.9630287.

[218] D. Kim *et al.*, 'EMG-based Simultaneous Estimations of Joint Angle and Torque during Hand Interactions with Environments', *IEEE Trans. Biomed. Eng.*, vol. PP, Dec. 2021, doi: 10.1109/TBME.2021.3134204.

[219] A. Bosy-Westphal *et al.*, 'Accuracy of Bioelectrical Impedance Consumer Devices for Measurement of Body Composition in Comparison to Whole Body Magnetic Resonance Imaging and Dual X-Ray Absorptiometry', *Obes. Facts*, vol. 1, no. 6, Art. no. 6, 2008, doi: 10.1159/000176061.

[220] D. A. Winter, *Biomechanics and Motor Control of Human Movement*. John Wiley & Sons, 2009.

[221] D. A. Belsey, E. Kuh, and R. E. Welsh, *Regression Diagnostics: Identifying Influential Data and Sources of Collinearity*. Willey, New York, 1980.

[222] N. Draper, *Applied regression analysis*. McGraw-Hill. Inc, 1998.

[223] S. Weisberg, *Applied linear regression*, 2nd Edition. Wiley, New York, 1985.

[224] J. R. Casley-Smith, *Lymphology*, vol. 27, no. 2, Art. no. 2, Jun. 1994.

[225] J. M. Deeb, C. G. DRURY, and D. R. PENDERGAST, 'An exponential model of isometric muscular fatigue as a function of age and muscle groups', *Ergonomics*, vol. 35, no. 7–8, pp. 899–918, 1992.

[226] C. Yi, K. W. Li, F. Tang, H. Zuo, L. Ma, and H. Hu, 'Pulling strength, muscular fatigue, and prediction of maximum endurance time for simulated pulling tasks', *PLOS ONE*, vol. 13, no. 11, p. e0207283, Nov. 2018, doi: 10.1371/journal.pone.0207283.

[227] K. W. Li, C. Yi, and M. Liu, 'Maximum endurance time modeling for push and pull tasks considering gender and handle height', *Hum. Factors Ergon. Manuf.*, vol. 31, no. 1, Art. no. 1, 2021, doi: 10.1002/hfm.20865.

[228] Y. Chen, S. Tian, and Y. Zou, 'Modeling of the maximum endurance time of coal miners muscle fatigue for one-handed carrying tasks', *J. Loss Prev. Process Ind.*, vol. 80, p. 104895, Dec. 2022, doi: 10.1016/j.jlp.2022.104895.

[229] T. Duan *et al.*, 'Real-time indicators and influence factors of muscle fatigue in push-type work', *Int. J. Ind. Ergon.*, vol. 80, p. 103046, Nov. 2020, doi: 10.1016/j.ergon.2020.103046.

[230] L. A. F. Law, J. E. Lee, T. R. McMullen, and T. Xia, 'Relationships between maximum holding time and ratings of pain and exertion differ for static and dynamic tasks', *Appl. Ergon.*, vol. 42, no. 1, pp. 9–15, 2010.

[231] J. S. Petrofsky, R. L. Burse, and A. R. Lind, 'Comparison of physiological responses of women and men to isometric exercise', *J. Appl. Physiol.*, vol. 38, no. 5, pp. 863–868, 1975.

[232] H. SATO and J. OHASHI, 'Sex differences in static muscular endurance', *J. Hum. Ergol. (Tokyo)*, vol. 18, no. 1, pp. 53–60, 1989.

[233] E. Bäckman, V. Johansson, B. Häger, P. Sjöblom, and K. Henriksson, 'Isometric muscle strength and muscular endurance in normal persons aged between 17 and 70 years.', *Scand. J. Rehabil. Med.*, vol. 27, no. 2, pp. 109–117, 1995.

[234] J. Sanchez, J. Pequignot, L. Peyrin, and H. Monod, 'Sex differences in the sympatho-adrenal response to isometric exercise', *Eur. J. Appl. Physiol.*, vol. 45, pp. 147–154, 1980.

[235] A. Garg, K. T. Hegmann, B. J. Schwoerer, and J. M. Kapellusch, 'The effect of maximum voluntary contraction on endurance times for the shoulder girdle', *Int. J. Ind. Ergon.*, vol. 30, no. 2, pp. 103–113, Aug. 2002, doi: 10.1016/S0169-8141(02)00078-1.

[236] Y. Soo, M. Sugi, H. Yokoi, T. Arai, R. Kato, and J. Ota, 'Quantitative estimation of muscle fatigue on cyclic handgrip tasks', *Int. J. Ind. Ergon.*, vol. 42, no. 1, pp. 103–112, Jan. 2012, doi: 10.1016/j.ergon.2011.10.004.

[237] P. De Leva, 'Adjustments to Zatsiorsky-Seluyanov's segment inertia parameters', *J. Biomech.*, vol. 29, no. 9, pp. 1223–1230, Sep. 1996, doi: 10.1016/0021-9290(95)00178-6.

[238] M. Adolphe, J. Clerval, Z. Kirchof, R. LACOMBE-DELPECH, and B. ZAGRODNY, 'Center of Mass of Human's Body Segments.', *Mech. Mech. Eng.*, vol. 21, no. 3, 2017.

[239] B. Liu, L. Ma, C. Chen, and Z. Zhang, 'Experimental validation of a subject-specific maximum endurance time model', *Ergonomics*, vol. 61, no. 6, pp. 806–817, Jun. 2018, doi: 10.1080/00140139.2017.1416180.

[240] N. K. Mamaghani, Y. Shimomura, K. Iwanaga, and T. Katsuura, 'Muscular Performance Modeling of the Upper Limb in Static Postures', *J. Physiol. Anthropol. Appl. Human Sci.*, vol. 22, no. 3, pp. 149–157, 2003, doi: 10.2114/jpa.22.149.

[241] B. Danneskiold-Samsøe *et al.*, 'Isokinetic and isometric muscle strength in a healthy population with special reference to age and gender', *Acta Physiol.*, vol. 197, no. s673, pp. 1–68, Oct. 2009, doi: 10.1111/j.1748-1716.2009.02022.x.

[242] P. O'Sullivan, 'SWIFTIES (Subject and Wearables data for Investigation of Fatiguing Tasks In Exension/flexion of Shoulder/elbow)'. Zenodo, May 16, 2024. doi: 10.5281/ZENODO.11202227.

[243] J. W. Garrett, 'The adult human hand: some anthropometric and biomechanical considerations', *Hum. Factors*, vol. 13, no. 2, pp. 117–131, 1971.

[244] E. E. Neumann *et al.*, 'Reference data on thickness and mechanics of tissue layers and anthropometry of musculoskeletal extremities', *Sci. Data*, vol. 5, no. 1, pp. 1–10, 2018.

[245] A. Freivalds, *Biomechanics of the upper limbs: mechanics, modeling and musculoskeletal injuries*. CRC press, 2011.

[246] 'Conventional Upper Skeleton Marker Set', Optitrack Conventional Upper (27). Accessed: Dec. 05, 2024. [Online]. Available: https://docs.optitrack.com/markersets/upper/conventional-upper-27

[247] M. Hagberg, 'Muscular endurance and surface electromyogram in isometric and dynamic exercise', *J. Appl. Physiol.*, vol. 51, no. 1, pp. 1–7, Jul. 1981, doi: 10.1152/jappl.1981.51.1.1.

[248] B. Elfving and Å. Dedering, 'Task dependency in back muscle fatigue – Correlations between two test methods', *Clin. Biomech.*, vol. 22, no. 1, pp. 28–33, Jan. 2007, doi: 10.1016/j.clinbiomech.2006.08.007.

[249] C. Yi, F. Tang, L. Peng, K. W. Li, L. Ma, and H. Hu, 'Modeling of maximum endurance time for static pulling tasks', *Work*, vol. 60, no. 3, pp. 455–463, 2018.

[250] S. K. Hunter, 'Sex differences in human fatigability: mechanisms and insight to physiological responses', *Acta Physiol.*, vol. 210, no. 4, pp. 768–789, 2014.

[251] B. Liu, L. Ma, W. Zhang, and Z. Zhang, 'Subject-specific hand grip fatigability indicator determined using parameter identification technique', *Hum. Factors Ergon. Manuf. Serv. Ind.*, vol. 29, no. 1, pp. 86–94, Jan. 2019, doi: 10.1002/hfm.20760.
[252] M. A. Nussbaum and X. Zhang, 'Heuristics for locating upper extremity joint centres from a reduced set of surface markers', *Hum. Mov. Sci.*, vol. 19, no. 5, pp. 797–816, Nov. 2000, doi: 10.1016/S0167-9457(00)00020-8.
[253] P. O'Sullivan, M. Menolotto, A. Visentin, B. O'Flynn, and D.-S. Komaris, 'AI-Based Task Classification With Pressure Insoles for Occupational Safety', *IEEE Access*, vol. 12, pp. 21347–21357, 2024, doi: 10.1109/ACCESS.2024.3361754.
[254] K. Renner, D. Williams, and R. Queen, 'The Reliability and Validity of the Loadsol® under Various Walking and Running Conditions', *Sensors*, vol. 19, no. 2, p. 265, Jan. 2019, doi: 10.3390/s19020265.
[255] M. Jönsson, T. Munkhammar, L. Norrbrand, and H. E. Berg, 'Foot centre of pressure and ground reaction force during quadriceps resistance exercises; a comparison between force plates and a pressure insole system', *J. Biomech.*, vol. 87, pp. 206–210, Apr. 2019, doi: 10.1016/j.jbiomech.2019.03.004.
[256] A. Forner Cordero, H. J. F. M. Koopman, and F. C. T. van der Helm, 'Use of pressure insoles to calculate the complete ground reaction forces', *J. Biomech.*, vol. 37, no. 9, pp. 1427–1432, Sep. 2004, doi: 10.1016/j.jbiomech.2003.12.016.
[257] G. S. Faber, A. S. Koopman, I. Kingma, C. C. Chang, J. T. Dennerlein, and J. H. Van Dieën, 'Continuous ambulatory hand force monitoring during manual materials handling using instrumented force shoes and an inertial motion capture suit', *J. Biomech.*, vol. 70, pp. 235–241, Mar. 2018, doi: 10.1016/j.jbiomech.2017.10.006.
[258] Y. Ma and S. Gallagher, 'A Machine Learning-Based Approach for Lifting Load Estimation', Auburn University, 2024. Accessed: Sep. 16, 2024. [Online]. Available: https://etd.auburn.edu//handle/10415/9408
[259] A. T. Peebles, K. R. Ford, J. B. Taylor, J. M. Hart, L. P. Sands, and R. M. Queen, 'Using force sensing insoles to predict kinetic knee symmetry during a stop jump', *J. Biomech.*, vol. 95, p. 109293, Oct. 2019, doi: 10.1016/j.jbiomech.2019.07.037.
[260] W. Seiberl, E. Jensen, J. Merker, M. Leitel, and A. Schwirtz, 'Accuracy and precision of loadsol ® insole force-sensors for the quantification of ground reaction force-based biomechanical running parameters', *Eur. J. Sport Sci.*, vol. 18, no. 8, pp. 1100–1109, Sep. 2018, doi: 10.1080/17461391.2018.1477993.
[261] V. Cigrovski, M. Očić, I. Bon, B. Matković, and P. Šagát, 'Inline Skating as an Additional Activity for Alpine Skiing: The Role of the Outside Leg in Short Turn Performance', *Int. J. Environ. Res. Public. Health*, vol. 19, no. 3, Art. no. 3, 2022, doi: 10.3390/ijerph19031747.
[262] D. Krumm, N. Kuske, M. Neubert, J. Buder, F. Hamker, and S. Odenwald, 'Determining push-off forces in speed skating imitation drills', *Sports Eng.*, vol. 24, no. 1, Art. no. 1, 2021, doi: 10.1007/s12283-021-00362-1.
[263] S. Tedesco *et al.*, 'A Wearable System for the Estimation of Performance-Related Metrics during Running and Jumping Tasks', *Appl. Sci.*, vol. 11, no. 11, p. 5258, Jun. 2021, doi: 10.3390/app11115258.
[264] J. Tao *et al.*, 'Real-time pressure mapping smart insole system based on a controllable vertical pore dielectric layer', *Microsyst. Nanoeng.*, vol. 6, no. 1, p. 62, Aug. 2020, doi: 10.1038/s41378-020-0171-1.
[265] Y. Gao *et al.*, 'Effects of novel diabetic therapeutic footwear on preventing ulcer recurrence in patients with a history of diabetic foot ulceration: study protocol for an open-label, randomized, controlled trial', *Trials*, vol. 22, no. 1, p. 151, Dec. 2021, doi: 10.1186/s13063-021-05098-8.
[266] A. Marcante *et al.*, 'Foot pressure wearable sensors for freezing of gait detection in parkinson's disease', *Sens. Switz.*, vol. 21, no. 1, Art. no. 1, 2021, doi: 10.3390/s21010128.
[267] M. F. Antwi-Afari, H. Li, J. Seo, and A. Y. L. Wong, 'Automated detection and classification of construction workers' loss of balance events using wearable insole pressure sensors', *Autom. Constr.*, vol. 96, pp. 189–199, Dec. 2018, doi: 10.1016/j.autcon.2018.09.010.
[268] E. S. Matijevich, P. Volgyesi, and K. E. Zelik, 'A promising wearable solution for the practical and accurate monitoring of low back loading in manual material handling', *Sens. Switz.*, vol. 21, no. 2, Art. no. 2, 2021, doi: 10.3390/s21020340.
[269] T. A. Ishtiaque, A. Cepuran, A. T. Salaj, O. Torp, and M. G. Diaconu, 'Developing an AI-powered smart insole system to reduce the possibility of back pain among older workers: lessons from the Norwegian construction industry', *IOP Conf. Ser. Earth Environ. Sci.*, vol. 1101, no. 3, p. 032027, Nov. 2022, doi: 10.1088/1755-1315/1101/3/032027.

[270] I. Conforti *et al.*, ‘Validation of a novel wearable solution for measuring L5/S1 load during manual material handling tasks’, presented at the 2020 IEEE International Workshop on Metrology for Industry 4.0 and IoT, MetroInd 4.0 and IoT 2020 - Proceedings, 2020, pp. 501–506. doi: 10.1109/MetroInd4.0IoT48571.2020.9138259.
[271] L. Kong, H. Li, Y. Yu, H. Luo, M. Skitmore, and M. F. Antwi-Afari, ‘Quantifying the physical intensity of construction workers, a mechanical energy approach’, *Adv. Eng. Inform.*, vol. 38, pp. 404–419, Oct. 2018, doi: 10.1016/j.aei.2018.08.005.
[272] Y. Yu, H. Li, X. Yang, and W. Umer, ‘Estimating Construction Workers’ Physical Workload by Fusing Computer Vision and Smart Insole Technologies’, presented at the 34th International Symposium on Automation and Robotics in Construction, Taipei, Taiwan, Jul. 2018. doi: 10.22260/ISARC2018/0168.
[273] M. F. Antwi-Afari *et al.*, ‘Quantifying workers’ gait patterns to identify safety hazards in construction using a wearable insole pressure system’, *Saf. Sci.*, vol. 129, p. 104855, Sep. 2020, doi: 10.1016/j.ssci.2020.104855.
[274] M. F. Antwi-Afari and H. Li, ‘Fall risk assessment of construction workers based on biomechanical gait stability parameters using wearable insole pressure system’, *Adv. Eng. Inform.*, vol. 38, pp. 683–694, Oct. 2018, doi: 10.1016/j.aei.2018.10.002.
[275] M. F. Antwi-Afari, H. Li, W. Umer, Y. Yu, and X. Xing, ‘Construction Activity Recognition and Ergonomic Risk Assessment Using a Wearable Insole Pressure System’, *J. Constr. Eng. Manag.*, vol. 146, no. 7, p. 04020077, Jul. 2020, doi: 10.1061/(ASCE)CO.1943-7862.0001849.
[276] M. F. Antwi-Afari *et al.*, ‘Machine learning-based identification and classification of physical fatigue levels: A novel method based on a wearable insole device’, *Int. J. Ind. Ergon.*, vol. 93, p. 103404, Jan. 2023, doi: 10.1016/j.ergon.2022.103404.
[277] S. Khandelwal and N. Wickström, ‘Evaluation of the performance of accelerometer-based gait event detection algorithms in different real-world scenarios using the MAREA gait database’, *Gait Posture*, vol. 51, pp. 84–90, Jan. 2017, doi: 10.1016/j.gaitpost.2016.09.023.
[278] H. Leutheuser, D. Schuldhaus, and B. M. Eskofier, ‘Hierarchical, Multi-Sensor Based Classification of Daily Life Activities: Comparison with State-of-the-Art Algorithms Using a Benchmark Dataset’, *PLoS ONE*, vol. 8, no. 10, p. e75196, Oct. 2013, doi: 10.1371/journal.pone.0075196.
[279] F. De la Torre *et al.*, ‘Guide to the carnegie mellon university multimodal activity (cmu-mmac) database’, 2009.
[280] A. R. De Pinho, P. H. F. S. Diniz, and H. Fuks, ‘Bottom-up Investigation: Human Activity Recognition Based on Feet Movement and Posture Information’, in *Proceedings of the 4th International Workshop on Sensor-based Activity Recognition and Interaction*, Rostock Germany: ACM, Sep. 2017, pp. 1–6. doi: 10.1145/3134230.3134240.
[281] Y. Hayakawa, Y. Kimata, K. Kida, Department of Control Engineering, National Institute of Technology, Nara College 22 Yata-cho, Yamatokoriyama, Nara 639-1058, Japan, and Advanced Mechanical Engineering Course, National Institute of Technology, Nara College 22 Yata-cho, Yamatokoriyama, Nara 639-1058, Japan, ‘Study on Human Behavior Classification by Using High-Performance Shoes Equipped with Pneumatic Actuators’, *J. Robot. Mechatron.*, vol. 32, no. 5, pp. 947–957, Oct. 2020, doi: 10.20965/jrm.2020.p0947.
[282] B. Oubre, S. Lane, S. Holmes, K. Boyer, and S. I. Lee, ‘Estimating ground reaction force and center of pressure using low-cost wearable devices’, *IEEE Trans. Biomed. Eng.*, vol. 69, no. 4, pp. 1461–1468, 2021.
[283] D. K. Agrawal, W. Usaha, S. Pojprapai, and P. Wattanapan, ‘Fall Risk Prediction Using Wireless Sensor Insoles With Machine Learning’, *IEEE Access*, vol. 11, pp. 23119–23126, 2023, doi: 10.1109/ACCESS.2023.3252886.
[284] D. Chen *et al.*, ‘Bring Gait Lab to Everyday Life: Gait Analysis in Terms of Activities of Daily Living’, *IEEE Internet Things J.*, vol. 7, no. 2, Art. no. 2, Feb. 2020, doi: 10.1109/JIOT.2019.2954387.
[285] W. Wei, Y. Kaiming, Z. Yu, Q. Yuyang, W. Chenhui, and L. Min, ‘Walking Speed Estimation From a Wearable Insole Pressure System Using a Bayesian Regularized Back Propagation Neural Network’, in *Volume 5: Biomedical and Biotechnology*, Virtual, Online: American Society of Mechanical Engineers, Nov. 2020, p. V005T05A001. doi: 10.1115/IMECE2020-23363.
[286] C. Chatzaki *et al.*, ‘The Smart-Insole Dataset: Gait Analysis Using Wearable Sensors with a Focus on Elderly and Parkinson’s Patients’, *Sensors*, vol. 21, no. 8, p. 2821, Apr. 2021, doi: 10.3390/s21082821.
[287] M. Hora, L. Soumar, H. Pontzer, and V. Sladek, ‘Body size and lower limb posture during walking in humans’, *PloS One*, vol. 12, no. 2, p. e0172112, 2017.

[288] J. Howcroft, E. D. Lemaire, and J. Kofman, 'Wearable sensor (accelerometer, pressure sensing insole) gait data of older adults - Update with Prospective Falls'. Borealis, 2017. doi: 10.5683/SP/VST2RC.
[289] J. Howcroft, J. Kofman, and E. D. Lemaire, 'Prospective Fall-Risk Prediction Models for Older Adults Based on Wearable Sensors', *IEEE Trans. Neural Syst. Rehabil. Eng.*, vol. 25, no. 10, pp. 1812–1820, Oct. 2017, doi: 10.1109/TNSRE.2017.2687100.
[290] V. Losing and M. Hasenjäger, 'Database (single file)'. figshare, p. 35823913732 Bytes, 2022. doi: 10.6084/M9.FIGSHARE.19834324.V1.
[291] V. Losing and M. Hasenjäger, 'A Multi-Modal Gait Database of Natural Everyday-Walk in an Urban Environment', *Sci. Data*, vol. 9, no. 1, p. 473, Aug. 2022, doi: 10.1038/s41597-022-01580-3.
[292] H. Wang, 'Raw data with small file sizes [individual subject files]'. Zenodo, Dec. 10, 2022. doi: 10.5281/ZENODO.7422043.
[293] H. Wang, 'Processed data with small file sizes [individual subject files]'. Zenodo, Dec. 10, 2022. doi: 10.5281/ZENODO.7422031.
[294] Yuzhu Guo *et al.*, 'Data for the paper "A new proxy measurement algorithm with applications to estimation of vertical ground reaction forces using wearable sensors"'. The University of Sheffield, p. 559039973 Bytes, 2017. doi: 10.15131/SHEF.DATA.5341309.
[295] Y. Guo *et al.*, 'A New Proxy Measurement Algorithm with Application to the Estimation of Vertical Ground Reaction Forces Using Wearable Sensors', *Sensors*, vol. 17, no. 10, p. 2181, Sep. 2017, doi: 10.3390/s17102181.
[296] M. Munoz-Organero, J. Parker, L. Powell, and S. Mawson, 'Assessing Walking Strategies Using Insole Pressure Sensors for Stroke Survivors', *Sensors*, vol. 16, no. 10, p. 1631, Oct. 2016, doi: 10.3390/s16101631.
[297] C. F. Martindale, S. Sprager, and B. M. Eskofier, 'Hidden Markov Model-Based Smart Annotation for Benchmark Cyclic Activity Recognition Database Using Wearables', *Sensors*, vol. 19, no. 8, p. 1820, Apr. 2019, doi: 10.3390/s19081820.
[298] D. Novak *et al.*, 'Automated detection of gait initiation and termination using wearable sensors', *Med. Eng. Phys.*, vol. 35, no. 12, pp. 1713–1720, Dec. 2013, doi: 10.1016/j.medengphy.2013.07.003.
[299] A. Choi, H. Jung, K. Y. Lee, S. Lee, and J. H. Mun, 'Machine learning approach to predict center of pressure trajectories in a complete gait cycle: a feedforward neural network vs. LSTM network', *Med. Biol. Eng. Comput.*, vol. 57, no. 12, pp. 2693–2703, Dec. 2019, doi: 10.1007/s11517-019-02056-0.
[300] S. R. Moore, C. Kranzinger, J. Fritz, T. Stöggl, J. Kröll, and H. Schwameder, 'Foot Strike Angle Prediction and Pattern Classification Using LoadsolTM Wearable Sensors: A Comparison of Machine Learning Techniques', *Sensors*, vol. 20, no. 23, p. 6737, Nov. 2020, doi: 10.3390/s20236737.
[301] J. Moon, D. Lee, H. Jung, A. Choi, and J. H. Mun, 'Machine Learning Strategies for Low-Cost Insole-Based Prediction of Center of Gravity during Gait in Healthy Males', *Sensors*, vol. 22, no. 9, p. 3499, May 2022, doi: 10.3390/s22093499.
[302] S. M. Lundberg and S.-I. Lee, 'A unified approach to interpreting model predictions', *Adv. Neural Inf. Process. Syst.*, vol. 30, 2017.
[303] D. Ren, N. Aubert-Kato, E. Anzai, Y. Ohta, and J. Tripette, 'Random forest algorithms for recognizing daily life activities using plantar pressure information: a smart-shoe study', *PeerJ*, vol. 8, p. e10170, 2020.
[304] E. Park *et al.*, 'Unobtrusive and Continuous Monitoring of Alcohol-impaired Gait Using Smart Shoes', *Methods Inf. Med.*, vol. 56, no. 01, pp. 74–82, 2017, doi: 10.3414/ME15-02-0008.
[305] K. Kitagawa, T. Nagasaki, S. Nakano, M. Hida, S. Okamatsu, and C. Wada, 'Comparison of Machine Learning Algorithms for Patient Handling Recognition based on Body Mechanics', in *2021 IEEE 3rd Global Conference on Life Sciences and Technologies (LifeTech)*, Nara, Japan: IEEE, Mar. 2021, pp. 77–79. doi: 10.1109/LifeTech52111.2021.9391968.
[306] W. Anderson, Z. Choffin, N. Jeong, M. Callihan, S. Jeong, and E. Sazonov, 'Empirical Study on Human Movement Classification Using Insole Footwear Sensor System and Machine Learning', *Sensors*, vol. 22, no. 7, p. 2743, Apr. 2022, doi: 10.3390/s22072743.
[307] M. F. Antwi-Afari, H. Li, J. Seo, S. Lee, D. J. Edwards, and A. Y. Lok Wong, 'Wearable insole pressure sensors for automated detection and classification of slip-trip-loss of balance events in construction workers', presented at the Construction Research Congress 2018, 2018, pp. 73–83.

[308] M. F. Antwi-Afari *et al.*, 'Deep learning-based networks for automated recognition and classification of awkward working postures in construction using wearable insole sensor data', *Autom. Constr.*, vol. 136, p. 104181, Apr. 2022, doi: 10.1016/j.autcon.2022.104181.

[309] K. Kitagawa *et al.*, 'Posture Recognition Method for Caregivers during Postural Change of a Patient on a Bed using Wearable Sensors', *Adv. Sci. Technol. Eng. Syst. J.*, vol. 5, no. 5, pp. 1093–1098, Oct. 2020, doi: 10.25046/aj0505133.

[310] K. Yuan *et al.*, 'Fuzzy-logic-based hybrid locomotion mode classification for an active pelvis orthosis: Preliminary results', presented at the 2015 37th Annual International Conference of the IEEE Engineering in Medicine and Biology Society (EMBC), IEEE, 2015, pp. 3893–3896.

[311] G. Wu *et al.*, 'ISB recommendation on definitions of joint coordinate systems of various joints for the reporting of human joint motion—Part II: shoulder, elbow, wrist and hand', *J. Biomech.*, vol. 38, no. 5, pp. 981–992, May 2005, doi: 10.1016/j.jbiomech.2004.05.042.

[312] S. Lim, A. Case, and C. D'Souza, 'Comparative Analysis of Inertial Sensor to Optical Motion Capture System Performance in Push-Pull Exertion Postures', *Proc. Hum. Factors Ergon. Soc. Annu. Meet.*, vol. 60, no. 1, pp. 970–974, Sep. 2016, doi: 10.1177/1541931213601224.

[313] R. Hubaut, R. Guichard, J. Greenfield, and M. Blandeau, 'Validation of an Embedded Motion-Capture and EMG Setup for the Analysis of Musculoskeletal Disorder Risks during Manhole Cover Handling', *Sensors*, vol. 22, no. 2, p. 436, Jan. 2022, doi: 10.3390/s22020436.

[314] A. C. Campbell, D. G. Lloyd, J. A. Alderson, and B. C. Elliott, 'MRI development and validation of two new predictive methods of glenohumeral joint centre location identification and comparison with established techniques', *J. Biomech.*, vol. 42, no. 10, pp. 1527–1532, Jul. 2009, doi: 10.1016/j.jbiomech.2009.03.039.

[315] A. Barre and S. Armand, 'Biomechanical ToolKit: Open-source framework to visualize and process biomechanical data', *Comput. Methods Programs Biomed.*, vol. 114, no. 1, pp. 80–87, Apr. 2014, doi: 10.1016/j.cmpb.2014.01.012.

[316] K. Lebel, P. Boissy, H. Nguyen, and C. Duval, 'Inertial measurement systems for segments and joints kinematics assessment: towards an understanding of the variations in sensors accuracy', *Biomed. Eng. OnLine*, vol. 16, no. 1, p. 56, Dec. 2017, doi: 10.1186/s12938-017-0347-6.

[317] L. R. Marusich and J. Z. Bakdash, 'rmcorrShiny: A web and standalone application for repeated measures correlation', *F1000Research*, vol. 10, p. 697, Jul. 2021, doi: 10.12688/f1000research.55027.1.

[318] J. J. De Koning *et al.*, 'Comparison of rating of perceived exertion scales during incremental and interval exercise', *Kinesiology*, vol. 51, no. 2, pp. 150–157, 2019, doi: 10.26582/k.51.2.1.

[319] S. M. S. Yamauchi, 'Rating of perceived exertion for quantification of the intensity of resistance exercise', *Int. J. Phys. Med. Rehabil.*, vol. 1, no. 09, 2013.

[320] N. Williams, 'The Borg Rating of Perceived Exertion (RPE) scale', *Occup. Med.*, vol. 67, no. 5, pp. 404–405, Jul. 2017, doi: 10.1093/occmed/kqx063.

[321] Y. Li *et al.*, 'Nicer: A new and improved consumed endurance and recovery metric to quantify muscle fatigue of mid-air interactions', *ACM Trans. Graph. TOG*, vol. 43, no. 4, pp. 1–14, 2024.

[322] M.-È. Chiasson, D. Imbeau, K. Aubry, and A. Delisle, 'Comparing the results of eight methods used to evaluate risk factors associated with musculoskeletal disorders', *Int. J. Ind. Ergon.*, vol. 42, no. 5, pp. 478–488, Sep. 2012, doi: 10.1016/j.ergon.2012.07.003.

[323] N. Arjmand, M. Amini, A. Shirazi-Adl, A. Plamondon, and M. Parnianpour, 'Revised NIOSH Lifting Equation May generate spine loads exceeding recommended limits', *Int. J. Ind. Ergon.*, vol. 47, pp. 1–8, May 2015, doi: 10.1016/j.ergon.2014.09.010.

[324] S. Kim and M. A. Nussbaum, 'Performance evaluation of a wearable inertial motion capture system for capturing physical exposures during manual material handling tasks', *Ergonomics*, vol. 56, no. 2, pp. 314–326, Feb. 2013, doi: 10.1080/00140139.2012.742932.

[325] X. Robert-Lachaine, H. Mecheri, C. Larue, and A. Plamondon, 'Validation of inertial measurement units with an optoelectronic system for whole-body motion analysis', *Med. Biol. Eng. Comput.*, vol. 55, no. 4, pp. 609–619, Apr. 2017, doi: 10.1007/s11517-016-1537-2.

[326] P. Picerno, A. Cereatti, and A. Cappozzo, 'Joint kinematics estimate using wearable inertial and magnetic sensing modules', *Gait Posture*, vol. 28, no. 4, pp. 588–595, 2008.

[327] H. J. Luinge, P. H. Veltink, and C. T. Baten, 'Ambulatory measurement of arm orientation', *J. Biomech.*, vol. 40, no. 1, pp. 78–85, 2007.

[328] A. Godwin, M. Agnew, and J. Stevenson, 'Accuracy of inertial motion sensors in static, quasistatic, and complex dynamic motion', 2009.

[329] C. Lins, S. Fudickar, A. Gerka, and A. Hein, 'A Wearable Vibrotactile Interface for Unfavorable Posture Awareness Warning':, in *Proceedings of the 4th International Conference on Information and Communication Technologies for Ageing Well and e-Health*, Funchal, Madeira,

Portugal: SCITEPRESS - Science and Technology Publications, 2018, pp. 178–183. doi: 10.5220/0006734901780183.
[330] C. Sun *et al.*, ‘Bilateral Asymmetry of Hand Force Production in Dynamic Physically-Coupled Tasks’, *IEEE J. Biomed. Health Inform.*, vol. 26, no. 4, pp. 1826–1834, Apr. 2022, doi: 10.1109/JBHI.2021.3112201.
[331] W. S. Marras and K. G. Davis, ‘Spine loading during asymmetric lifting using one versus two hands’, *Ergonomics*, vol. 41, no. 6, pp. 817–834, Jun. 1998, doi: 10.1080/001401398186667.
[332] P. O’Sullivan, ‘SWIFTIES (Subject and Wearables data for Investigation of Fatiguing Tasks In Extension/flexion of Shoulder/elbow)’. Zenodo, Sep. 17, 2024. doi: 10.5281/ZENODO.11202226.
[333] R. V. Vitali and N. C. Perkins, ‘Determining anatomical frames via inertial motion capture: A survey of methods’, *J. Biomech.*, vol. 106, p. 109832, Jun. 2020, doi: 10.1016/j.jbiomech.2020.109832.
[334] S. K. Hunter, ‘Sex differences in fatigability of dynamic contractions’, *Exp. Physiol.*, vol. 101, no. 2, pp. 250–255, Feb. 2016, doi: 10.1113/EP085370.
[335] M. Rosselli *et al.*, ‘Workers Fatigue Monitoring for Well-being Improvement in Manufacturing’, *IFAC-Pap.*, vol. 58, no. 19, pp. 61–66, 2024.
[336] G. Prisco *et al.*, ‘Capability of Machine Learning Algorithms to Classify Safe and Unsafe Postures during Weight Lifting Tasks Using Inertial Sensors’, *Diagnostics*, vol. 14, no. 6, p. 576, Mar. 2024, doi: 10.3390/diagnostics14060576.
[337] M. Menolotto, D.-S. Komaris, P. O’Sullivan, and B. O’Flynn, ‘Assessing Trust in Collaborative Robotics with Different Human-Robot Interfaces’, in *2024 IEEE International Instrumentation and Measurement Technology Conference (I2MTC)*, Glasgow, United Kingdom: IEEE, May 2024, pp. 1–6. doi: 10.1109/I2MTC60896.2024.10561211.
[338] L. Cavuoto and F. Megahed, ‘Understanding fatigue and the implications for worker safety’, presented at the ASSE Professional Development Conference and Exposition, ASSE, 2016, p. ASSE-16.
[339] M. Calzavara, D. Battini, D. Bogataj, F. Sgarbossa, and I. Zennaro, ‘Ageing workforce management in manufacturing systems: state of the art and future research agenda’, *Int. J. Prod. Res.*, vol. 58, no. 3, pp. 729–747, 2020.
[340] H. Nieminen, E.-P. Takala, J. Niemi, and E. Viikari-Juntura, ‘Muscular synergy in the shoulder during a fatiguing static contraction’, *Clin. Biomech.*, vol. 10, no. 6, pp. 309–317, Sep. 1995, doi: 10.1016/0268-0033(95)00041-I.
[341] D. M. Mulla, A. C. McDonald, and P. J. Keir, ‘Joint moment trade-offs across the upper extremity and trunk during repetitive work’, *Appl. Ergon.*, vol. 88, p. 103142, Oct. 2020, doi: 10.1016/j.apergo.2020.103142.
[342] J. Y. Kim, J. S. Park, D. J. Kim, and S. Im, ‘Evaluation of fatigue patterns in individual shoulder muscles under various external conditions’, *Appl. Ergon.*, vol. 91, p. 103280, Feb. 2021, doi: 10.1016/j.apergo.2020.103280.
[343] H. R. Zadry, S. Z. M. Dawal, and Z. Taha, ‘Development of statistical models for predicting muscle and mental activities during repetitive precision tasks’, *Int. J. Occup. Saf. Ergon.*, vol. 22, no. 3, pp. 374–383, Jul. 2016, doi: 10.1080/10803548.2016.1150094.
[344] H. Iridiastadi and M. A. Nussbaum, ‘Muscle fatigue and endurance during repetitive intermittent static efforts: development of prediction models’, *Ergonomics*, vol. 49, no. 4, pp. 344–360, Mar. 2006, doi: 10.1080/00140130500475666.
[345] E. Rashedi and M. A. Nussbaum, ‘Cycle time influences the development of muscle fatigue at low to moderate levels of intermittent muscle contraction’, *J. Electromyogr. Kinesiol.*, vol. 28, pp. 37–45, Jun. 2016, doi: 10.1016/j.jelekin.2016.03.001.
[346] W. K. D. S. Leite *et al.*, ‘Job rotations based on physical and psychological workloads: A proposal for the footwear industry’, *Comput. Ind. Eng.*, vol. 188, p. 109887, Feb. 2024, doi: 10.1016/j.cie.2024.109887.
[347] K. B. Martinez, M. Nazarahari, and H. Rouhani, ‘Breaking the Fatigue Cycle: Investigating the Effect of Work-Rest Schedules on Muscle Fatigue in Material Handling Jobs’, *Sensors*, vol. 23, no. 24, p. 9670, Dec. 2023, doi: 10.3390/s23249670.
[348] L. G. M. Bispo and F. G. Amaral, ‘The impact of Industry 4.0 on occupational health and safety: A systematic literature review’, *J. Safety Res.*, vol. 90, pp. 254–271, Sep. 2024, doi: 10.1016/j.jsr.2024.04.009.
[349] G. Beier *et al.*, ‘Implications of Industry 4.0 on industrial employment: A comparative survey from Brazilian, Chinese, and German practitioners’, *Technol. Soc.*, vol. 70, p. 102028, Aug. 2022, doi: 10.1016/j.techsoc.2022.102028.

[350] ‘Wearable Technology Market Size, Share & Industry Trends’, Markets and Markets, SE 2763, Feb. 2025.
[351] ‘Wearable Technology Market - Forecast(2025 - 2031)’, Industry ARC, ITR 40457. Accessed: Mar. 25, 2025. [Online]. Available: https://www.industryarc.com/Research/Wearable-Technology-Market-Research-504119
[352] ‘Wearable Technology Market Size, Share & Industry Analysis, By Type (Passive and Active), By Technology (IoT Based, AR and VR, and Others), By End Use (Health & Fitness, BFSI, Gaming & Entertainment, Fashion, Travel, Education, and Logistics & Warehouse), and Regional Forecast, 2024 – 2032 Source: https://www.fortunebusinessinsights.com/wearable-technology-market-106000’, Fortune Business Insights, FBI 106000, Mar. 2025. Accessed: Mar. 25, 2025. [Online]. Available: https://www.fortunebusinessinsights.com/wearable-technology-market-106000
[353] L. S. Dalenogare, M. M. Baseggio, N. F. Ayala, M.-A. Le Dain, and A. G. Frank, ‘The contribution of Smart Glasses for PSS’, *Procedia CIRP*, vol. 83, pp. 318–323, 2019.
[354] J. Min, Y. Kim, S. Lee, T.-W. Jang, I. Kim, and J. Song, ‘The Fourth Industrial Revolution and Its Impact on Occupational Health and Safety, Worker’s Compensation and Labor Conditions’, *Saf. Health Work*, vol. 10, no. 4, pp. 400–408, Dec. 2019, doi: 10.1016/j.shaw.2019.09.005.
[355] T. Luopajärvi, I. Kuorinka, M. Virolainen, and M. Holmberg, ‘Prevalence of tenosynovitis and other injuries of the upper extremities in repetitive work’, *Scand. J. Work. Environ. Health*, pp. 48–55, 1979.
[356] M. Madonna, L. Monica, S. Anastasi, and M. Di Nardo, ‘Evolution of Cognitive Demand in the Human–Machine Interaction Integrated with Industry 4.0 Technologies’, presented at the SAFE 2019, Ancona, Italy, Dec. 2019, pp. 13–19. doi: 10.2495/SAFE190021.
[357] P. Bałys, P. Buła, D. Dziedzic, and M. Uznańska, ‘The future of work in automated warehouse from the perspective of the employees’, in *Contemporary organisation and management. Challenges and trends*, A. Michałkiewicz and W. Mierzejewska, Eds., Wydawnictwo Uniwersytetu Łódzkiego, 2020, pp. 267–281. doi: 10.18778/8220-333-2.16.
[358] L. Lu, F. M. Megahed, R. F. Sesek, and L. A. Cavuoto, ‘A survey of the prevalence of fatigue, its precursors and individual coping mechanisms among U.S. manufacturing workers’, *Appl. Ergon.*, vol. 65, pp. 139–151, Nov. 2017, doi: 10.1016/j.apergo.2017.06.004.
[359] A. Yazdani *et al.*, ‘How compatible are participatory ergonomics programs with occupational health and safety management systems?’, *Scand. J. Work. Environ. Health*, vol. 41, no. 2, pp. 111–123, Mar. 2015, doi: 10.5271/sjweh.3467.
[360] F. Motta, T. Varrecchia, G. Chini, A. Ranavolo, and M. Galli, ‘The Use of Wearable Systems for Assessing Work-Related Risks Related to the Musculoskeletal System—A Systematic Review’, *Int. J. Environ. Res. Public. Health*, vol. 21, no. 12, p. 1567, Nov. 2024, doi: 10.3390/ijerph21121567.
[361] R. Wells, S. E. Mathiassen, L. Medbo, and J. Winkel, ‘Time—A key issue for musculoskeletal health and manufacturing’, *Appl. Ergon.*, vol. 38, no. 6, pp. 733–744, Nov. 2007, doi: 10.1016/j.apergo.2006.12.003.
[362] V. Orso, R. Ziviani, G. Bacchiega, G. Bondani, A. Spagnolli, and L. Gamberini, ‘Employee-centric innovation: Integrating participatory design and video-analysis to foster the transition to Industry 5.0’, *Comput. Ind. Eng.*, vol. 173, p. 108661, Nov. 2022, doi: 10.1016/j.cie.2022.108661.
[363] ‘Managing upper limb disorders in the workplace. A brief guide.’, HSE, UK, 01/20 INDG171(rev3), Jan. 2020. Accessed: Mar. 20, 2025. [Online]. Available: https://www.hse.gov.uk/pubns/indg171.htm
[364] S. Niehaus, M. Hartwig, P. H. Rosen, and S. Wischniewski, ‘An occupational safety and health perspective on human in control and AI’, *Front. Artif. Intell.*, vol. 5, p. 868382, 2022.
[365] M. Pigeon, B. O’Flynn, J. Barton, and P. O’Sullivan, ‘3D printed torso phantom for UHF WIMD measurements’, in *2021 IEEE International Symposium on Antennas and Propagation and USNC-URSI Radio Science Meeting (APS/URSI)*, Singapore, Singapore: IEEE, Dec. 2021, pp. 361–362. doi: 10.1109/APS/URSI47566.2021.9703848.
[366] P. O’Sullivan, J. Barton, and M. Pigeon, ‘Fully Integrated Circulatory System in a Torso Phantom for WIMD Read Range Performance Measurements’, in *2024 IEEE INC-USNC-URSI Radio Science Meeting (Joint with AP-S Symposium)*, Florence, Italy: IEEE, Jul. 2024, pp. 408–408. doi: 10.23919/INC-USNC-URSI61303.2024.10632410.
[367] M. M. Qirtas *et al.*, ‘Generalizing Perceived Fatigue Estimation Across Diverse Upper Limb Tasks Using Minimal Wearable Sensors’, *IEEE Sens. Lett.*, vol. 9, no. 9, pp. 1–4, Sep. 2025, doi: 10.1109/LSENS.2025.3596719.

[368] M. M. Qirtas *et al.*, ‘Hierarchical Modeling of Perceived Fatigue in Upper Limb Cross Tasks Using Wearable IMU and EMG Sensors’, *IEEE Access*, pp. 1–1, 2026, doi: 10.1109/ACCESS.2026.3659477.

[369] A. Shahid, K. Wilkinson, S. Marcu, and C. M. Shapiro, ‘Fatigue Assessment Scale (FAS)’, in *STOP, THAT and One Hundred Other Sleep Scales*, A. Shahid, K. Wilkinson, S. Marcu, and C. M. Shapiro, Eds., New York, NY: Springer New York, 2011, pp. 161–162. doi: 10.1007/978-1-4419-9893-4_33.

[370] J. Carifio and R. J. Perla, ‘Ten common misunderstandings, misconceptions, persistent myths and urban legends about Likert scales and Likert response formats and their antidotes’, *J. Soc. Sci.*, vol. 3, no. 3, pp. 106–116, 2007.

[371] S. J. Pedersen, C. M. Kitic, M.-L. Bird, C. P. Mainsbridge, and P. D. Cooley, ‘Is self-reporting workplace activity worthwhile? Validity and reliability of occupational sitting and physical activity questionnaire in desk-based workers’, *BMC Public Health*, vol. 16, no. 1, p. 836, Dec. 2016, doi: 10.1186/s12889-016-3537-4.

[372] K. Wick, O. Faude, S. Schwager, L. Zahner, and L. Donath, ‘Deviation between self-reported and measured occupational physical activity levels in office employees: effects of age and body composition’, *Int. Arch. Occup. Environ. Health*, vol. 89, no. 4, pp. 575–582, May 2016, doi: 10.1007/s00420-015-1095-1.

[373] G. P. Whitfield, K. K. Pettee Gabriel, and H. W. Kohl, ‘Assessing Sitting Across Contexts: Development of the Multicontext Sitting Time Questionnaire’, *Res. Q. Exerc. Sport*, vol. 84, no. 3, pp. 323–328, Sep. 2013, doi: 10.1080/02701367.2013.814041.

[374] R. Karasek, C. Brisson, N. Kawakami, I. Houtman, P. Bongers, and B. Amick, ‘The Job Content Questionnaire (JCQ): An instrument for internationally comparative assessments of psychosocial job characteristics.’, *J. Occup. Health Psychol.*, vol. 3, no. 4, pp. 322–355, 1998, doi: 10.1037/1076-8998.3.4.322.

[375] S. Grant *et al.*, ‘A Comparison of the Reproducibility and the Sensitivity to Change of Visual Analogue Scales, Borg Scales, and Likert Scales in Normal Subjects During Submaximal Exercise’, *Chest*, vol. 116, no. 5, pp. 1208–1217, Nov. 1999, doi: 10.1378/chest.116.5.1208.

[376] R. L. Brookham, J. N. Moreton, and C. R. Dickerson, ‘Perception of shoulder muscular effort during low-demand load transfer tasks’, *Work*, vol. 31, no. 4, pp. 417–424, 2008.

[377] J. Annett, ‘Subjective rating scales: science or art?’, *Ergonomics*, vol. 45, no. 14, pp. 966–987, Nov. 2002, doi: 10.1080/00140130210166951.

[378] G. Matthews, J. De Winter, and P. A. Hancock, ‘What do subjective workload scales really measure? Operational and representational solutions to divergence of workload measures’, *Theor. Issues Ergon. Sci.*, vol. 21, no. 4, pp. 369–396, Jul. 2020, doi: 10.1080/1463922X.2018.1547459.

[379] A. Dehghani, M. Snell, F. Guenzkofer, S. Kaltenbrunner, and E. Fendekova, ‘SERA: A Digital Risk Management Tool as the Basic of OSHM’, presented at the International Conference at Brno University of Technology, Faculty of Business and Management, 2021.

[380] M. Snell, ‘Digital Workplace Stress Management: A System for Digital Ergonomics Assessment in the BMW Group’, in *Proceedings of the XXXIVth Annual International Occupational Ergonomics and Safety Conference*, International Society for Occupational Ergonomics and Safety, Sep. 2022, pp. 69–71. doi: 10.47461/isoes.2022_snell.

[381] M. Snell, A. Dehghani, F. Guenzkofer, and S. Kaltenbrunner, ‘Safety and Ergonomics Risk Assessment (SERA): A Customized Ergonomics Assessment Tool for Automobile Manufacturing’, *Safety*, 2021.

[382] N. Warburton, ‘Operatives take a front seat in MSD risk reduction on Toyota’s production lines’, *IOSH Magazine*, pp. 44–50, Jan. 2019.

[383] E. N. Corlett and R. Bishop, ‘A technique for assessing postural discomfort’, *Ergonomics*, vol. 19, no. 2, pp. 175–182, 1976.

[384] J. Steven Moore and A. Garg, ‘The Strain Index: A Proposed Method to Analyze Jobs For Risk of Distal Upper Extremity Disorders’, *Am. Ind. Hyg. Assoc. J.*, vol. 56, no. 5, pp. 443–458, May 1995, doi: 10.1080/15428119591016863.

[385] D. Kee, ‘Systematic Comparison of OWAS, RULA, and REBA Based on a Literature Review’, *Int. J. Environ. Res. Public. Health*, vol. 19, no. 1, p. 595, Jan. 2022, doi: 10.3390/ijerph19010595.

[386] B. Jonsson, ‘Measurement and evaluation of local muscular strain in the shoulder during constrained work’, *J. Hum. Ergol. (Tokyo)*, vol. 11, no. 1, pp. 73–88, 1982.

[387] M. Björkstén and B. Jonsson, ‘Endurance limit of force in long-term intermittent static contractions’, *Scand. J. Work. Environ. Health*, pp. 23–27, 1977.

[388] L. V. Christensen, ‘Physiology and pathophysiology of skeletal muscle contractions: Part II. Static activity’, *J. Oral Rehabil.*, vol. 13, no. 5, pp. 463–477, Sep. 1986, doi: 10.1111/j.1365-2842.1986.tb01308.x.

[389] ‘How EU policy is decided’, European Union. Accessed: Aug. 13, 2024. [Online]. Available: https://european-union.europa.eu/institutions-law-budget/law/how-eu-policy-decided_en

[390] *International Organisation for Standardisation (ISO). ISO Strategy 2016-2020.*, Geneva, Switzerland., 2015.

[391] *International Organisation for Standardisation (ISO). ISO - 11226. Ergonmics - Evaluation of static working postures.*, Geneva, Switzerland., 2000.

[392] *International Organisation for Standardisation (ISO). ISO - 11228-1. Ergonmics - Manual Handling - Part 1: Lifting and carrying.*, Geneva, Switzerland., 2003.

[393] *International Organisation for Standardisation (ISO). ISO - 11228-2. Ergonmics - Manual Handling - Part 2: Pushing and pulling.*, Geneva, Switzerland., 2007.

[394] *International Organisation for Standardisation (ISO). ISO - 11228-3. Ergonmics - Manual Handling - Part 3: Handling of low loads at high frequency.*, Geneva, Switzerland., 2007.

[395] M. C. Brouwers, K. Kerkvliet, K. Spithoff, and AGREE Next Steps Consortium, ‘The AGREE Reporting Checklist: a tool to improve reporting of clinical practice guidelines’, *BMJ*, p. i1152, Mar. 2016, doi: 10.1136/bmj.i1152.

[396] ‘About the Total Worker Health® Approach’, Center for disease control and prevention. Accessed: Oct. 02, 2024. [Online]. Available: https://www.cdc.gov/niosh/twh/about/?CDC_AAref_Val=https://www.cdc.gov/niosh/twh/totalhealth.html

[397] ‘Scale Fit’. Accessed: Aug. 14, 2024. [Online]. Available: https://www.scalefit.de/home.html

[398] ‘Movella’s Motion Capture Technology Powers Workplace Ergonomic Improvements at BMW Group’, Movella, Henderson, NV, Jun. 2023. Accessed: Aug. 14, 2024. [Online]. Available: https://www.movella.com/company/press-room/movellas-motion-capture-technology-powers-workplace-ergonomic-improvements-at-bmw-group